

Print ISSN 2219-9764
Online ISSN 2617-8982



Diyala Journal of Medicine

Vol 28 Issue 1
April 2025



 www.djm.uodiyala.edu.iq
 editor@djm.uodiyala.edu.iq

مجلة دورية محكمة صادرة عن
كلية الطب - جامعة ديالى



DJM**Diyala Journal of Medicine*****Published by College of Medicine - University of Diyala - Diyala - Iraq.*****Editorial Board****Editor in Chief****Assistant Professor Dr. Anfal Shakir Motib****PhD in Molecular Microbiology – Department of Microbiology- College of Medicine - University of Diyala****anfal_shaker@yahoo.com****Editor Manager****Lecturer Dr. Saad Ahmed Ali Jadoo Al-ezzi****PhD in Community Medicine - College of Medicine - University of Diyala****saadalezzi@uodiyala.edu.iq****Editorial Board****Professor Dr. Ismail Ibrahim Latif**

PhD in Clinical Immunity- College of Medicine - University of Diyala

ismail_6725@yahoo.com**Professor Dr. Ghanim Mustafa Al-Sheikh**

PhD in Human Neurosciences - Imperial College London –UK

alsheikhg@gmail.com**Professor Dr. Karim Alwan Mohamed**

PhD in Pathology and Forensic Medicine - Head of Pathology Unit - Faculty of Medicine- SEGi University –Malaysia

jashamy@yahoo.com**Professor Dr. Talib Jawad Kadhum**

PhD in Anatomy- College of Medicine - University of Diyala

talibjwd@yahoo.com**Professor Dr. Saad Muhmood Hussain Arraki**

Board in Surgery – Newcastle University Medicine- Malaysia

Drsaad1961@gmail.com**Professor Dr. Jalil Ibrahim Alezzi**

FICMS, DCH in Medicine pediatrics- College of Medicine - University of Diyala

adil_alhusseiny@yahoo.com**Professor Dr. Amer Dawood Majeed**

PhD in Medical Physics - College of Medicine -University of Diyala

amer_dmk@yahoo.com**Professor Dr. Zuhair Maroof Hussain**

PhD in Biochemistry - College of Medicine - University of Diyala

zuhair@medicine.uodiyala.edu.iq**Professor Dr. Mehdi Shamkhi Gebir**

Board in Pediatrics - College of Medicine - University of Diyala

meh_sh2000@yahoo.com**Professor Dr. Ahmed Mohamed Badheeb**

Jordanian Board of Medical Oncology - Head of Medical Oncology department at King Khalid Hospital - Najran-Saudi Arabia

abadheeb@moh.gov.sa**Professor Dr. Salwa Sh. Abdul-Wahid**

PhD in Community Medicine - College of Medicine - University of Diyala

s_sh_abdulwahid@yahoo.co.uk**Professor Dr. Salih Mahdi Salman**

PhD in Organic Chemistry - College of Medicine - University of Diyala

salih@medicine.uodiyala.edu.iq**Professor Dr. Kamile Marakoglu**

PhD in Family Medicine - College of Medicine - University of Selcuk- Konya-Turkey

Professor Dr. Aydin beyatli

PhD in Ophthalmologist Medicine- Ankara University- Turkey

aydinbeyatli@hotmail.com**Professor Dr. Marwan Salih Al-Nimer**

PhD in Pharmacology and Therapeutics- College of Medicine - University of Diyala

marwanalnimer@yahoo.com**Professor Dr. Ali Mohammed Batarfi**

Board in Surgery- College of Medicine and Health, Sciences Roadstead- Hadhramout- Yemen

ambatarfi@yahoo.com**Assistant Professor Dr. Muqdad Fuad Abdulkareem**

Board in Surgery - College of Medicine-University of Diyala

muqdadfuad@yahoo.com**Assistant Professor Dr. Fayeze Alghofaili**

PhD in Medical Microbiology - College of Applied sciences -University of Majmaah-Saudi Arabia

F.alghofaily@mu.edu.sa**Assistant Professor Dr. Melike Emiroglu**

PhD in Child Health and Diseases- College of Medicine - University of Selcuk-Konya-Turkey

mkeser17@gmail.com**Dr. Omer Layth Qassid**

FRCPath(UK) IFCAP(USA)- University of Leicester-Consultant Histopathologist-The university hospitals of Leicester – United Kingdom

Omer.qassid@uhl-tr.nhs.uk**Assistant Professor Dr. Mustafa Ghani Taher**

PhD in Dentist- Oral and Maxillofacial Pathology- College of Medicine- University of Diyala

gheny@uodiyala.edu.iq**Professor Dr. Nadhim Ghazal Noaman**

Head of Community Medicine Department - College of Medicine - University of Diyala

drnadhimg@yahoo.com**DJM Design****Ahmed Jabbar Mohammed****ahmed.jabbar@uodiyala.edu.iq****Correspondence: DJM Office/ College of Medicine/ University of Diyala / PO Box (2) Baquba office/ Baquba/ Diyala/ Iraq.****E-mail: djm.diyala@yahoo.com , editor@djm.uodiyala.edu.iq**

Instruction to Authors

Papers are accepted on the understanding that the subject matter has not and will not be submitted simultaneously to another journal. The following notes are expected to be considered carefully in writing manuscripts:-

1- The manuscript including figures and tables should be submitted on line to <http://djm.uodiyala.edu.iq/index.php/djm/about/submissions> Or as an attachment to djmeditor@djm.uodiyala.edu.iq .

2- Manuscripts must be accompanied by a covering letter signed by all authors that the paper has not been published and will not be submitted to another journal if accepted in the Iraqi Medical Journal.

3- The title page should include:

Title of the paper is in Arabic and English

Correct first name, middle name and family name of all authors in Arabic and English as well as a maximum of two highest academic degrees for each author.

Name (s) and address (es) of the institution (s) where the work was carried out.

The name and address of the author responsible for correspondence together with telephone number, fax number and e-mail address (if any).

4- Abstract for original articles should contain a structured abstract of not more than 200 words in Arabic and English. Abstract heading include: background, objectives, Methods, Results, and conclusions. Abstracts in Arabic and English of review articles and case reports should be unstructured and of not more than 150 words.

5- Three to ten keywords should be provided on the same page as the abstract in English and Arabic. As far as possible, the keywords should be selected from the national library of medicine, medical subject headings.

6- The main text of the original article should be divided into section, each section should be started on a new page after the title page:

- **Introduction:** is should state clearly the purpose and rationale of the study.
- **Methods:** should include selection of subjects, identification of the methods, apparatus and chemicals used and include statistical analysis.
- **Results:** They presented in a logical sequence preferably with tables and illustrations emphasizing in the text only the important observation.
- **Discussion:** it emphasizes new findings of the study, implications and reference to other relevant studies.
- **Acknowledgement:** it is only to persons who have made substantive contribution to the study.
- **References:** should be in the Vancouver style. They should appear in the text by numbers in the order. List all authors when six or less; when seven or more, list only first six and add et al. journal titles should be abbreviated in accordance with Index Medicus. Examples of correct reference forms are given as follows:

Al-Salihi AR, Hasson EH, Al-Azzawi HT. A short review of snakes in Iraq with special reference to venomous snake bite and their treatment. Iraqi Med J 1987; 36:57-60.

Book chapter: Pen AS. Immunological features of myasthenia gravis. In: Aguayo AJ, Karapti G, editors. Topics in nerves and muscle research. 31st ed. Amsterdam: Experta Medica; 1975. p. 123-32.

7- Illustration: Photographs unmounted on glossy paper should be provided with magnification scale if appropriate. Lettering should be in either leterset or stencil of comparable size. Illustration should be marked on the back with the figure number, title of the paper and name (s) of the author (s) with soft pencil. All photographs, graphs and diagrams should be referred to as figures and should be numbered consecutively in the text. The legends to illustration should be typed on a separate sheet. Tables should be numbered consecutively in the text in and each typed on a separate sheet. Vertical lines normally will not be printed.

- 8-** Measurements are preferably expressed in SI (standard international) units.
- 9-** Authors are advised to follow the Webster's collegiate dictionary in spelling.
- 10-** Articles and abstracts which written in Arabic should follow the unified medical dictionary (council of Arab ministers of health/WHO/Arab medical union/ALESCO, 3rd edition)
- 11-** Use only SI standard abbreviations in the title and abstract. The full term for which the abbreviations stand should precede its first use the text.
- 12-** After the manuscripts has been accepted for publication, authors are required to supply the final version of the manuscript on CD IBM compatible disc in MS word 1997-2003 and more.
- 13-** Page proof will be sent to the corresponding author for proof correction. Major alterations from the text cannot be accepted.
- 14-** Through sending the manuscripts, authors from outside Iraq are requested to send upon acceptance of the paper, a publishing charge of 150 ID is required. For authors from Iraq, the total charge is 120\$ on sending the article.

No.	Paper Title	Page
1	Dietary phytoestrogen increases tumour size and the frequency of circulating Tregs in a B16-F10 murine melanoma tumour model Rafah Oday Hussian, Lee Richard Machado	1-13
2	Assessing the Appropriateness of Three-Dimensional Conformal Radiotherapy Technique Planning Treatment for Rectal Versus Cervical Cancer: A Comparative Study Ru'aa Emad Al-Khalidi, Nashwan Karkhi Abdulkareem, Arthur Saniotis, Rojgar Najat Yousif	14-24
3	The Significant Impact of Programmed Cell Death-1 Gene Polymorphism on HBV Infection and Viral Load Hiba Hadi Rashid, Hiba M. Al-Darraj, Müge FIRAT, Bassam Mohammed Mishkhal	25-35
4	Curcumin Oral Gel and its Relation to Salivary Tumor Necrosis Factor-Alpha and Interleukin-6 that Treated Oral Mucositis in Head and Neck Cancer Patients Undergoing Concurrent Chemoradiation Rou'aa S. Farhan, Fawaz D. Al-Aswad	36-47
5	Articular Eminence Inclination and Glenoid Fossa Measurements by CBCT in Patients with Temporomandibular Joint Disorders Hayder Mahdi Idan, Fawaz D. Al-Aswad	48-57
6	Comparison of Muscle to Nodule Strain Ratio Elastography with Parenchyma to Nodule Strain Ratio Elastography in Suspicious Thyroid Nodules Zainab Faisal Atiyah, Mohammed M.J. Al-khalissi	58-69
7	Relationship Between Entrance Surface Skin Exposure for Iraqi Women with Compressed Breast Thickness in Mammography Doaa Hameed kadhim, Zainab A. Hamoudi, Mawada M. Funjan, Rania Jamal Ahmed, Aya H. Hasan	70-78
8	Determination of meprin alpha enzyme and its relationship with some antioxidants and interleukin 12 in the blood serum of patients with colon cancer Hussein Mahmoud Khalaf, Wasan Nazhan Hussein, Alaa Hassan Mustafa	79-87
9	Assessment of development of children in Diyala province Haider Asad Mohammad, Najdat Sh. Mahmood, Jalil I. Alezzi	88-103
10	The Impact of Helicobacter pylori on Lesion Type and Matrix Metalloproteinase-9 Expression in Laryngeal Tumors Wasan Abdul-elah Bakir, Refif Sabih Al-Shawk, Mais Ibrahim Alsikafi, Shaimaa Rahem Al-Salihy	104-118
11	Recurrent Hidradenocarcinoma in the Abdominal Wall with no Distant Metastasis: A Case Report and Literature Review Yahia Hameed Al-Ani, Raid M. Al-Ani, Wassan Nori, Israa Mahdi Al-Sudani	119-125

Dietary Phytoestrogen Increases Tumour Size and the Frequency of Circulating Tregs in a B16-F10 Murine Melanoma Tumour Model

Rafah Oday Hussian ¹, Lee Richard Machado ²,

¹ Technical Institute of Baquba, Middle Technical university, Diyala, Iraq.

² Centre for Physical Activity and Life Sciences, University of Northampton, Northampton, UK.

OPEN ACCESS

Correspondence: Rafah Oday Hussian

Email: rafah.oday@mtu.edu.iq

Copyright: ©Authors, 2025, College of Medicine, University of Diyala. This is an open access article under the CC BY 4.0 license (<http://creativecommons.org/licenses/by/4.0/>)

Website:
<https://djm.uodiyala.edu.iq/index.php/djm>

Received: 27 January 2025

Accepted: 05 April 2025

Published: 25 April 2025

Abstract

Background: Clinical studies show strong associations between hormone levels, particularly estrogens and the development of skin cancers. Cutaneous melanoma is considered a hormone-related tumour; however, their role in melanoma progression remains unclear.

Objective: To investigate the effects of a phytoestrogen-rich diet on melanoma tumour initiation and development using a syngeneic mouse model.

Patients and Methods: Mice were fed either a phytoestrogen-rich or low control diet and injected subcutaneously with 5×10^5 syngeneic melanoma cells (B16-F10). After 10–12 weeks, tumours and spleens were collected. Tumour size and weight were measured, and quantitative PCR (qPCR) was performed to analyse the expression of estrogen receptor (ER) α and β . Regulatory T cells (Tregs) from splenocytes was assessed via flow cytometry.

Results: Mice consuming the phytoestrogen-rich diet exhibited significantly larger tumours compared to those on the control diet. Phytoestrogens in the diet up regulated ER β and down regulated ER α mRNA expression in tumour tissue. A significant increase in the proportion of splenic Tregs was observed in tumour-bearing mice fed a phytoestrogen-rich diet.

Conclusion: This study highlights the influence of dietary composition on tumour growth and associated immune responsiveness, emphasising the need to account for dietary factors in experimental designs and their potential impact on tumour biology.

Keywords: Phytoestrogen, T-regulatory cells, Murine melanoma tumours, Flow cytometry.

Introduction

Genetic, inflammatory and environmental factors have a significant role in the development of cancers (1). However, the impact of dietary components on outcomes in animal experiments is often underappreciated (2). A variety of commercial rodent diet formulations are available (3–5), many of which include Soy meal as a primary protein source (48). Soy meal is rich in phytoestrogens, plant-derived compounds structurally similar to endogenous estrogens, which can exert either estrogenic or anti-estrogenic effects through their interaction with estrogen receptors α (ER α) and ER β (6-50). Estrogen receptors belong to the nuclear receptor superfamily of transcription factors (7). Their activation elicits opposing effects on cancer growth and progression. Specifically, the expression of ER β is often reduced in various cancer cells (8). According to De Giorgi and colleagues, ER β expression counteracts the proliferative effects mediated by ER α in the skin (9,10). It is well established that expression of ER α is associated with abnormal proliferation, inflammation, tumorigenesis and the development of malignancy (7,8,11). These findings indicate that the effects of estrogens on cancer growth may depend on the relative ratio of ER α /ER β expression within a given

tumour cell or tissue (12). Estrogen receptors (ERs) can translocate from the cytoplasm to the nucleus, where they bind to transcriptional control regions of DNA or interact with small RNAs, subsequently inducing the expression of specific genes. Consequently, phytoestrogens have the potential to regulate estrogen-mediated processes, including the induction of sex hormones (13). High dietary phytoestrogen exposure can interfere with measurements in studies involving estrogenic activity, potentially affecting the interpretation of animal model experiments (14). Major natural dietary sources of phytoestrogens include soybeans, wheat, potatoes, rice, alfalfa, and oats (15-49). These compounds can bind to estrogen receptors, eliciting effects in animals, humans, and cultured cells. Consequently, studies of hormone-dependent or hormone-modulated conditions, such as animal models of cancer and investigations into steroid hormones like estrogen may be significantly compromised by the presence of high levels of dietary phytoestrogen (4). Several studies have reported significant differences in experimental outcomes when comparing diets with high phytoestrogen content to those with very low phytoestrogen levels (2,3). Phytoestrogens, particularly isoflavones, are recognised as endocrine disruptors with significant pathophysiological impacts. The Environmental Protection Agency (EPA) defines endocrine disruptors as substances that alter the structure and function of the endocrine system, leading to adverse effects (16). These disruptions may be attributed to the estrogenic activity, nutrient composition, and metabolizable energy of phytoestrogen-rich diets (17-19). In animal models, flavones have been shown to disrupt lactation, alter the timing of puberty, impair the ability to produce viable and fertile offspring, influence sex specific behaviours, accelerate reproductive ageing and compromise fertility (16). The role of

phytoestrogens in malignancy have been examined in a range of clinical and experimental studies. For example, in a recent large prospective cohort study, increased intake of total isoflavones, daidzein, glycitein, and formononetin was found to be associated with a reduced risk of pancreatic cancer among all participants and ever smokers (20). However, in ovarian cancer, associations between intake of phytoestrogens and cancer risk showed no major aetiological role (21). In a study of genistein supplementation on genome-wide DNA methylation and gene expression in patients with localised prostate cancer there were global gene expression changes and this had effects on molecular pathways involved in prostate tumorigenesis which included developmental pathways, markers of stem cells and proliferation and transcriptional regulation. The authors identified a reduction in MYC activity and a concomitant increase in PTEN activity (22). In a breast cancer soy supplementation study, cancer-related genes and pathways were examined and high plasma genistein identified a gene-signature with overexpression of FGFR2 and cell cycle progression and proliferation genes. Therefore, for a subset of women, soy may negatively affect gene expression in breast cancer (23). Although melanoma is traditionally considered a non-hormone-related cancer, growing evidence suggests a direct association between sex hormones, particularly estrogens, and melanoma progression (24). T-regulatory cells (Tregs) are recognised as significant barriers to effective anti-tumour immune responses, contributing to the development of an immunosuppressive tumour microenvironment (TME) (25,26). Tregs have been extensively studied in the peripheral blood and immune infiltrates of various cancers, with their accumulation strongly linked to poor prognosis in melanoma, breast, and colon cancers (27-30). Intracellular metabolism plays a critical role in

determining cell activity and function. Recent studies indicate that the metabolic and functional state of Tregs is shaped by local environmental conditions and the availability of specific metabolites. These metabolites, present in both the peripheral circulation and the TME, profoundly influence Treg differentiation, and phenotype stability (25). Tregs are classically characterised as CD4⁺CD25⁺ lymphocytes expressing the forkhead/winged helix family transcription factor FOXP3. In this study, we investigated the role of dietary phytoestrogens on B16-F10 melanoma tumour growth in C57BL/6 mice, examined the expression of tumour derived ERs, and assessed the frequency of peripheral treg populations.

Patients and Methods

Cell culture: Pigmented murine melanoma cells (B16-F10; kindly provided by Professor Steven Todryk, University of Northumbria, UK) were maintained DMEM/F-12 medium supplemented with 10% fetal calf serum (FCS), 100 IU/ml penicillin and 100 µg/ml streptomycin). To eliminate potential estrogen effects, the cells were cultured in phenol-free medium (31). Once the cells reached approximately 70% confluence, their viability (>90%) was assessed using trypan blue exclusion, and viable cells were counted with a haemocytometer.

Animals: The experiments were conducted using specific pathogen-free C57BL/6 black (6–8 weeks old) mice obtained from Jackson Laboratory 600 Main Street Bar Harbor, ME USA 04609. They were bred in the Preclinical Research Facility (PRF) at the University of Leicester and used with authority from the Home Office under the supervisor's project license P43308E3B, with approval from the institutional animal welfare and ethical review board on 11 July 2016. The mice were housed at 25°C under a 12-hour light/dark cycle and provided ad libitum access to food and water. Mice were divided randomly in two groups and fed either a

chow diet rich in phytoestrogen (5LF2; Test Diet ® product, 14.3% protein, 5.8% fat, 65% carbohydrate, up to 20% Soybean meal) or a low estrogenic control diet (58R1; Test Diet ® product, 14.8% protein, 4.8% fat, 73.9% carbohydrate, 0% Soybean meal) for 8 weeks, with sex and age matched between groups. Mice were then inoculated subcutaneously into the right flank with 5×10^5 B16-F10 murine melanoma cells suspended in 100 µl of PBS. Tumours were allowed to establish, and their size was measured daily using calipers until the endpoint, typically 10–14 days post-injection. Tumour volume was calculated using the formula $V = \pi/6 \times \text{length} \times \text{width}^2$. Tumour weight was measured using an analytical balance, and all weights are reported in milligrams (mg). At the conclusion of the experiment, all mice were sacrificed, and tumours and spleens were collected for analysis.

RNA extraction and quantitative real-time (RT-PCR): Total RNA was extracted from melanoma tumours using TRIzol reagent (Sigma-Aldrich, UK). Genomic DNA contamination was removed using an RNase-free DNase kit (Sigma-Aldrich). A total of 3 µg of RNA was retro-transcribed into cDNA following the manufacturer's instructions (Thermo Scientific). Gene-specific amplification was carried out using the SensiMix SYBR kit (Bioline Reagents Ltd., London) and analysed on a Corbett Rotor-Gene TM6000 machine to measure the expression of Estrogen Receptor α (ER α) and Estrogen Receptor β (ER β). The $\Delta\Delta\text{CT}$ method (Livak & Schmittgen, 2001) was used for relative quantification. Samples were analysed in triplicate, and GAPDH was used as the housekeeping gene. The primer sequences used were as follows: for Estrogen Receptor β (ER β), forward 5'-CAGTAACAAGGGCATGGAAC-3' and reverse 5'-GTACATGTCCCACTTCTGACA-3'; for GAPDH, forward 5'-

CCCTTAAGAGGGATGCTGCC-3' and reverse 5'-TACGGCCAAATCCGTTTACA-3'; and for Estrogen Receptor α (ER α), forward 5'-GACCAGATGGTCAGTGCCTT-3' and reverse 5'-ACTCGAGAAGGTGGACCTGA-3'.

Flow cytometry analysis: To detect T-regulatory cells, freshly isolated splenocytes (1×10^6 cells/100 μ l FACS buffer) from tumour-bearing mice fed the respective diets were pre-blocked with an Fc receptor-specific anti-mouse CD16/32 antibody (BioLegend) for 30 minutes on ice. Following the blocking step, cells were stained with PE and APC-conjugated antibodies targeting CD4, CD25, and FOXP3 (mouse, 130-094-165) for 30 minutes on ice in the dark. After staining, the cells were washed and re-suspended in 400 μ l PBS supplemented with 3% (v/v) FCS. The stained cells were then transferred into polypropylene tubes for flow cytometry analysis. Spectral overlap of fluorochromes was compensated where necessary, and flow cytometry data were acquired using BD FACS Diva™ software version 8.0. Splenocytes from three tumour-bearing mice per dietary group were used.

Statistical analysis

The data were expressed as the mean \pm SD for bar charts. Box-and-whisker plots display the distribution of the data, with the box representing the interquartile range (IQR) (25th to 75th percentile) and the line inside the box indicating the median. Whiskers extend to the minimum and maximum values, showing the full data range. Individual values are also shown. Analysis was performed using GraphPad Prism 10 (GraphPad, San Diego, California, USA). Tests for normality were conducted by inspecting QQ-plots and employing the Shapiro-Wilk test to confirm the assumption of a normal distribution. Statistical significance was determined using Unpaired t-tests (or the non-parametric equivalent) and indicated by exact p-values where alpha was set

to < 0.05 . Effect sizes were calculated using η^2 (eta squared) to quantify the proportion of variance explained by group differences. For parametric tests, η^2 was derived from the t-statistic, while for non-parametric tests, it was calculated using the Z-score (Mann-Whitney U/Wilcoxon). For qPCR analyses, the results were presented as the fold change in gene expression normalised to the housekeeping gene.

Results

A phytoestrogen rich diet enhances melanoma tumour weight and size: To investigate the impact of any difference in tumour weight of tumour bearing mice fed on chow diet rich in phytoestrogen (5LF2) or control diet low in estrogen (58R1), C57BL/6 mice were inoculated subcutaneously into the right flank with 5×10^5 B16-F10 murine melanoma cells. The results demonstrated statistically significant differences in tumour weight between the two diet groups (Figure 1).

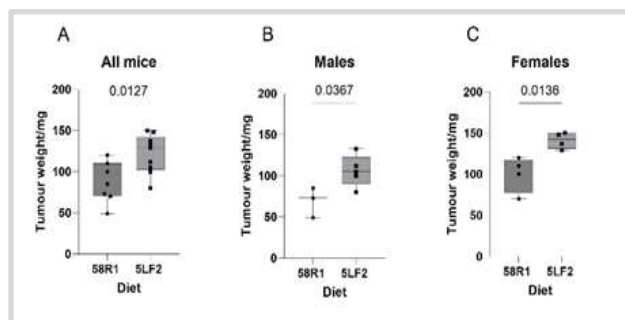


Figure 1. Melanoma tumour weight in C57BL/6 mice after administration of estrogenic or control diets. The effect of estrogenic (5LF2) and control diets (58R1) on tumour weight in melanoma-bearing mice. (A) The tumour weight in all mice following an estrogen-rich or poor diet (B) The tumour weight in males following an estrogen-rich or poor diet. (C) The tumour weight in females following an estrogen-rich or poor diet. The data are presented as box plots, including individual data points, the median, and the quartiles. Statistical significance was assessed using an unpaired t-test, with exact p values provided. * $p < 0.05$.

In the all-mice group, the 5LF2 diet resulted in a mean tumour weight 34.84 grams higher than the 58R1 diet ($P = 0.0127$), with a moderate effect size (Figure 1A, $R^2 = 0.3680$). In males, the mean

difference was 37.00 grams ($P = 0.0367$), with a larger effect size (Figure 1B, $R^2 = 0.5442$), while in females, the mean difference was 41.00 grams ($P = 0.0136$), showing the largest effect size (Figure 1C, $R^2 = 0.6655$). In all groups, the unpaired t-tests yielded significant P values ($P < 0.05$), indicating that the 5LF2 diet had a notable impact on tumour weight. These findings suggest that the 5LF2 diet significantly influenced tumour weight, with the most pronounced effect observed in female mice. The analysis of tumour size across all mice, males, and females fed either a phytoestrogen-rich 5LF2 diet or a control 58R1 diet revealed significant differences in tumour size between the two diet groups Figure 2. For all mice, the 5LF2 diet resulted in a mean tumour size 48.56 mm³ larger than the 58R1 diet ($P = 0.0258$), with a moderate effect size (Figure 2C, $R^2 = 0.3074$). In males, the 5LF2 diet caused a mean tumour size increase of 61.60 mm³ ($P = 0.0159$), showing a large effect size (Figure 2B, $R^2 = 0.6485$). In females, the 5LF2 diet led to a 50.75 mm³ larger tumour size ($P = 0.0238$), with a strong effect size (Figure 2C, $R^2 = 0.6010$). The unpaired t-tests for all groups showed significant differences ($P < 0.05$), indicating that the 5LF2 diet significantly influenced tumour size. These results suggest that the phytoestrogen-rich 5LF2 diet significantly impacted tumour size across all groups, with the most pronounced effect in males, followed closely by females.

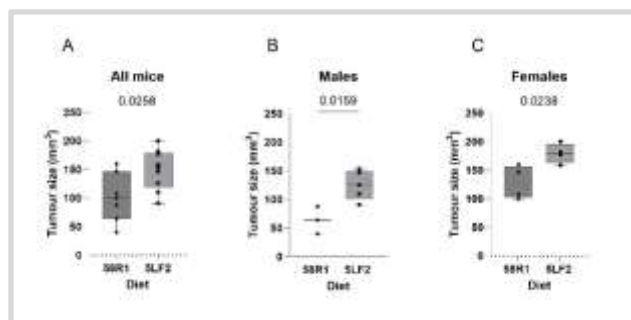


Figure 2. Effect of consuming a phytoestrogenic diet on tumour size in C57BL/6 mice. The effect of estrogenic (5LF2) and control diets (58R1) on tumour size (mm³) in melanoma-bearing mice. (A) The tumour size (mm³) in all mice following an estrogen-rich or poor diet (B) The tumour size (mm³) in males following an estrogen-rich or

poor diet. (C) The tumour size (mm³) in females following an estrogen-rich or poor diet. The data are presented as box plots, including individual data points, the median, and the quartiles. Statistical significance was assessed using an unpaired t-test, with exact p values provided. * $p < 0.05$.

A phytoestrogen diet is associated with upregulated estrogen receptor β in B16-F10 tumours:

As a transcription factor, ER β regulates the transcription of various genes, which binds to estrogen response elements (ERE) upstream of the target genes (Hayashi et al., 2003). Therefore, we investigated the effect of a diet rich in phytoestrogen on the expression of ER β in mice bearing melanoma tumours. To investigate the effect of a high phytoestrogen diet (5LF2) and control low phytoestrogen diet (58R1) on ER β mRNA levels, melanoma tumours were isolated, and fold change quantified using qPCR. The comparison of fold change in mRNA expression of ER β between the 5LF2 and 58R1 diets showed significant differences in both male (Figure 3B) and female mice (Figure 3C), but no significant difference in the overall group (Figure 3A). In male mice, the 5LF2 diet significantly increased ER β expression compared to the 58R1 diet ($P = 0.0155$), with a large effect size ($R^2 = 0.9692$). A similar significant increase was observed in female mice ($P = 0.0188$, $R^2 = 0.9627$). However, in the combined data for all mice, no significant difference was found ($P = 0.1828$), likely due to higher variability in this group. Overall, the 5LF2 diet had significantly upregulated tumour ER β mRNA expression, in males and females individually with ER β expression higher in females than males for both diets.

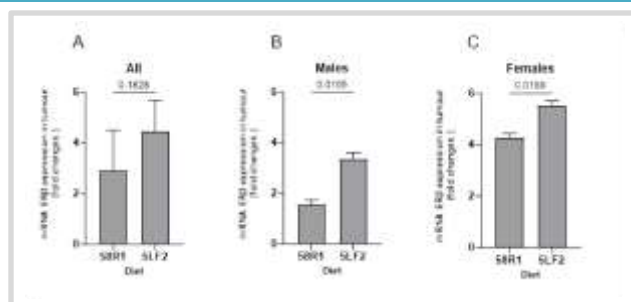


Figure 3. Effect of estrogenic (5LF2) and control (58R1) diets on ER β mRNA expression in B16-F10 tumours from melanoma-bearing mice (All n=4, Females n=2, Males n=2). The study examined the impact of estrogenic (5LF2) and control (58R1) diets on ER β mRNA expression in B16-F10 tumours from melanoma-bearing mice. Fold changes in ER β mRNA expression were assessed using the $\Delta\Delta CT$ method, with normalisation to GAPDH. Results showed differences in tumour ER β expression across (A) all mice, as well as in (B) male and (C) female subgroups, following either an estrogen-rich or estrogen-poor diet. Data are presented as mean \pm SD (n = 3). Statistical significance was determined using an unpaired t-test, with exact p-values reported (*p < 0.05).

Consumption of a phytoestrogenic diet significantly increases splenic Tregs in tumour bearing mice: Splenic Tregs (CD4+CD25+ cells as a percentage of CD4 T cells) were next examined using flow cytometry across all mice, male, and female animals fed either the phytoestrogen-rich 5LF2 diet or the control 58R1 diet and showed significant differences between the two diet groups (Figure 4, Supplementary Figure 1). For all mice, the 5LF2 diet resulted in an increase of 1.743% in the Treg percentage compared to the 58R1 diet (P = 0.0397), with a moderate effect size ($R^2 = 0.2687$). In males, the 5LF2 diet caused a 2.080% increase in the Treg percentage (P = 0.0441), reflecting a moderate effect size ($R^2 = 0.5180$). In females, the 5LF2 diet led to a 1.950% increase in Treg percentage (P = 0.0453), with a moderate effect size ($R^2 = 0.5140$). These significant differences indicate that the 5LF2 diet significantly influenced the percentage of splenic Tregs. These results suggest that the 5LF2 diet has a significant effect on the percentage of Tregs across all groups, with

moderate effect sizes observed in both male and female mice.

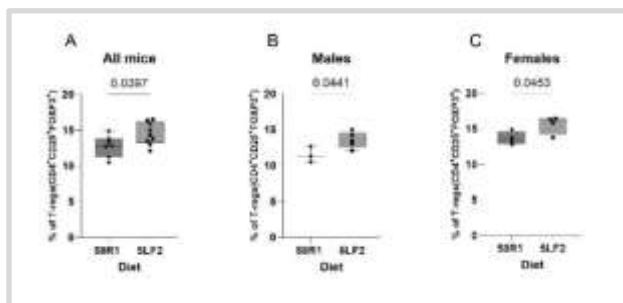


Figure 4. Flow cytometry analysis of Treg cell populations in splenocytes of tumour bearing mice fed on estrogen rich (5LF2) and poor (58R1) diets. The effect of estrogenic (5LF2) and control diets (58R1) on Treg frequencies in melanoma-bearing mice. (A) Splenic CD4+CD25+Foxp3+ cells in all mice following an estrogen-rich or poor diet (B) Splenic CD4+CD25+Foxp3+ cells in males following an estrogen-rich or poor diet. (C) Splenic CD4+CD25+Foxp3+ cells in females following an estrogen-rich or poor diet. The data are presented as box plots, including individual data points, the median, and the quartiles. Statistical significance was assessed using an unpaired t-test, with exact p values provided. *p < 0.05.

A phytoestrogen diet is associated with downregulated estrogen receptor α in B16-F10 tumours: We next investigated the effect of a diet rich in phytoestrogen on the expression of ER α in mice bearing melanoma tumours (Figure 5). The comparison of fold change in mRNA expression of ER α between the 5LF2 and 58R1 diets showed significant differences in male and female mice, but no significant difference in the overall group. In male mice (Figure 5B), the 5LF2 diet significantly decreased ER α expression compared to the 58R1 diet (P = 0.0203), with a large effect size ($R^2 = 0.9599$). Similarly, in female mice (Figure 5C), a significant decrease was observed (P = 0.0105, $R^2 = 0.9792$). However, in the combined data for all mice, no significant difference was found (P = 0.0788), likely due to higher variability in this group due to sex specific ER α levels. Overall, the high phytoestrogen 5LF2 diet resulted in significant downregulation of ER α mRNA expression in both male and female groups.

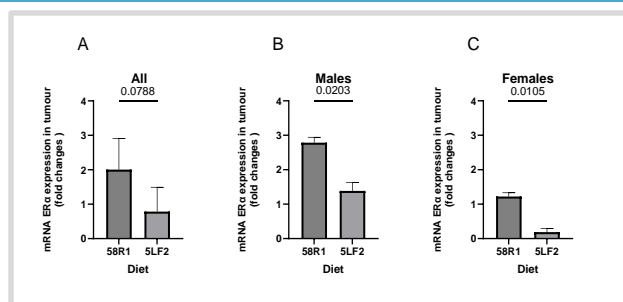


Figure 5. Effect of estrogenic (5LF2) and control (58R1) diets on ER α mRNA expression in B16-F10 tumours from melanoma-bearing mice (All n=4, Females n=2, Males n=2). The study examined the impact of estrogenic (5LF2) and control (58R1) diets on ER α mRNA expression in B16-F10 tumours from melanoma-bearing mice. Fold changes in ER α mRNA expression were assessed using the $\Delta\Delta\text{CT}$ method, with normalisation to GAPDH. Results showed differences in tumour ER α expression across (A) all mice, as well as in (B) male and (C) female subgroups, following either an estrogen-rich or estrogen-poor diet. Data are presented as mean \pm SD (n = 3). Statistical significance was determined using an unpaired t-test, with exact p-values reported (*p < 0.05).

Discussion

The aim of this study was to investigate the impact of phytoestrogen-rich diets on melanoma tumour growth. We show that B16-F10 tumours were larger in size and unregulated ER β mRNA and down regulated ER α . In addition, splenic Tregs isolated from tumour-bearing mice showed an increased frequency in the CD4 $^{+}$ T cell population. This agrees with previous studies that suggest animal diets containing phytoestrogens can significantly influence the outcomes of tumour studies and hormonal cellular endpoints. Therefore, diet selection is critically important, and can directly affect experimental results (3). Despite studies which indicate the anti-angiogenic and anti-cancer effects of consuming a diet rich in phytoestrogen, there is ongoing concern about the potential risks associated with consuming high levels of these compounds (32,33). Commercial rodent diets formulated with soy as a protein source are typically provided to animals daily, resulting in the

consumption of large doses of phytoestrogens, particularly isoflavones (34). These results in a sustained high serum concentration of isoflavones compared to animals fed on free or low soy diet (4). Thigpen and colleagues (2004) found that dietary isoflavones can affect the reproductive, skeletal, and cardiovascular systems (3). As a result, this may influence and alter the outcomes of experiments focused on comparative estrogenicity, endocrine disruption and carcinogenicity. Sex-related factors are intriguing aspects of melanoma tumour growth. Premenopausal women developed melanoma tumours more slowly than men and experience better survival rates, potentially due to the influence of sex hormone levels and the expression of estrogen receptors (35). These observations support the role of sex hormones in melanoma development and progression (11). However, our measurements of tumour weight revealed that mice fed a high estrogenic diet (5LF2) had larger tumours compared to those fed on the 58R1 diet. This aligns with previous work showing that B16 tumours grow more rapidly in female C57BL/6 mice than in males. They also demonstrate that sex and estrogen receptors signalling mechanisms may impact tumour development and immune cell infiltration (36). Our results align with a study reporting an increase in the incidence of vulvar carcinomas in female 129/J mice fed soy protein containing daidzein and genistein for three months, compared to other groups fed phytoestrogen-free diets (3). Female athymic nude mice fed dietary phytoestrogens across a wide concentration range (125–1,000 μg) exhibited increased tumour size, comparable to the estradiol control group. Long-term exposure to dietary soy isoflavones significantly enhances proliferation of estrogen-dependent tumours and increased total plasma genistein concentrations (37). Similarly, soy-derived isoflavones, with genistein as a key component, stimulated tumour

progression and prevented tumour regression in a mammary cancer model, resulting in significantly larger tumours compared to controls after three months of feeding (38). In contrast, our findings do not agree with work that showed dietary supplementation with isoflavones resulted in the development of smaller tumours in a dose-dependent manner (2.5-20% soybean protein) in an experimental metastasis model (39). This discrepancy may be attributed to the lower number of B16-F10 cells for tumour implantation (0.5×10^5), which was nearly 10 times fewer than the numbers used in our study (39). Additionally, their study employed a mouse melanoma B16 cell line which is different from the B16-F10 line and used lower doses of soybean protein in their diets compared to those used in this study (up to 20%). Importantly their study used an intravenous injection model which contrasts with the subcutaneous injection model used in this study. Another study supporting a protective role of phytoestrogens showed that the administration of 15 mg/kg of a soybean-based diet for five days reduced tumour-induced angiogenesis in syngeneic 6-8-week-old female C57BL/6 mice intraperitoneally injected with 1×10^5 B16-F10 cells (40). However, the study employed the less aggressive parental B16-F0 cell line, (31). Furthermore, the previous study injected 1×10^5 B16-F10 cells intraperitoneally, five times fewer cells than used in our study, and employed a different injection site. Collectively, these differences suggest that the effect of dietary phytoestrogens may depend on factors such as the route of injection, duration of exposure, soybean diet dosage, number of cells used, and the specific animal model. Our investigation revealed that mice fed a high-estrogenic diet (5LF2) exhibited a significantly higher proportion of splenic Tregs compared to mice on a low-estrogenic diet (58R1). This result concurs with a previous study demonstrating that estrogen (17- β -estradiol, E2) administered at

physiological doses enhances Treg expansion and upregulates Foxp3 and IL-10 expression in multiple tissues of immunocompetent ovariectomized female mouse models (41). Additionally, others have reported that increased estrogen (17- β -estradiol, E2) levels stimulate Foxp3 expression in both naïve and syngeneic pregnant female C57BL/6 mice. This finding is particularly significant given the accumulation of FoxP3+ Tregs in tumours is a well-established predictor of poor prognosis in various cancers (26,42,43). Our results revealed significantly higher ER β mRNA expression in tumours from mice fed a high-estrogenic diet (5LF2) compared to a low-estrogenic diet (58R1), with females exhibiting higher expression than males fed on the same diets. Similar findings were obtained by de Giorgi et al. (2009) that reported higher ER β mRNA levels in primary compared with metastatic melanomas (9,10). Additionally, immunohistochemistry has confirmed the presence of ER β protein, but not ER α , in human malignant melanoma cells (45). ER β is thought to play a protective role in tumour suppression by reducing uncontrolled proliferation and enhancing apoptotic activity, with its activation shown to inhibit cutaneous melanoma cell growth (8,46). Conversely, ER α mRNA expression was lower in tumours of mice fed a phytoestrogen-rich diet compared to controls, and expression was also lower in males compared to females. This finding contrasts with studies suggesting that ER α promotes the proliferation of various cancerous cells (47). The findings from our study are consistent with existing literature, which suggests that mouse melanoma tumours express both estrogen receptors (ER α and ER β). Specifically, the interaction of phytoestrogens, which are chemically similar to estrogen, in the diet appears to stimulate a decrease in ER α expression, potentially promoting cell proliferation and enhancing tumour progression.

This is accompanied by an increase in the splenic Treg population. In contrast, the expression of ER β may counteract tumour growth mechanisms. This could occur through the activation of ER β or by disrupting the activity of ER α , potentially through the formation of ER α /ER β heterodimers. Such interactions may exert an anti-proliferative effect, leading to reduced tumour growth and a lower percentage of splenic T-regs. This study adopts a well-established murine melanoma model, with dietary manipulation to simulate phytoestrogen exposure and the quantification of immune cell subsets. We incorporate efforts to adhere to the 3Rs (Replacement, Reduction, and Refinement) by using the minimum number of animals necessary to achieve meaningful results, and statistical tests appropriate for small sample sizes were applied. However, there are several limitations and although the all-mouse group included larger numbers (>6), stratified sex-based analysis involved a smaller sample size per group. Therefore, the stratified analysis should be interpreted more cautiously. Additionally, the analysis of ER expression examined only mRNA expression and not protein expression and therefore expression may not fully reflect functional ER activity. We also note the limited scope of immune cell profiling and the lack of long-term tumour monitoring.

Conclusions

Despite significant contradictions in findings regarding the effects of dietary phytoestrogens on tumour growth, there is growing clinical and preclinical evidence suggesting that phytoestrogen-rich diets in animal models may influence cancer research outcomes. Variations in dietary isoflavone levels, particularly in soy-based laboratory diets, have been identified as a key factor contributing to inconsistent results across studies.

Recommendations

This study highlights the need to consider animal

diets as an essential experimental variable that should be carefully controlled to ensure reproducible and reliable animal models. For certain experimental designs, an isoflavone-free or low diet may be required to prevent dietary interference with experimental outcomes. Therefore, selecting an appropriate diet is crucial for the validity and reliability of carcinogenicity studies.

Source of funding: No source of funding.

Ethical clearance: Approval of the programme of work was granted by the institutional Animal Welfare and Ethics Subcommittee (item AWERB/15/24) and by the Secretary of State of the UK Home Office (license P43308E3B) on 11 July 2016.

Conflict of interest: None.

Acknowledgements:

We thank the technical support provided by the University of Leicester animal house staff for their dedicated care and maintenance of the animals used in this study. We also thank Dr Simon Byrne for his technical advice during the project.

References

1. Dunnick JK, Hailey JR. Phenolphthalein exposure causes multiple carcinogenic effects in experimental model systems. *Cancer Res.* 1996 1;56(21):4922–6.
2. Thigpen JE, Setchell KDR, Kissling GE, Locklear J, Caviness GF, Whiteside T, et al. The estrogenic content of rodent diets, bedding, cages, and water bottles and its effect on bisphenol A studies. *J Am Assoc Lab Anim Sci.* 2013 Mar;52(2):130–41.
3. Thigpen JE, Setchell KDR, Saunders HE, Haseman JK, Grant MG, Forsythe DB. Selecting the appropriate rodent diet for endocrine disruptor research and testing studies. *ILAR*(2004) <https://doi.org/10.1093/ilar.45.4.401>.

4. Brown NM, Setchell KDR. Animal models impacted by phytoestrogens in commercial chow: implications for pathways influenced by hormones. *LabInvest* (2001).
<https://doi.org/10.1038/labinvest.3780282>.
5. Barnard DE, Lewis SM, Teter BB, Thigpen JE. Open- and Closed-Formula Laboratory Animal Diets and Their Importance to Research. *J Am Assoc Lab Anim Sci*(2009).
<https://doi.org/10.1038/labinvest.3780282>.
6. Lai YC, Yew YW. Tofu, urinary phytoestrogens, and melanoma: An analysis of a national database in the United States. *Dermatologica Sinica*. 2015 1;33(4):210–4.
<https://doi.org/10.1016/j.dsi.2015.05.003>.
7. Thomas C, Gustafsson JÅ. The different roles of ER subtypes in cancer biology and therapy. *Nature Review Cancer* 2011.
<https://doi.org/10.1038/nrc3093>.
8. Marzagalli M, Marelli MM, Casati L, Fontana F, Moretti RM, Limonta P. Estrogen Receptor β in Melanoma: From Molecular Insights to Potential Clinical Utility. *Front Endocrinol (Lausanne)* .2016
<https://doi.org/10.3389/fendo.2016.00140>.
9. de Giorgi V, Mavilia C, Massi D, Sestini S, Grazzini M, Brandi ML, et al. The role of estrogens in melanoma and skin cancer. *Carcinogenesis*2009.
<https://doi.org/10.1093/carcin/bgp025>.
10. De Giorgi V, Mavilia C, Massi D, Gozzini A, Aragona P, Tanini A, et al. Estrogen receptor expression in cutaneous melanoma: a real-time reverse transcriptase-polymerase chain reaction and immunohistochemical study. *Arch Dermatol* 2009.
<https://doi.org/10.1001/archdermatol.2008.537>.
11. Janik ME, Belkot K, Przybylo M. Is oestrogen an important player in melanoma progression? *Contemp Oncol (Pozn)* 2014
<https://doi.org/10.5114/wo.2014.43938>.
12. Warner M, Gustafsson JÅ. The role of estrogen receptor beta (ERbeta) in malignant diseases--a new potential target for antiproliferative drugs in prevention and treatment of cancer. *Biochemical and Biophysical Research Communications* 2010.
<https://doi.org/10.1016/j.bbrc.2010.02.144>.
13. AV S, AH H. Phytoestrogens and their effects *European Journal of Pharmacology*2014.
<https://doi.org/10.1016/j.ejphar.2014.07.057>.
14. Thigpen JE, Setchell KD, Ahlmark KB, Locklear J, Spahr T, Caviness GF, et al. Phytoestrogen content of purified, open- and closed-formula laboratory animal diets. *Laboratory Animal Science*. 1999.
15. Desmawati D, Sulastri D. Phytoestrogens and Their Health Effect. *Open Access Maced J Med Sci* 2019.
16. Patisaul HB, Jefferson W. The pros and cons of phytoestrogens. *Front Neuroendocrinol* 2010.
17. Thigpen JE, Haseman JK, Saunders H, Locklear J, Caviness G, Grant M, et al. Dietary factors affecting uterine weights of immature CD-1 mice used in uterotrophic bioassays. *Cancer Detect Prev* 2002.
18. Thigpen JE, Haseman JK, Saunders HE, Setchell KDR, Grant MG, Forsythe DB. Dietary phytoestrogens accelerate the time of vaginal opening in immature CD-1 mice. *Comp Med*. 2003 Dec;53(6):607–15.
19. Thigpen JE, Setchell KDR, Padilla-Banks E, Haseman JK, Saunders HE, Caviness GF, et al. Variations in phytoestrogen content between different mill dates of the same diet produces significant differences in the time of vaginal opening in CD-1 mice and F344 rats but not in CD Sprague-Dawley rats. *Environ Health Perspect* 2007.
20. Liu C, Reger M, Fan H, Wang J, Zhang J. Dietary intake of isoflavones and coumestrol and risk of pancreatic cancer in

the prostate, lung, colorectal, and ovarian cancer screening trial. *Br J Cancer* 2025.

21. Hedelin M, Lö M, Andersson TML, Adlercreutz H, Weiderpass E. Dietary phytoestrogens and the risk of ovarian cancer in the women's lifestyle and health cohort study. *Cancer Epidemiol Biomarkers Prev.* 2011.

22. Bilir B, Sharma N V., Lee J, Hammarstrom B, Svindland A, Kucuk O, et al. Effects of genistein supplementation on genome wide DNA methylation and gene expression in patients with localized prostate cancer. *Int J Oncol* 2017.

23. Shike M, Doane AS, Russo L, Cabal R, Reis-Filho JS, Gerald W, et al. The effects of soy supplementation on gene expression in breast cancer: a randomized placebo-controlled study. *J Natl Cancer Inst* 2014.

24. Dika E, Patrizi A, Lambertini M, Manuelpillai N, Fiorentino M, Altimari A, et al. Estrogen Receptors and Melanoma: A Review. *Cells* 2019.

25. Galgani M, De Rosa V, La Cava A, Matarese G. Role of Metabolism in the Immunobiology of Regulatory T Cells. *J Immunology* 2016.

26. Chaudhary B, Elkord E. Regulatory T Cells in the Tumor Microenvironment and Cancer Progression: Role and Therapeutic Targeting. *Vaccines (Basel)* 2016.

27. Nishikawa H, Sakaguchi S. Regulatory T cells in cancer immunotherapy. *Curr Opin Immunol* 2014.

28. Chaudhary B, Khaled YS, Ammori BJ, Elkord E. Neuropilin 1: function and therapeutic potential in cancer. *Cancer Immunol Immunother* 2014.

29. DeLeeuw RJ, Kost SE, Kakal JA, Nelson BH. The prognostic value of FoxP3+ tumor-infiltrating lymphocytes in cancer: a critical review of the literature. *Clin Cancer* 2012.

30. Shang B, Liu Y, Jiang SJ, Liu Y. Prognostic

value of tumor-infiltrating FoxP3+ regulatory T cells in cancers: a systematic review and meta-analysis. *Sci Rep* 2015.

31. Overwijk WW, Restifo NP. B16 as a mouse model for human melanoma. *Curr Protoc Immunol* 2001.

32. Dagdemir A, Durif J, Ngollo M, Bignon YJ, Bernard-Gallon D. Histone lysine trimethylation or acetylation can be modulated by phytoestrogen, estrogen or anti-HDAC in breast cancer cell lines. *Epigenomics* 2013.

33. Rice S, Whitehead SA. Phytoestrogens and breast cancer--promoters or protectors? *Endocr RelatCancer*2006.

34. Jensen MN, Ritskes-Hoitinga M. How isoflavone levels in common rodent diets can interfere with the value of animal models and with experimental results. *Lab Anim* 2007.

35. Roh MR, Eliades P, Gupta S, Grant-Kels JM, Tsao H. Cutaneous melanoma in women. *Int J Womens Dermatol* 2017.

36. Wilkinson HN, Hardman MJ. The role of estrogen in cutaneous ageing and repair. *Maturitas* 2017.

37. Ju YH, Doerge DR, Allred KF, Allred CD, Helferich WG. Dietary genistein negates the inhibitory effect of tamoxifen on growth of estrogen-dependent human breast cancer (MCF-7) cells implanted in athymic mice. *Cancer Res.* 2002 May 1;62(9):2474–7.

38. Allred CD, Allred KF, Ju YH, Goeppinger TS, Doerge DR, Helferich WG. Soy processing influences growth of estrogen-dependent breast cancer tumors. *Carcinogenesis* 2004.

39. Li B, Ding J, Larson A, Song S. Tumor tissue recycling--a new combination treatment for solid tumors: experimental and preliminary clinical research. *In Vivo.* 1999;13(5):433–8.

40. Farina HG, Pomies M, Alonso DF, Gomez DE. Antitumor and antiangiogenic activity of soy isoflavone genistein in mouse models

- melanoma and breast cancer. *Oncol Rep* 2006 tumors: experimental and preliminary clinical research. *In Vivo*. 1999;13(5):433–8.
41. Tai P, Wang J, Jin H, Song X, Yan J, Kang Y, et al. Induction of regulatory T cells by physiological level estrogen. *J Cell Physiol* 2008.
 42. Polanczyk MJ, Carson BD, Subramanian S, Afentoulis M, Vandenbark AA, Ziegler SF, et al. Cutting Edge: Estrogen Drives Expansion of the CD4+CD25+ Regulatory T Cell Compartment. *The Journal of Immunology*, 2004.
<https://doi.org/10.4049/jimmunol.173.4.2227>.
 43. Fontenot JD, Gavin MA, Rudensky AY. Foxp3 programs the development and function of CD4+CD25+ regulatory T cells. *Nature Immunology* 2003.
<https://doi.org/10.1038/ni904>
 44. Morito K, Hirose T, Kinjo J, Hirakawa T, Okawa M, Nohara T, et al. Interaction of phytoestrogens with estrogen receptors alpha and beta. *Biological and Pharmaceutical Bulletin* 2001.
<https://doi.org/10.1248/bpb.24.35144>.
 45. Ohata C, Tadokoro T, Itami S. Expression of estrogen receptor beta in normal skin, melanocytic nevi and malignant melanomas. *Journal of Dermatology*. 2008.
<https://doi.org/10.1111/j.13468138.2008.00447>.
 46. Topi G, Satapathy SR, Dash P, Fred Mehrabi S, Ehrnström R, Olsson R, et al. Tumour-suppressive effect of oestrogen receptor β in colorectal cancer patients, colon cancer cells, and a zebrafish model. *Journal of Pathology* 2020. <https://doi.org/10.1002/path.5453>
 47. Yuan B, Cheng L, Gupta K, Chiang HC, Gupta HB, Sareddy GR, et al. Tyrosine phosphorylation regulates ER β ubiquitination, protein turnover, and inhibition of breast cancer. *Oncotarget*. 2016.
<https://doi.org/10.18632/oncotarget.10018>
 48. Torrens-Mas M, Roca P. Phytoestrogens for Cancer Prevention and Treatment. *Biology (Basel)*. 2020
<https://doi.org/10.3390/biology9120427>
 49. Messina M, Nechuta S. A Review of the Clinical and Epidemiologic Evidence Relevant to the Impact of Postdiagnosis Isoflavone Intake on Breast Cancer Outcomes. *Current Nutrition Reports* 2025
<https://doi.org/10.1007/s13668-025-00640-5>
<https://orcid.org/10.1007/s13668-025-00640-5>.
 50. Chakraborty B, Byemerwa J, Krebs T, Lim F, Chang CY, McDonnell DP. Estrogen Receptor Signaling in the Immune System. *Endocrine Reviews*. 2023.
<https://doi.org/10.1210/endrev/bnac017>.

الغذاء الغني بالفيتواستروجين يزيد من حجم الورام وزيادة في معدلات الخلايا تي التنظيمية الدوارة في نموذج ورم الميلانوما الفاري B16F10

^١ رفاه عدي حسين، ^٢ لي ريتشارد ماشادو

المخلص

الخلفية: تُظهر الدراسات السريرية ارتباطاً وثيقاً بين مستويات الهرمونات، وخاصة الإستروجين، وتطور سرطانات الجلد. يُعتبر الورم الميلانيني الجلدي (Cutaneous melanoma) من الأورام المرتبطة بالهرمونات؛ ومع ذلك لا تزال أدوارها في تطو سرطان الجلد لا يزال غير واضح لحد الآن.

الأهداف: هو التحقق من تأثير النظام الغذائي الغني بالفيتواستروجينات على بدء وتطور الورم الميلانيني باستخدام نموذج الفئران المتماثلة جينياً (syngeneic mouse model).

المرضى والطرق: تم تغذية الفئران إما بنظام غذائي غني بالفيتواستروجينات أو نظام غذائي منخفض (وتم حقنها تحت الجلد بـ ١٠٥ × ٥ خلايا ميلانوما متماثلة جينياً B16-F10) وبعد ١٠-١٢ أسبوعاً، تم جمع الأورام والطحال. تم قياس حجم ووزن الأورام، كما أُجري تفاعل البوليميرز المتسلسل الكمي (qPCR) لتحليل تعبير مستقبلات الإستروجين (ER) α و β وتم تقييم الخلايا التائية التنظيمية (Tregs) من خلايا الطحال باستخدام قياس التدفق الخلوي (flow cytometry).

النتائج: أظهرت الفئران التي استهلكت النظام الغذائي الغني بالفيتواستروجينات أوراماً أكبر حجماً مقارنةً بتلك التي تغذت على النظام الغذائي المراقب. أدت الفيتواستروجينات في النظام الغذائي إلى زيادة تعبير مستقبل الإستروجين ER β وخفض تعبير ER α في أنسجة الورم. كما لوحظت زيادة كبيرة في نسبة الخلايا التائية التنظيمية (Tregs) في الطحال لدى الفئران الحاملة للأورام التي استهلكت النظام الغذائي الغني بالفيتواستروجينات.

الاستنتاج: تسلط هذه الدراسة الضوء على أهمية تأثير مكونات النظام الغذائية على نمو الورام والاستجابة المناعية المرتبطة به، وتؤكد على الحاجة إلى مراعاة تركيبة النظام الغذائية عند تصميم التجارب لما لها من تأثير محتمل على بيولوجيا الورم.

الكلمات المفتاحية: الاستروجين النباتي، الخلايا التنظيمية التائية، أورام الميلانوما لدى الفئران، قياس التدفق الخلوي.

المؤلف المراسل: رفاه عدي حسين

الايمل: rafah.oday@mtu.edu.iq

تاريخ الاستلام: ٢٧ كانون الثاني ٢٠٢٥





تاريخ القبول: ٥ نيسان ٢٠٢٥

تاريخ النشر: ٢٥ نيسان ٢٠٢٥

^١ المعهد التقني بعقوبة - الجامعة التقنية الوسطى - ديالى - العراق.

^٢ مركز النشاط البدني وعلوم الحياة - جامعة نورثامبتون - نورثامبتون - المملكة المتحدة.

Assessing the Appropriateness of Three-Dimensional Conformal Radiotherapy Technique Planning Treatment for Rectal Versus Cervical Cancer: A Comparative Study

Ruaa Emad Al-Khalidi ¹, Nashwan Karkhi Abdulkareem ², Arthur Saniotis ³, Rojgar Najat Yousif ⁴

^{1,2} Department of pharmacology and medical physics and clinical biochemistry, college of medicine, Hawler Medical University, Erbil, Iraq.

³ School of Biomedicine, Faculty of Health and Medical Sciences, The University of Adelaide, South Australia, Australia.

⁴ Department of plan and dosimetry, Awat Radiation Oncology Center, Erbil, Iraq.

OPEN ACCESS

Correspondence: Ruaa Emad Al-Khalidi
Email: ruaa.hussien@hmu.edu.krd
Copyright: ©Authors, 2025, College of Medicine, University of Diyala. This is an open access article under the [CC BY 4.0](http://creativecommons.org/licenses/by/4.0/) license (<http://creativecommons.org/licenses/by/4.0/>)
Website: <https://djm.uodiyala.edu.iq/index.php/djm>

Received: 10 October 2024
Accepted: 08 January 2025
Published: 25 April 2025

Abstract

Background: Radiotherapy is an important part of the treatment paradigm for many patients with rectal and cervical malignancies. With the development of more powerful 3D conformal treatment planning tools, the clinical application of three-dimensional conformal radiation therapy (3D-CRT) has gained recognition for its potential to enhance treatment results for these patients.

Objective: To assess which cancer type benefits more from the (3D-CRT) technique by comparing its effectiveness for rectal and cervical cancer, with a focus on dosimetric outcomes.

Patients and Methods: A retrospective analysis conducted from August 2023 to January 2024 assessed ten cases of rectal cancer and ten cases of cervical cancer, who treated with 3D-CRT technique at Awat Radiation Oncology Center (AROC), Erbil. Many dosimetric parameters, including mean dose (Dmean), minimum dose (Dmin), maximum dose (Dmax), target volume coverage (D95%), homogeneity index HI, conformity index CI, and the dose that is received by the organ at risk, have been evaluated in order to determine the efficacy of 3D-CRT technique for both cancers.

Results: Rectal cancer showed higher conformity and homogeneity index in the PTV int_sum phase (0.87 ± 0.05), (0.16 ± 0.02) compared to cervical cancer (0.66 ± 0.21), (0.19 ± 0.01), indicating better alignment of prescribed dose with target volume and more consistent dose distribution within the target volume. For organs small bowel ($V45 < 195\text{cc}$) and bladder ($V45 < 50\%$), rectal cancer exhibits very high significantly superior sparing in comparison to cervical cancer, displaying lower average volumes and percentages of these organs receiving 45 Gy ($p < 0.001$ for both).

Conclusion: The investigation demonstrated that 3D-CRT offered better target coverage, dose homogeneity, and conformity for rectal cancer. Plans for rectal cancer also showed improved bladder and rectum sparing.

Keywords: Rectal cancer, Cervix cancer, Homogeneity index (HI), Conformity index (CI).

Introduction

Rectal cancer is a significant oncological health issue. It would be the third leading cause of

mortality in the world due to oncological diseases. For radiotherapy treatment, it is crucial to rely on optimization techniques that can treat the target volume while also minimizing the amount of dosage that reaches the organs at risk (OARs) (1-2). Cervical cancer (CaCx) is a prevalent malignancy in women, affecting over 500,000 globally. Annually, 233,000 women die, primarily in poor nations. Treatment mainly involves external beam radiation and intravital brachytherapy for locally advanced cases (3). Radiotherapy has an established role in the curative treatment of rectal and cervical cancers (4). Choosing the right radiotherapy technique for rectal and cervical cancers is crucial. Different techniques, such as 3D-CRT, Intensity-modulated radiation therapy (IMRT), or Volumetric modulated arc therapy (VMAT), can improve tumor coverage and reduce the risk of recurrence. Careful selection of methods also helps spare critical organs-at-risk, reducing side effects. Personalized strategies enhance patient quality of life and treatment success rates (5). Three-dimensional conformal radiotherapy (3D-CRT) uses 3D anatomic information to provide an appropriate dosage to tumors and healthy tissue. Delivering high doses of ionizing radiation to the target volume and minimum doses to the OARs. And uses for treat both rectal and cervical cancers (6). Despite the widespread use of 3D-CRT for both cancer types, there is limited research directly comparing its effectiveness between rectal and cervical cancers. Understanding the dosimetric differences is critical, as anatomical and physiological variations can significantly impact treatment outcomes. This study addresses this gap by examining dose coverage,

conformity, homogeneity, and organ-at-risk sparing, providing insights into the suitability of 3D-CRT for these two distinct malignancies. This study aims to assess and compare the dosimetric results of the 3D-CRT technique for

rectal and cervical cancers, intending to identify the more appropriate cancer type for this treatment technique.

Patients and Methods

Patients' selection: In this study, 20 patients with two different types of cancer were included: 10 cases of rectal cancer, with a mean age of 52.6 years, six female patients (60%) and four male patients (40%); and 10 cases of cervical cancer, with a mean age of 59.2 years, all of them were female as shown in Table 1. They were treated with the 3D-CRT technique at the Awat Radiation Oncology Center, in Erbil from August 2023 to January 2024.

Table 1. Patient characteristics.

Characteristics	Rectal Cancer (n=10)	Cervical Cancer (n=10)
Mean age (years)	52.6 (35-85)	59.2 (67-55)
Sex:		
Male	4 (40%)	-
Female	6 (60%)	10(100%)

CT simulation: Each patient will receive radiation therapy imaging using a CT scan with a 2–5 mm slice separation according to the size, type, and location of the tumor. They all scanned in the headfirst orientation in the supine position with an (A) headrest. The arms were either on the chest or raised up. All patients were breathing freely during the scan with an empty rectum and no contrast. We followed the bladder protocol, and patients were asked to drink 4-5 glasses of water to ensure a full bladder, which helps keep the bowel from moving into the pelvis. The isocenter location was in the middle of the pelvis, and the scan started from the upper abdomen to the mid-thigh for all patients. The image sets will be transferred to the Monaco treatment planning system version 5.51.02 for contouring and planning.

Target volumes and OARs contour: The

radiation oncologist outlined the target volumes and OARs. Target volume includes gross target volume (GTV), clinical target volume (CTV), and planning target volume (PTV). The organs at risk were the small bowel, bladder, and right and left femoral heads for both rectal and cervical cancers as shown in figure 1 and 2, respectively. Contouring for rectal cancer, the GTV was defined as all gross disease; the CTV includes the GTV with a minimum of 1.5–2 cm superior and inferior margin as well as the entire rectum, mesorectum, and presacral space and internal iliac and obturator lymph node. The PTV includes the CTV + 5mm (7). In the cases of cervical cancers, the GTV is also defined as all gross tumors; the CTV consists of the common, external, and internal iliac and presacral lymph nodes with a 7 mm margin around the vessels and any additional visible lymph nodes, lymphoceles, or pertinent surgical clips, and the PTV initial (PTVinit.) included CTV + 7 mm, and the PTVboost included CTV, vaginal cuff + parametrium (8).

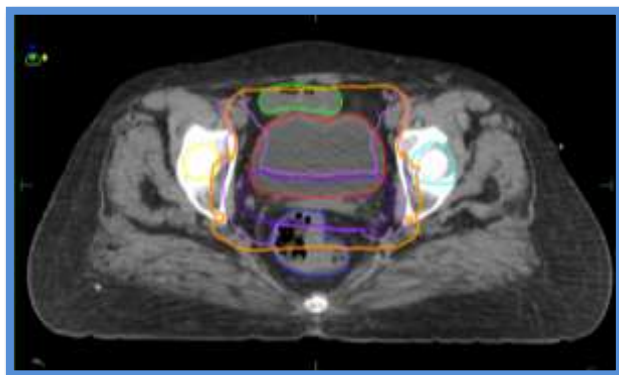


Figure 1. Axial image for patient with rectal cancer in AROC, bladder (red), small bowel (green), LFH (light blue), RFH (yellow), PTVinit.45Gy (pink), PTV boost 5.4Gy (purple), rectum (dark blue).

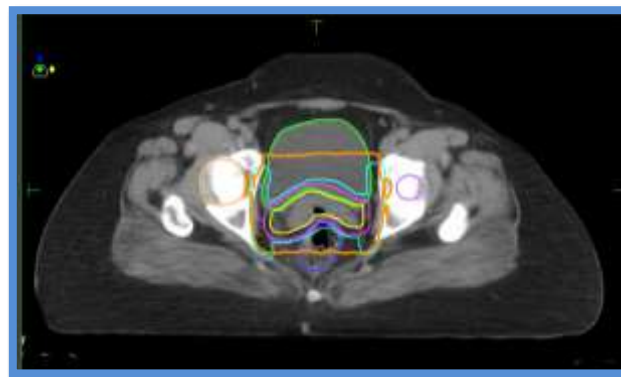


Figure 2. Axial image for patient with cervical cancer in AROC, bladder (green), LFH (dark purple), RFH (orange), PTV inti. 45Gy (turquoise), PTVboost 5.4Gy (pink), CTV (yellow), rectum (dark blue).

Treatment planning: For both rectal and cervical cancers, the prescribed dose was 1.8 Gy/fraction to 45Gy for the PTVinit. and 1.8 Gy/fraction to 5.4Gy for the PTV boost, which received a cumulative dose of 50.4 Gy. 3D-CRT plans were developed using Elekta's Monaco treatment planning system (TPS), which can accurately calculate 3D-CRT, IMRT, VMAT, SRS, and Brachytherapy plans using advanced algorithms such as Monte Carlo algorithm (the most accurate dose calculation available), pencil beam, and collapsed cone. Each of the 3D-CRT plans employs an isocentric technique and contained four photon beams: posteroanterior (PA), anteroposterior (AP), and two opposing lateral fields as shown in figure 3, with varying gantry angles (0°, 90°, 180°, and 270°), utilizing 10 MV of energy, provided by an Elekta infinity linear accelerator machine. To accomplish a consistent dose distribution and meet clinical objectives.

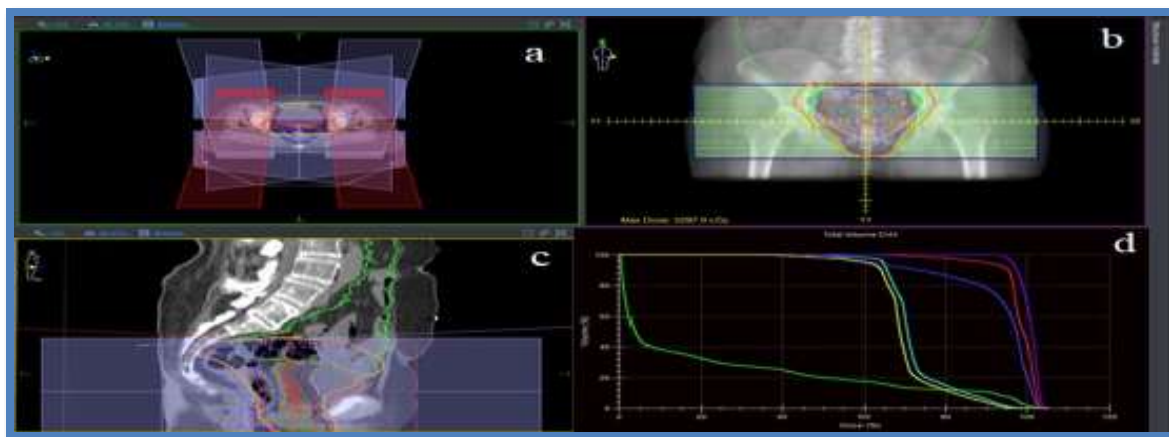


Figure 3. Screenshot for a treatment plan with 4 beams: PA, AP, and two opposing lateral fields, with three views: a: axial, b: coronal, c: sagittal, and d: the Dose-Volume Histograms (DVH) for patient with rectal cancer at AROC.

Plan evaluation: A distinction was made between the global plan, comprising the sum of both phases, and the results corresponding to each phase. PTV int._sum and PTV boost_sum is the same as PTV int. and PTV boost. The phrase "_sum" indicates that the related evaluated parameters (Dmean, Dmax, Dmin, HI, CI, D98%, and D2%) of each of them apply to the sum plan rather than the separate phase plans. The parameters of the individual phase plans have specifications for PTV int. and PTV boost. Plans were compared using the Dose-Volume Histograms (DVHs). For the PTV, the following data were analyzed: Dmean, Dmax, Dmin, D95%, The 95% of the prescribed dose of the PTV is helps to evaluate the dosimetry plans. The goal of the dosimetry plan is to cover at least 95% of the PTV (V95%) with 95% of the prescribed dose. A Homogeneity Index (HI) is a fast and easy-to-use scoring tool used to assess and quantify dose homogeneity in a target volume. The formula used in this study to calculate HI was suggested by ICRU-83 (9).

$$HI = \frac{D_{2\%} - D_{98\%}}{D_P}$$

Where, D2% denotes the maximum dose that will be delivered to 2% of the PTV, Dp denotes the prescribed dose for the PTV, and D98%

denotes the minimum dose calculated for the remaining 98% of the PTV. Conformity index (CI) is defined as the ratio of dosage volumes covered to PTV volume. In the present study, we use the following equation to calculate CI (9):

$$CI = \frac{\text{volume covered by 95\% of prescribed dose}}{\text{volume of PTV}}$$

The small bowel, bladder, and femoral heads were the OARs examined in this study. The OAR doses were evaluated on the global plan and compared with the constraints in QUANTIC and RTOG protocols (10). The constraint doses for small bowel, bladder, and right and left femoral heads were $V_{45} < 195$ cc, $V_{45} < 50\%$, and $V_{45} < 15\%$, respectively, for both types of cancer.

Statistical analysis

Data entry and analysis were conducted using the Statistical Package for Social Sciences (SPSS) version 26. Two approaches were used: in the first approach the descriptive statistics to calculate frequencies and percentages. While in the second approach: we used an independent t-test for normally distributed groups and a Mann-Whitney test for non-normally distributed data. A P-value ≤ 0.05 is regarded as statistically

significant. Shapiro's test is used to assess the normality of the data.

Results

Dosimetric parameters for PTV: The study revealed significant variations in dosimetric parameters between rectal cancer and cervical cancer as shown in Table 2. Rectal cancer demonstrated a notably higher minimum dose Dmin to the PTV int_sum (4040 ± 213.43 cGy) compared to cervical cancer (3496.68 ± 213.81 cGy), with a p-value of <0.001 , indicating superior coverage. However, the minimum dose for the PTV boost_sum did not differ significantly between rectal cancer (4577.49 ± 190.13 cGy) and cervical cancer (4410.20 ± 262.85 cGy, $p = 0.09$). The Dmax of the PTV int_sum was not significantly different between rectal cancer (5339.51 ± 49.24 cGy) and cervical cancer (5311.89 ± 39.94 cGy, $p = 0.18$), but rectal

cancer had a very high significant maximum dose for the PTV boost_sum (5353.75 ± 30.11 cGy) compared to cervical cancer (5312.75 ± 9.76 cGy, $p < 0.001$). Additionally, the mean dose Dmean to the PTV int_sum was slightly higher in rectal cancer (5025.26 ± 100.33 cGy) than cervical cancer (4907 ± 148.80 cGy, $p = 0.05$), and similar results were observed for the PTV boost. Rectal cancer also had a very high significant D95% dose for the PTV int_sum (4539.72 ± 165.76 cGy) compared to cervical cancer (4315.18 ± 103.28 cGy, $p = 0.002$), indicating better target coverage in rectal cancer. Conversely, the D95% dose for the PTV boost_sum did not show a significant difference. These results demonstrate that, rectal cancer generally received higher doses and achieved better target coverage.

Table 2. Dosimetric parameters for PTV.

	Rectal Cancer (Mean \pm SD)	Cervical Cancer (Mean \pm SD)	p-value
Dmin for PTV init._sum (cGy)	4040 \pm 213.43	3496.68 \pm 213.81	<0.001
Dmin for PTV boost_sum (cGy)	4577.49 \pm 190.13	4410.20 \pm 262.85	0.09
Dmax for PTV init._sum (cGy)	5339.51 \pm 49.24	5311.89 \pm 39.94	0.18
Dmax for PTV boost_sum (cGy)	5353.75 \pm 30.11	5312.75 \pm 9.76	<0.001
Dmean for PTV init._sum (cGy)	5025.26 \pm 100.33	4907 \pm 148.80	0.05
Dmean for PTVboost_sum (cGy)	5167.150 \pm 53.45	5114.55 \pm 54.04	0.04
D95% for PTVinit._sum (cGy)	4539.72 \pm 165.76	4315.18 \pm 103.28	0.002
D95% for PTVboost_ sum (cGy)	5068.87 \pm 195.04	5010.82 \pm 186.73	0.50

Physical Indices: There were marked variations in dose homogeneity and conformity between rectal cancer and cervical cancer as shown in Table 3. In the PTV inti. sum phase, rectal cancer exhibited significantly higher conformity (0.87 ± 0.05).

compared to cervical cancer (0.66 ± 0.21) with a p-value of 0.01, indicating better alignment of the prescribed dose with the target volume for rectal cancer. When it

comes to the PTV boost_sum phase, the conformity index was very high significantly between rectal cancer (0.98 ± 0.01) and cervical cancer (0.97 ± 0.05), with ($p = 0.008$). As for the homogeneity index, which measures the uniformity of dose distribution within the target volume, rectal cancer also displayed superior dose homogeneity in the PTV int_sum phase (0.16 ± 0.02) compared to cervical cancer (0.19 ± 0.01), with a p-value of 0.003, indicating a more consistent dose distribution for rectal cancer. In the PTV boost_sum phase,

both rectal cancer and cervical cancer had similar homogeneity indices (0.086 ± 0.02 and 0.085 ± 0.01 , respectively), with no significant difference ($p = 0.89$). These findings suggest that rectal cancer generally achieved better dose conformity and homogeneity, particularly in the initial phase, which could have implications for optimizing treatment precision and minimizing exposure to surrounding healthy tissues.

Table 3. Homogeneity index (HI) and conformity index (CI).

	Rectal Cancer (Mean \pm SD)	Cervical Cancer (Mean \pm SD)	p-value
CI for PTV int_sum	0.87 ± 0.05	0.66 ± 0.21	0.01
CI for PTV boost_sum	0.98 ± 0.01	0.97 ± 0.05	0.008
HI for PTV int_sum	0.16 ± 0.02	0.19 ± 0.01	0.003
HI for PTV boost_sum	0.086 ± 0.02	0.085 ± 0.01	0.89

Organ at risk: The comparison of organ sparing between rectal cancer and cervical cancer shows notable differences for certain organs as shown in Table (4) and Figure (4). For the organs small bowel ($V_{45} < 195$ cc) and bladder ($V_{45} < 50\%$), rectal cancer exhibits very high significantly superior sparing (120.15 ± 36.16 and 65.84 ± 13.31 , respectively) in comparison to cervical cancer (197.87 ± 7.70 and 36.55 ± 12.52 , respectively), displaying lower average volumes

and percentages of these organs receiving 45 Gy ($p < 0.001$). However, for organs RFH and LFH (both $V_{45} < 15\%$), there are no statistically significant differences in sparing between rectal cancer and cervical cancer ($p = 0.40$ and $p = 0.96$, respectively). These results imply potential variations in treatment planning or tumor characteristics that impact organ sparing for different cancer types.

Table 4. Organ at risk (OAR) sparing.

OAR	Rectal Cancer			Cervical Cancer			Mann-Whitney U	Z	p-value
	Mean \pm SD	Median	Mean rank	Mean \pm SD	Median	Mean rank			
SB, $V_{45}(\text{cc})$	120.15 ± 36.16	-	-	197.87 ± 7.70	-	-	-	-	< 0.001
Bladder, $V_{45}(\%)$	36.55 ± 12.52	-	-	65.84 ± 13.31	-	-	-	-	< 0.001
RFH, $V_{45}(\%)$	0.28 ± 0.50	0	11.40	0.32 ± 0.99	0	9.60	41	0.839	0.40*
LFH, $V_{45}(\%)$	1.33 ± 1.99	0.39	10.45	2.22 ± 2.49	1.10	10.55	49	0.039	0.96*

*Mann-Whitney U test

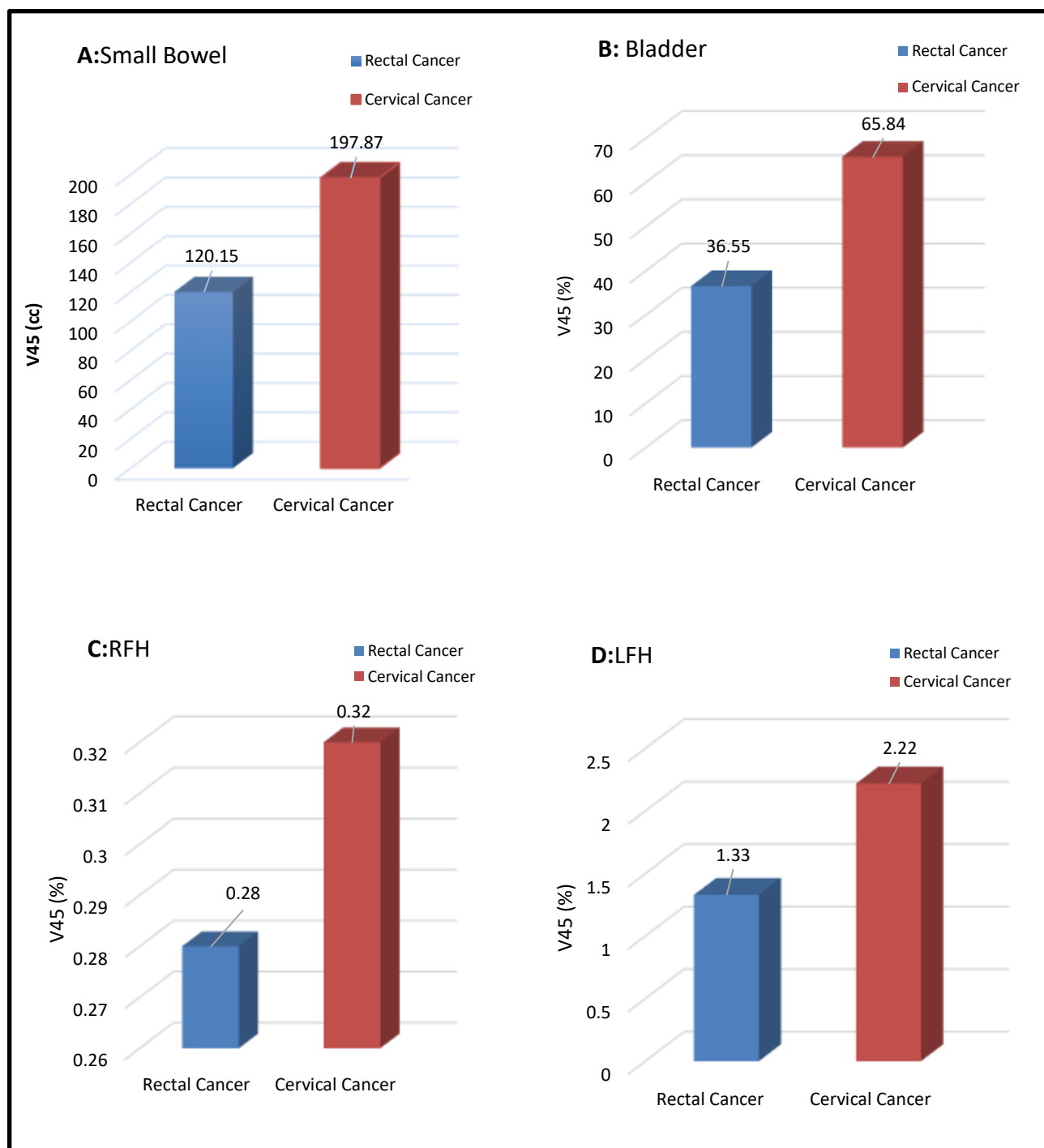


Figure 4. Bar graphs of (A) a comparison of the small bowel volume received 45Gy for rectum and cervical cancer, (B) a comparison of the bladder volume % received 45Gy for rectum and cervical cancer, (C) a comparison of the RFH volume % received 45Gy for rectum and cervical cancer, (D) a comparison of the LFH volume % received 45Gy for rectum and cervical cancer.

Discussion

The results of the study show that 3D-CRT technique, is usually more effective for rectal cancer than cervical cancer in regards to dose coverage (D95%), homogeneity index (HI), conformity index (CI), and sparing of organs at risk (OARs). This study shows that, in comparison to cervical cancer, rectal cancer has a better dose coverage (D95%) with 3D-CRT treatment. This is primarily because of the rectum's anatomical stability. These results align with previous studies. For example, a study conducted in 2016 by Simson DK et al. (11) demonstrated that 3D-CRT offers sufficient dose coverage for rectal cancer and that most patients achieve favorable D95% results because of the relatively fixed position of the rectum within the pelvis. Conversely, studies on cervical cancer by Urban R et al. (2022) (12) supported our findings that D95% outcomes are less consistent for cervical cancer by demonstrating difficulties in achieving optimal D95% with 3D-CRT due to the cervix's variable position and movement caused by bladder and bowel filling. The results of this study, which show that the CI and HI are more advantageous for rectal cancer than for cervical cancer when utilizing 3D-CRT, are consistent with earlier research. For rectal cancer, Jun Zhao et al. (2016) (13) found that 3D-CRT could achieve satisfactory CI and HI due to the simpler geometry and fewer variations in target position. On the other hand, Zeng et al. (2024) (14) found that in the case of cervical cancer, the uneven form of the cervix and the mobility of surrounding organs typically result in inadequate CI and HI after 3D-CRT, necessitating the employment of more sophisticated techniques like IMRT to improve these

indices. This confirms the finding that these anatomical difficulties may make 3D-CRT less effective for cervical cancer. Regarding OAR sparing, this study indicates that 3D-CRT is more appropriate for rectal cancer than for cervical cancer in terms of OAR sparing. In rectal cancer, the results of other studies, like those by Georgios Kouklidis et al. (2023) (15), which showed that 3D-CRT enables better organ sparing of nearby organs, like the small bowel and bladder, because the tumor is more localized and there is less overlap with critical structures, are consistent with this finding. While those in cervix cancer this technique couldn't protect the small bowel, due to the specific shape of the pelvic floor and iliac lymph node. After a hysterectomy, a significant portion of the small bowel is situated in the pelvic space, leading to a larger volume of intestine receiving a high dose (16). The study results indicate that the average small bowel volume for patients with cervical cancer exceeded the tolerance dose. Therefore, it's crucial to minimize the dose to the small bowel to prevent gastrointestinal toxicity. According to Minsky et al. (1995) (16), there is a strong correlation between gastrointestinal toxicity and the volume of irradiated small bowel. However, because of the close proximity of the bladder and bowel to the cervix, several studies including one by Lv Y et al. (2014) (17) have demonstrated that OAR sparing is more difficult with 3D-CRT for cervical cancer. This results in higher rates of toxicity when these organs unintentionally receive radiation. The 3D-CRT technique is effective in protecting the bladder from high doses in patients with rectal cancer, while for patients with cervical cancer, it was ineffective. For the bladder in cervical cancer, our results cast a new light on the results for the patients who were treated with PD 50.4 Gy. All the percentage patients' bladder volumes were above the tolerance volume, the mean \pm SD of the volume that receive 45Gy for cervical was 65.84 ± 13.31 . And that is mean the 3D-CRT technique cannot protect the bladder from

the high dose in cervical cancers. However, when comparing our results to those of older studies, the findings are directly in line with Lv Y et al.(2014) (17) the mean for V45(%) were 65.48, which was more than 50%.

Conclusions

This study demonstrates that 3D-CRT is generally more effective for treating rectal cancer compared to cervical cancer due to differences in anatomical structure, tumor positioning, and organ stability. Rectal cancer showed superior dose coverage (D95%), homogeneity index (HI), and conformity index (CI), as well as better sparing of organs at risk (OARs). Conversely, the mobility and variable position of the cervix and adjacent organs, such as the bladder and bowel, present significant challenges for achieving optimal outcomes in cervical cancer treatment with 3D-CRT.

Recommendations

Given the limitations observed in 3D-CRT for cervical cancer, it is recommended that further research explore alternative radiotherapy techniques to determine whether they offer superior outcomes, particularly in terms of organ sparing and dose homogeneity.

Source of funding: No source of funding.

Ethical clearance: The study was approved by the Ethical Committee of Hawler Medical University / college of medicine (KR, meeting code:1, paper code:1, date: 22/9/2024).

Conflict of interest: None.

Acknowledgements:

We would like to express our sincere gratitude to all those who contributed to the completion of this research. Our heartfelt thanks go to our colleagues and mentors for their continuous support, and to the Hawler Medical University / college of medicine.

References

1. AlQudah M, Salmo E, Haboubi N. The effect of radiotherapy on rectal cancer: a histopathological appraisal and prognostic indicators. *Radiat Oncol J*. 2020 Jun;38(2):77–83.
<https://doi.org/10.3857/roj.2020.00010>
2. Motib MS, Mustaf AHMH, Alrubaye MFA, Al-Hamami HAJ. Influence of lymphovascular invasion on outcome of colon cancer. *Diyala Journal of Medicine*. 2024 Oct 25;27(1):25–34.
<https://doi.org/10.26505/djm.v27i1.1139>
3. Elnaggar M, Motaweh HA, Zard K. Comparative Study of Dose Distribution Homogeneity between 3D-Brachytherapy and Intensity Modulated Radiation Therapy Techniques in Cervix Cancer Tumors. *Int J Med Phys Clin Eng Radiat Oncol*. 2019 Aug 14;8(3):163–74.
<https://doi.org/10.4236/ijmpcero.2019.83015>
4. Al-Maliki SAK, Musstaf AH, Al-Haidary YAD. Comparative Study of Cardiac Radiation Dose With Different Types of Surgery in Breast Cancer Patients. *djm*. 2024 Dec 25;27(2):53–64.
<https://doi.org/10.26505/djm.v23i2.956>
5. Raina P, Singh S. Comparison between Three-Dimensional Conformal Radiation Therapy (3DCRT) and Intensity-Modulated Radiation Therapy (IMRT) for Radiotherapy of Cervical Carcinoma: A Heterogeneous Phantom Study. *J Biomed Phys Eng*. 2022 Oct 1;12(5):465–76.
<https://doi.org/10.31661/jbpe.v0i0.2101-1257>
6. Morris DE, Emami B, Mauch PM, Konski AA, Tao ML, Ng AK, et al. Evidence-based review of three-dimensional conformal radiotherapy for localized prostate cancer: An ASTRO outcomes initiative. *Int J Radiat Oncol*. 2005 May;62(1):3–19.
<https://doi.org/10.1016/j.ijrobp.2004.07.666>
7. Myerson RJ, Garofalo MC, Naqa IE, Abrams RA, Apte A, Bosch WR, et al. Elective Clinical Target Volumes for Conformal Therapy in Anorectal Cancer: An RTOG Consensus Panel Contouring Atlas. *Int J Radiat Oncol Biol Phys*. 2009 Jul 1;74(3):824–30.
<https://doi.org/10.1016/j.ijrobp.2008.08.070>
8. Lim K, Small W, Portelance L, Creutzberg C, Jürgenliemk-Schulz IM, Mundt A, et al. Consensus

Guidelines for Delineation of Clinical Target Volume for Intensity-Modulated Pelvic Radiotherapy for the Definitive Treatment of Cervix Cancer. *Int J Radiat Oncol.* 2011 Feb 1;79(2):348–55.

<https://doi.org/10.1016/j.ijrobp.2009.10.075>

9. Özseven A, Elif Özkan E. Dosimetric evaluation of field-in-field and sliding-window IMRT in endometrium cancer patients with a new approach for the conformity index. *Int J Radiat Res.* 2020 Oct 10;18(4):853–62.

<https://doi.org/10.52547/ijrr.18.4.853>

10. Dumen E, Inal A, Segul A, Cecen Y, Yavuz M. Dosimetric comparison of different treatment planning techniques with International Commission on Radiation Units and Measurements Report-83 recommendations in adjuvant pelvic radiotherapy of gynecological malignancies. *J Cancer Res Ther.* 2016; 12(2): 975-980.

<https://doi.org/10.4103/0973-1482.179189>

11. Simson DK, Mitra S, Ahlawat P, Sharma MK, Yadav G, Mishra MB. Dosimetric Comparison between Intensity Modulated Radiotherapy and 3 Dimensional Conformal Radiotherapy in the Treatment of Rectal Cancer. *Asian Pac J Cancer Prev APJCP.* 2016;17(11):4935–7.

<https://doi.org/10.22034/APJCP.2016.17.11.4935>

12. Urban R, Wong J, Lim P, Zhang S, Spadinger I, Olson R, et al. Cervical cancer patient reported gastrointestinal outcomes: intensity/volumetric modulated vs. 3D conformal radiation therapy. *J Gynecol Oncol.* 2022 Jul 7;33(5):e70.

<https://doi.org/10.3802/jgo.2022.33.e70>

13. Zhao J, Hu W, Cai G, Wang J, Xie J, Peng J, et al. Dosimetric comparisons of VMAT, IMRT and 3DCRT for locally advanced rectal cancer with simultaneous integrated boost. *Oncotarget.* 2015 Nov 26;7(5):6345–51.

<https://doi.org/10.18632/oncotarget.6401>

14. Zeng Z, Zhu J, Wang Z, Wang G, Yan J, Zhang F. Pelvic target volume inter-fractional motion during radiotherapy for cervical cancer with daily iterative cone beam computed tomography. *Radiat Oncol Lond Engl.* 2024 Apr 15;19:48.

<https://doi.org/10.1186/s13014-024-02438-1>

15. Kouklidis G, Nikolopoulos M, Ahmed O, Eskander B, Masters B. A Retrospective Comparison of Toxicity, Response and Survival of Intensity-Modulated Radiotherapy Versus Three-Dimensional Conformal Radiation Therapy in the Treatment of Rectal Carcinoma. *Cureus.* 15(11):e48128.

<https://doi.org/10.7759/cureus.48128>

16. Minsky BD, Conti JA, Huang Y, Knopf K. Relationship of acute gastrointestinal toxicity and the volume of irradiated small bowel in patients receiving combined modality therapy for rectal cancer. *J Clin Oncol Off J Am Soc Clin Oncol.* 1995 Jun;13(6):1409–16.

<https://doi.org/10.1200/JCO.1995.13.6.1409>

17. Lv Y, Wang F, Yang L, Sun G. Intensity-modulated whole pelvic radiotherapy provides effective dosimetric outcomes for cervical cancer treatment with lower toxicities. *Cancer Radiother J Soc Francaise Radiother Oncol.* 2014 Dec;18(8):745–52.

<https://doi.org/10.1016/j.canrad.2014.08.005>

تقييم ملائمة تخطيط تقنية العلاج الإشعاعي ثلاثي الأبعاد لعلاج سرطان المستقيم مقابل سرطان عنق الرحم: دراسة مقارنة

^١ رؤى عماد الخالدي، ^٢ نشوان كرخي عبد الكريم، ^٣ آرثر سانيوتيس، ^٤ روزكار نجات يوسف

المخلص

الخلفية: يُعتبر العلاج الإشعاعي جزءاً مهماً من بروتوكول العلاج للعديد من المرضى الذين يعانون من أورام المستقيم وعنق الرحم. ومع تطور أدوات تخطيط العلاج ثلاثية الأبعاد الأكثر قوة، اكتسب تطبيق العلاج الإشعاعي ثلاثي الأبعاد (3D-CRT) اعترافاً بإمكانياته في تحسين نتائج العلاج لهؤلاء المرضى.

الأهداف: لتقييم أي نوع من السرطان يستفيد أكثر من تقنية العلاج الإشعاعي ثلاثي الأبعاد (3D-CRT) من خلال مقارنة فعاليتها بين سرطان المستقيم وسرطان عنق الرحم، مع التركيز على النتائج الجرعية.

المرضى والطرق: تم إجراء تحليل بائر رجعي للفترة من آب ٢٠٢٣ إلى كانون الثاني ٢٠٢٤ لتقييم عشر حالات من سرطان المستقيم وعشر حالات من سرطان عنق الرحم تم علاجهم باستخدام تقنية العلاج الإشعاعي ثلاثي الأبعاد (3D-CRT) في مركز أوات للأورام الإشعاعية (AROC) في أربيل. تم تقييم العديد من معايير الجرعات، بما في ذلك الجرعة المتوسطة (Dmean)، الجرعة الدنيا (Dmin)، الجرعة القصوى (Dmax)، تغطية حجم الهدف (D95%)، مؤشر توزيع الجرعات (HI)، مؤشر مطابقة الجرعة الإشعاعية لشكل الهدف (CI)، والجرعة التي يتلقاها العضو المعرض للخطر، لتحديد فعالية التقنية في كلا النوعين من السرطان.

النتائج: أظهر سرطان المستقيم مؤشر لتوزيع الجرعات و مدى مطابقة الجرعة الإشعاعية لشكل الهدف (PTV) أعلى في مرحلة PTV int_sum (0.87 ± 0.05)، مقارنة بسرطان عنق الرحم (0.66 ± 0.21)، (0.16 ± 0.02) مقارنة بسرطان عنق الرحم (0.19 ± 0.01)، مما يشير إلى تحسين توزيع الجرعة ضمن حجم الهدف وتطابق أفضل بين الجرعة الموصوفة وحجم الهدف. بالنسبة للأعضاء المعرضة للخطر مثل الأمعاء الدقيقة (V45 < 195cm³) والمثانة (V45 < 50%)، أظهر سرطان المستقيم تفضيلاً كبيراً في الحماية مقارنة بسرطان عنق الرحم، مع تسجيل أحجام ومتوسطات أقل بشكل كبير من هذه الأعضاء التي تتلقى 45 Gy، (p < 0.001) لكلتا الحالتين.

الاستنتاج: أظهرت الدراسة أن تقنية العلاج الإشعاعي ثلاثي الأبعاد وفرت تغطية أفضل للهدف وتمثل لتوزيع الجرعات، ومطابقة الجرعة الإشعاعية لشكل الهدف لسرطان المستقيم. كما أظهرت خطط سرطان المستقيم تحسناً في حماية المثانة والمستقيم.

الكلمات المفتاحية: سرطان المستقيم، سرطان عنق الرحم، مؤشر التجانس (HI)، مؤشر المطابقة (CI).

المؤلف المراسل: رؤى عماد الخالدي

الايمل: ruaa.hussien@hmu.edu.krd

تاريخ الاستلام: ١٠ تشرين الأول ٢٠٢٤

تاريخ القبول: ٨ كانون الثاني ٢٠٢٥





تاريخ النشر: ٢٥ نيسان ٢٠٢٥

^{٢٠١} قسم الأدوية والفيزياء الطبية والكيمياء الحياتية السريرية - كلية الطب - جامعة هوليير الطبية - أربيل - العراق.

^٣ كلية الطب الحيوي، كلية الصحة والعلوم الطبية - جامعة أديليد - جنوب استراليا - استراليا.

^٤ قسم التخطيط والجرعات - مركز أوات لعلاج الأورام بالإشعاع - أربيل - العراق.

The Significant Impact of Programmed Cell Death-1 Gene Polymorphism on HBV Infection and Viral Load

Hiba Hadi Rashid ¹, Hiba M. Al-Darraj ², Müge FIRAT ³,
Bassam Mohammed Mishkhal ⁴

^{1,2} Department of Microbiology, College of Medicine, University of Diyala, Diyala, Iraq.

³ Sabanözü Vocational High School, Veterinary Department, Cankiri Karatekin, University, Ankara, Turkey.

⁴ Department of Family Medicine, Albatoool-Teaching Hospital, Diyala Health, Diyala, Iraq.

OPEN ACCESS

Correspondence: Hiba Hadi Rashid

Email: hiba@uodiyala.edu.iq

Copyright: ©Authors, 2025, College of Medicine, University of Diyala. This is an open access article under the [CC BY 4.0](http://creativecommons.org/licenses/by/4.0/) license (<http://creativecommons.org/licenses/by/4.0/>)

Website:
<https://djm.uodiyala.edu.iq/index.php/djm>

Received: 20 November 2024

Accepted: 29 March 2025

Published: 25 April 2025

Abstract

Background: Hepatitis B virus (HBV) is a common and international problem associated with severe liver diseases. Programmed cell death-1 (PCD-1) is an immunosuppressive molecule that negatively regulates T-cell activity. Genetic variation in PCD-1 gene could impact the encoded protein, and, thus HBV infection.

Objective: To assess the single nucleotide polymorphisms (SNPs) in the PCD-1 gene's promotor area effect of viral load and HBV infection.

Patients and Methods: This case-control study recruited 117 subjects (67 patients with HBV and 50 apparently healthy persons as control). From June 2024 to November 2024, all subjects had been selected at the Gastroenterology and Liver Hospital-Medical City (Baghdad, Iraq). Every participant donates about 5 mL of blood extracted from a vein and stored at -80 °C until it was needed. Blood samples were used to obtain genomic DNA, and gene fragment corresponding the rs38084323 polymorphism in PCD-1 gene was amplified and genotyping by polymerase chain reaction-restriction fragment length polymorphism (PCR-RFLP).

Results: The patients' and controls' mean ages did not differ significantly, out of the 67 patients, 39 (43.28%) had an acute infection, and 38 (56.7%) had a chronic infection. Merely 34.33% of the patients were receiving HBV-specific therapy. Patients having the mutant homozygous genotype (GG) of rs38084323 were significantly more likely to have it (28.36% vs. 14%) (OR= 3.34, 95%CI= 1.07-10.38, p= 0.037). On the level with allele, the G allele was more often found in patients than in healthy subjects (54.48% vs. 41%), demonstrating an important disparity (OR=1.72, 95% CI=1.02-2.91, p=0.042). The various genotypes did not substantially affect the progression of infection to a chronic status. Although, 30.77% of patients carrying the AA genotype had viral ≥ 200000 IU/ml compared with 5.71% for AG carriers and 15.79% for GG carries with such a viral load, and these results were shown significant difference.

Conclusion: The homozygous mutant genotype (GG) and G allele may be regarded as an indicator of risk for HBV infection. However, their impact on viral load is negligible.

Keywords: Hepatitis B virus, Programmed cell death-1, Promoter, Single nucleotide polymorphism, Apoptosis.

Introduction

The World Health Organization (WHO) projected that by 2024, there will be 254 million people with a chronic HBV infection, a 3.2% global seroprevalence of hepatitis B surface antigen (HBsAg), and around 820,000 deaths from HBV-related causes (1). Hepatitis B virus is recognized as a source of several viral diseases, including acute hepatitis B, which may resolve naturally, and chronic infection, which increases the risk of fatalities from hepatocellular carcinoma (2). The clinical consequences of HBV infection rely on the intricate interplay between the host immune response and viral replication. Innate immunity has a significant influence in the initial stages of the disease. However, HBV evades identification by the host innate immune system through stealth (3). The complete elimination of the virus during acute infection is contingent upon an individual's immune system. Generally, individuals infected with HBV can eradicate the virus; nevertheless, acute infection may progress to chronic infection in cases of immunological inadequacy (4). Adaptive immunity, comprising a variety of cell types, has both preventive and detrimental functions in generating an antiviral acquired response. Numerous strong arguments demonstrate that the human cellular immune response which is enabled by CD8⁺ and CD4⁺T cells, predominantly HBV-specific CD8⁺T cells is essential for HBV pathogenesis (5-7). If the virus is not completely eradicated from the body, HBV persists.

A dynamic equilibrium between the host's immune response and viral replication is established, ultimately leading to immunological tolerance and T cell dysfunction in the long term. The depletion of HBV-specific CD8⁺ T cells predominantly occurs through the stimulation the immunosuppressive checkpoint PCD-1/PCD-L1 signaling cascade. Genetic factors donated in advancement of diversity of HBV

disease extension including single nucleotide polymorphism of diversity genes such as Programmed cell death -1 (PCD-1) (8). The PCD-1 gene is situated on chromosome 2 at position q37.3 areas, and over thirty single nucleotide polymorphism (SNPs) sites are in various areas of the gene comprising exon, promoter, intron and 3'UTR area (9-10). PD-1(also known CD 279) is 55-KD protein and a kind of the immunoglobulin subfamily which are immunological sensor revert to the CD28/CTLA-4 that recognized to be restraint of receptor (11,12). PCD-1 offered at the level on trigger B lymphocytes, natural killer cells, T cells, myeloid dendritic cells, and can found in elevated amount at T lymphocytes that get in the repose phase (13). Studies have announced that there are newly genetic interrelation reports had examined genetic variant of (PCD-1) and its ligand (PCDL-L1) with cancer, autoimmune and certain disease in various world people (14,15). Given the significant function of PCD-1 in T-cell activity within the immune response specific to HBV, it is essential to consider the potential effects of gene polymorphism regarding the expression or functional alteration of PCD-1 and its implications for immunological reaction. In this condition, it we conducted a case-control research with the objective of defining the correlation between HBV infection and the SNP rs36084323. Therefore, the objective of this study was to assess the single nucleotide polymorphism (SNPs) in the gene's promotor area effect of viral load and HBV infection.

Patients and Methods

The study design: One Hundred and seventeen subjects registered in this case- control research, encompass 67 patients with HBV and compared with 50 healthy persons. All subjects enlisted at Gastroenterology and liver Hospital-Medical City (Baghdad, Iraq) from June 2024 to November 2024. Diagnosis was executed for HBs Ag by laboratory tests involving enzyme-

linked immunosorbent assays (ELISAs) and asserts these tests by viral load specified by real time-PCR.

Data and sample collection: Written agreement was acquired from all group's previous enrollment in the research project. Data on gender, age, body mass index (BMI), residence, family history of HBV and comorbidities was taken from each subject through direct interview in a preformed formula. Type of infection and treatment assorted under clinical features. Approximately 5 mL of blood taken from a vein gained from everyone who participated, this volume divided into two part 3 µl utilized for serological analysis and 2 µl utilized for molecular assay and both of these kept at -80 °C til be utilized.

Serum preparation and storage: To ensure full clotting, the tubes were centrifuged for 10 minutes at 1900 x g at 4 °C after being kept at room temperature (15–25 °C) for 20 minutes. Ultimately, the supernatant was cautiously moved to a fresh tube. For HBs Ag.

Determination of Hepatitis B surface antigen (HBs Ag) by ELISA: All 117 samples were examined for detection of (HBs Ag) by ELISA kit (Cat. No: BXEO741C ,CAMP/Romania). The procedure according to the manufacture, Once the necessary number of strips had been removed, they were secured into the micro well. The ELISA working sheet was followed when adding the specimens. 100 µl of samples were added to the test well, and 100 µl of HBs Ag positive, negative control was added to the control well. To every well, one hundred microliters of conjugate were added. After 50 minutes of incubation at 37 °C, the well was rinsed four times with wash buffer. After 50 minutes of incubation at 37 °C, the well was rinsed four times with wash buffer. After adding 90 µl of TMB substrates, the mixture was incubated for 20 minutes at 37 °C in a dark environment. The well becomes blue. Lastly, 50

µl of stop solution was carefully added, convert the color to yellow. The result was measured at 450 nm in 15 minutes.

Isolation DNA and Polymerase Chain Reaction and restriction fragment length polymorphism (RFLP): A commercial kit (Gsync TM DNA extraction kit quick organizer, Cat.No: GS100, Geneaid, Taiwan) was utilized for Genomic DNA extraction as stated by steps by the manufacturer. Biospec Nano spectrophotometer identified extracted DNA concentration the at 260 nm/280 nm (A260/A280). Polymerase chain reaction – restriction fragment length polymorphism (PCR-RFLP) was employed to inspect the -538 locus (rs3608423). For this purpose, two primers utilized (16):

Forward (F): 5'-CTCAACCCCACTCCCATTTCT-3' and reverse for above F (R) 5'-TTCTAGCCTCGCTTCGGTTA-3' with an expected fragment length of 552 bp. The ABI 9600 (Hybaid / England) was employed in PCR in entire volume of 25 µl comprising 50 ng of genomic DNA, 1.5 µl of 10×PCR buffer, 0.3 µl of 10mM dNTPs, 0.25 µl of 10pmol/µl of every primer, and 1.25 U of Taq DNA polymerase (Cat. No: K-2012, Bioneer, Korea). The cycling parameters included preliminary denaturation at 94 °C for 5 minutes, subsequently 30 cycles of 1 min. at 94 °C, 1 min. at 56 °C, 1 min. at 72 °C and finally extension step at 72 °C for 5 min. The PCR products underwent enzymatic digestion with 5 U MspI (Cat.No: E091, Sib Enzyme Russia) adhering to the manufacturer's guidelines. Individuals' genotypes were identified based on the length of digested parts subsequent 2% agarose gel electrophoresis, which was colored with ethidium bromide. Allele differentiation was determined by fragment size post- digestion which was 227 bp for G allele and 282 bp for A allele.

Quantitation of HBV DNA: For the purpose of

quantifying HBV DNA in all 117 samples, we employed the COBAS AmpliPrep/COBAS TaqMan HBV Test (Roche Diagnostics, Laval, QC, Canada), a nucleic acid amplification test, in conjunction with an automated real-time PCR assay. An HBV DNA fragment from the S gene served as the primer for the HBV DNA quantification.

Statistical analysis

The analyses were executed employed SPSS 25.0 (SPSS, Chicago). The mean and standard deviation of Continual information were presented, and the student t-test was employed for analysis. The Chi-square test assessed variables with categories, noted as numbers and percentages. The relationship between HBV infection and rs36084323, positioned in the promoter area of the PCD-1 gene, was assessed through binary logistic regression analysis. The odds ratio (OR) and in line with 95% confidence interval (CI) were determined from this test. Any change regarded statistically significant had a p-value of less than 0.05.

Results

Demographic features of the patients: There was no substantial disparity in the mean age of the patients and controls, the previous processing range was 14–75 years and the last one possessing a range of 44.98±9.5 29 years. Despite being less common in patients than in controls (47.76% vs. 56%), the variation was not substantial significant. Similarly, there were no appreciable variations between the two groups' BMIs or places of residence. However, there existed a notable disparity between the 19.4% of patients and the 6% of control group who had a family history of HBV. Diabetes mellitus (DM) and hypertension were prevalent co-occurring conditions in both the patient and control groups, with no discernible variations in the occurrence of these conditions between them as shown in Table 1.

Table 1. Presents the demographic features of the study population.

Variables	Patients (n=67)	Controls (n=50)	p-value
Age, years			0.363
Mean±SD	42.72±15.47	44.98±9.5	
Range	14-75	17-62	
Gender			0.378
Male	35(52.24%)	22(44%)	
Female	32(47.76%)	28(56%)	
BMI, kg/m ²			0.101
Mean±SD	26.2± 3.76	25.26±3.6	
Range	17.42-35.8	21.67-28.73	
Residence			0.697
Rural	53(79.1%)	41(82%)	
Urban	14(20.9%)	9(18%)	
Family history			0.037
No	54(80.6%)	47(94%)	
Yes	13(19.4%)	3(6%)	
Comorbidity			0.614
No	51(76.12%)	36(72%)	
DM	7(10.45%)	5(10%)	0.741
Hypertension	8(11.94%)	5(10%)	0.131
Others	3(4.48%)	6(12%)	
SD: standard deviation, BMI: body mass index, DM			

Clinical characteristics of the patients: Acute infection was reported in 39 patients out of 67 (43.28%), while chronic infection was found in 38 patients (56.7%). Only 34.33% of the patients were under specific treatment for HBV. Viral load was ≥ 200000 IU/ml in 9 patients (13.43%) as shown in Table 2.

Table 2. Patient clinical features.

Variables	Values
Type of infection	
Acute	29(43.28%)
Chronic	38(56.72%)
Treatment	
No	44(65.67%)
Yes	23(34.33%)
Viral load, IU/ml	
<200000	56(83.58%)
≥200000	9(13.43%)

Molecular assay: This study examined the relationship between HBV infection and the SNP rs36084323, which is situated in the promoter region of the PD-1 gene. RFLP was used for the genotyping process, as shown in Figure 1, display the PCR products prior to digestion, Lane M is 1:100 bp ladder, primarily all samples explained in 1 to14 lanes gave positive result for PD-1.1 primers with product length 552bp before utilized the restriction enzyme. Following digestion with the MspI restriction enzyme, three genotypes for this SNP were identified: AA, AG, and GG, as illustrated in Figure 2. Current study announced about 13 patients and 16 controls carrying AA genotype, 35 patients and 27 controls carrying AG genotype and 19 patients and 7controls carrying GG genotyping.

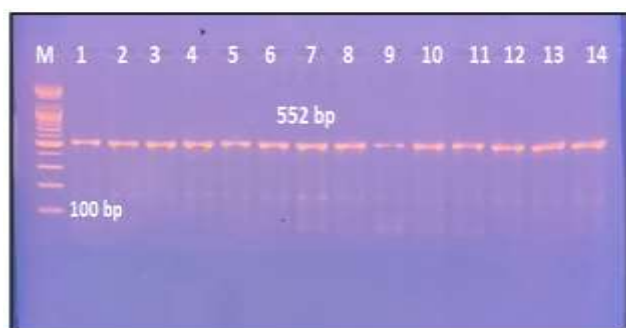


Figure 1. Gel electrophoresis of the PD-1-606 G/A gene polymorphism amplified with an identifiable primer pair via conventional PCR. The PCR result was dyed with ethidium bromide. The fragment's size measured 552 base pairs.



Figure 2. Genotype variations in PD-1-606 G/A in patients with HBV following digestion with the MspI restriction enzyme, shown under U.V light after colored with ethidium bromide. Lanes M is 1:100 bp ladder, Lanes 1, 4, and 8: AA genotype; lanes 2, 3, 6, 9, 10, and 12: GA genotype; lanes 5, 7, and 11: GG genotype; M: 100 bp molecular ladder.

Association of rs36084323 with HBV Infection: Both wild type homozygous and heterozygous genotypes were less frequent in patients (19.4% and 52.24%, respectively) than controls (32% and 54%, respectively) although the differences were not significant. Conversely, the mutant homozygous genotype (GG) was increased frequency in patients than (28.36% vs. 14%) with a substantial disparity (OR= 3.34, 95%CI= 1.07-10.38, p= 0.037). In dominant approach, the rate of GG genotype was higher in patients compared to controls (28.36% vs. 14%) with no substantial disparity. At the allelic level, the G allele was greater prevalent in patients compared to controls (54.48% vs. 41%), exhibiting an important distinction (OR=1.72, 95%CI=1.02-2.91, p=0.042), as illustrated in Table 3.

Table 3. The prevalence of various genotypes and alleles of the rs36084323 polymorphism in HBV patients and healthy subjects.

rs36084323 Polymorphism	Patients (n=67)	Controls (n=50)	P-value	OR (95%CI)
Genotypes				
AA	13(19.4%)	16(32%)	0.113	1.0
AG	35(52.24%)	27(54%)	0.148	2.1(0.77-5.7)
GG	19(28.36%)	7(14%)	0.037	3.34(1.07-10.38)
HWE	0.663	0.411		
Dominant model				
AA+AG	48(71.64%)	43(86%)	0.069	1.0
GG	19(28.36%)	7(14%)		2.43(0.93-6.35)
Recessive model				
AA	13(19.4%)	16(32%)	0.121	1.0
AG+GG	54(80.6%)	34(68%)		1.96(0.84-4.57)
Alleles				
A	61(45.52%)	59(59%)	0.042	1.0
G	73(54.48%)	41(41%)		1.72(1.02-2.91)

Correlation of various genotypes of rs36084323 with the clinical attributes of patients: There was no discernible effect of different genotypes of rs36084323 polymorphism on the development of infection into chronic status.

Although, 30.77% of patients carrying AA genotype had viral load ≥ 200000 IU/ml compared with 5.71% for AG carriers and 15.79% for GG carries with such a viral load, the change was not substantial as shown in Table 4.

Table 4. Correlation of various genotypes of rs36084323 with the clinical attributes of patients.

Variables	AA (n=13)	AG (n=35)	GG (n=19)	p-value
Type of infection				
Acute	3(3.08%)	16(45.71%)	10(52.63%)	0.232
Chronic	10(76.9%)	19(54.9%)	9(47.37%)	
Viral load, IU/ml				
<200000	9(69.23%)	32(91.43%)	14(73.68%)	0.072
≥ 200000	4(30.77%)	2(5.71%)	3(15.79%)	

Discussion

This study found no variation in impact related to age between patients and controls, also the findings contradict previous studies conducted in Iraq, Iran, and China, which indicated that age was related with a raised risk of infection. (17-19). The study found no variation in impact based on gender, BMI, or residence; however, a positive association was observed between family history and HBV prevalence. This result compared with previous study from Iraq showed that the proportion of family members of infected people who received the HBV vaccine was much lower than those who did not (20). This finding aligns with the report from Ethiopia. (21), Vietnam, (22) in Northeast China (23), and Africa Uganda. (24) In contrast, this is in consistent with other reports (25,26). This result may from insufficient understanding of HBV transmission methods, inadequate caution when sharing sharp objects, traditional practices, or unsafe sexual practices. The transmission of viruses occurs through various methods, including blood transfusion. Additionally, individuals within the same household may be exposed to similar external risk factors. For instance, family members engaging in the same conventional medical practices may significantly elevate the risk of infection through

various means, including intravenous drug use, unsafe healthcare-related injections, blood transfusions, and dialysis. Additionally, exposure to infected blood via razors and nail clippers can contribute to infection, as can the use of contaminated piercing instruments, tattoos, and other cosmetic procedures. New sexual discharge and an additional fluid, such as saliva (26-28). Additionally, HBV infection can be transmitted from a mother with HBsAg at birth or through postnatal blood exposure. Research indicates that children of HBsAg positive individuals face a heightened risk of HBV infection through the exchange of items containing infected bodily secretions, such as chewing gum or toothbrushes (29-30). Several factors contribute to the variation in HBV infection outcomes, encompassing host, viral, and environmental elements. Genetic polymorphism and specific comorbidities, such as diabetes are recognized as host factors influencing on clinical outcomes of HBV infection. The viral determinants encompass HBV viral load. This study indicated no variation in impact concerning specific comorbidities and viral load between patients and controls, which contradicts previous research suggesting a positive association

between specific comorbidities and viral load with the outcomes of HBV infection (31). This study examines the host genetic polymorphism associated with HBV infection outcomes, particularly detecting the SNPs in the promoter area of PCD-1.1 (-538G/A) (rs36084323). A multitude of studies has examined the identified connection between PCD.1 gene polymorphisms and diverse disorders (32-33). In this context, additional studies examined the connection between PD-1.1 gene polymorphism and colorectal cancer in Iranian patients, they showed that A and G alleles are correlated with raised risk of colon cancer (34). The prior report detailed the risk of various PD-1 variants in myocardial infarction (MI), no association was identified between PCD-1.1 alleles or genotypes and MI. They noted a limited protective effect of the PD-1.3A allele regarding myocardial infarction (35). A recent study assessed PCD-1 mRNA expression levels in Peripheral Blood Mononuclear Cells (PMCs) and examined its correlation with clinical characteristics of hepatitis B infection and the genotypes kinds of PCD-1 rs10204525, which includes three kinds genotypes: AA, GA, and GG. The findings indicated whom patients with chronic HBV infection displayed a notable higher PCD-1 mRNA expression compared to the healthy control group (36). Currently, there limited number of published research demonstrating a relationship between the PCD-1.1 (-538G/A) gene polymorphism and vulnerability to HBV infection. This research is confirmed and indicated a significantly higher prevalence of the GG genotype and G allele at position -538G/A of PCD.1 in HBV patients compared to the normal group. Conversely, the results indicated a lower frequency of the AA genotype and A allele in HBV patients compared to the normal group. Our research and prior studies indicated a strong correlation between elevated PD-1 expression and heightened HBV viral

transcription levels (2,37). Furthermore, efficient viral transcription of HBV contributes to the advance of disease in patients, characterized by elevated expression of PCD-1 on HBV-specific CD8+ T cells, CD4+ T cells, and CD25+ regulatory T cells. This is attributed to increased RNA polymerase activity at the promoter area of the gene, resulting in impaired T cell functionality and persistent HBV infection (38). This polymorphism may serve as a target for designing immunotherapy strategies and assessment and selecting patients with HBV based on specific genetic immunological profiles, potentially enhancing future immunotherapy approaches for hepatitis B virus disease (39).

Conclusions

The mutant homozygous mutant genotype (GG) and G allele may be regarded as an indicator of risk for HBV infection. The detection of HBs Ag and employed real time PCR is the best way that assert the infection with virus. However, their impact on viral load is negligible. Expanding screening methods should be the main focus of future work since it is crucial to better therapy.

Recommendations

recommended for using another primer in another region of gene for obtain the additional risk factors for HBV infection and recommended for diagnose another gene.

Source of funding: No source of funding.

Ethical clearance: Ethical approval to perform the research acquired from the scientific and ethical committees / College of Medicine / University of Diyala (No:2025HHR898 Date:19/2/2025).

Conflict of interest: None.

Acknowledgments:

The authors would like to express their sincere gratitude to the Gastroenterology

and Liver Hospital – Medical City (Baghdad, Iraq) for their valuable support and collaboration in this study

References

1. Razavi-Shearer D, Gamkrelidze, I, Pan C, Jia J, Berg T, Gray R, et al. Global prevalence, cascade of care, and prophylaxis coverage of hepatitis B in 2022: a modelling study. *The lancet Gastroenterology & hepatology*.2023; 8(10), 879-907.
2. Hoan NX, Huyen PTM, Binh MT, Trung NT, Giang DP, Linh, BT, & Song LH. Genetic variants of programmed cell death 1 are associated with HBV infection and liver disease progression. *Scientific Reports*. (2021); 11(1): 7772.
<https://doi.org/10.1038/s41598-021-87537-9>.
3. Zheng P, Dou Y, & Wang Q. Immune response and treatment targets of chronic hepatitis B virus infection: Innate and adaptive immunity. *Frontiers in Cellular and Infection Microbiology*. 2023; 13: 1206720.
<https://doi.org/10.3389/fcimb.2023.1206720>.
4. Soleimani F, Arabzadeh SAM, Mollaei H, Iranmanesh Z, Nikpour N & Motahar M. Evaluation of the frequency of precore/core mutation in patients with chronic hepatitis B, Kerman, Southeast of Iran. *Asian pacific journal of tropical disease*.2016; 6(8):603-607.
[https://doi.org/10.1016/S2222-1808\(16\)61093-9](https://doi.org/10.1016/S2222-1808(16)61093-9).
5. Aduagna A. "Antigen recognition and immune response to acute and chronic hepatitis B virus infection." *Journal of Inflammation Research*. 2023;2159-2166.
<https://doi.org/10.2147/JIR.S411492>.
6. Li M, Lu Y, Zhang L, Wang XY, Ran CP, Hao HX, et al. Association of cytokines with alanine aminotransferase, hepatitis b virus surface antigen and hepatitis b envelope antigen levels in chronic hepatitis b. *Chin Med J*. 2018; 131 (15):1813–8.

<https://doi.org/10.4103/03666999.237394>.

7. Vittal A, Ghany MG. WHO guidelines for prevention, care and treatment of individuals infected with HBV: A US perspective. *Clinics liver Dis*. 2019; 23 (3):417–32.
<https://doi.org/10.1016/j.cld.2019.04.008>.
8. Zhang G, Liu Z, Duan S, Han Q, Li Z. Lv Y, et al . Association of polymorphisms of programmed cell death–1 gene with chronic hepatitis B virus infection. *Human immunology*.2010; 71(12); 1209-1213.
<https://doi.org/10.1016/j.humimm.2010.08.014>.
9. Wang Y, Wu L, Tian C& Zhang Y . "PD-1-PD-L1 immune-checkpoint blockade in malignant lymphomas." *Annals of Hematology*. 2018; 97: 229-237.
<https://doi.org/10.1007/s00277-017-3176-6>
10. Zasada M, Lenart M, Rutkowska-Zapala, M, Stec, M Durlak W, et al . "Analysis of PD-1 expression in the monocyte subsets from non-septic and septic preterm neonates." *PLoS One*. 2017; 12(10): e0186819.
<https://doi.org/10.1371/journal.pone.0186819>
11. Xibing G, Y Xiaojuan, and W Juanhua. "PD-1 expression on CTL may be related to more severe liver damage in CHB patients with HBV genotype C than in those with genotype B infection." *Journal of Viral Hepatitis*.2013; 20(4): e1-e2. <https://doi.org/10.1111/jvh.12009>
12. Teng XY, Wang P, Zhou XG, Shen B, Sun L, & Lang Z W. "PD-1/PD-L1 expressions in liver tissues of patients with chronic HBV infection. *Chinese Journal of Hepatology* . 2011;19(5): 345-348.
<https://doi.org/10.3760/cma.j.issn.1007-3418.2011.05.008>.
13. Yazdanpanah S, Geramizadeh B, Nikeghbalian S & Malek-Hosseini SA. "Hepatocellular Carcinoma and Its Precursors in 103 HBV-Related Cirrhotic Explanted Livers: A Study from South Iran." *Hepatitis Monthly*.2016;

- 16(8). <https://doi.org/10.5812/hepatmon.38584>
14. Salmaninejad A, Khoramshahi V, Azani A, Soltaninejad E, Aslani S, Zamani MR, et al. "PD-1 and cancer: molecular mechanisms and polymorphisms. Immunogenetics.2018; 70: 73-86. <https://doi.org/10.1007/s00251-017-1015-5>
15. Yeo MK, Choi SY, Seong IO, Suh KS, Kim JM & Kim KH. Association of PD-L1 expression and PD-L1 gene polymorphism with poor prognosis in lung adenocarcinoma and squamous cell carcinoma. Human Pathology.2017;68: 103–111. <https://doi.org/10.1016/j.humpath.2017.08.016>
16. Shamsdin SA, Karimi MH, Hosseini SV, Geramizadeh B, Fattahi MR, Mehrabani D& Moravej A. Associations of ICOS and PD. 1 gene variants with colon cancer risk in the Iranian population. Asian Pacific journal of cancer prevention.2018; 19(3): 693. <https://doi.org/10.22034/APJCP.2018.19.3.693>.
17. Hussein NR, Zana ZS, Ibrahim NM, Assafi MS, Daniel S. The prevalence of HBV infection in renal transplant recipients and the impact of infection on graft survival. Acta Medica Iranica. 2019;381–4. <https://doi.org/10.18502/acta.v57i6.1884>
18. Alavian SM, Tabatabaei SV, Ghadimi T, Beedrapour F, Kafi-Abad SA, Gharehbaghian A, et al. Seroprevalence of hepatitis B virus infection and its risk factors in the west of Iran: a population-based study. International Journal of preventive medicine. 2012; 3(11):770. PMID: PMC3506088 PMID: 23189228.
19. Li X, Zheng Y, Liao A, Cai B, Ye D, Huang F, et al. Hepatitis B virus infections and risk factors among the general population in Anhui Province, China: an epidemiological study. BMC Public Health. 2012; 12:1–7. <https://doi.org/10.1186/1471-2458-12-272>.
20. Abdul-Rahman SM, Mahmud MA, Hassan ZI, & Jafaar AM. Prevalence of hepatitis B virus infection among general people and hemophilia patients in Erbil City, Iraq during 2020-2021. The Egyptian Journal of Hospital Medicine. 2022; 89(2), 8023-8033.
21. Dagne M, Million Y, Gizachew M, Eshetie S, Yitayew G, Asrade L, et al. Hepatitis B and C viruses infection and associated factors among pregnant women in the Amhara region. Implications for prevention of vertical transmission. 2020. <https://doi.org/10.21203/rs.3.rs-30519/v1>
22. Thanh PN, Tho NTT, Phu TD, Dai Quang T, Duong NT, Chien VC, et al. Prevalence and factors associated with chronic Hepatitis B infection among adults in the Central Highland, Vietnam. AIMS Medical Science. 2020; 7(4):337-346. <https://doi.org/10.3934/medsci.2020023>
23. Zhang H, Li Q, Sun J, Wang C, Gu Q, Feng X, et al. Seroprevalence and risk factors for hepatitis B infection in an adult population in Northeast China. Int J Med Sci. 2011; 8(4):321-331. <https://doi.org/10.7150/ijms.8.321>
24. Kayondo SP, Byamugisha JK & Ntuyo P. Prevalence of hepatitis B virus infection and associated risk factors among pregnant women attending antenatal clinic in Mulago Hospital, Uganda: a cross-sectional study. BMJ open. 2020;10(6):e033043. <https://doi.org/10.1136/bmjopen-2019-033043>
25. Amsalu A. Prevalence, infectivity and associated risk factors of Hepatitis B virus among pregnant women in Yirgalem Hospital, southern Ethiopia: Implication of screening to control mother-to-child transmission? 28th Annual Conference 2016. 2017. <https://doi.org/10.1155/2018/8435910>.
26. Yohanes T, Zerdo Z & Chufamo N. Seroprevalence and predictors of hepatitis B virus infection among pregnant women attending routine antenatal care in Arba Minch Hospital, South Ethiopia. Hepatitis research and

treatment.2016;(1):9290163.

<https://doi.org/10.1155/2016/9290163>

27. Ali AT & Othman SM. Needle stick injuries and their safety measures among nurses in Erbil Hospitals. Diyala Journal of Medicine, 2022; 23(2),1-13.

<https://doi.org/10.26505/djm.v23i2.942>

28. MacLachlan JH, Locarnini S & Cowie BC. Estimating the global prevalence of hepatitis B. The Lancet.2015;386(10003):1515-1517.

29. Al-Majmaie, IME, Alezzi, J I & Batarfi AM. Diversity in Medical Education: A Review Article. Diyala Journal of Medicine, 2023; 25(2),145-155.

<https://doi.org/10.26505/djm.v25i2.105830>.

Gupta S, Gupta R, Joshi YK & Singh S. Role of horizontal transmission in hepatitis B virus spread among household contacts in north India. Intervirology. 2008; 51(1):7-13.

<https://doi.org/10.1159/000118790>.

31. Martinson FE, Weigle KA, Royce RA, Weber DJ, Suchindran CM & Lemon, SM. Risk factors for horizontal transmission of hepatitis B virus in a rural district in Ghana. American journal of epidemiology.1998; 147(5): 478-487.

<https://doi.org/10.1159/000118790>

32. Xu J, Zhan Q, Fan Y, Yu Y & Zeng Z. Human genetic susceptibility to hepatitis B virus infection. Infection Genetics and Evolution. 2021;87:104663.

<https://doi.org/10.1016/j.meegid.2020.104663>

33. Hezave YA, Sharifi Z, & Shahabi M. The association of polymorphisms (rs2227981 and rs10204525) of PDCD1 gene with susceptibility to human T-cell leukemia virus type 1. Microbial Pathogenesis.2021; 158, 105049.

34. Yousefi AR, Karimi MH, Shamsdin SA, et

al . PD-1 gene polymorphisms in Iranian

patients with colorectal cancer. Lab Med.2013; 44(3),241-4.

<https://doi.org/10.1309/LMG1BS4J3TAONRQ>

35. Bennet AM, Alarcon-Riquelme M, Wiman B, de Faire U, & Prokunina-Olsson L. Decreased risk for myocardial infarction and lower tumor necrosis factor-alpha levels in carriers of variants of the PDCD1 gene. Hum Immunol, 2006; 67(9): 700-705.

<https://doi.org/10.1016/j.humimm.2006.05.005>.

36. Ghorbani P, Mollaei H, Arabzadeh S & Zahedi M. Upregulation of single nucleotide polymorphism of PD-1 gene (rs10204525) in chronic hepatitis B patients. Int. Arch. Med. Microbiol. 2019; 2(1): 1-8.

<https://doi.org/10.23937/26434008%2F1710009>

37. Huyen PTM, Dung DTN, Weiß P J, Hoan PQ, Giang DP, Uyen NT, et al. Circulating level of sPD-1 and PD-1 genetic variants are associated with hepatitis B infection and related liver disease progression. International Journal of Infectious Diseases. 2022; 115: 229-236.

<https://doi.org/10.1016/j.ijid.2021.12.325>.

38. Li D, R Chen, YW Wang, AJ Fornace, Li HH, et al. Prior irradiation results in elevated programmed cell death protein 1 (PD-1) in T Cells. Int J Radiat Biol .2018; 94(5):488-494.

<https://doi.org/10.1080/09553002.2017.1400192>

2

39. Ludin A, Zon LI. The dark side of PD-1 receptor inhibition. Cancer immunotherapy. Nature .2017;552(7683): 41-42.

التأثير الكبير لتعدد اشكال جين موت الخلية المبرمج - ١ على عدوى فيروس التهاب الكبد نوع ب والحمل الفيروسي

^١ هبة هادي رشيد ، ^٢ هبة محمد جاسم حمادة ، ^٣ موكا فرات ، ^٤ بسام محمد مشخال

الملخص

الخلفية: فيروس التهاب الكبد نوع ب هو مشكلة عامة شائعة مرتبطة بالتهاب الكبد الشديد. موت الخلايا المبرمج ١ هو جزئى مثبط ينظم نشاط الخلايا التائية بشكل سلبي يمكن ان يؤثر الاختلاف الجيني في جين موت الخلية المبرمج النوع ١ على البروتين المشفر وبالتالي على عدوى فيروس التهاب الكبد نوع ب.

الأهداف: تقييم دور تعدد الاشكال النيوكليوتيدات المفردة في منطقة المحفز لجين (موت الخلايا المبرمج-١) في عدوى فيروس التهاب الكبد نوع ب والتركيز الفيروسي.

المرضى والطرق: شملت الدراسة الحالية ١١٧ شخصا (٦٧ مريضا بالتهاب الكبد الفيروسي نوع ب و ٥٠ شخصا سليما ظاهريا كمجموعة تحكم) تم استخراج الحمض النووي الجينومي من عينات الدم ومن ثم تم تضخيم جزء الجين المقابل لتعدد اشكال ٣٨٠٨٤٣٢٣ في جين موت الخلايا المبرمج-١ والنمط الجيني عن طريق تفاعل البلمرة المتسلسل - تعدد الاشكال- القطع باستخدام الانزيم القاطع).

النتائج: كان النمط الجيني المتمثل المتحور نوع (ج ج) ل ٣٨٠٨٤٣٢٣ اكثر شيوعا لدى المرضى (٢٨,٣٦٪ مقابل ١٤ على المستوى الاليلي كان الاليل (ج) اكثر شيوعا لدى المرضى مقارنة بمجموعة الاصحاء مع وجود فرق كبير . لم يكن هناك تأثير كبير للأنماط الجينية المختلفة على تطور العدوى الفايروسية الى عدوى مزمنة وعلى الرغم من ان ٣٠,٧٧٪ المرضى الحاملين للنمط الجيني (أ أ) كان لديهم حمولة فيروسية ≤ 200000 وحدة دولية مقارنة ب ٥,٧١ لحاملي النمط الجيني (أ ج) و ١٥,٧٩ لحاملي النمط الجيني (ج ج) مع مثل هذا الحمل الفيروسي , الا ان الفرق لم يكن كبيرا.

الاستنتاج: يمكن اعتبار النمط الجيني المتمثل المتحور (ج ج) والاليل (ج) من العوامل الخطورة للإصابة بفيروس التهاب الكبد الفيروسي نوع ب ومع ذلك فان تأثيرها على الحمل الفيروسي لا يذكر.

الكلمات المفتاحية: فيروس التهاب الكبد نوع ب , موت الخلايا المبرمج-١ , منطقة المحفز, تعدد الاشكال للنيوكليوتيد المفرد.

المؤلف المراسل: هبة هادي رشيد

الايمل: hiba@uodiyala.edu.iq

تاريخ الاستلام: ٢٠ تشرين الثاني ٢٠٢٤

تاريخ القبول: ٢٩ آذار ٢٠٢٥



تاريخ النشر: ٢٥ نيسان ٢٠٢٥

^{٢,١} فرع الاحياء المجهرية - كلية الطب - جامعة ديالى - ديالى - العراق.

^٣ كلية الطب البيطري - جامعة جنكيري - انقرة - تركيا.

^٤ وزارة الصحة - دائرة صحة ديالى - مستشفى البتول التعليمي - ديالى - العراق.

Curcumin Oral Gel and its Relation to Salivary Tumor Necrosis Factor-Alpha and Interleukin-6 that Treated Oral Mucositis in Head and Neck Cancer Patients Undergoing Concurrent Chemoradiation

Rouaa S. Farhan ¹, Fawaz D. Al-Aswad ²

^{1,2} College of Dentistry, University of Baghdad, Baghdad, Iraq.

OPEN ACCESS

Correspondence: Rouaa S. Farhan

Email: dr.rouaa.alkhaleedy@gmail.com

Copyright: ©Authors, 2025, College of Medicine, University of Diyala. This is an open access article under the [CC BY 4.0](http://creativecommons.org/licenses/by/4.0/) license (<http://creativecommons.org/licenses/by/4.0/>)

Website: <https://djm.uodiyala.edu.iq/index.php/djm>

Received: 14 December 2024

Accepted: 19 March 2025

Published: 25 April 2025

Abstract

Background: Curcumin oral gel is one example of a traditional herbal medication, it has shown potential in several pharmaceutical uses. Oral mucositis is commonly prevent and treat using magic solution, a mouthwash that contains a combination of pharmaceuticals. Tumor necrosis factor- α and Interleukin-6 are salivary cytokines stimulates the immune response and promotes inflammation during infection or other tissue damage causes inflammation.

Objective: To determine the effect of curcumin oral gel on salivary tumor necrosis factor- α and interleukin-6 levels in head and neck cancer patients under concurrent chemoradiation induced oral mucositis.

Patients and Methods: Two groups of forty-five patients each, with a total of ninety head and neck cancer patients receiving concurrent chemoradiation. Enzyme-linked immunosorbent assay measured salivary tumor necrosis factor-alpha and interleukin-6 levels. Oral mucositis was assessed by WHO scale.

Results: Patients who took oral curcumin gel had less severe oral mucositis and lower salivary levels of tumor necrosis factor-alpha and interleukin-6. WHO scale between the two groups showed significant differences at 2 weeks ($P = 0.041$) and 6 weeks ($P=0.02$).

Conclusion: Study concludes that curcumin oral gel might reduced salivary tumor necrosis factor-alpha and interleukin-6 levels and may serve as an alternative treatment for oral mucositis resulting from chemoradiation.

Keywords: Head and neck cancer, Concurrent chemoradiotherapy, Oral mucositis, Curcumin, Tumor necrosis factor-alpha, Interleukin-6.

Introduction

Curcumin goes under another name, The Zingiberaceae family includes turmeric. One to two percent curcuminoids and three to twelve percent volatile oil are the two main components of the root. A phenolic compound with possible health benefits, dimethylsulfoxide is also known as curcumin. (1, 2). Numerous clinical investigations have shown the extensive variety of pharmacologic capabilities exhibited by Curcumin oral gel. These features include the ability to

enhance wound healing, anti-inflammatory, antifungal, antibacterial, and anticarcinogenic actions (3, 4). Curcumin improves epithelialization and wound healing by protecting and activating keratinocytes while scavenging reactive oxygen species and serving as an antioxidant (5, 6). Curcumin may potentially increase the effectiveness of morphine by decreasing pain transmission channels and promoting the production of serotonin, dopamine, and noradrenaline at large dosage (7). Head and neck cancers(HNC) involve a wide range of malignancies that may develop in salivary glands, paranasal sinuses, the larynx, pharynx, and oral cavity (8). When head and neck cancer has spread locally, first line of treatment choice is a chemotherapy combined with radiotherapy (9). Cytotoxic concurrent chemoradiotherapy causes oral mucositis (OM), an inflammatory condition of the mouth and throat that is a major problem in oncology (10). Oral mucositis may progress to deep, confluent ulcers if left untreated. The level of functioning and the standard of living of a patient are often compromised by pain caused by mucositis (11, 12). In cells such as macrophages, epithelial, endothelial, and mesenchymal cells, the transcription nuclear factor- κ B(NF- κ B) is made active by concurrent chemotherapy and radiation (CCRT). The result is an increase in genes that are upregulated and the generation of cytokines that promote inflammation, like tumour necrosis factor- α (TNF- α) and interleukin-6 (IL-6). The transcription of genes encoding cyclooxygenase 2 (COX2), mitogen-activated protein kinase (MAPK) and tyrosine-kinase signaling molecules is induced by cytokines that enhance the main signal or activate nuclear factor- κ B in other cells. In the cell epithelium and lamina propria, matrix metalloproteinase (MMP-1 and MMP-3), is activated by both TNF- α and IL-6, leading to tissue injury (13, 14).

Aim of this study: To determine the effect of curcumin oral gel on salivary tumor necrosis factor- α and interleukin-6 levels in head and neck cancer patients under concurrent chemoradiation induced oral mucositis.

Patients and Methods

From March 2023 to June 2024, this study was carried out. Protocol number: 934724 indicates that the study was given the go light by the Research Ethics Committee of the University of Baghdad, College of Dentistry. There were 90 HNC patients that took part in the research. There were two groups created: the experimental group and the comparison group.

Subjects: For the trial, 45 patients were given oral gel containing curcumin, whereas 45 patients were given magic-solution as a control.

Inclusion criteria: included being between the ages of 30 and 70, diagnosed with cancer of the head and neck and being scheduled for concurrent chemoradiotherapy. Patients were also required to wear mask of head and neck during radiation therapy, and their oral cavity mucosa had to be within the radiation range. Chemotherapy was cisplatin 40 mg/m² administered weekly, and radiotherapy consisted of 33 fractions scheduled 5 times a week for 6 weeks with 50 and 70 Gray (Gy).

Exclusion criteria: were individuals receiving only radiation and those having palliative radiotherapy.

Assessment of oral mucositis Clinical: On the 2nd week of chemoradiation and the last day of the chemoradiation treatments, patients were examined and scored on a scale from 0 to 4 developed by the World Health Organization WHO. With a score of 0, no symptoms are present; with a score of 1, the oral mucosa is red and uncomfortable; and a score of 2 indicates that the mouth is ulcerous and makes it hard to eat normally. At 3, the ulcer has already developed, and the patient is limited to drinking fluids; at 4, the patient is unable to eat or drink anything (15).

Curcuma longa oral gel: The subjects in the

curcumin group were given Curenext[®], a product made by (Abbott Healthcare, India) which includes 10 milligrams of Curcuma longa root extract (rhizome) per gram of gel. Patients were told to use a cotton swab or finger to apply the gel three times a day beginning with the initial saliva sample collection until their chemoradiotherapy treatment was finished. A standard mouthwash consisting of nystatin, dexamethasone, lidocaine, and tetracycline was administered to patients in the magic-solution group (16, 17).

Saliva sample collection and storage: Each of the 90 patients had three complete saliva samples taken: once before chemoradiation, once after the second week of treatment, and again at the six-week chemoradiation. Patients spat into a plastic tube that was marked with their name, group, and visit date in order to collect their unstimulated saliva. The next step was to place it in an icebox and freeze it stored at a temperature of -80°C till the time of analysis comes.

Laboratory analysis: Salivary TNF- α and IL6 levels were examined using the enzyme-linked immunosorbent test (ELISA). (ELISA) is a type of solid phase immunoassay in which antigens or antibodies are covalently bound with suitable enzymes that can catalyze the change of substrates into dyed products. It is an approved

technique to investigate different biological markers Commercial quantitative sandwich assay (ELISA) kits from Cloud-clone Corp (CCC, USA) were used in compliance with the manufacturer's recommendations (18). To find the levels of TNF- α and IL6, saliva samples were taken, using phosphate-buffered saline as a negative control and a manufacturer-supplied standard curve.

Statistical analysis

The data was handled in an Excel spreadsheet. Analysis was carried out using SPSS version 22. Statistical tests were used: a paired t-test, an independent t-test, a Bonferroni test, a Wilcoxon Signed Ranks test, and chi-square (χ^2) test. A P-value below 0.05 was defined significant.

Results

When comparing the two groups according to age and sex, no statistically significant differences were found.

Salivary tumor necrosis factor- α (TNF- α):

The comparison between the two studied groups with respect to TNF- α marker, along different of an experimental periods, results shows that mean values are decreases clearly over the time periods, and at a lower levels with respect to treated with curcumin group (Table 1 , Figure 1).

Table 1. Summary statistics of TNF- α (pg/ml) marker along different periods of the studied groups.

Periods	Groups	No.	Mean	Std. D.	Std. E.	95% C. I. for Mean		Min.	Max.
						L.b.	U.b.		
Initiation period	Curcumin	45	208.0	34.95	5.21	197.51	218.52	113.29	282.61
	Magic Solution	45	266.4	77.50	11.55	243.08	289.64	135.99	391.84
After 2 weeks	Curcumin	45	142.6	27.73	4.13	134.26	150.92	104	216.96
	Magic Solution	45	218.3	47.78	7.12	203.91	232.62	100.45	295.76
After 6 weeks	Curcumin	45	88.95	9.44	1.41	86.12	91.79	74.49	111.6
	Magic Solution	45	182.8	55.76	8.31	166.05	199.56	116.17	324.32

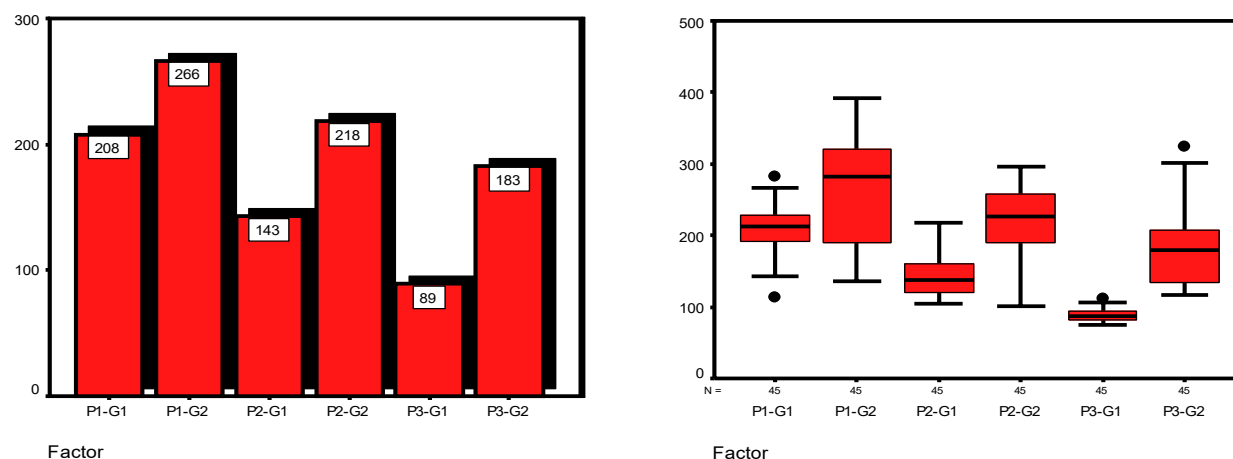


Figure 1. Stem-leaf plot and Bar Chart for exploring behavior of TNF- α marker reading's distribution along the study of the sequential periods in each group.

Means salivary TNF- α were highly significantly ($P = 0.000$) decreased two and six weeks after chemoradiotherapy compared to that before chemoradiotherapy and six weeks after chemoradiotherapy compared to that at two weeks after chemoradiotherapy in both study groups. The decrement in TNF- α two and six weeks after chemoradiotherapy was considerably significantly higher in the curcumin group than that treated with magic solution compared to that before chemoradiotherapy ($P < 0.05$) in Table 2.

Salivary interleukin 6 (IL-6): The comparison between the two studied groups concerning the "IL6" marker along different

experimental periods. The results show that mean values decrease clearly over the periods and at lower levels concerning the curcumin group (Table 3, Figure 2).

Table 4 shows the means salivary IL-6 were highly significantly ($P = 0.000$) decreased two and six weeks after chemoradiotherapy compared to that before chemoradiotherapy and six weeks after chemoradiotherapy compared to that at two weeks after chemoradiotherapy in both study groups. The decrement in IL-6 two and six weeks after chemoradiotherapy group treated with curcumin had a significantly higher than that treated with magic solution compared to that before chemoradiotherapy ($P < 0.05$).

Table 2. Significant levels for testing covariate of TNF- α (pg/ml) marker's readings in each group independently over the sequential periods.

Groups	Pairwise Comparisons		Mean Diff. (I-J)	Std. lError	Sig. (*) Level	95% C. I. for Diff.	
	(I) TNF- α	(J) TNF- α				L.b.	U.b.
Curcumin	Initiation	After 2 w.	-20.02	4.416	0.000	-28.92	-11.1
		After 6 w.	33.62	2.211	0.000	29.17	38.1
	After 2 w.	After 6 w.	53.64	4.129	0.000	45.32	62.0
Magic Solution	Initiation	After 2 w.	-147.78	11.471	0.000	-170.90	-124.7
		After 6 w.	-64.23	8.381	0.000	-81.12	-47.3
	After 2 w.	After 6 w.	83.55	10.036	0.000	63.33	103.8

(*) HS: Highly Sig. at $P < 0.01$; S: Sig. at $P < 0.05$; Testing is based on repeated measurers of several related groups, through using adjustment for multiple comparisons by "Bonferroni" test.

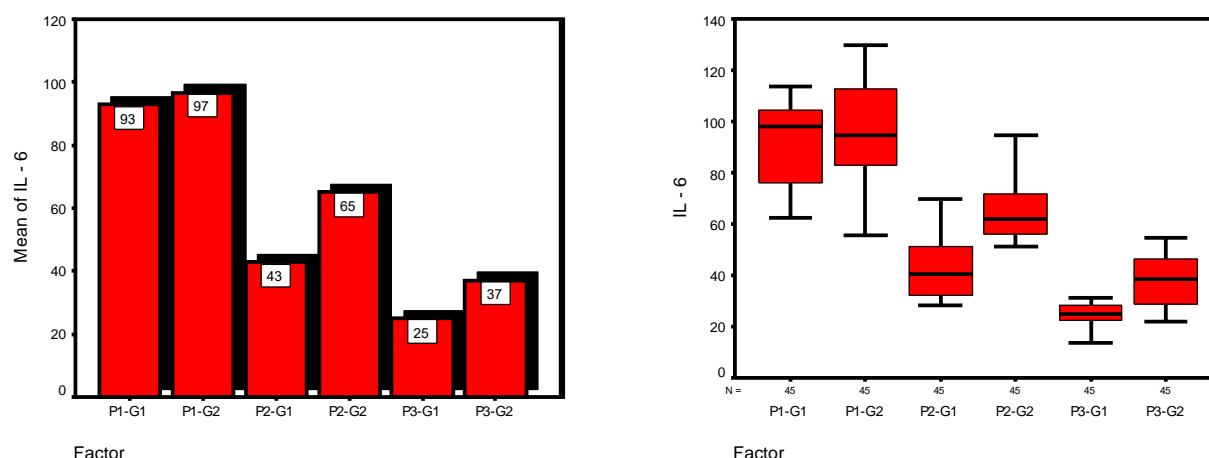


Figure 2. Bar Chart, and stem-leaf plot for explore behavior of IL-6 marker reading's distribution along the studied of sequential periods in each group.

Table 3. Summary Statistics of IL-6 (pg/ml) marker along different periods of the studied groups.

Periods	Groups	No.	Mean	Std. D.	Std. E.	95% C. I. for Mean		Min.	Max.
						L.b.	U.b.		
Initiation period	Curcumin	45	92.88	15.39	2.29	88.26	97.51	62.27	113.75
	Magic Solution	45	96.69	19.60	2.92	90.80	102.58	55.71	129.76
After 2 weeks	Curcumin	45	42.80	12.42	1.85	39.07	46.53	28.30	69.65
	Magic Solution	45	65.17	11.89	1.77	61.60	68.74	51.03	94.79
After 6 weeks	Curcumin	45	24.99	3.90	0.58	23.82	26.16	13.68	31.00
	Magic Solution	45	37.15	9.43	1.41	34.31	39.98	21.89	54.87

Table 4. Significant levels for testing covariate of IL-6 (pg/ml) marker readings in each group independently over the sequential periods.

Groups	Pairwise Comparisons		Mean Diff. (I-J)	Std. Error	Sig. Level	95% C. I. for Diff.	
	(I) IL-6	(J) IL-6				L.b.	U.b.
Curcumin	Initiation	After 2 w.	50.086	2.570	0.000	43.69	56.48
		After 6 w.	67.895	2.167	0.000	62.50	73.29
	After 2 w.	After 6 w.	17.809	1.741	0.000	13.48	22.14
Non Curcumin	Initiation	After 2 w.	31.515	3.089	0.000	23.83	39.20
		After 6 w.	59.540	3.624	0.000	50.52	68.56
	After 2 w.	After 6 w.	28.025	2.261	0.000	22.40	33.65

(*) HS: Highly Sig. at P<0.01; Testing are based on repeated measurers of several related groups, through using adjustment for multiple comparisons by "Bonferroni" test.

Clinical evaluation of oral mucositis

world health organization scale: Table 5 and Figure 3 at both the two-week and six-week chemoradiation evaluations, the curcumin group had a significantly lower mean WHO score than the magic-solution

group. Results in Table 6 demonstrate WHO score readings that too highly significant differences are accounted at P<0.01 concerning all probable pairwise comparisons grade of mucositis GOM, either for curcumin or magic solution groups % independently.

Table 5. Summary Statistics of Grade of Mucositis WHO score along different periods of the studied groups.

Groups	Statistics	Periods		
		Initiation	After 2 weeks	After 6 weeks
Curcumin	Mean of Score	0.000	1.667	1.178
	Interquartile Range	0.000	1.000	1.000
	Minimum score	0.000	1.000	1.000
	Maximum score	0.000	3.000	2.000
Magic solution	Mean of Score	0.000	1.689	1.378
	Interquartile Range	0.000	0.000	1.000
	Minimum score	0.000	1.000	1.000
	Maximum score	0.000	3.000	3.000

Table 6. Significant levels for testing of GOM score's readings in each group independently over the sequential periods.

Groups	Pairwise Comparisons		Z-value	Sig. Level
	(I) GOM	(J) GOM		
Curcumin	Initiation	After 2 w.	-5.964	0.000
		After 6 w.	-6.283	0.000
	After 2 w.	After 6 w.	-4.491	0.000
Magic Solution	Initiation	After 2 w.	-5.970	0.000
		After 6 w.	-6.081	0.000
	After 2 w.	After 6 w.	-3.300	0.001
(*) HS: Highly Sig. at P<0.01; Testing are based on the "Wilcoxon Signed Ranks" test.				

Grade of mucositis between study groups:

Table 7 shows the comparison in grade of mucositis between study groups after chemoradiotherapy. After two weeks, 66.7% of patients in curcumin group were graded I compared to 42.3% in magic solution group;

with statistical significance p-value = 0.041. After six weeks, 82.2% of patients in the curcumin group were graded I compared to 60% in the magic solution the group, a statistically significant difference (P=0.02) was seen.

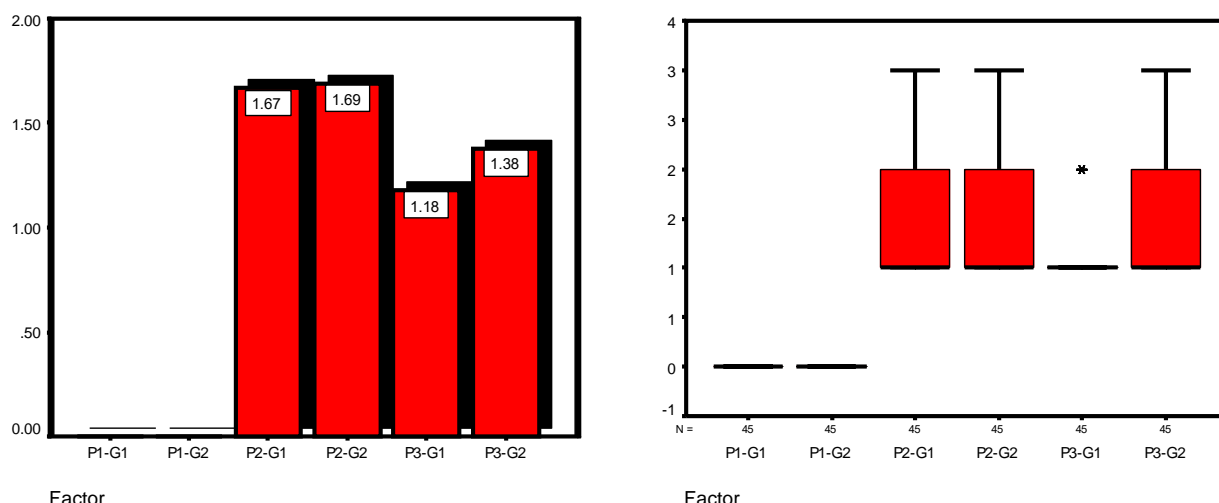


Figure 3. Bar Chart, and stem-leaf plot for exploring behavior of GOM Score reading's distribution along the studied of sequential periods in each group.

Table 7. Comparison between study groups by grade of mucositis.

Grade of mucositis (WHO)	Study group		X ² test	P - Value
	Curcumin (%) n= 45	Magic Solution (%) n= 45		
Two weeks after chemoradiotherapy				
1	30 (66.7)	19 (42.3)	6.351	0.041
2	11 (24.4)	15 (33.3)		
3	4 (8.9)	11 (24.4)		
Six weeks after chemoradiotherapy				
1	37 (82.2)	27 (60.0)	7.75	0.02
2	8 (17.8)	13 (28.9)		
3	0 (0)	5 (11.1)		
WHO: World Health Organization. X ² : chi-square test.				

Discussion

Since it is simpler to apply, absorbs quickly, topical curcumin treatment, in the form of an oral gel, offers several benefits over systemic curcumin because it interacts with surrounding tissues, prolonging the contact period that increases its benefits, and because it has fewer evident bad effects. For individuals suffering from dysphagia or gastrointestinal issues, oral gel formulations may be helpful in reducing side effects (15-17,19). Concurrent chemoradiotherapy causes basal epithelial cell death, which may occur as a result of free radical production.

The activation of second messengers by these free radicals transmits signals from surface receptors on cells to their inner surroundings, leading to an increase in inflammatory cytokines, harm to tissues, and cell death. Macrophages secrete cytokines that promote inflammation, including TNF- α and IL-6, intensify mucosal damage; moreover, a superimposed infection of the ulcerated mucosa might trigger the generation of these pro-inflammatory cytokines (20-22).

TNF- α is a cytokine that promotes inflammation released by macrophages, endothelial cells, and fibroblasts. It is plays an important in the formation and development of OM in in patients with head and neck cancer receiving CCRT. Typically, it goes

undetected in healthy people. However, in cases of inflammation or infection, it is found to be highly concentrated in both serum and tissues. The severity of an infection is correlated with the salivary and serum levels. A wide range of cells have the ability to create $\text{TNF-}\alpha$, such as monocyte/macrophage, neutrophils, natural killer cells (NK), T and B lymphocytes, smooth and cardiac muscle cells, osteoclasts, endothelial cells, fibroblasts (23, 24). Patients with oral cancer had significantly higher

levels of salivary $\text{TNF-}\alpha$, according to Deepthi's research (25). IL-6 is a cytokine that promotes inflammation and an anti-inflammatory myokine secreted by T cells and macrophages when an infection or other kind of tissue injury causes inflammation (26). After chemotherapy drugs have been administered, many investigations showed that nuclear factor $\text{NF-}\kappa\text{B}$ and pro-inflammatory cytokines ($\text{TNF-}\alpha$, interleukin IL-6 and IL-1 β) are altered in both blood and tissue expression (27, 28). Study by Alburgaiba et al. showed patients with HNC had a significant increase in salivary $\text{TNF-}\alpha$ and IL-6 levels, after completing radiation (29). This study demonstrates that the salivary $\text{TNF-}\alpha$ and IL-6 levels are much lower after chemoradiotherapy compared to before, and that the severity of OM is reduced when curcumin oral gel is used, which is in accordance with Sufiawati et al. study indicated that cancer patients receiving chemotherapy induced oral mucositis may benefit from using a magic mouthwash containing curcuma xanthorrhiza, as it dramatically reduced salivary $\text{TNF-}\alpha$ levels (30). Curcumin may be able to suppress $\text{NF-}\kappa\text{B}$, according to Aggarwal et al. reported that curcumin inhibits the expression of several genes controlled by nuclear factor ($\text{NF-}\kappa\text{B}$) (31). These include nitric oxide synthase

(NOS), chemokines, cell surface adhesion molecules, TNF , IL-6, matrix metalloproteinase-9, and cyclooxygenase-2. The anti-inflammatory actions of curcumin are explained by lowering the expression of these genes, which are essential regulators of inflammation (32, 33). Also, in this study the majority of participants using curcumin experienced only mild mucositis grade 1 at the end of the chemoradiotherapy sessions; a few had grades 2 but none had severe mucositis (grades 3 and 4) whereas patients in magic solution group experienced grade 2 and grade 3 mucositis. These findings are in agreement with those of Alsalm et al., 2024 reported that after the completion of radiation treatments, most patients treated with curcumin had no mucositis (grade 0), mild mucositis (grades 1 and 2) occurred in a few of individuals in this group, but severe mucositis (grades 3 and 4) did not (34). And results are consistent with those of the Shah study shown that grade 3 mucositis did not occur in the curcumin group, unlike the control group (1). In addition, Patil's research demonstrated significantly difference between two groups in WHO grades (33). When it comes to reducing the severity of chemoradiotherapy-induced oral mucositis in HNC patients, curcuma long a gel outperformed both chlorhexidine gel (17) and placebo gel (16). Also, results are coincided with the study done by Arun et al., 2020 that the majority of patients in the curcumin group experienced only grade 1 mucositis after four weeks of treatment (35).

Conclusions

Using topical curcumin oral gel compared to magic solution significantly reduced levels of $\text{TNF-}\alpha$ and IL-6 in saliva from patients with HNC undergoing concurrent chemoradiotherapy, suggesting that it effectively prevents and manages oral mucositis caused by concurrent chemoradiation, and could be used as an alternative treatment for this condition.

Recommendations

It was recommended that head and neck cancer patients use curcumin oral gel as a preventive agent

for chemoradiation-induced oral mucositis before concurrent chemoradiotherapy. In addition, a multicenter study is essential to achieve a sufficient sample size and increase the likelihood of obtaining reliable evidence for evaluating biomarkers that assist in treating mucositis. Furthermore, it was recommended that each oncology center should establish a dental unit staffed by highly trained dentists to provide adequate care for patients with oral mucositis and other dental-related disorders during cancer therapy.

Source of funding: No source of funding

Ethical clearance: Approved by a protocol number 934724 by the Research Ethics Committee of the University of Baghdad, College of Dentistry.

Conflict of interest: None

Acknowledgments:

Authors thank Baghdad Center of Radiation Therapy and Nuclear Medicine in Medical City, Baghdad, Iraq and all patients participated in this study.

References

- Shah S, Rath H, Sharma G, Senapati SN, Mishra E. Effectiveness of curcumin mouthwash on radiation-induced oral mucositis among head and neck cancer patients: A triple-blind, pilot randomised controlled trial. *Indian J Dent Res.* 2020Sep-Oct;31(5):718-727. https://doi.org/10.4103/ijdr.IJDR_822_18
- Liu Z, Smart JD, Pannala AS. Recent developments in formulation design for improving oral bioavailability of curcumin: A review. *Journal of Drug Delivery Science and Technology.* 2020;60:102082. <https://doi.org/10.1016/j.jddst.2020.102082>
- Jagiello K, Uchańska O, Matyja K, Jackowski M, Wiatrak B, Kubasiewicz-Ross P, et al. Supporting the Wound Healing Process-Curcumin, Resveratrol and Baicalin in In Vitro Wound Healing Studies. *Pharmaceuticals (Basel).* 2023 Jan6;16(1):82. <https://doi.org/10.3390/ph16010082>
- Jaafar NS, Jaafar IS. Natural Products as A Promising Therapy for SARS COV-2; An Overview. *Iraqi J Pharm Sci.* 2021;30(1):29-40. <https://doi.org/10.31351/vol30iss1pp29-40>
- Ghani BA. Histological evaluation of the effect of topical application of Curcumin powder and essential oil on skin wound healing. *Journal of Baghdad College of Dentistry.* 2015;27(3):58-63. <https://jbcd.uobaghdad.edu.iq/index.php/jbcd/article/view/807>
- Shamash MSA, Zaidan TF. Effect of topical curcumin on the healing of major oral mucosal ulceration. *EurAsian Journal of BioSciences.* 2020;14(2):4653-4660.
- Ramezani V, Ghadirian S, Shabani M, Boroumand MA, Daneshvar R, Saghaei F. Efficacy of curcumin for amelioration of radiotherapy-induced oral mucositis: a preliminary randomized controlled clinical trial. *BMC Cancer.* 2023 Apr 17;23(1):354. <https://doi.org/10.1186/s12885-023-10730-8>
- Idan HM, Motib AS. Incidence of head and neck cancer among Baquba Teaching Hospital Patients. *Diyala Journal of Medicine.* 2024 Oct 25;27(1):86-96. <https://doi.org/10.26505/djm.v27i1.1144>
- Du C, Ying H, Zhou J, Hu C, Zhang Y. Experience with combination of docetaxel, cisplatin plus 5-fluorouracil chemotherapy, and intensity-modulated radiotherapy for locoregionally advanced nasopharyngeal carcinoma. *International Journal of Clinical Oncology.* 2013;18:464-71. <https://doi.org/10.1007/s10147-012-0403-y>
- Baydar M, Dikilitas M, Sevinc A, Aydogdu I. Prevention of Oral Mucositis Due to 5-Fluorouracil Treatment with Oral Cryotherapy. *J Natl Med Assoc.* 2005; 97(8): 1161-1164. <https://pubmed.ncbi.nlm.nih.gov/articles/PMC2575965/>
- Al-Ansari S, Zecha J a. EM, Barasch A, de Lange J, Rozema FR, Raber-Durlacher JE. Oral

- Mucositis Induced By Anticancer Therapies. *Curr Oral Heal Reports*. 2015; 2(4):202–211. <https://doi.org/10.1007/s40496-015-0069-4>
12. Muhammad RT, Alzubaidee AF. Oral complications of cancer medication in hemato-oncologic patients. *Diyala Journal of Medicine*. 2020 Dec.
13. Sonis ST. The pathobiology of mucositis. *Nat Rev Cancer*. 2004; 4(4): 277–84. <https://doi.org/10.1038/nrc1318>
14. Ben Salem M, Affes H, Athmouni K, Ksouda K, Dhouibi R, Sahnoun Z, Hammami S, Zeghal KM. Chemicals Compositions, Antioxidant and Anti-Inflammatory Activity of *Cynara scolymus* Leaves Extracts, and Analysis of Major Bioactive Polyphenols by HPLC. *Evidence-based Complement Altern Med*. 2017; 2017. <https://doi.org/10.1155/2017/4951937>
15. Zhang L, Tang G, Wei Z. Prophylactic and Therapeutic Effects of Curcumin on Treatment- Induced Oral Mucositis in Patients with Head and Neck Cancer: A Meta-Analysis of Randomized Controlled Trials. *Nutr Cancer*. 2021; 73(5): 740-749. <https://doi.org/10.1080/01635581.2020.1776884>
16. Charantimath S. Use of curcumin in radiochemotherapy induced oral mucositis patients: A control trial study. *International Journal of Medical and Health Sciences*. 2016; 10(3): 147-52. <https://pubmed.ncbi.nlm.nih.gov/26436049/>
17. Mansourian A, Amanlou M, Shirazian S, Moosavian JZ, Amirian A. The effect of “Curcuma Longa” topical gel on radiation-induced oral mucositis in patients with head and neck cancer. *Int J Radiat Res*. 2015;13(3):269-74. <https://doi.org/10.5339/jemtac.2024.uncidc.4>
18. Hussein, A.A., Motib, A.S., & Hadi, L.M. "Evaluation of ELISA and HBsAg Rapid Test Cassette Assay in Detection of Hepatitis B Virus." *Journal of Pharmaceutical Sciences and Research* 10.12 (2018): 3157.
19. Budi HS, Anitasari S, Ulfa NM, Juliastuti WS, Aljunaid M, Ramadan DE, Muzari K, Shen YK. Topical Medicine Potency of *Musa paradisiaca* var. *sapientum* (L.) *kuntze* as Oral Gel for Wound Healing: An In Vitro, In Vivo Study. *Eur J Dent*. 2022 Oct;16(4):848-855. <https://doi.org/10.1055/s-0041-1740226>
20. Trucci VM, Veeck EB, Morosolli AR. Current strategies for the management of oral mucositis induced by radiotherapy or chemotherapy. *Rev Odonto Cienc*. 2009;24(3):309–314. <https://revistaseletronicas.pucrs.br/fo/article/view/4854>
21. Sultani M, Stringer AM, Bowen JM, Gibson RJ. Anti-Inflammatory Cytokines: Important Immunoregulatory Factors Contributing to Chemotherapy-Induced Gastrointestinal Mucositis. *Chemother Res Pract*. 2012;2012:1–11. <https://doi.org/10.1155/2012/490804>
22. Lalla R V., Sonis ST, Peterson DE. Management of Oral Mucositis in Patients with Cancer. *Dent Clin North Am*. 2008; 52(1):1–17. <https://doi.org/10.1016/j.cden.2007.10.002>
23. Bradley J. TNF-mediated inflammatory disease. *J Pathol*. 2008; 214: 149–160. <https://doi.org/10.1002/path.2287>
24. Aggarwal BB, Kohr WJ, Hass PE, Moffat B, Spencer SA, Henzel WJ, et al. Human tumor necrosis factor. Production, purification, and characterization. *J Biol Chem*. 1985; 260(4): 2345–2354. <https://pubmed.ncbi.nlm.nih.gov/3871770/>
25. Deepthi G, S R K Nandan, Pavan G Kulkarni. Salivary Tumour Necrosis Factor- α as a Biomarker in Oral Leukoplakia and Oral Squamous Cell Carcinoma. *Asian Pac J Cancer Prev*. 2019;20(7):2087-2093. Published 2019 Jul 1. <https://pubmed.ncbi.nlm.nih.gov/31350970/>
26. Rincon M. Interleukin-6: from an inflammatory marker to a target for inflammatory diseases. *Trends Immunol* 2012; 33: 571-577.

<https://doi.org/10.1016/j.it.2012.07.003>

27. Sakamoto K, Takeda S, Kanekiyo S, Nishiyama M, Kitahara M, Ueno T, Yamamoto S, Yoshino S, Hazama S, Okayama N, Nagano H. Association of tumor necrosis factor- α polymorphism with chemotherapy-induced oral mucositis in patients with esophageal cancer. *Mol Clin Oncol*. 2017;6(1):125–129.

<https://doi.org/10.3892/mco.2016.1081>

28. Steer JH, Kroeger KM, Abraham LJ, Joyce DA. Glucocorticoids Suppress Tumor Necrosis Factor-Alpha Expression By Human Monocytic THP-1 Cells By Suppressing Transactivation Through Adjacent NF- κ B And C-Jun-Activating Transcription Factor- 2 Binding Sites In The Promoter. *J Biol Chem*. 2000;275(24):18432–18440.

<https://doi.org/10.1074/jbc.m906304199>

29. Mohammed H. Alburgaiba, Fawaz D. Al-Aswad, Haider N. Salh. Salivary tumor necrosis factor- α and interleukin-6 in patients with head and neck cancer before and after radiotherapy. *SRP*. (2019), [cited March 29, 2021]; 10(1): 146-150.

<https://dx.doi.org/10.5530/srp.2019.1.27>

30. Sufiawati Irna, Indra Gunawan, Indra Wijaya, Taofik Rusdiana and Anas Subarnas. “Reduction of salivary tumor necrosis factor alpha levels in response to magic mouthwash with Curcuma xanthorrhiza in cancer patients undergoing chemotherapy.” *Journal of Research in Pharmacy* (2018): n. pag.

<https://doi.org/10.12991/jrp.2018.00>

31. Aggarwal BB. Anticancer Potential Of Curcumin: preclinical and clinical studies. *Anticancer Res*. 2003; 23(1A): 363– 398. <https://pubmed.ncbi.nlm.nih.gov/12680238/>

32. van’t Land B, Blijlevens NM a, Marteijs J, Timal S, Donnelly JP, de Witte TJ, M'Rabet L. Role of curcumin and the inhibition of TNF- κ B in the onset of chemotherapy-induced mucosal barrier injury. *Leukemia*. 2004;18(2):

<http://dx.doi.org/10.1177/09636897221086969>

33. Patil K, Guledgud MV, Kulkarni PK, Keshari D, Tayal S. Use of Curcumin Mouthrinse in Radio-Chemotherapy Induced Oral Mucositis Patients: A Pilot Study. *J Clin Diagn Res*. 2015;9(8): ZC59–ZC62.

<https://doi.org/10.7860/JCDR/2015/13034.6345>

34. Alsalim SA, Diajil AR. The effect of curcumin oral gel on radiation- induced oral mucositis in relation to salivary epidermal growth factor. *Journal of Emergency Medicine, Trauma & Acute Care*. 2024(2):4

<http://dx.doi.org/10.5339/jemtac.2024.uncidc.4>

35. Arun P, Sagayaraj A, Azeem Mohiyuddin SM, Santosh D. Role of turmeric extract in minimising mucositis in patients receiving radiotherapy for head and neck squamous cell cancer: a randomised, placebo-controlled trial. *J Laryngol Otol*. Published online February 7, 2020.

<https://doi.org/10.1017/s0022215120000316>

جل الكركمين الفموي وعلاقته بعامل نخر الورم اللعابي ألفا وإنترلوكين ٦ المستخدم في علاج التهاب الغشاء المخاطي الفموي لدى مرضى سرطان الرأس والرقبة الذين يخضعون للعلاج الكيميائي الإشعاعي المتزامن

^١ رؤى شاكور فرحان ، ^٢ فواز داود الاسود

الملخص

الخلفية: يُعد هلام الكركمين الفموي أحد الأمثلة على الأدوية العشبية التقليدية، وقد أظهر إمكانات في العديد من الاستخدامات الصيدلانية. التهاب الغشاء المخاطي للفم عادة ما يمنع ويعالج باستخدام المحلول السحري ، وهو غسول للفم يحتوي على مزيج من الأدوية. عامل نخر الورم ألفا وإنترلوكين-٦، هما ساييتوكينات لعابية، تحفز الاستجابة المناعية وتعزز الالتهاب أثناء العدوى أو تلف الأنسجة الأخرى الذي يسبب الالتهاب

الأهداف: تحديد تأثير هلام الكركمين الفموي على مستويات عامل نخر الورم ألفا وإنترلوكين-٦ في اللعاب لدى مرضى سرطان الرأس والرقبة الذين يتلقون العلاج الكيميائي الإشعاعي المتزامن الناجم عنه التهاب الغشاء المخاطي الفموي.

المرضى والطرق: أجريت الدراسة على مجموعتين، كل مجموعة تضم خمسة وأربعين مريضاً، بإجمالي تسعين مريضاً بسرطان الرأس والرقبة يتلقون العلاج الكيميائي الإشعاعي المتزامن. مقايسة الممتز المناعي المرتبط بالإنزيم قاس مستويات عامل نخر الورم ألفا وإنترلوكين-٦ في اللعاب. قُيِّم التهاب الغشاء المخاطي الفموي وفقاً لمقياس منظمة الصحة العالمية.

النتائج: أظهر المرضى الذين تناولوا جل الكركمين الفموي التهاباً أقل حدة في الغشاء المخاطي الفموي، ومستويات أقل من عامل نخر الورم ألفا وإنترلوكين-٦ في اللعاب. أظهر مقياس منظمة الصحة العالمية بين المجموعتين اختلافات كبيرة عند أسبوعين ($P = 0.041$) و ٦ أسابيع ($P = 0.02$).

الاستنتاج: خلصت الدراسة إلى أن جل الكركمين الفموي قد يخفض مستويات عامل نخر الورم ألفا وإنترلوكين-٦ في اللعاب، وقد يُستخدم كعلاج بديل لالتهاب الغشاء المخاطي الفموي الناتج عن العلاج الكيميائي والإشعاعي.

الكلمات المفتاحية: سرطان الرأس والرقبة، العلاج الكيميائي والإشعاعي المتزامن، التهاب الغشاء المخاطي الفموي، الكركمين، عامل نخر الورم ألفا، الإنترلوكين-٦.

المؤلف المراسل: رؤى شاكور فرحان

الابميل: dr.rouaa.alkhaledy@gmail.com

تاريخ الاستلام: ١٤ كانون الأول ٢٠٢٤

تاريخ القبول: ١٩ آذار ٢٠٢٥

تاريخ النشر: ٢٥ نيسان ٢٠٢٥

^{٢٠١} كلية طب الاسنان - جامعة بغداد - بغداد - العراق.

Articular Eminence Inclination and Glenoid Fossa Measurements by CBCT in Patients with Temporomandibular Joint Disorders

Hayder Mahdi Idan ¹, Fawaz D. Al-Aswad ²

¹ Department of Clinical Dental sciences, College of Dentistry, University of Diyala, Diyala, Iraq.

² College of Dentistry, University of Baghdad, Baghdad, Iraq.

OPEN ACCESS

Correspondence: Hayder Mahdi Idan
Email: haider.m@uodiyala.edu.iq
Copyright: ©Authors, 2025, College of Medicine, University of Diyala. This is an open access article under the [CC BY 4.0](http://creativecommons.org/licenses/by/4.0/) license (<http://creativecommons.org/licenses/by/4.0/>)
Website: <https://djm.uodiyala.edu.iq/index.php/djm>

Received: 09 November 2024
Accepted: 14 February 2025
Published: 25 April 2025

Abstract

Background: The increasing frequency of temporomandibular joint dysfunction requires the promotion of diagnostic and therapeutic approaches. The several etiologies of dysfunction are still poorly understood. Numerous studies have talked articular eminence shape as a probable causative factor for this dysfunction.

Aims of the study: The aim of this study was to measure of articular eminence inclination, depth of glenoid fossa and width by cone beam computed tomography in patients with temporomandibular joint disorder conferring gender and side and compared with healthy control.

Patients and Methods: Study samples embraced of fifty-five individuals (110 joints), were twenty patients with intra articular disorders of temporomandibular joint, fifteen patients with degenerative disorders of temporomandibular joint and twenty control group with age range from (20-55) years old.

Results: The results display females appear to stay more affected by disorders of temporomandibular joint. The articular eminence inclination showed higher mean value in the right side than left side and in males than females. Also, glenoid fossa depth and width was higher mean value in the right side than left side and in males than females. The results recorded mean value of articular eminence inclination in control group higher than patients with temporomandibular joint disorders, while mean value of glenoid fossa depth and width in control group less than patients with temporomandibular joint disorders.

Conclusion: Females look to be more affected by temporomandibular joint disorders. The glenoid fossa width and depth were also less in the control individuals.

Keywords: Articular eminence, Glenoid fossa, Depth, Cone beam computed tomography.

Introduction

The complex articular system identified as temporomandibular joint (TMJ) is positioned between jaw and temporal bone. Bony components of the TMJ, amongst other effects, have an important impact on how much the mandible moves (1). The mandibular condyle, articular eminence, which is a constituent of the temporal bone, and the glenoid fossa make up the bony portions of the joint. (2). The mandibular ramus connects to the condylar process, an ellipsoid hard tissue (bony structure) with a thin neckline. One significant anatomical feature of the mandible is the condylar processes,

which are accountable for the sagittal and vertical development of the mandibular bone (3). The condyle is essential to move anteriorly and inferiorly more when articular eminence is steeper. As a consequence, as the jaw opens, the condyle, mandible, and mandibular arch move more vertically (4). The zone of temporal fossa across which condyle-disk complex moves while acting different mandibular movements is known as the articular eminence. It is frequently disorganized with the articular tubercle, a totally dissimilar feature (4). Articular section of the squamous segment of temporal bone is entitled articular fossa. Consuming the articular eminence vertex as an indication point, the articular fossa shows a medium depth for female patients (4.34 mm) and for male patients (4.73 mm) (5). Condyle and articular disc compound slide below the articular eminence (AE) during the opening and closing of the mouth. That movement is finished possible by the morphology of the AE; it varies from individual to individual and may alter according on factors such as sex, age and masticatory function (6). The formation of inside problems and bone changes conferring to the useful load in this zone, beside individual factors like age and gender, have been clarified by the morphology of TMJ bone components (7-9). The normal variety for this inclination's degree measurement is amongst 30 and 60 degrees (10). AEs are considered as flat beneath 30 degrees and steep beyond 60 degrees, (11) and internal articulation abnormalities seem to be linked with both classes. Degenerative bone illnesses in both the AE and the condyle may consequence from these conditions (10). There is controversy concerning the linking between temporomandibular joint disorder (TMD) and TMJ morphology. While some research has revealed evidence directing to higher articular eminence as a probable risk factor for TMD, other studies have not been able to document

this issue. Furthermore, numerous research displays that healthy control group had a higher slope than TMD patients (12). Cone-beam computed tomography (CBCT) is beneficial for oral and maxillofacial demands because of its fast image time and high-resolution images. CBCT is effective for a variety of conditions, including TMJ disorders (13,14). There are no sufficient studies display the association among the width and depth of glenoid fossa and incidence of TMD. This study was designed to determine the association between the inclination of articular eminence, width of glenoid fossa and depth in TMD patients and controls without symptom via CBCT in Diyala population.

Patients and Methods

The study samples composed of fifty-five individuals (110 joints), twenty patients with intra articular disorders of TMJ (8 male and 12 females), fifteen patients with degenerative disorders of TMJ (4 male and 11 females) and twenty control group (8 male and 12 females) with age range from (20-55) years old. Conferring to the Diagnostic Criteria for Temporomandibular Disorders (15) temporomandibular joint disorders were clinically diagnosed and their control group who came the dental center for scanning of cone beam computed tomography for many investigative purposes did not consume TMD based on a clinical investigation. All patients and control involved in this study with normal occlusion, non-edentulous patients, no history of trauma, no facial asymmetry, no fracture and no cystic lesion of TMJ. The depth of glenoid fossa and width were measured based on methods defined by Paknahad et al. (12) via calculating the perpendicular distance among uppermost point of glenoid fossa and line extend from posterior glenoid process to the utmost lower point on the AE, the depth of glenoid fossa was measured. Distance between

posterior glenoid process and utmost inferior point on the AE was used to fix glenoid fossa width (Figure 1). The inclination of the AE was measured based on the methods labeled by Abdul-Nabi and Al-Nakib (1) the inclination of eminence was measured in two pathways. Firstly, Best-fit line method: - In the sagittal section, the posterior surface of the eminence was drowned. The horizontal Frankfort plane was also, drew. The angle designed between these two planes in the sagittal section, was measured and referred to as eminence inclination. This procedure was applied to the sides (left and right) Figure 2. Secondly, Top-roof line method: - Angle between the horizontal plane (Frankfort) in sagittal section and plane that passes through the points (the uppermost point of fossa and lowermost point of articular eminence) is recognized as articular eminence inclination. For both sides (left and right) Figure 3.

Statistical analysis

In this investigation, the t-test was applied to comparison means statistically via program of Statistical Analysis System (SAS) (2018), the effect of the control and patient groups'

differences in the study parameters were determined.

Results

Distribution of sample study according to gender and location: The results showed females look to be more affected by TMD, out of 55 cases 12 (60.00%) intra articular disorders and 11 (73.33%) degenerative disorders as shown in Table 1.

Table 1. Distribution of sample study according difference gender in difference groups.

Factors		Male No (%)	Female No (%)	P-value
Groups	Control (No. =20)	8 (40.00%)	12 (60.00%)	0.371 NS
	Intra articular disorders (No. =20)	8 (40.00%)	12 (60.00%)	0.371 NS
	Degenerative disorders (No. =15)	4 (26.67%)	11 (73.33%)	0.0488 *
P-value		0.445 NS	0.969 NS	---
* (P≤0.05), NS: Non-Significant.				

In the existing study articular eminence inclination by two methods, have higher mean value in the right side than left side and in males than females. Also, glenoid fossa depth and width have higher mean value in the right side than left side and in males than females as shown in Table 2.

Table 2. Comparison between control, intra articular and degenerative disorders groups according to gender and side.

Group		Top roof		Best fit		Glenoid fossa height		Glenoid fossa width	
		Right°	Left°	Right°	Left°	Right	Left	Right	Left
Control	Male	39.21 ±2.05 a	38.86 ±2.18 a	57.68 ±2.72 a	53.95 ±3.29 a	10.70 ±0.56 a	9.43 ±0.72 b	20.42 ±1.04	20.28 ±1.27
	Female	37.66 ±1.87 ab	36.15 ±2.06 ab	55.26 ±2.44 ab	50.75 ±2.68 b	8.45 ±0.62 b	8.38 ±0.60 b	18.22 ±0.79	18.11 ±0.87
Intra articular disorders	Male	35.73 ±1.39 b	35.31 ±1.81 b	53.48 ±3.07 bc	51.67 ±1.98 ab	10.91 ±0.73 a	10.73 ±0.75 a	20.68 ±1.15	19.68 ±1.28
	Female	35.39 ±1.62 b	33.88 ±1.59 bc	50.18 ±2.84 cd	49.92 ±2.07 b	10.44 ±0.64 ab	10.14 ±0.81 ab	19.03 ±0.94	18.70 ±1.07
Degenerative disorders	Male	35.57 ±1.27 b	36.15 ±2.02 ab	54.35 ±2.27 ab	52.20 ±2.61 ab	10.32 ±0.71 ab	10.3 ±0.76 ab	19.67 ±1.15	19.12 ±2.37
	Female	32.1 ±1.08 c	31.60 ±1.26 c	47.18 ±2.37 d	45.32 ±2.35 c	9.70 ±0.62 ab	9.04 ±0.71 ab	18.94 ±0.92	18.76 ±1.28
Mean	Total	35.84 ±1.75 b	35.02 ±1.53 b	52.56 ±3.01 bc	50.19 ±2.09 b	9.95 ±0.70 ab	9.53 ±0.80 ab	19.32 ±0.87	18.99 ±1.53
LSD		3.062 **	2.977 **	3.473 **	2.637 *	2.216 *	1.955 *	2.704 NS	2.544 NS
P-value		0.0057	0.0039	0.00314	0.0192	0.0369	0.0377	0.268	0.251
Means having with the different letters in same column differed significantly * (P≤0.05), ** (P≤0.01), NS: Non-Significant.									

Articular eminence inclination and glenoid fossa (height and width) in different groups:

The results showed inclination of articular eminence by two methods (top roof and best fit) in both sides (right and left), control group have documented mean value (right 38.28 °, left 37.24 °) (right 56.23 °, left 52.03 °), higher than patients with intra articular disorders (right 35.53°, left 34.45°) (right 51.50°, left 50.62°), as shown in Table 3.

The results showed articular eminence inclination by two methods (top roof and best fit) in both sides (right and left), control group have documented mean value (right 38.28 °, left 37.24 °) (right 56.23 °, left 52.03 °), higher than patients with degenerative disorders (right 33.02°, left 32.81°) (right 49.09°, left 47.16°), as shown in table 3. The results showed articular eminence inclination by two methods (top roof and best fit) in both sides (right and left), intra articular disorders have documented higher mean value (right 35.53 °, left 34.45 °) (right

51.50 °, left 50.62 °), then patients with degenerative disorders (right 33.02°, left 32.81°) (right 49.09°, left 47.16°), as shown in Table 3.

Glenoid fossa height and width in both sides (right and left), mean value of control group (right 9.35 mm, left 8.81mm) (right 19.10 mm, left 18.98 mm) have recorded less than patients with intra articular disorders (right 10.63 mm, left 10.38mm) (right 19.69 mm, left 19.10 mm), as shown in table 3. Regarding to glenoid fossa height in both sides (right and left), control group have verified less mean value (right 9.35mm, left 8.81mm), than patients with degenerative disorders (right 9.87mm, left 9.38mm), as shown in table 3. Regarding to glenoid fossa height and width in both sides (right and left), intra articular disorders has documented higher mean value (right 10.63 mm, left 10.38 mm) (right 19.69 mm, left 19.10 mm), than patients with degenerative disorders (right 19.69 mm, left 19.10 mm) (right 19.14 mm, left 18.86 mm), as shown in Table 3.

Table 3. Comparison between difference groups in articular eminence inclination, glenoid fossa height and width.

Group	Top roof		Best fit		Glenoid height		Glenoid width	
	Right	Left	Right	Left	Right	Left	Right	Left
Control	38.28 ±0.92 a	37.24 ±0.64 a	56.23 ±0.61 a	52.03 ±1.36 a	9.35 ±0.34 b	8.81 ±0.39 b	19.10 ±0.43	18.98 ±0.53
Intra articular disorders	35.53 ±0.77 b	34.45 ±0.89 b	51.50 ±1.56 b	50.62 ±1.52 ab	10.63 ±0.19 a	10.38 ±0.16 a	19.69 ±0.46	19.10 ±0.31
Degenerative disorders	33.02 ±0.91 b	32.81 ±1.38 b	49.09 ±1.34 b	47.16 ±1.46 b	9.87 ±0.28 ab	9.38 ±0.26 b	19.14 ±0.44	18.86 ±0.60
LSD	2.507 **	2.717 **	3.532 **	4.193 *	0.804 **	0.849 **	1.289 NS	1.377 NS
P-value	0.0006	0.0074	0.0007	0.050	0.0059	0.0010	0.570	0.943
Means having with the different letters in same column differed significantly. * (P≤0.05), ** (P≤0.01), NS: Non-Significant.								

The results showed inclination of articular eminence by two methods (top roof and best fit) in both sides, control group have documented higher than in patients with intra articular disorders with a statistically significant relationship as shown in Table 4. The results showed articular eminence inclination by two methods (top roof and best fit) in both sides, control group have documented higher than patients with degenerative disorders, with a statistically highly significant relationship as

shown in Table 4. Glenoid fossa height in both sides, control has recorded less than patients with intra articular disorders with a statistically highly significant relationship as shown in Table 4. The CBCT picture shows the measurements depth and width of glenoid fossa in the sagittal section as in Figure 1. The CBCT picture shows the measurements of articular eminence inclination (Best-fit line method) and (Top-roof line method) in the sagittal section as in Figure 2, and Figure 3.

Table 4. Comparison between control, intra articular and degenerative disorders groups in parameters study.

Groups			T-test (right)	P-value (right)	T-test (left)	P-value (left)
Top roof	Control	Intra articular	2.45 *	0.0283	2.21 *	0.0152
		Degenerative	2.71 **	0.0004	2.86 **	0.0034
	Intra articular	Degenerative	2.430 *	0.0439	3.205 NS	0.305
Best fit	Control	Intra articular	3.40 **	0.0076	4.14 NS	0.495
		Degenerative	2.76 **	0.0001	4.120 *	0.0218
	Intra articular	Degenerative	4.371 NS	0.269	4.417 NS	0.120
Glenoid fossa height	Control	Intra articular	0.797 **	0.0025	0.861 **	0.0007
		Degenerative	0.942 NS	0.277	1.036 NS	0.267
	Intra articular	Degenerative	0.670 *	0.027	0.608 **	0.0021
Glenoid fossa width	Control	Intra articular	1.278 NS	0.356	1.247 NS	0.853
		Degenerative	1.283 NS	0.956	1.643 NS	0.878
	Intra articular	Degenerative	1.338 NS	0.405	1.279 NS	0.705
* (P≤0.05), ** (P≤0.01), NS: Non-Significant.						

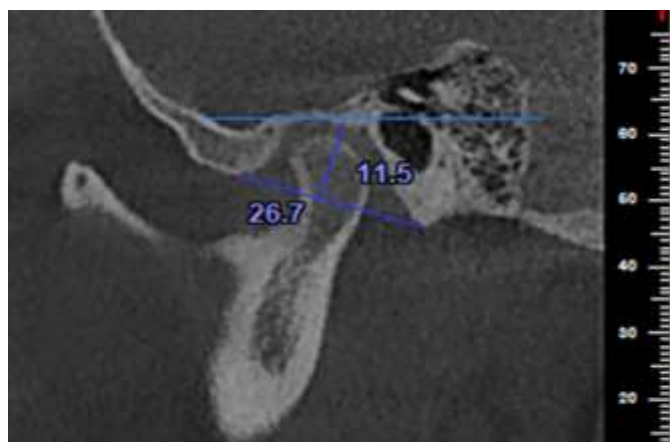


Figure 1. CBCT showed the measurements depth and width of glenoid fossa.

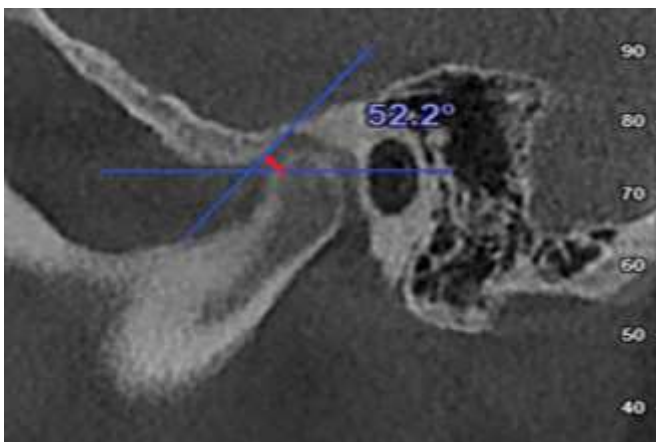


Figure 2. CBCT showed the measurements of articular eminence inclination (Best-fit line method).

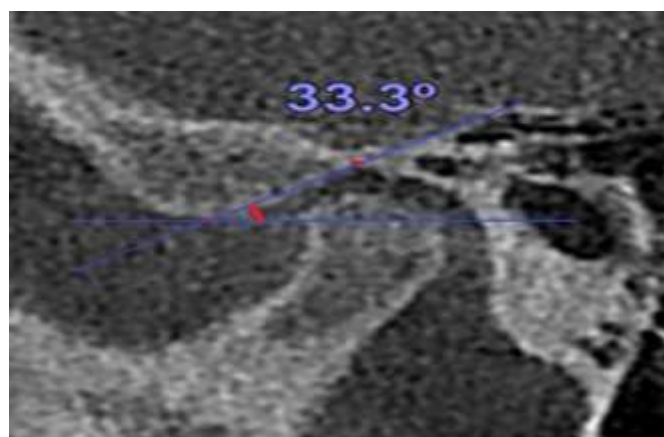


Figure 3. CBCT showed the measurements of articular eminence inclination (Top-roof line method).

Discussion

Several researches have looked into the linking between the morphometric and morphological variances of TMJ and pathological changes constructed on age and gender (6,16).

Disorders of TMJ look to be more affected by females in the current study as numerous authors have designated a female preference of symptoms and signs connected with TMDs, this may be produced by androgenic hormones (17). In the current study glenoid fossa depth have higher mean value in intra articular disorders group followed by degenerative disorders and then control group and the right side more than left side, this agrees with other investigations

(18) they detailed that associated to the left fossa, the right fossa was deeper. Similarly, to investigate of Paknahad et al., (12) current research found that fossa depth in TMD group was higher than in control group. Also, similar to research of Paknahad et al., (12) the existing study found that fossa depth in females was lesser than those of males. These findings support sexual dimorphism, which may be associated to gender-specific differences in the quantity of masticatory force acting on the joint. Paknahad et al., (12) also, signifying larger width of fossa in the TMD group related to control group, which is constant with the existing results. Opposing to current results, Alkhader et al., (19)

projected that TMJs with osseous anomalies had lesser fossa widths than TMJs without such abnormalities. These controversies may result from variations in imaging modalities, measurement methods, sample sizes, age distributions, and other population differences. In the existing study the articular eminence inclination was found to be higher in the control group than in patient group. This correspondence with the study finished by Çağlayan et al., and Sümbüllü et al., (8,20) They display that control group had a steeper eminence inclination. This might be explained by fact that mandibular movement is affected by AE characteristics, such as shape, and that mandibular movement is additional conditioned by dental absence, (11,21) age, (11,22) skeletal malocclusion, (9) gender, and masticatory loading. (23) The mandibular condyle's shape and degenerative bone disorders may possibly have an influence on AEI (24). The existing study disagrees with several other investigations (25,26). They display that the eminence slope in the TMD group was steeper than in the symptom-free group.

Conclusions

Females look to be more affected by temporomandibular joint disorders, and articular eminence inclination in the control group is higher than patients with temporomandibular joint disorders. The glenoid fossa width and depth were also less in the control individuals.

Recommendations

More patients with temporomandibular joint disorders are involved in a recent study. Study other measurements of the TMJ and determine their relationship to joint diseases.

Source of funding: No source of funding.

Ethical clearance: The Scientific and Ethical Committee of the College of Medicine at the University of Diyala approved this study with

Code No. (2024HMI866).

Conflict of interest: None.

Acknowledgments:

Many thanks to everyone who contributed and cooperated in completing this research and to all members of the staff of second specialized dental center in Diyala city, Iraq.

References

1. Abdul-Nabi L.A, Al-Nakib L.H, flattening of the posterior slope of the articular eminence of completely edentulous patients compared to patients with maintained occlusion in relation to age using computed tomography. J Bagh Coll Dentistry 2015; 27(2):66-71. <http://dx.doi.org/10.12816/0015297>
2. Idan, H. M., & Al-Aswad, F. D. (2020). Measurements of Horizontal condylar inclination by using Cadiax compactII in patients with TMJ clicking before and after different treatments modalities. Medico-legal Update, 20(1), 1071. <http://dx.doi.org/10.37506/v20/i1/2020/mlu/194443>
3. Idan, H. M. (2024). The effect of gender and site on the condylar head measurements in Diyala. Diyala Journal of Medicine, 26(2), 80-89. <https://doi.org/10.26505/djm.v26i2.1099>
4. Chaurasia, A., Katheriya, G., & Patil, R. (2016). Morphometric analysis of articular eminence of temporomandibular joint in Indian Ethnicity-A cone beam computed tomography study. Journal of oral medicine, oral surgery, oral pathology and oral radiology, 2(4), 196-202. <http://10.0.71.55/2395-6194.2016.0001>
5. de Pontes MLC, Melo SLS, Bento PM, Campos PSF, de Melo DP. Correlation between temporomandibular joint morphometric measurements and gender, disk position, and condylar position. Oral Surg Oral Med Oral Pathol Oral Radiol 2019;128:538-42. <http://10.1016/j.oooo.2019.07.011>.

6. Saione Cruz SA, Saulo Leonardo Sousa MELO, Daniela Pita de MELO, Deborah Queiroz FREITAS, Paulo Sérgio Flores CAMPOS. Relationship between articular eminence inclination and alterations of the mandibular condyle: a CBCT study. *Braz. Oral Res.* 2017;31:e25: <http://doi.org/10.1590/1807-3107BOR-2017.vol31.0025>.
7. Ejima K, Schulze D, Stippig A, Matsumoto K, Rottke D, Honda K. Relationship between the thickness of the roof of glenoid fossa, condyle morphology and remaining teeth in asymptomatic European patients based on cone beam CT data sets. *Dentomaxillofac Radiol.* 2013;42(3):90929410. <https://doi.org/10.1259/dmfr/90929410>
8. Çağlayan F, Sümbüllü MA, Akgül HM. Associations between the articular eminence inclination and condylar bone changes, condylar movements, and condyle and fossa shapes. *Oral Radiol.* 2014;30(1):84-91. <https://doi.org/10.1007/s11282-013-0149-x>
9. İlgüy D, İlgüy M, Fişekçioğlu E, Dölekoğlu S, Ersan N. Articular eminence inclination, height, and condyle morphology on cone beam computed tomography. *Sci World J.* Volume 2014, Article ID 761714, 6 pages. <https://doi.org/10.1155/2014/761714>
10. Ozkan A, Altug HA, Sencimen M, Senel B. Evaluation of articular eminence morphology and inclination in TMJ internal derangement patients with MRI. *Int J Morphol.* 2012;30(2):740-4. <https://doi.org/10.4067/S0717-95022012000200064>
11. Katsavrias EG. Changes in articular eminence inclination during the craniofacial growth period. *Angle Orthod.* 2002;72(3):258-64. [https://doi.org/10.1043/00033219\(2002\)0722.0.CO;2](https://doi.org/10.1043/00033219(2002)0722.0.CO;2)
12. Paknahad M, Shahidi S, Akhlaghian M, and Abolvardi M. Is Mandibular Fossa Morphology and Articular Eminence Inclination Associated with Temporomandibular Dysfunction? *J Dent (Shiraz).* 2016 Jun; 17(2): 134–141. PMID: PMC4885671; PMID: 27284559.
13. Katayama K, Yamaguchi T, Sugiura M, Haga S, Maki K. Evaluation of mandibular volume using tomography cephalometric cone-beam and computed correlation values. with Angle Orthod. 2014;84:337–342. <http://doi.org/10.2319/012913-87.1>
14. Nakawaki T, Yamaguchi T, Tomita D, et al. Evaluation of mandibular volume classified by vertical skeletal dimensions with cone-beam computed tomography. *Angle Orthod.* 2016;86:949–954. <http://doi.org/10.2319/103015-732.1>
15. Schiffman E., Ohrbach R., Truelove, E., Look, J., Anderson, G., Goulet, J.P., List, T. Svensson, P., et al., Diagnostic criteria for temporomandibular disorders (DC/TMD) for clinical and research applications: recommendations of the International RDC/TMD Consortium Network and Orofacial Pain Special Interest Group. *Journal of oral & facial pain and headache*, 2014; 28(1):6-27. <http://doi.org/10.11607/jop.1151>
16. Ahmed NF, Samir SM, Ashmawy MS, et al. Cone beam computed tomographic assessment of mandibular condyle in Kennedy class I patients. *Oral Radiol* 2020;36:356-64. <http://doi.org/10.1007/s11282-019-00413-1>
17. Coombs, M. C., Bonthius, D. J., Nie, X., Lecholop, M. K., Steed, M. B., & Yao, H. (2019). Effect of measurement technique on TMJ mandibular condyle and articular disc morphometry: CBCT, MRI, and physical measurements. *Journal of Oral and Maxillofacial Surgery*, 77(1), 42-53. <http://doi.org/10.1016/j.joms.2018.06.175>
18. Jasinevicius T.R., Pyle M.A,

Lalumandier J.A., Nelson S., Kohrs K.J., Türp J.C., Asymmetry of the Articular Eminence in Dentate and Partially Edentulous Populations: the Journal of Craniomandibular Practice 24(2):85-94 May 2006.

<http://doi.org/10.1179/crn.2006.014>

19. Alkhader M, Al-Sadhan R, Al-Shawaf R. Cone-beam computed tomography findings of temporomandibular joints with osseous abnormalities. Oral Radiology. 2012; 28: 82–86.

<http://doi.org/10.1007/s11282-012-0094-0>

20. Sümbüllü MA, Çağlayan F, Akgül HM, Yilmaz AB. Radiological examination of the articular eminence morphology using cone beam CT. Dentomaxillofac Radiol. 2012; 41: 234–240.

<http://doi.org/10.1259/dmfr/24780643>

21. Kwon, O.K.; Yang, S.W.; Kim, J.H. Correlation between sagittal condylar guidance angles obtained using radiographic and protrusive occlusal record methods. J. Adv. Prosthodont. 2017, 9, 302–307.

<http://doi.org/10.4047/jap.2017.9.4.302>

22. Arieta-Miranda, J.M.; Silva-Valencia, M.; Flores-Mir, C.; Paredes-Sampen, N.A.; Arriola-Guillen, L.E. Spatial analysis of condyle position according to sagittal skeletal relationship, assessed by cone beam computed tomography. Prog. Orthod. 2013, 14, 36.

<http://doi.org/10.1186/2196-1042-14-36>

23. Costa, E.D.D.; Peyneau, P.D.; Roque-Torres, G.D.;

Freitas, D.Q.; Ramírez-Sotelo, L.R.; Ambrosano, G.M.B.; Verner, F.S. The relationship of articular eminence and mandibular fossa morphology to facial profile and gender determined by cone beam computed tomography. Oral Surg. Oral Med. Oral Pathol. Oral Radiol. 2019, 128, 660–666.

<http://doi.org/10.1016/j.oooo.2019.07.007>

24. Al-Saleh, M.A.; Alsufyani, N.A.; Saltaji, H.; Jaremko, J.L.; Major, P.W. MRI and CBCT image registration of temporomandibular joint: A systematic review. J. Otolaryngol. Head Neck Surg. 2016, 45, 30.

<http://doi.org/10.1186/s40463-016-0144-4>

25. Sülün T, Cemgil T, Duc JM, Rammelsberg P, Jäger L, Gernet W. Morphology of the mandibular fossa and inclination of the articular eminence in patients with internal derangement and in symptom-free volunteers. Oral Surg Oral Med Oral Pathol Oral Radiol Endod. 2001; 92: 98–107.

<http://doi.org/10.1067/moe.2001.114621>

26. Sato S, Kawamura H, Motegi K, Takahashi K. Morphology of the mandibular fossa and the articular eminence in temporomandibular joints with anterior disk displacement. Int J Oral Maxillofac Surg. 1996; 25: 236–238.

[http://doi.org/10.1016/s0901-5027\(96\)80037-3](http://doi.org/10.1016/s0901-5027(96)80037-3)

الميل المفصلي وقياسات الحفرة الحقائية بواسطة التصوير المقطعي المحوسب بالحزمة المخروطية في المرضى الذين يعانون من اضطرابات المفصل الصدغي الفكي

^١ حيدر مهدي عيدان ، ^٢ فواز داود الاسود

الملخص

الخلفية: إن التكرار المتزايد لخلل المفصل الصدغي الفكي يتطلب تعزيز الأساليب التشخيصية والعلاجية. لا تزال مسببات الخلل الوظيفي المتعددة غير مفهومة جيداً. لقد تحدثت العديد من الدراسات عن شكل البروز المفصلي كعامل مسبب محتمل لهذا الخلل الوظيفي.

الأهداف: كان الهدف من هذه الدراسة هو قياس ميل البروز المفصلي وعمق الحفرة الحقائية وعرضها بواسطة التصوير المقطعي المحوسب بالحزمة المخروطية في المرضى الذين يعانون من اضطرابات المفصل الصدغي الفكي الذي يمنح الجنس والجانب ومقارنتها مع السيطرة الصحية.

المرضى والطرق: عينات الدراسة شملت خمسة وخمسين فرداً (١١٠ مفصل)، عشرين مريضاً يعانون من اضطرابات داخل المفصل في المفصل الفكي الصدغي، وخمسة عشر مريضاً يعانون من اضطرابات تنكسية في المفصل الفكي وعشرين مجموعة ضابطة تتراوح أعمارهم بين (٢٠-٥٥) سنة.

النتائج: أظهرت النتائج أن الإناث يبدون أكثر تأثراً باضطرابات المفصل الصدغي الفكي. أظهر ميل البروز المفصلي قيمة متوسطة أعلى في الجانب الأيمن من الجانب الأيسر وعند الذكور مقارنة بالإناث. كما أن عمق وعرض الحفرة الحقائية كان أعلى في الجانب الأيمن منه في الجانب الأيسر وفي الذكور منه في الإناث. سجلت النتائج متوسط قيمة ميل البروز المفصلي في المجموعة الضابطة أعلى من المرضى الذين يعانون من اضطرابات المفصل الصدغي الفكي، في حين أن متوسط قيمة عمق وعرض الحفرة الحقائية في المجموعة الضابطة أقل من المرضى الذين يعانون من اضطرابات المفصل الصدغي الفكي.

الاستنتاج: يبدو أن الإناث أكثر تأثراً باضطرابات المفصل الصدغي الفكي. كان عرض الحفرة الحقائية وعمقها أقل أيضاً لدى أفراد التحكم.

الكلمات المفتاحية: البروز المفصلي، الحفرة الحقائية، العمق، التصوير المقطعي المحوسب بالحزمة المخروطية.

المؤلف المراسل: حيدر مهدي عيدان

الايمل: haider.m@uodiyala.edu.iq

تاريخ الاستلام: ٩ تشرين الثاني ٢٠٢٤

تاريخ القبول: ١٤ شباط ٢٠٢٥

تاريخ النشر: ٢٥ نيسان ٢٠٢٥

^١ كلية طب الاسنان – جامعة ديالى – ديالى - العراق.

^٢ كلية طب الاسنان – جامعة بغداد – بغداد - العراق.

Comparison of Muscle to Nodule Strain Ratio Elastography with Parenchyma to Nodule Strain Ratio Elastography in Suspicious Thyroid Nodules

Zainab Faisal Atiyah ¹, Mohammed M.J. Al-khalissi ²

¹ Al Imamein Al Kadhimein medical city, Baghdad, Iraq.

² Department of Radiotechnology, AL-Hadi University College, Baghdad, Iraq.

OPEN ACCESS

Correspondence: Zainab Faisal Atiyah
Email: Zainab.faisal137@gmail.com
Copyright: ©Authors, 2025, College of Medicine, University of Diyala. This is an open access article under the [CC BY 4.0](http://creativecommons.org/licenses/by/4.0/) license (<http://creativecommons.org/licenses/by/4.0/>)
Website:
<https://djm.uodiyala.edu.iq/index.php/djm>

Received: 17 July 2024
Accepted: 08 January 2025
Published: 25 April 2025

Abstract

Background: Ultrasound elastography (USE) is a non-invasive technique for distinguishing benign from malignant thyroid nodules. It uses strain ratio to determine thyroid nodular stiffness, however it has limitations when no normal thyroid tissue is present.

Objective: To assess the diagnostic performance of USE in the prediction of malignant thyroid nodules by assessing the strain ratio comparing the normal thyroid tissues as a reference and sternocleidomastoid muscle as a second reference.

Patients and Methods: The study was conducted on 33 patients with single TIRADS III or IV nodules at Al-Imamein Al-Kadhimein Medical City in Baghdad-Iraq for 5 months (August 25th, 2020 to January 15th, 2021), using both gray scale and real-time USE on a Voluson- E6 Ultrasound machine. Final diagnosis has been obtained by cytology and/or histopathology.

Results: The study involved a total of 33 patients, with 78.8% female and 21.2% male. Of these, 72.7% were benign, and 27.3% were malignant. The thyroid nodules were hypoechoic, taller, and micro calcified. The parenchymal-nodular SR of all thyroid nodules ranged from 0.55-6.0, while the muscle-nodular SR ranged from 0.42-5.25. The best (strain ratio) SR cutoff value was (≥ 3.63) for parenchymal-nodular SR, with sensitivity, specificity, and accuracy rates were 100%, 85%, and 89.2%, respectively.

Conclusion: The study found that sternocleidomastoid muscle has high sensitivity, specificity, and accuracy in predicting thyroid malignancy and differentiating benign from malignant nodules so making it safe for use in certain cases.

Keywords: Elastography, Thyroid nodules, Strain ratio, Muscle.

Introduction

Thyroid nodules are a prevalent concern in the general population, with an incidence of 5% in women and 1% in men in iodine-sufficient areas, and 19-68% detected using high-resolution ultrasound (1,2) Most thyroid nodules remain benign, with only 5% existence malignant (3). Diagnosing benign or malignant thyroid nodules is crucial for treatment. Fine needle aspiration biopsy (FNAB) is recommended for the diagnosis but has limitations (4). Ultrasound perceives thyroid nodules, their location, size, composition, and histopathology (5). It's crucial for identifying cancerous nodules due to their high prevalence (6). For solid thyroid nodules, parameters like echotexture, shape, borders, intramodular calcifications, and peri nodular halo should be evaluated (7). The American Thyroid Association [ACR] has developed the Thyroid Imaging Reporting and Data System [ACR-TIRADS], a sonographic technique for evaluating nodular features (8).

The American Thyroid Association (ACR) strategies (9) declared that apart from worrisome cervical lymphadenopathy, no single sonographic characteristic or combination is sensitive enough to identify all malignant nodules. Elastography is an emerging sonographic technology that needs additional confirmation (10). Ultrasound elastography (USE) is an imaging method that detects tissue stiffness. It was first described in the 1990s and has since been further developed and enhanced to allow quantitative measurements of tissue stiffness (11). The elasticity of the thyroid gland depends on the structural features of the tissue matrix. Unlike conventional ultrasound (US) which determines reflectivity based on microscopic structure, elastography affords image contrast depending on histologic tissue structure, allowing discrimination between normal and parenchymal disorders (10). The normal thyroid has a soft advent, with variability in elastography appearance due to parenchymal hyperplasia and involution (12). Combining thyroid USE with B-mode US can enhance the capability to differentiate benign from malignant thyroid nodules and diminish the number of desired FNAs (13). Elastography methods can distinguish precious from normal tissue for investigative applications. Conservative ultrasound is a low-priced, adaptable, and commonly available modality, which also applies to USE (14). Elastography evaluates tissue elasticity, or the ability of tissue to resist deformation or regain its original shape after force is applied (11,15). Techniques include free-hand quasi-static or strain elastography [SE], which measures shape-deformation using a probe compression (10), and shear-wave elastography (SWE), a new technique that uses acoustic pressure from the probe to provide real-time elastic information (16). SE measures the shape-deformation and lesion stiffness compared to surrounding tissue, while SWE

detects the transverse component of particle displacement caused by an acoustic pulse from the probe (10). Strain elastography is a method used to measure the stiffness of thyroid nodules by analyzing changes in size and shape corresponding to the route of the investigative force (17),(18). The strain data are presented as a semitransparent color map termed an electrogram, which is placed on the B-mode picture (19). The strain ratio is a pseudo-quantitative measurement that indicates the ratio of strain recorded in a neighboring reference tissue region of interest and strain measured in a target lesion ROI (20). Thyroid ultrasound strain imaging investigations can be classified based on the stimuli used and the grading systems employed. The most common stimulus utilized in thyroid ultrasound strain imaging is operator-applied external compression through the ultrasound transducer (14). Thyroid ultrasound strain imaging scoring systems include two qualitative elasticity scores (Asteria criterion, a 4-point score (21) or Rago criteria, a 5-point score) (22) and a semi-quantitative thyroid stiffness index, which measures the strain in the background normal thyroid tissue versus the strain in the thyroid nodule (23). The Asteria criteria are based on four classes of tissue stiffness, whereas the Rago criteria range from score 1 (even elasticity throughout the nodule) to score 5 (no elasticity in the nodule or the area of posterior shadowing) (22). The real-time elastography (RTE) appearance of thyroid nodules is assessed subjectively using the elasticity score (ES) (23) and strain ratio (SR). The latter involves placing two similar ROIs at similar depths, resulting in a strain ratio that may be more accurate than elasticity imaging (24-26). Combining these measurements is assumed to be superior for malignancy assessment, as they provide independent measures (11).tissue as the first reference and

SCM muscle as the second reference. The current study's purpose was to assess the diagnostic performance of USE in the prediction of malignant thyroid nodules by assessing the strain ratio compared to sternocleidomastoid muscle and normal thyroid tissue as references.

Patients and Methods

This prospective study was conducted at the US unit of the Radiological Department at Al Imamein Al Kadhimein Medical City in Baghdad from August 25th, 2020, to January 15th, 2021. The study included 33 patients aged 18 years or older, with solitary thyroid nodules, including TIRADS III nodules of more than 25 mm and TIRADS IV nodules of more than 15 mm. The patients were examined using B-mode ultrasound and sonoelastography before undergoing fine-needle aspiration (FNA). Exclusion criteria included patients with inconclusive histopathology, TIRADS I and II, multiple thyroid nodules, abnormal thyroid parenchyma, neck surgery affecting the sternocleidomastoid muscle (SCM) or partial thyroidectomy, abnormal thyroid function tests, and thyroid nodules with eggshell calcification.

Imaging Methods:

Gray-scale US: The thyroid ultrasonic examination was carried out utilizing the Voluson-E6 Ultrasound machine (GE Healthcare, USA) with a 5 to 12 MHz linear array transducer. Thyroid nodule criteria were obtained with the patient resting supine with an exposed neck and a minor neck extension. The thyroid gland is scanned at axial, sagittal, and oblique planes. The size, margin, composition, echogenicity, orientation, and presence of calcification were all measured and documented. **Real-time Elastographic US:** Elastographic US of the nodules were carried out immediately after the B-mode US. The operator placed the linear probe perpendicular to the skin on the neck. A box was then highlighted that included

the selected thyroid nodule and an adequate surrounding normal thyroid tissue at the same depth as possible. This was followed by the inclusion of the same thyroid nodule and the other reference tissue (SCM muscle). To reduce motion artifacts, patients were instructed to hold their breath and refrain from swallowing during the examination. The probe exerted slight external compression until an ideal pressure was achieved, as indicated by the presence of a green color on the indicator bar in the upper left corner of the screen. The elastogram was displayed as a color scale over the grayscale image of the US. The color scale varied from red, which indicated components with the greatest elastic strain (softest components), to blue, which indicated components without strain (hardest components). Two SR were measured for each nodule by placing a selected ROI within the reference tissue and another ROI on the thyroid nodule as follows:

1. The parenchymal-nodular strain ratio (PNSR) measures the strain between the thyroid nodule and the surrounding normal thyroid tissue.
2. Muscle-nodular strain ratio (MNSR): the strain of the thyroid nodule with the second reference tissue the SCM muscle.

The average value for each selected nodule was calculated (at least three measurements were recorded), and the average was used to calculate the result.

Statistical analysis

The data were statistically analyzed using the Statistical Package for Social Sciences (SPSS) version 22 for Windows. Descriptive data are reported as mean \pm SD and frequencies as percentages. Chi-square and Fisher's exact tests were used for categorical variables when appropriate. The t-test was used for continuous variables. Sensitivity, specificity, accuracy, and

the cut-off value of each SR was calculated. In all statistical analyses, a P-value of < 0.05 was considered statistically significant.

Results

The histopathological distribution of the benign and malignant thyroid nodules according to age and gender:

The results of this study showed that the final histopathological diagnosis of thyroid nodules was 24 (72.7%) benign and 9 (27.3%) malignant. The patient's age was ranging from (18 – 68) years, with mean \pm SD = 43.4 ± 10.7 years. In benign nodules, patients' ages ranged from 18 to 68 years., with mean \pm SD= 41.29 ± 12.89 years, whereas in malignant cases, the age ranged from 32 to 60 years, mean \pm SD= 44 ± 8.32 years, with non-statistically significant result; P-value 0.88. The majority of patients with thyroid nodules were females 26 [78.8%], and most of the females had benign thyroid nodules 21 [87.5%]. However, the result was not significant. This is demonstrated in Table 1.

Table 1. Demographical characteristics of the studied sample distributed by the type of the thyroid nodules.

Parameters	Benign n=24	Malignant n=9	P-value
Gender, n (%)			
Female	3(12.5)	4 (44.4)	0.68
Male	21(87.5)	5(55.6)	
Age			
Mean \pm SD	41.2 \pm 12.8	44 \pm 8.32	0.8
Min	18	32	
Max	68	60	
*The result was non-significant at P- value <0.05			

The sonographic characteristic of the thyroid nodules.

Echogenicity: The majority of the thyroid nodules were isoechoic 21(63.6%), 10 (30.3%)

were hypoechoic, and 2 (6.1%) were hyperechoic. Most of the benign thyroid nodules were isoechoic 18 (75%), and 4 (16.7%) of them were hypoechoic. While the malignant thyroid nodules, 6 (66.7%) of them were hypoechoic and 3 (33.3%) of them were isoechoic. The result was statistically significant P-value 0.019, as demonstrated in Table 2.

Composition: Most of the thyroid nodules were solid 26 (78.8%), most of the benign thyroid nodules were solid 19 (79.2%), and 5 [20.8%] of them were mixed. Most of the malignant thyroid nodules were solid 7 (77.8%), and only 2 (22.2%) of them were mixed. However, the result was not significant. This is demonstrated in Table 2.

Margin: Most of the thyroid nodules had well-defined margins 29 (87.9%). 23 (95.8%) of the benign thyroid nodule had well-defined margin. 6 (66.7%) of the malignant thyroid nodules had well defined margin. One third of the malignant thyroid nodules had ill- defined margin with significant result P- value = 0.047. These findings were demonstrated in Table 2.

Orientation: Most thyroid nodules were wider than taller 31 (93.9%). All the benign nodules were wider than taller 24 (100%). According to the study, most malignant nodules were wider than taller, and on the other hand, all nodules that were taller than wide (22.2%) had significant outcomes and were malignant. These findings were demonstrated in Table 2.

Calcification: 11 (45.8%) of the benign nodules showed no calcification, and 10 (41.7%) had macrocalcification. In the present study, most of the malignant nodules (8 from 9 cases =88.9 %) had calcification. Microcalcification was most frequently encountered which is present in 5 cases (55.6%), while macro calcification is present in (3 from 9 cases=33.35). These findings were demonstrated in Table 2.

The TIRADS of selected thyroid nodules in relation to histopathological results: 12 of the benign thyroid nodules were TIRADS III, and 12 cases were of TIRADS IV.

All malignant nodules were of TIRADS IV with significant result, P-value < 0.05. These findings were demonstrated in Table 2.

Table 2. the association of the sonographic characteristic of the thyroid nodules with histopathological type of the nodules.

Parameters	Benign		Malignant		P-value
	No.	%	No.	%	
Echogenicity					0.019*
Hyperechoic	2	8.34	0	0	
Isoechoic	18	75	3	33.3	
Hypoechoic	4	16.7	6	66.7	
Composition					0.63
Solid	19	7.2	7	77.8	
mixed	5	20.8	2	22.2	
Margin					0.047*
Well-defined margin	23	95.8	6	66.7	
Ill-defined margin	1	4.2	3	33.3	
Orientation					0.017*
Wider than taller [oval]	24	100	7	77.8	
Taller than wider [oval]	0		2	22.2	
Calcifications					0.02*
No calcification	11	45.8	1	11.1	
Microcalcification	3	12.5	5	55.6	
Macrocalcification	10	41.7	3	33.3	
TIRADS					0.012*
TIRADS III	12	50	0	0	
TIRADS IV	12	50	9	100	
*The result was significant at P-value <0.05, TIRADS: Thyroid Imaging Reporting and Data System					

The association of the histopathological type of thyroid nodules with their PNSR and MNSR: The PNSR of all thyroid nodules were ranging from (0.55-6.0) with mean±SD of 2.95 ±1.5. The mean±SD of benign nodules were 2.26±0.95, ranging from 0.55 to 4.33, while the mean±SD of malignant nodules were 4.87±1.11 ranging from (6-3.16). The MNSR of all thyroid nodules were ranging from (0.42-5.25) with mean±SD of 2.44 ±1.28. The mean± SD of benign nodules were 1.81±0.75, ranging from 0.42 to 3.13, while the mean±SD of malignant

nodules were 4.1±0.8 ranging from 2.45-5.25 with significant P-value for both SR, as shown in Table 3.

Table 3. SR ratios of thyroid nodules for benign and malignant lesions among the patients.

Parameter		N	Mean	SD	Min	Max	P-value
PNSR	Benign	24	2.26	0.95	0.55	4.33	<0.001*
	Malignant	9	4.78	1.11	3.16	6.0	
MNSR	Benign	24	1.81	0.75	0.42	3.13	<0.001*
	Malignant	9	4.1	0.8	2.45	5.25	

The cutoff value for PNSR and MNSR to differentiate between benign and malignant Nodule: The best strain ratio Cutoff value derived from analysis was (≥ 3.63) for PNSR (higher values were more indicative of malignant thyroid nodules, whereas values below this cut-off value, suggestive of benign nodule). The strain ratios of PNSR and MNS were represented by the ROC Curve in Figure 1.

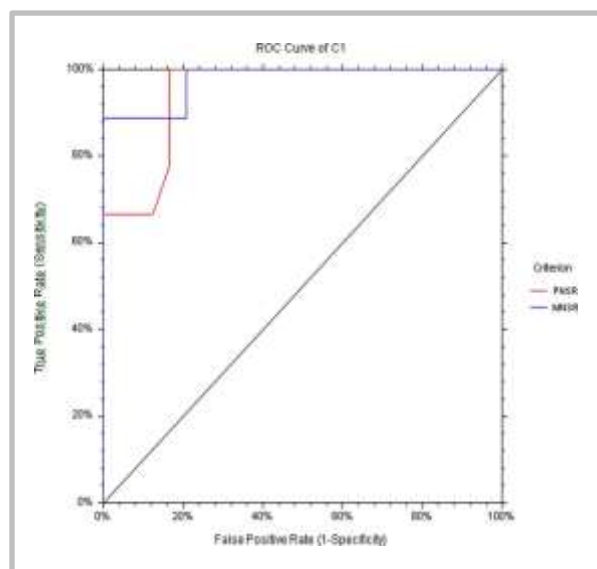


Figure 1. The Strain ratio at ROC curve.

The best cut off value for parenchyma-nodule strain ratio is 3.63 with highest sensitivity, specificity and accuracy of 100%, 85.3% and 89.2% respectively, this indicates that all cases with pathological findings were accurately detected when the strain ratio exceeded 3.63. and suggests that 85.3% of non-pathological nodules were correctly classified as benign using this cutoff value. as seen in Table 4.

Table 4. PNSR Cutoff value to differentiate between benign and malignant thyroid nodules among the patients.

PNSR	AUC	P-value	Accuracy	Asymptotic 95% Confidence Interval	
				Lower Bound	Upper Bound
	0.946	<0.001*	89.2%	0.874	1.000
Positive if				Sensitivity	Specificity
≥ 2.88				100.0	82.7
≥ 3.63				100.0	85.3
≥ 3.73				98.8	87.5
≥ 4.08				77.8	94.3
≥ 4.50				66.7	100.0

The best cutoff value for muscle –nodule strain ratio is 3.20 with highest sensitivity, specificity and accuracy of 100%, 91.1% and 93.3% respectively. This indicates that at MNSR ≥ 3.20 all pathological nodules were accurately detected as malignant and 91.1% of non-pathological nodules were correctly classified as benign at this cutoff, as demonstrated in Table 5.

Table 5. MNSR Cutoff value to differentiate between benign and malignant thyroid nodules among the patients.

MNSR	AUC	P-value	Accuracy	Asymptotic 95% Confidence Interval	
				Lower Bound	Upper Bound
	0.976	<0.001*	93.3%	0.927	1.000
Positive if				Sensitivity	Specificity
≥ 2.8				100.0	83.3
≥ 3.20				100.0	91.1
≥ 3.53				77.8	100
≥ 4.09				66.8	100

Discussion

In this study, there was no significant link between patient's age or gender and histological diagnosis. US examination can detect these nodules with irregular margins, microcalcification, and hypo echogenicity indicating biopsy these criteria may correlate with thyroid malignancy (27). FNA is necessary for distinguishing benign from malignant nodules, but it's invasive and may cause sampling errors. Approximately 15-20% of thyroid nodules yield non-diagnostic cytology or inadequate sampling (28), making it crucial to determine which nodules require follow-up and which necessitate re-aspiration.

Ultrasound elastography is a non-invasive technique used to differentiate benign and malignant thyroid nodules (29). However, it has limitations when there's no normal surrounding thyroid tissue, like multinodular goiter or Hashimoto's thyroiditis (29). A new reference tissue, SCM muscle, has been developed. There was no significant link between patient's age or gender and histological diagnosis, which is similar with other studies (30,32).

In terms of echogenicity, the current investigation found a statistically significant link between the echogenicity of thyroid nodules on US and histological diagnosis. This is consistent with recent research (33,34), which found a substantial association between the echogenicity of thyroid nodules and the prediction of malignancy. Furthermore, current study discovered a substantial relationship between the border of thyroid nodules and histological diagnosis, consistent with previous research (30,35) indicating that ill-defined or irregular margins significantly predict malignancy. Additionally, the orientation of thyroid nodules was found to have a highly significant correlation with malignancy prediction (35, 33). Moreover, the study found a significant

correlation between microcalcification and malignancy prediction, but these features alone are not accurate (36). The study also found a significant correlation between TIRADS (III and IV) and the distinction between benign and malignant thyroid nodules. Also, the study reveals a significant difference in the stiffness of benign and malignant thyroid nodules using US elastography for both PNSR and MNSR with P-value <0.001 , similar to results documented in previous studies (30,37) revealing more rigidity in malignant nodules than in normal ones. Moreover, the study indicated that the best cut-off value for predicting malignant nodules is ≥ 3.63 , with 100% sensitivity, 85% specificity, and 89.2% accuracy, respectively. Previous studies have used the normal thyroid parenchyma's SR as a reference for discriminating between benign and malignant thyroid nodules, with a wide range of optimal cut-off values, from SR 1.1 in Rago et al. study [86% sensitivity and 90% specificity] to SR 4.2 in Ning et al. study with a sensitivity of 81.8% (22)

Additionally, the study indicated that the muscle-nodule strain ratio elastography (MNSR) for predicting malignant nodules was ≥ 3.2 , with a 100% sensitivity, 91.1 specificity, and 93.3% accuracy rate, respectively. This is higher than previous studies (30,38) which set MNSRs of over 1.85 with sensitivity, specificity, and accuracy of 95.6%, 92.8%, and 93.4%, and above 2.31 for malignant thyroid nodules (39) Görgülü's (37) study set the highest MNSR cutoff value (>5.75), with the highest sensitivity and specificity (100% and 96.3%). The muscle-nodule SR was also variable compared to other studies. The variability in the cutoff value of SR (PNSR and MNSR) between previous studies and the current study can be attributed to differences in sampling criteria, examination techniques due to different machines and operators, and a lack

of uniformity in procedures, such as compression forces applied by operators. The current study found a statistically significant similarity between PNSR and MNSR in differentiation between benign and malignant thyroid nodules (p-value <0.001 for both) with better sensitivity, specificity, and accuracy rate of MNSR in comparison with PNSR. This result was concomitant with Görgülü study (37). Another study done by Aydin et al (30) shows no significant difference between PNSR and MNSR in the form of sensitivity, specificity, and accuracy rate in the prediction of malignant thyroid nodules, the sensitivity, specificity, and accuracy rate were 95.6%, 93.4%, and 94.3% respectively for PNSR and for MNSR, the sensitivity, specificity, and accuracy rate were 95.6%, 92.8%, 93.4% respectively with p-value < 0.001. This could be related to subtle inflammation of the thyroid parenchyma, which may be missed by the radiologist.

Conclusions

The study found that USE has high diagnostic accuracy in distinguishing benign from malignant thyroid nodules, while SCM muscle has high sensitivity, specificity, and accuracy in predicting nodular thyroid malignancy. MNSR had a better cutoff value of 3.2 compared to PNSR's 3.63 in the differentiation of benign and malignant thyroid nodules, suggesting it could be used safely in cases where PNSR has limitations.

Recommendations

The study advocates for the use of elastography and Gray-scale US for assessing thyroid nodules and suggests using sternocleidomastoid muscle as a reference point in addition to normal thyroid parenchyma for better strain ratio measurement.

Source of funding: No source of funding.

Ethical clearance: The ethical approval was taken from the scientific committee of the Iraqi Board of Diagnostic Radiology, by the number

of 45 in (25/8/2020) An oral informed consent was taken from all patients.

Conflict of interest: None.

Acknowledgements:

I am grateful to the institute of radiology in AL-Imamein AlKadhimein Medical city.

References

1. Milas M, Mandel SJ, Langer JE. Advanced Thyroid and Parathyroid Ultrasound. *Advanced Thyroid and Parathyroid Ultrasound*. 2017 Mar 27;1–468.
2. Abdulkareem Salman M. Prevalence of Thyroid Hormones Test Abnormality In Females At Reproductive Age Attending Al-batool Maternity Teaching Hospital. *Diyala Journal of Medicine*. 2023 Jun 30;24(2):93–9. <https://doi.org/10.26505/djm.v24i2.1000>
3. Duick DS, Levine RA, Lupo MA. Thyroid and parathyroid ultrasound and ultrasound-guided FNA. *Thyroid and Parathyroid Ultrasound and Ultrasound-Guided FNA*. 2017 Dec 9;1–546.
4. Kagoya R, Monobe H, Tojima H. Utility of elastography for differential diagnosis of benign and malignant thyroid nodules. *Otolaryngology–Head and Neck Surgery*. 2010 Aug 1;143(2):230–4. <https://doi.org/10.1016/j.otohns.2010.04.006>
5. Patnaik M, Patnaik G, Swain J, Kanwar J. Rapidly Progressing Non-Hodgkin's Lymphoma of Thyroid Gland. *AL-Kindy College Medical Journal*. 2024 Apr 1 20(1):74–7. <https://doi.org/10.47723/nrpvbk52>
6. Idan, H. M., & Motib, A. S. (2024). Incidence of head and neck cancer among Baquba Teaching Hospital Patients. *Diyala Journal of Medicine*, 27(1), 86-96. <https://doi.org/10.26505/DJM.27018820708>.
7. Ji YK, Chang HL, Soo YK, Woo KJ, Jin HK, Su KA, et al. Radiologic and pathologic findings of nonpalpable thyroid carcinomas detected by ultrasonography in a medical

- screening center. J Ultrasound Med. 2008;27(2):215–23.
<https://doi.org/10.7863/jum.2008.27.2.215>
8. Omer Bahabara , Jamal, Salem Basabaa , Ahmed, Mohammed Bin Thalab , Abeer, Yeslam Baothman , Sameer, Khamis Alakbary , Mohammed, Salim Musiaan N. Correlation Between the Thyroid Imaging Reporting and Data System and Bethesda System of Cytology in Thyroid Nodule Evaluation. Diyala Journal of Medicine. 2024 Jun 25;26(2):1–13.
<https://doi.org/10.26505/djm.v26i2.1092>
9. Cooper DS, Doherty GM, Haugen BR, Kloos RT, Lee SL, Mandel SJ, et al. Revised American Thyroid Association management guidelines for patients with thyroid nodules and differentiated thyroid cancer. Thyroid. 2009Nov1;19(11):1167–214.
<https://doi.org/10.1089/thy.2009.0110>
10. Cantisani V, Lodise P, Grazhdani H, Mancuso E, Maggini E, Di Rocco G, et al. Ultrasound elastography in the evaluation of thyroid pathology. Current status. Eur J Radiol. 2014 Mar;83(3):420–8.
<https://doi.org/10.1016/j.ejrad.2013.05.008>
11. Sigrist RMS, Liao J, Kaffas A El, Chammas MC, Willmann JK. Ultrasound Elastography: Review of Techniques and Clinical Applications. Theranostics. 2017 ;7(5):1303–29.
<https://doi.org/10.7150/thno.18650>
12. Melmed S, Polonsky KS, Larsen PR, Kronenberg HM. Williams Textbook of Endocrinology, Twelfth Edition. Williams Textbook of Endocrinology, Twelfth Edition. Elsevier; 2011. 1–1898 p. Available from: <http://www.sciencedirect.com:5070/book/9781437703245/williams-textbook-of-endocrinology>
13. Shiina T, Nightingale KR, Palmeri ML, Hall TJ, Bamber JC, Barr RG, et al. WFUMB guidelines and recommendations for clinical use of ultrasound elastography: Part 1: basic principles and terminology. Ultrasound Med Biol. 2015 May 1;41(5):1126–47.
<https://doi.org/10.1016/j.ultrasmedbio.2015.03.009>
14. Kamaya A, Machtaler S, Safari Sanjani S, Nikoozadeh A, Graham Sommer F, (Pierre) Khuri-Yakub BT, et al. New technologies in clinical ultrasound. Semin Roentgenol. 2013 Jul;48(3):214–23.
<https://doi.org/10.1053/j.ro.2013.03.009>
15. Abdulqader S, Nori W, Akram N, Al-Kinani M. Radiological Modalities for the Assessment of Fetal Growth Restriction: A Comprehensive Review. AL-Kindy College Medical Journal. 2024 Apr 1;20(1):4–13.
<https://doi.org/10.47723/nz221421>
16. Sebag F, Vaillant-Lombard J, Berbis J, Griset V, Henry JF, Petit P, et al. Shear Wave Elastography: A New Ultrasound Imaging Mode for the Differential Diagnosis of Benign and Malignant Thyroid Nodules. J Clin Endocrinol Metab. 2010 Dec 1 ;95(12):5281–8.
<https://doi.org/10.1210/jc.2010-0766>
17. Magri F, Chytiris S, Chiovato L. The role of elastography in thyroid ultrasonography. Curr Opin Endocrinol Diabetes Obes. 2016 ;23(5):416–22.
<https://doi.org/10.1097/MED.0000000000000074>
18. Abdulqader SK, Al-Ani YAA, Akram NN, Nori W, Al-Kinani M. Metastatic Ovarian Tumor from Incidental Renal Cell Carcinoma: A Case Report and Literature Review. Al-Anbar Medical Journal. 2024 Jun 1 ;20(1):113–6.
<https://doi.org/10.33091/amj.2024.145878.1521>
19. Gennisson JL, Deffieux T, Fink M, Tanter M. Ultrasound elastography: principles and techniques. Diagn Interv Imaging. 2013;94(5):487–95.
<https://doi.org/10.1016/j.diii.2013.01.022>
20. Choi YJ, Lee JH, Baek JH. Ultrasound elastography for evaluation of cervical lymph nodes. Ultrasonography.

2015;34(3):157–64.

<https://doi.org/10.14366/usg.15007>

21. Asteria C, Giovanardi A, Pizzocaro A, Cozzaglio L, Morabito A, Somalvico F, et al. US-elastography in the differential diagnosis of benign and malignant thyroid nodules. *Thyroid*. 2008 May 1;18(5):523–31.

<https://doi.org/10.1089/thy.2007.0323>

22. Rago T, Santini F, Scutari M, Pinchera A, Vitti P. Elastography: New Developments in Ultrasound for Predicting Malignancy in Thyroid Nodules. *J Clin Endocrinol Metab*. 2007 Aug 1;92(8):2917–22.

<https://doi.org/10.1210/jc.2007-0641>

23. Dighe M, Bae U, Richardson ML, Dubinsky TJ, Minoshima S, Kim Y. Differential Diagnosis of Thyroid Nodules with US Elastography Using Carotid Artery Pulsation1.. *2008Aug1;248(2):662–9.*

<https://doi.org/10.1148/radiol.2482071758>

24. Wang HL, Zhang S, Xin XJ, Zhao LH, Li CX, Mu JL, et al. Application of Real-time Ultrasound Elastography in Diagnosing Benign and Malignant Thyroid Solid Nodules. *Cancer Biol Med*. 2012 Jun;9(2):124–7.

<https://doi.org/10.4103/2156-7514.197074>

25. Guazzaroni M, Spinelli A, Coco I, Del Giudice C, Girardi V, Simonetti G. Value of strain-ratio on thyroid real-time sonoelastography. *Radiol Med*. 2014 Mar 1;119(3):149–55.

<https://doi.org/10.1007/s11547-013-0320-9>

26. El-Hariri MA, Taha Ali TF, Tawab MA, Magid AMA, El-Shiekh AF. The clinical value of ultrasound elastography in predicting malignant thyroid nodules. *The Egyptian Journal of Radiology and Nuclear Medicine*. 2014 Jun 1;45(2):353–9.

<https://doi.org/10.1016/j.ejrnm.2014.03.006>

27. Kim HG, Moon HJ, Kwak JY, Kim EK. Diagnostic accuracy of the ultrasonographic features for subcentimeter thyroid nodules suggested by the revised American Thyroid

Association guidelines. *Thyroid*. 2013 Dec 1;23(12):1583–9.

<https://doi.org/10.1089/thy.2012.0586>

28. Chow LS, Gharib H, Goellner JR, Van Heerden JA. Nondiagnostic thyroid fine-needle aspiration cytology: management dilemmas. *Thyroid*. 2001;11(12):1147–51.

<https://doi.org/10.1089/10507250152740993>

29. Bojunga J, Herrmann E, Meyer G, Weber S, Zeuzem S, Friedrich-Rust M. Real-time elastography for the differentiation of benign and malignant thyroid nodules: a meta-analysis. *Thyroid*. 2010 Oct 1;20(10):1145–50.

<https://doi.org/10.1089/thy.2010.0079>

30. Aydin R, Elmali M, Polat AV, Danaci M, Akpolat I. Comparison of muscle-to-nodule and parenchyma-to-nodule strain ratios in the differentiation of benign and malignant thyroid nodules: which one should we use? *Eur J Radiol*. 2014 Mar;83(3).

<https://doi.org/10.1016/j.ejrad.2013.12.003>

31. Zhang WB, Xu W, Fu WJ, He BL, Liu H, Deng WF. Comparison of ACR TI-RADS, Kwak TI-RADS, ATA guidelines and KTA/KSThR guidelines in combination with SWE in the diagnosis of thyroid nodules. *Clin Hemorheol Microcirc*. 2021 Feb 10 ;78(2):163–74.

<https://doi.org/10.3233/CH-221507>

32. Abdulqader SK, Bakr GM an, Ahmed SA, Hassan QA, Al-Kinani M. Gender Distribution of Coronary Artery Calcium Score and Degree of Stenosis Assessed by Computed Tomography Angiography in Iraqi Patients with Chest Pain: *Al-Rafidain Journal of Medical Sciences* (ISSN 2789-3219). 2024 Jul 20;7(1):78–84.

<https://doi.org/10.54133/ajms.v7i1.1032>

33. Colakoglu B, Yildirim D, Alis D, Ucar G, Samanci C, Ustabasioglu F, et al. Elastography in Distinguishing Benign from Malignant Thyroid Nodules. *J Clin Imaging Sci*. 2016 Oct 1;6(4).

<https://doi.org/10.4103/2156-7514.197074>

34. Muhi AM, Kamal AM, Dawood SN, Kareem TF, Fakhri RTT, Al-Attar Z. The Role of Strain Elastography in Evaluating Borderline Axillary Lymph nodes. AL-Kindy College Medical Journal. 2022 May 5;18(1):68–72.

<https://doi.org/10.47723/kcmj.v18i1.692>

35. Shin JH, Baek JH, Chung J, Ha EJ, Kim JH, Lee YH, et al. Ultrasonography Diagnosis and Imaging-Based Management of Thyroid Nodules: Revised Korean Society of Thyroid Radiology Consensus Statement and Recommendations. Korean J Radiol. 2016 May 1;17(3):370–95.

<https://doi.org/10.3348/kjr.2016.17.3.370>

36. Slapa R, Jakubowski W, Slowinska-Srzednicka J, Szopin

ski K. Advantages and disadvantages of 3D ultrasound of thyroid nodules including thin slice volume rendering. Thyroid Res. 2011;4(1):1.

<https://doi.org/10.1186/1756-6614-4-1>

37. Görgülü FF. Which Is the Best Reference Tissue for Strain Elastography in Predicting Malignancy in Thyroid Nodules, the Sternocleidomastoid Muscle or the Thyroid Parenchyma? J Ultrasound Med. 2019 Nov 1;38(11):3053–64.

<https://doi.org/10.1002/jum.15013>

38. Abdulqader SK. Thyroid Imaging Reporting and Data System (TI-RADS) Stratification for Thyroid Incidentalomas in Iraqi Sample. Kirkuk Journal of Medical Sciences. 2024 Oct 1;12(2):13–20.

<https://doi.org/10.32894/kjms.2024.152350.1117>

39. Çiledag N, Arda K, Aribas BK, Aktas E, Köse SK. The utility of ultrasound elastography and MicroPure imaging in the differentiation of benign and malignant thyroid nodules. AJR Am J Roentgenol. 2012 Mar;198(3).

<https://doi.org/10.2214/AJR.11.6763>

مقارنة نسبة اجهاد انعضلات إلى العقيدات مع نسبة اجهاد نسيج الغدة الدرقية إلى العقيدات باستخدام فحص مرونة النسجة بجهاز الموجات فوق الصوتية في عقيدات الغدة الدرقية المشبوهة

^١ زينب فيصل عطية ، ^٢ محمد محمد جواد

الملخص

الخلفية: ان التصوير بالموجات فوق الصوتية هة تقنية غير جراحية تم تطويرها حديثا، وهي مفيدة في تمييز العقيدات الحميدة من عقيدات الغدة الدرقية الخبيثة. وقد أظهر قياس تصلب الغدة الدرقية بواسطة نسبة الاجهاد نتائج واعدة. ومع ذلك توجد قيود كبيرة على نسبة الاجهاد عندما يكون هناك نقص في أنسجة الغدة الدرقية الطبيعية المحيطة.

الأهداف: كان الهدف من الدراسة هو تقييم الأداء التشخيصي في التنبؤ بالعقيدات الدرقية من خلا تقييم نسبة الاجهاد باستخدام انسجة الغدة الدرقية الطبيعية والعضلة القصية الترقوية الخائية كمرجع.

المرضى والطرق: أجريت دراسة استباقية على 33 مريضا مختارا من ذوي العقيدات الوحيدة من الثالث أو الرابع الذين حضروا وحدة الموجات فوق الصوتية في مدينة الامامين الكاظمين الطبية في بغداد – العراق في الفترة من 25 آب / أغسطس 2020 إلى 15 كانون الثاني /يناير 2021. تم فحص جميع المرضى بمقياس رمادي واستخدم الوقت الحقيقي بواسطة جهاز الموجات فوق الصوتية. Volution-E6 وقد تم الحصول على التشخيصات النهائية عن طريق علم الخلايا و/أو علم التنسج.

النتائج: كان متوسط عمر المرضى (18-68) سنة بمدى (43.4 ± ١٠.٧) 26 (78.8 %) منهم من الاناث و ٧ (21.2 %) من الذكور. 24 (72.7 %) كانت حميدة و ٩ (27.3 %) كانت عقيدات خبيثة. كانت العقيدات الدرقية الخبيثة ناقصة الصدى بشكل ملحوظ، واطول من الاعرض، وتظهر التكلس الدقيق. تراوحت نسبة الاجهاد العقدي المتني لجميع عقيدات الغدة الدرقية من (٠.٥٥-٦.٠) بمتوسط ± انحراف معياري من ١.٥ ± ٢.٩٥ ، وبالنسبة للعضلات العقدية كانت تتراوح نسبة الاجهاد من ٠.٤٢ - ٥.٢٥ بمتوسط ± انحراف معياري يبلغ ± ٢.٤٤. ١.٢٨. أفضل قيمة قطع كانت (٣.٦٣ ≤) ل نسبة الاجهاد العقدي المتني مع حساسية و نوعية ومعدل دقة (١٠٠% ، ٨٥% ، ٨٩.٢% على التوالي) ، وأفضل قيمة قطع لنسبة الاجهاد العضلي العقدي كانت (٣.٢ ≤) مع الحساسية ، والخصوصية ، ومعدل الدقة البالغ (١٠٠% ، ٩١.١ ، ٩٣.٣% على التوالي).

الاستنتاج: أظهرت العضلة القصية الترقوية الخشائية حساسية عالية وخصوصية ودقة في التنبؤ بأورام الغدة الدرقية. كان هناك تشابه بين نسبة أجهاد العقدي المتني و نسبة الاجهاد العضلي الغدي في الدقة التشخيصية التمييز بين عقيدات الغدة الدرقية الحميدة والخبيثة. لذلك يمكن استخدام نسبة الاجهاد العضلي العقدي بأمان في الحالات التي يوجد فيها قيود على قياس الاجهاد المتني العقدي

الكلمات المفتاحية: فحص مرونة النسجة، عقيدات الغدة الدرقية، نسبة الاجهاد.

المؤلف المراسل: زينب فيصل عطية

الايمل: Zainab.faisal137@gmail.com

تاريخ الاستلام: ١٧ تموز ٢٠٢٤

تاريخ القبول: ٨ كانون الثاني ٢٠٢٥

تاريخ النشر: ٢٥ نيسان ٢٠٢٥

^١ مدينة الإمامين الكاظمين الطبية – بغداد – العراق.

^٢ قسم تكنولوجيا الراديو – كلية الهادي الجامعة – بغداد – العراق.

Relationship Between Entrance Surface Skin Exposure for Iraqi Women with Compressed Breast Thickness in Mammography

Doaa Hameed kadhim ¹, Zainab A. Hamoudi ², Mawada M. Funjan ³, Rania Jamal Ahmed ⁴, Aya H. Hasan ⁵

¹ Department of Physiology, College of Medicine, Mustansiriyah University, Baghdad, Iraq.

² Department of X-ray techniques, Al-Nisour University College, Baghdad, Iraq.

³ Department of Physiology, College of Medicine, University of Baghdad, Baghdad, Iraq.

⁴ AL-ESRAA University, College of Health & Medical Techniques, Department of Radiology Techniques, Baghdad, Iraq.

⁵ Communication Technology Engineering Department, Technical College, Imam Ja'afar Al-Sadiq University, Baghdad, Iraq.

Abstract

Background: The evaluation of compressed breast thickness has been conducted based on the results of mammography examinations. While it is well-established that breast compression influences breast tissue, its effect on the axillary (armpit) region remains unclear. Increased compression of breast tissue in women can lead to a reduction in breast tissue thickness.

Objective: To determine the correlation between entrance surface skin exposure with compressed breast thickness and compare the mean of entrance surface skin exposure results from mammography in Iraq with other studies.

Patients and Methods: A study was conducted at Al-Alwiya Teaching hospital from December 2023 to January 2024 and involved 100 Iraqi women. The study used a mammography (model GE healthcare) to determine compressed breast thickness and skin exposure for craniocaudal and mediolateral oblique projections.

Results: The mammography findings revealed a statistically significant correlation between entrance surface skin exposure (ESE) and compression breast thickness (CBT) in Iraqi women. Specifically, it was observed that increased CBT was associated with higher ESE values.

Conclusion: The study demonstrates that breast compression thickness and radiation exposure were notably higher in the mediolateral oblique (MLO) view compared to the craniocaudal (CC) view. A significant positive correlation was observed between compression breast thickness and radiation dose. These findings underscore the importance of region-specific guidelines and standards in mammography practices to ensure optimal patient care and safety.

Keywords: Axillary region, Breast parenchyma, Entrance surface skin exposure, Mammography, Compressed breast thickness.

OPEN ACCESS

Correspondence: Doaa Hameed kadhim

Email:

doaa.hameed2208m@comed.uobaghdad.edu.iq

Copyright: ©Authors, 2025, College of Medicine, University of Diyala. This is an open access article under the [CC BY 4.0](http://creativecommons.org/licenses/by/4.0/) license (<http://creativecommons.org/licenses/by/4.0/>)

Website:

<https://djm.uodiyala.edu.iq/index.php/djm>

Received: 04 January 2025

Accepted: 17 March 2025

Published: 25 April 2025

Introduction

The female breast is a complex anatomical structure primarily composed of glandular, fibrous, and adipose tissues (1). The glandular component is organized into lobules and ducts, which are crucial for milk production and transport during lactation. The fibrous stroma provides essential structural

support. Adipose tissue surrounds these elements and significantly influences the breast's overall size and shape. In addition, the breast contains an intricate network of blood vessels, lymphatic channels, and nerves, which collectively contribute to its physiological functions and immunological defense (2,3,4). There are several reasons for applying firm (but not painful) compression to the breast during the mammographic examination (5). Compression causes breast tissues to be spread out, minimizing superposition from different planes and thereby improving the conspicuity of structures.

This effect may be accentuated by the fact that different tissues (fatty, fibrous, glandular, and cancerous) exhibit varying elasticity (6,7,8), resulting in the tissues being spread out to different extents and potentially making a cancer more visible. As in other areas of radiography, scattered radiation reduces contrast in mammograms. The use of compression decreases the ratio of scattered to directly transmitted radiation reaching the image receptor (9).

The effect of breast thickness on scatter is quantified. Compression also decreases the distance from any plane within the breast to the image receptor, thereby reducing geometric unsharpness. The compressed breast provides lower overall attenuation to the incident X-ray beam, allowing the radiation dose to be reduced. The compressed breast also provides more uniform attenuation over the image. This reduces the exposure range that must be recorded by the imaging system, and in screen-film mammography, allows a film with a higher gradient to be employed. Finally, compression provides a clamping action, which reduces

anatomical motion during the exposure, thereby reducing this source of image un-sharpness, it is essential that the breast (10-12) be compressed as uniformly as possible and that the edge of the compression plate at the chest wall be straight and aligned with both the focal spot and image receptor to maximize the amount of breast tissue (13, 14) that is included in the image. The mechanical properties of the breast are non-

linear; after a certain reduction in thickness, application of additional pressure provides little benefit in terms of improved image quality and only contributes to patient discomfort. Specialized mechanisms have been introduced by several manufacturers to try to achieve better compression while minimizing the risk of overcompression (15,17,18).

This research seeks to estimate and compare the ESE from mammography procedures in Iraq with those reported in other studies. Additionally, it aims to explore the relationship between ESE and breast compression thickness.

Patients and Methods

Study design: The study involved 100 Iraqi women, aged between 30 and 60 years, who were referred to Al-Alwiya Teaching Hospital between December 2023 and January 2024. ESE and compressed breast thickness (CBT) measurements for craniocaudal (CC) and mediolateral oblique (MLO) views from mammography were recorded for both breasts. Various anode-filter pairings were considered, including Mo/Mo, Mo/Rh, and Rh/Rh.

Exclusion Criteria:

1. Patients with a history of radiation therapy.
2. Patients exhibiting symptoms of mastitis or breast abscess.
3. Patients with any inflammatory condition that may increase skin thickness beyond normal limits, potentially resulting in a higher radiation dose.

Data analysis: Analysis of the data was carried out using the Statistical Package for the Social Sciences, version 24 (SPSS-24). Data were presented in simple measures of mean, standard deviation, and range. The significance of the difference between different means (quantitative data) was tested using Student's t-test for the difference between two independent means or the Paired T-Test for a difference between paired

observations (or two dependent means).

The scattering distribution curve was used for correlation analysis. Statistical significance was considered whenever the p-value was equal or less than 0.05.

Results

Age distribution: The age distribution of our data, collected from 100 Iraqi women, is shown

in Figure 1.

The study groups were divided into smaller groups according to their ages, and the results showed that the percentage of the age range of patients of 30-39 years was 18.0%, it was 38.0% of patients within 40-49 years, and 44.0% for patients within the age range of 50 to 59 years old.

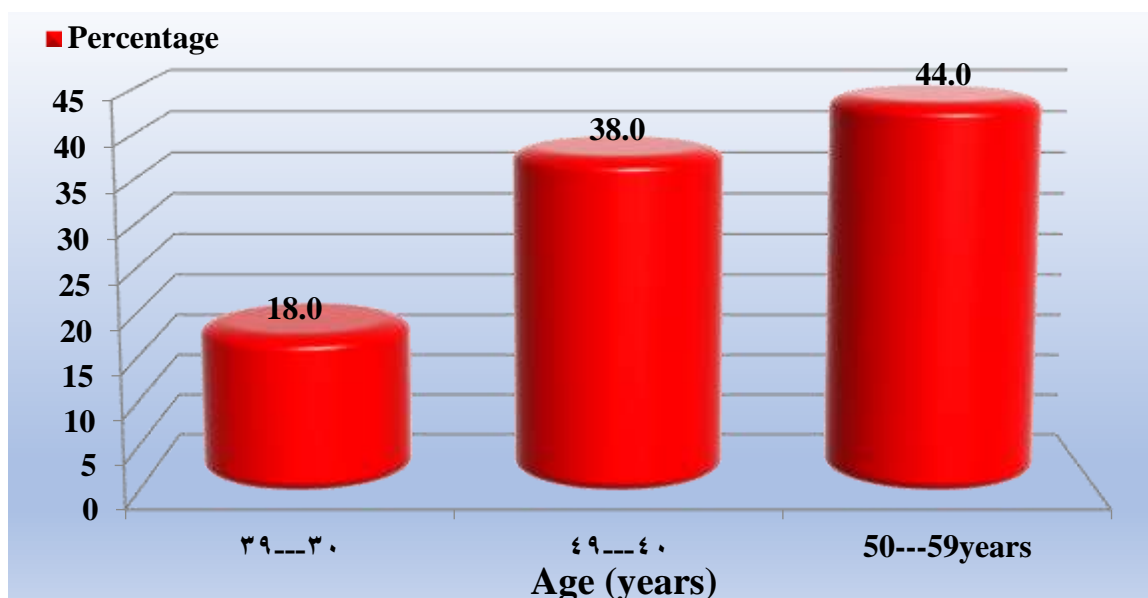


Figure 1. Age distribution of Iraqi women used in the current study at Al-Alwiya hospital.

These measurements are provided separately for the right breast, left breast, and combined for both breasts. Additionally, the range of values for each category is included.

Breast Thickness: For the cranio-caudal (CC) projection, the average compressed breast thickness for the right breast is 50.62 mm with a standard deviation of 9.62. The range of values for this measurement extends from 30.0 mm to 77.0 mm. Similarly, for the left breast, the mean thickness is 50.35 mm with a standard deviation of 9.38, and the range was from 30.0 mm to 75.0 mm. When both breasts are considered together, the average thickness was slightly higher at 50.90 mm, with a standard deviation of 9.89 and

a range of 30.0 mm to 77.0 mm. In the mediolateral oblique (MLO) projection, the compressed breast thickness is generally more significant than in the CC projection. The mean thickness for the right breast is 61.12 mm, with a standard deviation of 12.57, and the range spans from 33.0 mm to 89.0 mm. For the left breast, the average thickness is 60.28 mm, with a standard deviation of 12.86, and the range is identical at 33.0 mm to 89.0 mm. When both breasts are analyzed together, the mean compressed thickness increases slightly to 61.97 mm, with a standard deviation of 12.27 and a range of 37.0 mm to 89.0 mm these shown at Table 1.

Table 1. The mean and standard deviation of compression breast thickness.

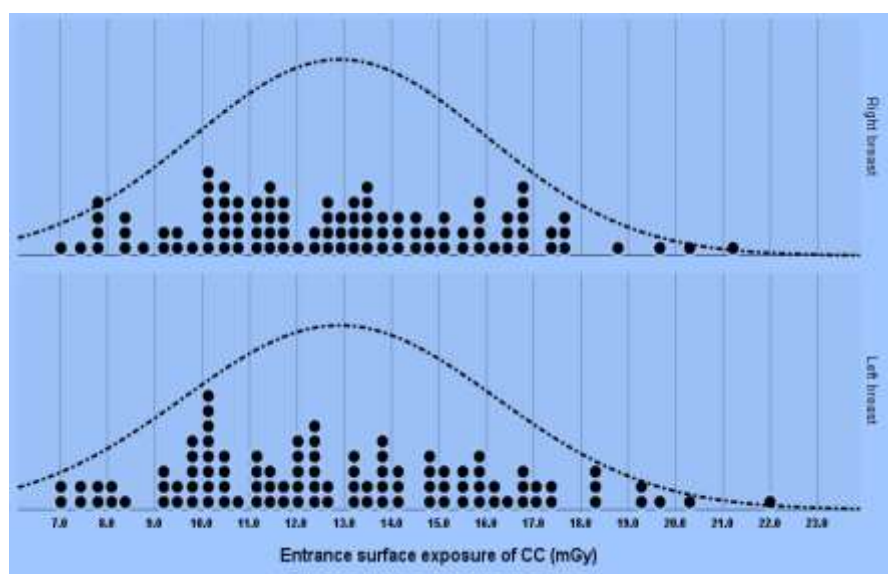
Physical parameters of mammography	Mean \pm SD (Range) For right breasts	Mean \pm SD (Range) For left breasts	Mean \pm SD (Range) For both breasts
Compression breast thickness for CC (mm)	50.62 \pm 9.62 (30.0-77.0)	50.35 \pm 9.38 (30.0-75.0)	50.90 \pm 9.89 (30.0-77.0)
Compression breast thickness for MLO (mm)	61.12 \pm 12.57 (33.0-89.0)	60.28 \pm 12.86 (33.0-89.0)	61.97 \pm 12.27 (37.0-89.0)

Entrance Surface Exposure: Based on Table 2 and Figure 2 which show the craniocaudal (CC) projection, the entrance surface exposure for the right breast has a mean value of 12.91 mGy, with a standard deviation of 3.19. The exposure values range from 7.0 mGy to 21.99 mGy. Similarly, for the left breast, the mean exposure was 12.91 mGy, with a standard deviation of 3.10, and the range is from 7.0 mGy to 21.21 mGy. When the data for both breasts are combined, the mean remains consistent at 12.91 mGy, with a slightly lower standard deviation of 3.10, and the range spans from 7.02 mGy to

21.99 mGy in mediolateral oblique (MLO) projection, the entrance surface exposure is slightly higher compared to the CC projection. For the right breast, the mean exposure is 15.38 mGy, with a standard deviation of 4.73, and the range is from 6.22 mGy to 37.09 mGy. While in the left breast, the mean exposure was 15.31 mGy, with a standard deviation of 4.88, and the range was from 7.41 mGy to 37.09 mGy. When both breasts are analyzed together, the mean exposure was 15.45 mGy, with a standard deviation of 4.61, and the range spans from 6.22 mGy to 31.25 mGy.

Table 2. Comparison of Entrance Surface Exposure (mGy) in Mammography.

Radiation factors	Mean \pm SD (Range) For right breasts	Mean \pm SD (Range) For left breasts	Mean \pm SD (Range) For both breasts
Entrance surface exposure of CC (mGy)	12.91 \pm 3.19 (7.0-21.99)	12.91 \pm 3.10 (7.0-21.21)	12.91 \pm 3.30 (7.02-21.99)
Entrance surface exposure of MLO (mGy)	15.38 \pm 4.73 (6.22-37.09)	15.31 \pm 4.88 (7.41-37.09)	15.45 \pm 4.61 (6.22-31.25)


Figure 2. Analysis of radiation dose in CC and MLO mammography projection for left and right breast.

Breast Thickness and Radiation Doses: Table 3 provides an analysis of the correlation between compressed breast thickness (CBT) and radiation doses during mammography for the cranio-caudal (CC) and mediolateral oblique (MLO) projections. The relationship is assessed using the Pearson correlation coefficient (R) and the corresponding p-values (P), which indicate the statistical significance of the results.

Correlation Coefficient: For the CC projection, the correlation coefficient \textcircled{R} between entrance surface exposure (ESE) and breast compression thickness was 0.401. This value signifies a moderate positive correlation, meaning that as breast thickness increases, the radiation dose required for the CC projection also increases. The associated p-value for this correlation is 0.0001, which was considered highly significant. This strong statistical significance underscores the reliability of the relationship between CBT and radiation dose in this projection.

In the case of the MLO projection, the correlation coefficient between ESE and CBT is slightly lower at 0.337, which also indicates a moderate positive correlation. Similar to the CC projection, this relationship implies that thicker breast tissue requires a higher radiation dose for adequate imaging. The p-value for this correlation is also 0.0001, demonstrating a high level of statistical significance. Despite being slightly weaker than the CC projection, the correlation remains important for understanding the factors influencing radiation dose during mammography.

When looking at the overall correlation between CBT and ESE in the MLO projection, the relationship becomes stronger, with a correlation coefficient of 0.654. This indicates a strong positive correlation, suggesting that breast thickness has an even greater impact on radiation dose in the MLO projection. The p-

value remains at 0.0001 which confirms the high statistical significance of this correlation.

Table 3. Correlation between compressed breast tissue and radiation doses. (*Correlation is significant at the 0.05 level, **Correlation is highly significant at the 0.01 level).

Radiation doses		CBT For CC	CBT For MLO
ESE For CC	R	0.401**	0.337**
	P	0.0001	0.0001
ESE For MLO	R	0.305**	0.654**
	P	0.0001	0.0001

Discussion

Our study shows that the majority of women visiting Al-Alwiya Hospital are aged 50–59 years (44%), followed by those aged 40–49 years (38%), with the lowest percentage in the 30–39 years group (18%). This suggests that older women seek medical care more frequently, likely due to age-related health issues or routine check-ups (19). The current study reveals that breast compression thickness is slightly higher in the MLO view compared to the CC view. Measurements are consistent between right and left breasts, with ranges of 30–77 mm (CC) and 33–89 mm (MLO). This ensures reliable imaging for both views. MLO view has been reported to have a higher radiation exposure than the CC view, with consistent values between right and left breasts. Mean ESE ranges from 12.91 mGy (CC) to 15.38 mGy (MLO). The study results revealed a positive correlation between radiation doses (ESE) and mammography techniques (CBT) in both CC and MLO positions, with a highly significant statistical level of 0.01. In the CC position, the correlation coefficient \textcircled{R} was 0.401, indicating a moderate positive correlation. This can be explained by the fact that increased breast tissue density or thickness in this position requires higher radiation doses to achieve diagnostic image quality. In the MLO position, the correlation coefficient was 0.337, reflecting a

mild to moderate positive correlation. This is because the MLO position captures more glandular tissue (20, 21), resulting in higher radiation exposure; however, the correlation is lower than in the CC position due to differences in imaging angles and tissue distribution.

The highest correlation was observed between radiation doses and the MLO position, with an R value of 0.654. This can be attributed to the broader tissue area covered in this position, requiring higher radiation doses for effective penetration. These findings are attributed to several factors, including the differences in tissue density, breast thickness, and imaging angles. Additionally, the quality and calibration of imaging devices directly influence the radiation required dose. A comparison of the Entrance Surface Exposure (ESE) values in mammography between this study and a Sudanese study revealed significantly lower ESE values in this study across all views (RCC, RMLO, LCC, LMLO) compared to the Sudanese study (18). This difference could be attributed to advancements in mammography technology (10), stricter radiation safety protocols, and differences in patient characteristics. The lower ESE enhances patient safety by minimizing radiation exposure while maintaining diagnostic quality. However, this result does not align with the study conducted by Myug-Su Ko et al in 2013, where the mean of ESE was 5.98 ± 1.22 , which is significantly lower than our findings. This discrepancy could be explained by the fact that the device used in their study has a higher level of safety compared to the one used in our study.

Conclusions

The study found that most patients involved here were within the age range of 50–59 years. Breast compression thickness and radiation exposure were higher in the MLO view, with a positive correlation between thickness and dose. The

ESE values were significantly lower, which indicates that the mammography device used in this study is very advanced.

Recommendations

It is recommended to increase the number of patients to obtain accurate results and incorporate additional studies to compare the Entrance Skin Exposure (ESE) of mammography devices in other countries with those in Iraq, thereby ensuring greater accuracy and reliability of the results.

Source of funding: No source of funding.

Ethical considerations: The study received ethical approval from the University of Baghdad, College of Medicine, in partnership with the Ministry of Health (specifically, the outpatient Al-Alwiya Teaching Hospital), number 495 on 2/4/2024.

Conflict of interest: None.

Acknowledgements:

The authors thank Mustansiriyah University, Baghdad, Iraq, for its support of the presented work.

References

1. Radhi EA, Kamil MY. Anisotropic Diffusion Method for Speckle Noise Reduction in Breast Ultrasound Images. *International Journal of Intelligent Engineering and Systems*. 2024;17(2):621-31.
<https://doi.org/10.22266/ijies2024.0430.50>
2. Hamza SA, Mohammed RS, Marjani MFA, Bekhit MM. Antibiotic Susceptibility Profile of Carbapenem-Resistant *Klebsiella pneumoniae* Isolates after Exposure to NonThermal Plasma. *Al-Mustansiriyah Journal of Science*. 2025;36(1):14-21.
<https://doi.org/10.23851/mjs.v36i1.1583>
3. Ahmed RI, Shakir SA, Hamad MT, Ibrahim NS. Epidemiological Study of CA Breast in Diyala. *Diyala Journal of Medicine*

.2022;22(2):8--17.

<https://doi.org/10.26505/DJM.22026190823>

4. Bazira PJ, Ellis H, Mahadevan V. Anatomy and physiology of the breast. Surgery (Oxford). 2022;40(2):79-83.

<https://doi.org/10.1016/j.mpsur.2021.11.015>

5. Al-Karawi AS, Kadhim AS, Mohammed AA, Alajeeli F, Lippi G. The Impact of Spirulina Supplementation on Iraqi Obese Females: A Cohort Study. Al-Mustansiriyah Journal of Science. 2024;35(4):24-30.

<https://doi.org/10.23851/mjs.v35i4.1545>

6. Hertel M, Makvandi R, Kappler S, Nanke R, Bildhauer P, Saalfeld S, et al. Towards a biomechanical breast model to simulate and investigate breast compression and its effects in mammography and tomosynthesis. Physics in Medicine & Biology. 2023;68(8):085007.

<https://doi.org/10.1088/1361-6560/acc30b>

7. Branderhorst W, de Groot JE, Highnam R, Chan A, Böhm-Vélez M, Broeders MJM, et al. Mammographic compression – A need for mechanical standardization. European Journal of Radiology. 2015;84(4):596-602.

<https://doi.org/10.1016/j.ejrad.2014.12.012>

8. Mays Najem Al-Adilee HMA-A. The Role of Caspase-8, MLKL and RIPK1 in Iraqi Patients' Women with Breast Cancer. Al-Mustansiriyah Journal of Science. 2025;36(1):22-33.

<https://doi.org/10.23851/mjs.v36i1.1596>

9. Serwan E, Matthews D, Davies J, Chau M. Mechanical standardisation of mammographic compression using Volpara software. Radiography. 2021;27(3):789-94.

<https://doi.org/10.1016/j.radi.2020.12.009>

10. Farhan AH, Kamil MY. Texture Analysis of Mammogram Using Local Binary Pattern Method. Journal of Physics: Conference Series; 2020: Institute of Physics Publishing.

<https://doi.org/10.1088/17426596/1530/1/01201>

11. Radhi EA, Kamil MY. Breast tumor

segmentation in mammography image via Chan-Vese technique. Indonesian Journal of Electrical Engineering and Computer Science. 2021;22(2):809-17.

<https://doi.org/10.11591/ijeecs.v22.i2.pp809-817>

12. Mohammed SS, Al-sharuee IF, Ali AM, Elrayah A. Theoretical Study of the Structural and Electronic Properties of NIPAM Polymer Dosimetry Gel. Al-Mustansiriyah Journal of Science. 2024;35(4):72-9.

<https://doi.org/10.23851/mjs.v35i4.1571>

13. Hameed D, Funjan MM, Al-Sabbagh AA. Relationship Between Anthropometric Measurements with Radiation Dose During Screening Mammography. Journal of Ecohumanism. 2024;3(4):1598-605.

<https://doi.org/10.62754/joe.v3i4.3690>

14. Radhi EA, Kamil MY. Segmentation of breast mammogram images using level set method. AIP Conference Proceedings. 2022;2398(1). <https://doi.org/10.1063/5.0093693>

15. Salim DA, Mhana WJ, Ishnayin HG, Mahdi KH. Theoretical Study of the Quadruple Gamma Transitions of Radioactive Radon and Radium Isotopes Based on Half-Life. Al-Mustansiriyah Journal of Science. 2024;35(4):42-51.

<https://doi.org/10.23851/mjs.v35i4.1550>

16. Marouf SS. The Relations Between High Body Mass Index and Breast Cancer Characteristics. Diyala Journal of Medicine. 2024;26(2):69-79.

<https://doi.org/10.26505/djm.v26i2.1098>

17. Abu Elmola AM, Sudan Academy of Sciences, Khartoum (Sudan). Assessment of mean glandular dose for patients in mammography in some Hospitals in Khartoum state. 2016. <https://inis.iaea.org/records/fz1gc-mb772>

18. Alukic E, Bravhar P, Mekis N. Does the use of self-compression in mammography affect compression force, breast thickness, and mean

glandular dose? European Journal of Radiology. 2021;139:109694.

<https://doi.org/10.1016/j.ejrad.2021.109694>

19. Ko MS, Kim HH, Cha JH, Shin HJ, Kim JH, Kim MJ. Dose reduction in automatic optimization parameter of full field digital mammography: breast phantom study. J Breast Cancer. 2013;16(1):90-6.

<https://doi.org/10.4048/jbc.2013.16.1.90>

20. Al Hrouf R, Ayasrah M, Noor Azman NZ. Assessing Mean Glandular Dose in Mammography in Jordan According to

American College of Radiology (ACR) Standards. Cancer Manag Res. 2025;17:11-22

<https://doi.org/10.2147/CMAR.S497104>

21. Noor KAM, Norsuddin NM, Karim MKA, Isa INC, Ulaganathan V. Evaluating Factors Affecting Mean Glandular Dose in Mammography: Insights from a Retrospective Study in Dubai. Diagnostics. 2024; 14(22):2568.

<https://doi.org/10.3390/diagnostics14222568>

العلاقة بين تعرض الجلد للإشعاع لدى النساء العراقيات وسُمك الثدي المضغوط في التصوير الشعاعي للثدي

^١ دعاء حميد كاظم، ^٢ زينب احمد حمودي، ^٣ مودة موسى فنجان، ^٤ رانية جمال احمد، ^٥ ايه حميد حسن

الملخص

الخلفية: يجري تقييم سُمك الثدي المضغوط (CBT) بشكل أساسي من خلال فحوصات الماموغرافي. وعلى الرغم من التأكيد العلمي على أن الضغط على الثدي يؤثر بشكل ملحوظ على خصائص أنسجة الثدي، إلا أن التأثير المحدد لهذا الضغط على منطقة الإبط لا يزال غير واضح. إذ قد يؤدي زيادة الضغط إلى تقليل سُمك أنسجة الثدي، مما يؤثر بدوره على جودة التصوير ومعايير التعرض للإشعاع.

الأهداف: تهدف هذه الدراسة إلى تحديد العلاقة بين التعرض السطحي للجلد (ESE) وسُمك الثدي المضغوط (CBT) لدى النساء العراقيات، بالإضافة إلى مقارنة المتوسط الحسابي لقيم التعرض السطحي للجلد الناتجة عن فحوصات التصوير الشعاعي للثدي في العراق بقيم وردت في الدراسات الأخرى.

المرضى والطرق: أجريت دراسة مقطعية في مستشفى التعليمي "العلوية" خلال الفترة من ديسمبر ٢٠٢٣ إلى يناير ٢٠٢٤، وشارك فيها ١٠٠ امرأة عراقية. تم إجراء فحوصات الماموغرافي باستخدام جهاز من طراز GE Healthcare، مع استخدام كل من الإسقاطات الأمامية-الخلفية (CC) والجانبية المائلة (MLO) لتقييم سُمك الثدي المضغوط والتعرض السطحي للجلد.

النتائج: أظهرت النتائج وجود علاقة إيجابية ذات دلالة إحصائية بين التعرض السطحي للجلد (ESE) وسُمك الثدي المضغوط (CBT). وبشكل محدد، لوحظ أن زيادة سُمك الثدي المضغوط كانت مرتبطة بارتفاع قيم التعرض السطحي للجلد. علاوة على ذلك، كان متوسط قيم التعرض السطحي للجلد المسجلة في هذه الدراسة أقل بكثير مقارنةً بالمتوسط الحسابي للقيم المُبلغ عنها في دراسات مماثلة أُجريت في السودان.

الاستنتاج: تُظهر الدراسة أن سُمك الثدي المضغوط والتعرض للإشعاع يكونان أعلى بشكل ملحوظ في الإسقاط الجانبية المائل (MLO) مقارنةً بالإسقاط الأمامي-الخلفي (CC). كما تم رصد علاقة إيجابية قوية بين سُمك الثدي المضغوط وجرعة الإشعاع. بالإضافة إلى ذلك، كانت قيم التعرض السطحي للجلد في هذه الدراسة أقل بكثير من تلك التي وُجدت في الدراسات المماثلة في السودان. وتؤكد هذه النتائج على ضرورة اعتماد إرشادات ومعايير إقليمية خاصة في ممارسات الماموغرافي لضمان توفير الرعاية المثلى للمرضى وسلامتهم.

الكلمات المفتاحية: منطقة الإبط، نسيج الثدي، التعرض السطحي للجلد (ESE)، التصوير الشعاعي للثدي، سُمك الثدي المضغوط.

المؤلف المراسل: دعاء حميد كاظم

الايمل: doaa.hameed2208m@comed.uobaghdad.edu.iq

تاريخ الاستلام: ٠٤ كانون الثاني ٢٠٢٥

تاريخ القبول: ١٧ آذار ٢٠٢٥

تاريخ النشر: ٢٥ نيسان ٢٠٢٥

^١ فرع الفلسفة - كلية الطب - الجامعة المستنصرية - بغداد - العراق.




^٢ قسم تقنيات الاشعة - كلية النور الجامعة - بغداد - العراق.

^٣ فرع الفلسفة - كلية الطب - جامعة بغداد - بغداد - العراق.

^٤ قسم تقنيات الاشعة - كلية التقنيات الصحية والطبية - جامعة الاسراء - بغداد - العراق.

^٥ قسم هندسة تقنيات الاتصالات - الكلية التقنية - جامعة الامام جعفر الصادق - بغداد - العراق.

Determination of Meprin Alpha Enzyme and its Relationship with Some Antioxidants and Interleukin 12 in the Blood Serum of Patients with Colon Cancer

Hussein Mahmoud Khalaf ¹, Wasan Nazhan Hussein ², Alaa Hassan Musstaf ³

^{1,2} Department of Chemistry, College of Education for Pure Sciences, Tikrit University, Tikrit, Iraq.

³ General Medicine and Surgery, College of Medicine, Al-Kindi University, Baghdad, Iraq.

OPEN ACCESS

Correspondence: Hussein Mahmoud Khalaf
Email: HM230043pep@st.tu.edu.iq
Copyright: ©Authors, 2025, College of Medicine, University of Diyala. This is an open access article under the [CC BY 4.0](http://creativecommons.org/licenses/by/4.0/) license (<http://creativecommons.org/licenses/by/4.0/>)
Website: <https://djm.uodiyala.edu.iq/index.php/djm>

Received: 25 November 2024
Accepted: 05 March 2025
Published: 25 April 2025

Abstract

Background: Colon cancer is an uncontrolled growth of cells that begins in a part of the large intestine called the colon. The colon is the first and longest section of the large intestine. The possible causes of colon cancer are genetic, environmental and nutritional factors. This study was prepared to help in identifying the causes and predicting the occurrence of colon cancer.

Objective: To identify the possible factors as causes of colon cancer in a group of patients in Diyala Governorate - Iraq.

Patients and Methods: In this study, blood serum samples were collected from 60 patients with colon cancer. 30 serum samples were collected from non-colon cancer patients who were considered a control group. The levels of alpha-meprin enzyme, catalase enzyme, nitric oxide and interleukin 12 were measured by immunoassay using the ELISA device.

Results: The results showed that the levels of Meprin alpha and interleukin 12 had statistically significant values, as their levels were higher than the control group, while the levels of catalase and nitric oxide were low when compared to the control group.

Conclusion: It was found that there is a significant positive correlation between meprin alpha and interleukin 12, and there was an inverse correlation between meprin alpha and catalase and nitric oxide. The results of our study indicated that the reason for the increase in meprin alpha and interleukin 12 is related to colon cancer.

Keywords: Antioxidants, Interleukin 12, Meprin alpha, Catalase, Nitric oxide.

Introduction

Colon cancer is a type of cancer that affects the large intestine and usually arises from benign tumors that turn into cancerous cells over time (1). Colon cancer affects the colon and causes a health problem. It is a very common disease, with high rates of infection and death reaching almost half of those infected (2). Colon cancer was the cause of 10% of cancer deaths in 2010. Colon cancer is becoming more common among people aged 45 to 50, regardless of age (3) Colon Cancer is one of the most common types of cancer in the world, with more than a million new cases each year around the world (3). Malignant tumors of the lymphocytes are known as lymphomas. They begin in B or T lymphocytes. The gastrointestinal tract is the most common site for lymphomas outside the lymph nodes (4). Therefore, it is considered the third most common type of cancer and the fourth most

common type of cancer in terms of cancer-related deaths (5). Among the causes of infection are behavioral factors that affect the development of colon cancer, including age, lifestyle, environmental, and genetic factors (6). Meprin alpha is a metalloproteinase that contains zinc and is associated with the cell membrane, from which it is secreted. Many of these enzymes (metalloproteins) are secreted from cell membranes; some of them are associated with the cell membrane, and their work is both outside and inside the cell. These metalloproteins are crucial in various disorders and diseases, including inflammatory conditions and cancers (7). Interleukin 12 is a key member of the IL-12 cytokine family and a powerful stimulator of antitumor immunity. IL-12 was initially identified in the late 1980s as a factor that acts as a stimulator of natural killer cells with multiple biological effects on peripheral blood lymphocytes (8). It is mainly produced by antigen-presenting cells such as dendritic cells, monocytes, macrophages, and B cells. It consists of two covalently linked chains of 40 KDa and 35 KDa. IL-12 has been reported to have a potent antitumor effect (9, 10). Catalase plays an important role in decomposing hydrogen peroxide into oxygen and water. Catalase removes high concentrations of hydrogen peroxide due to its antioxidant action. Catalase is distinguished from other enzymes by its highest turnover rates, with a single molecule capable of converting 83,000 hydrogen peroxide molecules into water and oxygen per second. Catalase also resists the formation of Peroxynitrite by oxidizing nitric oxide in the presence of hydrogen peroxide. Overall, these catalytic properties enhance the antioxidant defense systems of cells mediated by catalase (11). Nitric oxide plays a significant role in the physiology of living organisms. It has a significant regulatory role at the physiological level in vital processes such as neurotransmission. It also has an essential role in

responding to inflammation and cardiovascular diseases and is involved in defense mechanisms and regulating inflammatory and immune mechanisms (12). Arginine acts as a building block for protein and a precursor for nitric oxide synthesis (13). Nitric oxide is a vasodilator, neurotransmitter, metabolic regulator, and bactericidal, fungicidal, and virucidal agent (14). This study investigates the meprin alpha enzyme's effect on cancer cells, the associated biochemical alterations in colon cancer patients, and its potential future implications.

Patients and Methods

Study design: Blood samples were taken from 60 patients with colon cancer, and 30 samples were used as a control group for the period from 11/1/2023 to 3/1/2024. Blood samples (4-5 ml) were drawn from patients and healthy people and transferred to gel tubes. Serum was obtained by centrifugation at 3000 rpm for 15 minutes. The serum was stored at -20 °C until the tests were performed.

Serological tests: Serological tests were performed in Baghdad, Iraq's Scientific Center for Chemical Analysis laboratories. The effectiveness and levels of the study variables were determined using the sandwich method and the ELISA device. The concentration of the study variables in the blood serum was estimated using a ready-made test kit from the American company Clond-Clond Corp, which produced a yellow compound whose absorption intensity could be measured at a wavelength of 450 nanometers.

Statistical analysis

The results were analyzed statistically, and the values were expressed as (mean \pm standard deviation), and the level of statistical significance was determined using the SPSS program (statistical package for the social sciences), and the difference between the two groups were not considered statistically significant unless (P value) was less than

0.05, and Pearson's correlation coefficient (r) was used to test the relationship between the two coefficients.

Results

Meprin alpha enzyme level assessment: The activity and level of meprin alpha enzyme were estimated in the blood of healthy people and patients with colon cancer. The research results included the statistical values for colon cancer patients that were estimated in the blood of patients with colon cancer and the control group, where it was found when conducting a statistical comparison between the activity of meprin alpha enzyme in the blood of patients and controls,

it was found that there was a significant increase at a probability level ($P \leq 0.05$) in the activity of the enzyme in patients, where it was (316.696 ± 53.131) and in the control, where it was (223.385 ± 40.820) and shown in Figure 1.

Catalase enzyme level assessment: Catalase enzyme levels were investigated in the serum of patients with colon cancer compared to healthy controls. A statistically significant decrease was observed at the probability level of $P \leq 0.05$, where the values of Mean \pm SD in healthy and infected patients were 21.479 ± 3.835 and 3.175 ± 0.718 , respectively, as shown in Figure 2.

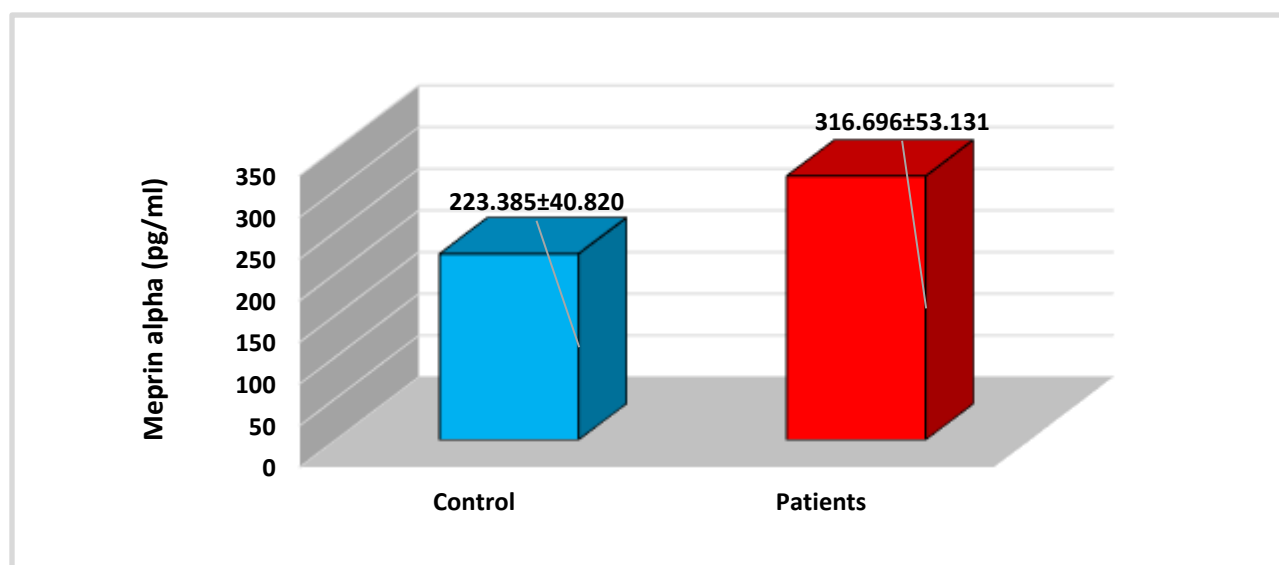


Figure 1. The activity of meprin alpha enzyme in the blood of colon cancer patients and the control group.

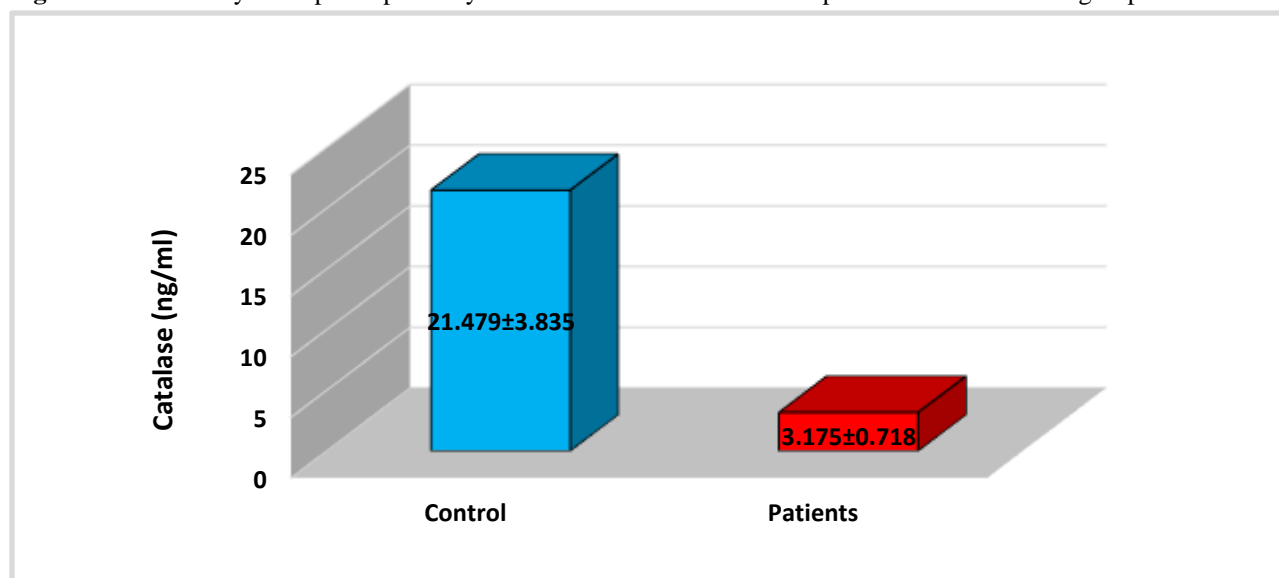


Figure 2. shows the concentration of catalase enzyme in the blood of colon cancer patients and the control group.

Nitric oxide level assessment: The results showed a statistically significant decrease at the probability level of $P \leq 0.05$ in the level of nitric oxide in the group of colon cancer patients, where the results in patients were (4.496 ± 0.987) compared to the control group (17.972 ± 2.953) as shown in Figure 3.

Interleukin-12 level assessment: By studying

the levels of interleukin 12 in the serum of healthy people and those with colon cancer, the results showed a significant increase with statistical significance at the probability level of $P \leq 0.05$ in patients compared to healthy people, as the mean \pm SD in patients was (377.891 ± 80.119) and healthy people (136.927 ± 33.929) as shown in Figure 4.

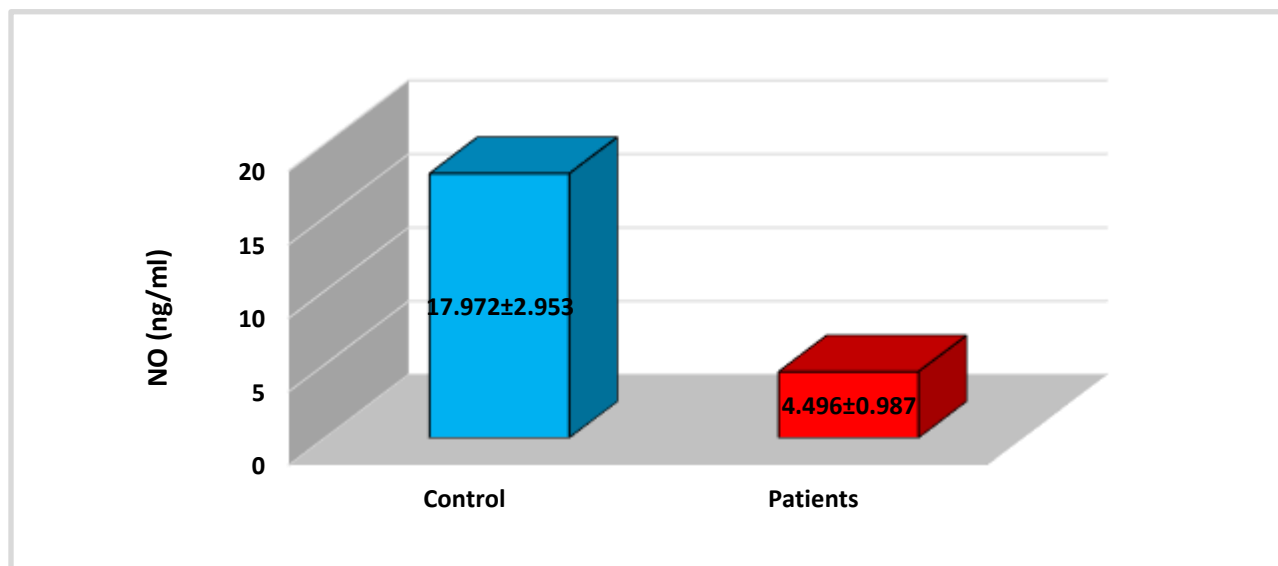


Figure 3. Shows the concentration of nitric oxide in the blood of colon cancer patients and the control group.

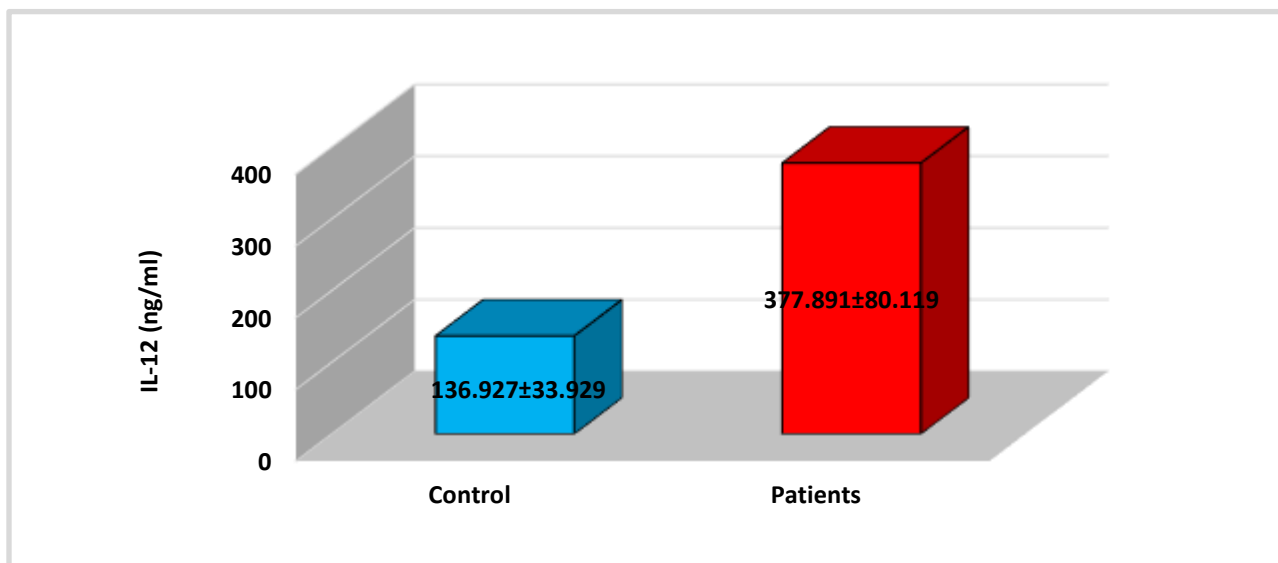


Figure 4. The concentration of interleukin-12 in the blood of colon cancer patients and the control group.

The correlation relationships of the enzyme meprin alpha with the variables under study:

To find the relationship between the enzyme meprin alpha and the clinical variables studied in the research for patients with colon cancer, it is necessary to find the correlation coefficient (linear correlation) between the enzyme and the variables, as the correlation coefficient r : is a measure of the degree of association or commitment between two independent variables and is used to describe the relationship and degree of association between the various measurements studied, as follows:

The binding relationship between meprin alpha and catalase: The correlation between the

enzyme meprin alpha and the enzyme catalase was studied in people with colon cancer and an inverse correlation was found as shown in Figure 5.

The binding relationship between meprin alpha and nitric oxide: The relationship between meprin alpha and nitric oxide was studied in people with colon cancer and an inverse relationship was found as shown in Figure 6.

The binding relationship between Meprin alpha and IL-12: The relationship between meprin alpha and interleukin-12 was studied in people with colon cancer and a direct correlation was found as shown in Figure 7.

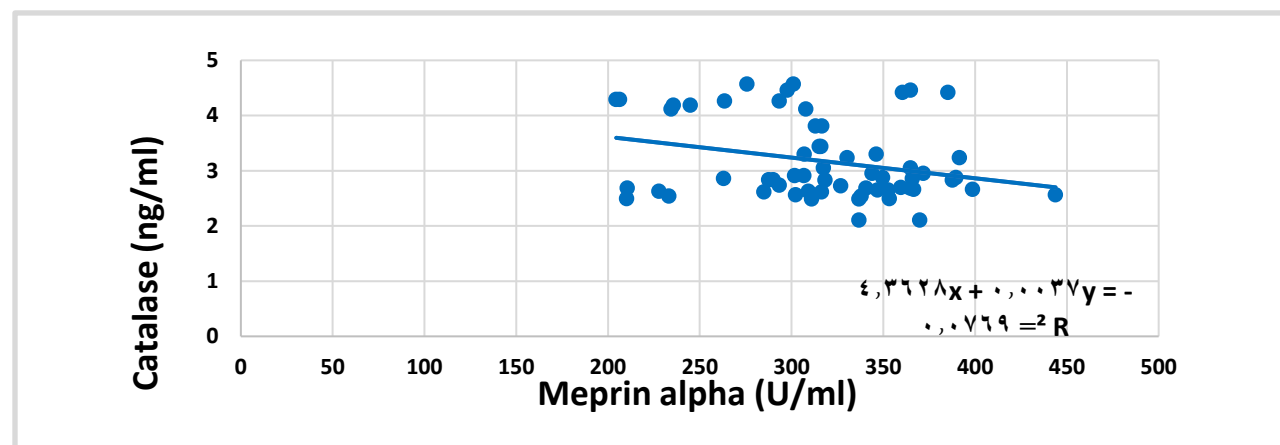


Figure 5. The linear relationship between the enzyme meprin alpha and the enzyme catalase in the blood serum of patients with colon cancer.

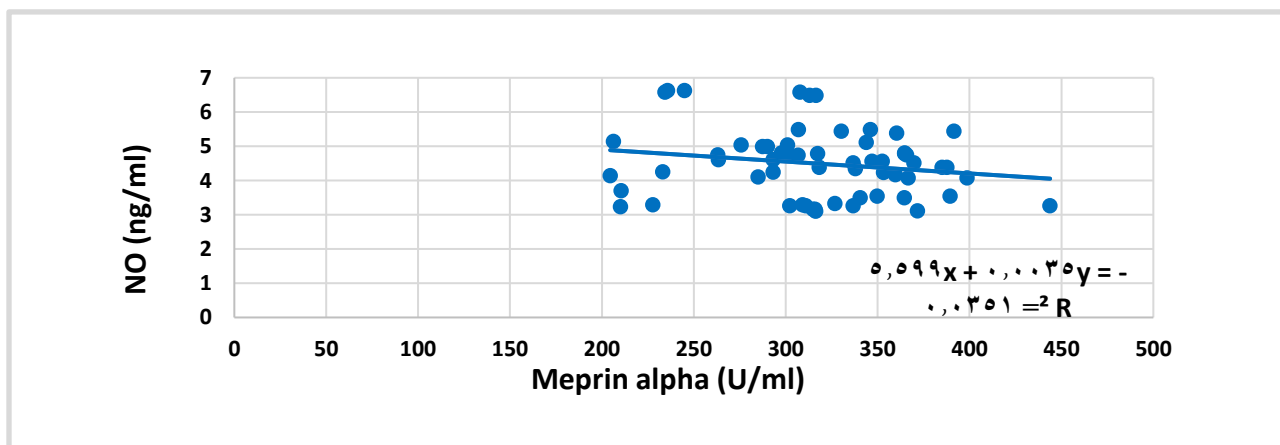


Figure 6. The linear relationship between the enzyme meprin alpha and nitric oxide in the blood serum of patients with colon cancer.

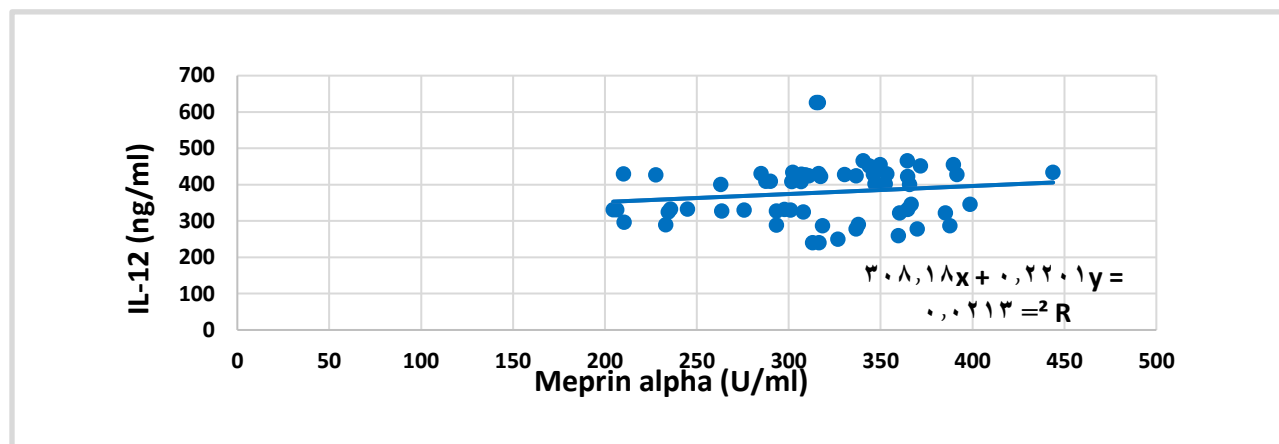


Figure 7. The linear relationship between the enzyme meprin alpha and interleukin-12 in the blood serum of patients with colon cancer.

Discussion

Colon cancer is an uncontrolled growth of cells that begins in a part of the large intestine called the colon. The possible causes of colon cancer include genetic, environmental, and nutritional factors. This study was designed to help determine the causes and predict the occurrence of colon cancer. The results of our study showed lower levels of catalase and nitric oxide in people with colon cancer and higher levels of interleukin 12 and mebrin alpha in people with colon cancer. The study conducted by researchers Lutaz, Daniel, and their group was consistent with the results of our study, which indicated that mebrin alpha contributes to tumor progression by facilitating the migration of cancer cells and their entry into the blood vessels and their metastasis in patients compared to healthy individuals (15). Peters and colleagues observed that mebrin alpha levels were highly abundant in intestinal cells of both sexes, and their expression was associated with different stages of colon cancer. conditions (16). Anwar and colleagues noted that catalase is the major antioxidant enzyme that efficiently degrades hydrogen peroxide into water and oxygen, reducing oxidative stress and preventing cellular and molecular disintegration. This enzyme plays a crucial role in maintaining cellular redox balance. Its dysregulation is

associated with the delicate balance between generating reactive oxygen species (ROS) and antioxidant defenses such as catalase, which is particularly vital in conditions such as cancer, where catalase can play a dual role in the survival of normal and cancer cells (17). Panneerselvan suggested that the reason for the lower levels of nitric oxide in patients with colon cancer compared to healthy individuals is due to the antioxidant and pro-oxidant properties of nitric oxide (18,19). Yin, X. L. demonstrated that IL-12 is a potent cytokine that plays a key role in the initiation of cell-mediated immunity by regulating biological groups as a growth factor for natural killer cells and activated T cells, favoring the formation of cytotoxic T cells, and stimulating the production of several cytokines (20,21).

Conclusions

The change in immune response due to colon cancer resulted in high responsive concentrations of interleukin 12 and meprin alpha, with a strong association between them.

Recommendations

It was recommended to study the relationship between meprin alpha enzyme and other cancer cases, such as lung and liver cancer. In addition, it was essential to

study the effect of genes encoding the meprin alpha enzyme on patients with colon cancer and other cancers. Furthermore, it was recommended that the relationship between meprin alpha activity and oxidative stress be found, and the role of meprin alpha in remodeling the extracellular matrix be studied.

Source of funding: No source of funding.

Ethical clearance: This study was conducted based on the ethical standards stipulated in the Declaration of Helsinki. Before taking the sample, the patient's informed written and verbal agreement was obtained, after the review and approval of the study protocol and subject's information by the local ethics committee according to the document number 12118 (including the number and the date in 9/11/2023) to get this approval by Task Facilitation Committee of Diyala Health Directorate in coordination with Tikrit University, College of Education for Pure Sciences, Department of Chemistry.

Conflict of interest: None.

Acknowledgements:

The authors extend they're thanks to all participants in the study, starting with Tikrit University, College of Education for Pure Sciences, Department of Chemistry, and with the staff of the Oncology Center at Baqubah General Hospital, and I pray for the recovery of the patients and mercy for those who have passed away.

References

1. Sachdeo RA, Charde MS, Chakole RD. Colorectal cancer: An overview. Asian Journal of Research in Pharmaceutical Science. 2020;10(3):211-23.
<https://doi.org/10.5958/2231-5659.2020.00040.5>
2. Wang Y-H, Li J-Q, Shi J-F, Que J-Y, Liu J-J, Lappin JM, et al. Depression and anxiety in relation to cancer incidence and mortality: a

systematic review and meta-analysis of cohort studies. Molecular psychiatry. 2020;25(7):1487-99. <https://doi.org/10.1038/s41380-019-0595-x>.

3- Motib, M. S., Mustaf, A. H. M. H., Alrubaye, M. F. A., & Al-Hamami, H. A. J. (2024). Influence of lymphovascular invasion on outcome of colon cancer. Diyala Journal of Medicine, 27(1), 25-34.

<https://doi.org/10.26505/DJM.27018260212>.

4. Morgan, E., Arnold, M., Gini, A., Lorenzoni, V., Cabasag, C. J., Laversanne, M., ... & Bray, F. (2023). Global Burden of Colorectal Cancer in 2020 and 2040: Incidence and Mortality Estimates from GLOBOCAN. Gut, 72(2), 338-344.

<https://doi.org/10.1136/gutjnl-2022-327736>

5- Idan, H. M., & Motib, A. S. (2024). Incidence of head and neck cancer among Baquba Teaching Hospital Patients. Diyala Journal of Medicine, 27(1), 86-96.

<https://doi.org/10.26505/DJM.27018820708>

6. Ahmed M. Colon cancer: a clinician's perspective in 2019. Gastroenterology research. 2020;13(1):1.

<https://doi.org/10.14740/gr1239>

7. Chan AT, Giovannucci EL. Primary prevention of colorectal cancer. Gastroenterology. 2010;138(6):2029-43. e10. <https://doi.org/10.1053/j.gastro.2010.01.057>

8. Sterchi EE, Stöcker W, Bond JS. Meprins, membrane-bound and secreted astacin metalloproteinases. Molecular aspects of medicine.2008;29(5):309-28.

<https://doi.org/10.1016/j.mam.2008.08.002>

9. Peignier, A., Kim, J., Lemenze, A., & Parker, D. (2024). Monocyte-regulated interleukin 12 production drives clearance of Staphylococcus aureus. PLoS pathogens, 20(10), e1012648.

<https://doi.org/10.3390/cancers13030373>

10. Medzhitov R. Toll-like receptors and innate immunity. *Nature Reviews Immunology*. 2001;1(2):135-45.
<https://doi.org/10.1038/35100529>
11. Manetti R, Parronchi P, Giudizi MG, Piccinni M-P, Maggi E, Trinchieri G, et al. Natural killer cell stimulatory factor (interleukin 12 [IL-12]) induces T helper type 1 (Th1)-specific immune responses and inhibits the development of IL-4-producing Th cells. *The Journal of experimental medicine*. 1993;177(4):1199-204.
<https://doi.org/10.1084/jem.177.4.1199>
12. Góth L, Rass P, Páy A. Catalase enzyme mutations and their association with diseases. *Molecular Diagnosis*. 2004;8:141-9.
<https://doi.org/10.1007/BF03260057>
13. León J, Costa-Broseta Á. Present knowledge and controversies, deficiencies, and misconceptions on nitric oxide synthesis, sensing, and signaling in plants. *Plant, Cell & Environment*. 2020;43(1):1-15.
<https://doi.org/10.1111/pce.13617>
14. Wu G, Meininger CJ, McNeal CJ, Bazer FW, Rhoads JM. Role of L-arginine in nitric oxide synthesis and health in humans. *Amino acids in nutrition and health: Amino acids in gene expression, metabolic regulation, and exercising performance*. 2021:167-87.
https://doi.org/10.1007/978-3-030-74180-8_10
15. Kurhaluk, N., & Tkaczenko, H. (2025). L-Arginine and Nitric Oxide in Vascular Regulation—Experimental Findings in the Context of Blood Donation. *Nutrients*, 17(4), 665. <https://doi.org/10.3390/nu17040665>
16. Dumermuth E, Sterchi E, Jiang W, Wolz R, Bond JS, Flannery A, et al. The astacin family of metalloendopeptidases. *Journal of Biological Chemistry*. 1991;266(32):21381-5.
[https://doi.org/10.1016/S0021-9258\(18\)54648-2](https://doi.org/10.1016/S0021-9258(18)54648-2)
17. Peters F, Becker-Pauly C. Role of meprin metalloproteases in metastasis and tumor microenvironment. *Cancer and Metastasis Reviews*. 2019;38(3):347-56.
<https://doi.org/10.1007/s10555-019-09805-5>
18. Anwar S, Alrumaihi F, Sarwar T, Babiker AY, Khan AA, Prabhu SV, et al. Exploring Therapeutic Potential of Catalase: Strategies in Disease Prevention and Management. *Biomolecules*. 2024;14(6):697.
<https://doi.org/10.3390/biom14060697>
19. Ballardín M, Barsacchi R, Bodei L, Caraccio N, Cristofani R, Di Martino F, et al. Oxidative and genotoxic damage after radio-iodine therapy of Graves' hyperthyroidism. *International journal of radiation biology*. 2004;80(3):209-16.
<https://doi.org/10.1080/0955300042000205555>
20. Yin X-l, Wang N, Wei X, Xie G-f, Li J-j, Liang H-j. Interleukin-12 inhibits the survival of human colon cancer stem cells in vitro and their tumor initiating capacity in mice. *Cancer letters*. 2012;322(1):92-7.
<https://doi.org/10.1016/j.canlet.2012.02.015>
21. Al-Hasso IKQ. Evaluation of Interleukin-22 and TLR-2 as an Immunological Biomarkers in Breast Cancer Patients. *Al-Kindy College Medical Journal*. 2024;20(2):97-100.
<https://doi.org/10.47723/3sfb2q82>

محدد انزيم الفازيم ميبرين وعلاقته المضادة للاكسدة وانترولوكين ١٢ في مصل الدم لمرضى القولون العصبي

^١ حسين محمود خلف ، ^٢ وسن نزهان حسين ، ^٣ علاء حسن مصطفى

الملخص

الخلفية: القولون العصبي: هو القولون غير المضبط للخلايا يبدأ في جزء من الامعاء الغليظة. القولون هو القسم الاول والاطول من الامعاء الغليظة. الاسباب المحتملة لسرطان القولون هي العوامل الضارة والبيئية والغذائي. وعدت هذه الدراسة للمساعدة في تحديد لاسباب والتننبؤ بحدوث سرطان القولون.

الأهداف: تحديد العامل المحتمل كمسببات لسرطان القولون في مجموعة من المرضى في محافظة ديالى - العراق.

المرضى والطرق: في هذه الدراسة تم جمع عينات من الدم من ٦٠ مريضاً للكولسترول. تم جمع ٣٠ عينة من المرضى المصابين بالمرض والكولسترول والذين اعتبروا مجموعة المرضى. تم قياس مستويات انزيم الفا ميبرين وانزيم الكاتالاز واكسيد نيتريك وانترولوكين ١٢ بواسطة المقاييس المناعية باستخدام جهاز الاليزا.

النتائج: أن مستويات الميبرين لسيارة فولفو والانترولوكين ١٢ كانت ذات قيم ذات دلالة إحصائية، حيث كانت مستوياتها أعلى من المجموعة الضابطة، في حين كانت مستويات الكاتالاز وأكسيد النيتريك دون وجوداً بالمجموعة الضابطة. بالإضافة إلى: هناك أن هناك ارتباطاً إيجابياً يهم بين الميبرين فولكس فاجن والانترولوكين ١٢، وهناك ارتباط عكسي بين الميبرين فولفو والكاتالاز وأكسيد النيتريك. أشارت دراستنا إلى سبب زيادة الميبرين لسيارة فول الصويا والانترولوكين ١٢ المرتبط بالقولون العصبي.

الاستنتاج: وُجد ارتباط إيجابي كبير بين الميبرين ألفا والانترولوكين ١٢، وارتباط عكسي بين الميبرين ألفا والكاتالاز وأكسيد النيتريك. وأشارت نتائج دراستنا إلى أن سبب ارتفاع مستويات الميبرين ألفا والانترولوكين ١٢ مرتبطاً بسرطان القولون.

الكلمات المفتاحية: مضادات التغذية، الانترولوكين ١٢، الميبرين فولفو، الكاتالاز، قرص نيتريك.

المؤلف المراسل: حسين محمود خلف

الايمل: HM230043pep@st.tu.edu.iq

تاريخ الاستلام: ٢٥ تشرين الثاني ٢٠٢٤




تاريخ القبول: ٥ آذار ٢٠٢٥

تاريخ النشر: ٢٥ نيسان ٢٠٢٥

^{٢,١} قسم الكيمياء - كلية التربية للعلوم الصرفة - جامعة تكريت - تكريت - العراق.

^٣ كلية طب الكندي - جامعة بغداد - بغداد - العراق.

Assessment of Development of Children in Diyala Province

Haider Asad Mohammad ¹, Najdat Sh. Mahmood ², Jalil I. Alezzi ³

¹ Diyala Health Directorate, Diyala, Iraq.

^{2,3} College of Medicine, University of Diyala, Diyala, Iraq.

OPEN ACCESS

Correspondence: Haider Asad Mohammad

Email: haider1991asad@yahoo.com

Copyright: ©Authors, 2025, College of Medicine, University of Diyala. This is an open access article under the [CC BY 4.0](http://creativecommons.org/licenses/by/4.0/) license (<http://creativecommons.org/licenses/by/4.0/>)

Website:
<https://djm.uodiyala.edu.iq/index.php/djm>

Received: 09 July 2023

Accepted: 06 August 2024

Published: 25 April 2025

Abstract

Background: Developmental assessment is a systematic and comprehensive process that evaluates a child's progress across multiple domains of development to identify potential developmental delays or disabilities.

Objective: This study aimed to assess the development of Iraqi children aged 2-60 months residing in Diyala province, compare it to other states, and estimate the prevalence of developmental delay.

Patients and Methods: A total of 330 samples from children were recruited from Al-Batool Teaching Hospital for Maternity and Children over a six-month period, from October 2022 to March 2023. The Ages and Stages Questionnaire (ASQ3) was used to assess the children's development. The ASQ3 is a standardized tool used to screen for developmental delays in children aged 2-60 months. The ASQ3 scores are divided into three areas: white (normal development), black (delayed development), and gray (critical zone).

Results: The study results showed that most of the children (97.6%) had normal development across all domains of development. However, 2.42% of the children had developmental delay, including two children (0.6%) with delayed speech and communication only and six children (1.8%) with global developmental delay in all areas. In addition, a proportion of children were situated within the gray area of the ASQ3 system, which indicates the need for further assessment to evaluate specific aspects of a child's development that may warrant closer attention. The proportion of children in the gray area ranged from 0% to 34.5%, depending on the development domain.

Conclusion: The results of this study suggest that most children in Diyala province have normal development. However, a small percentage of children have developmental delays, and a proportion of children are situated in the critical area and need further assessment.

Keywords: Developmental assessment, Developmental delay, Diyala, ASQ3.

Introduction

Child development is a complex and intricate process involving biological, psychological, and emotional changes that occur predictably and continuously from birth through adolescence. Some children may face developmental delays, failing to acquire skills and reach milestones according to the expected timeline (1,2). A combination of biomedical and socio-cultural factors influences child development. Some factors, such as nutrition, emotional support, and education, are modifiable and can be actively addressed. On the other hand, certain factors like child gender, consanguinity between parents, parents' ages, and educational level are non-modifiable. Socio-cultural factors, including poverty and exposure to violence, can also significantly impact a child's development (1). Developmental evaluation plays a critical role in assessing a child's progress in achieving age-appropriate developmental milestones and identifying any potential concerns or delays. Healthcare professionals, such as pediatricians or developmental psychologists, conduct these evaluations using

standardized tools to measure various aspects of a child's development, including cognitive, motor, communication, and social-emotional skills (3,4). The American Academy of Pediatrics recommends conducting regular developmental evaluations throughout a child's early years to identify and address any delays or concerns as early as possible. Early detection and intervention for developmental delays can significantly improve a child's outcomes and increase their chances of success in school and life. Parents and caregivers also play a crucial role in the developmental evaluation process by monitoring their child's progress and sharing any concerns with their healthcare provider (5,6). According to the Global Burden of Disease Study, approximately 52.9 million children under 5 worldwide experience delayed development, with 95% living in low- and middle-income countries (7). The American Academy of Pediatrics (AAP) recommends the routine and periodic use of standardized tools during each well-child clinic visit, with specific screenings conducted at 9, 18, and 24 or 30 months of age. The Ages and Stages Questionnaire (ASQ-3) is one of the screening tools chosen for its cultural sensitivity and availability in the native spoken language (8). Primary healthcare professionals, particularly family physicians, are critical in promoting child development. They are well-positioned to monitor children's growth and development and educate mothers or caregivers on providing the optimum environment for their child's growth.

Patients and Methods

Using a convenient sampling method, this cross-sectional study was conducted at the College of Medicine, University of Diyala, in the Pediatric Department. The study included 330 children from various socioeconomic backgrounds, selected from AlBatoool Teaching Hospital for Maternity and Children over a period of six months. The study utilized the Ages and Stages

Questionnaire (ASQ-3) system to categorize the enrolled children as normally developed or experiencing abnormal development. The ASQ3 is a parent-completed developmental screening instrument for children aged 2 to 60 months. Each questionnaire consists of 30 questions covering five developmental areas: communication, gross motor skills, fine motor skills, problem-solving, and personal-social skills. For each item, parents provide responses of "Yes," "Sometimes," or "Not yet," which are scored as 10, 5, or 0, respectively. The overall domain scores are obtained by summing the scores of all items within each domain, with a maximum score of 60 points per domain. Based on these domain scores, children are classified as normally developed (white area), developmentally delayed (black area), or at risk (gray area). Completing the ASQ-3 questionnaire typically takes 10-15 minutes for each child (Figure 1).

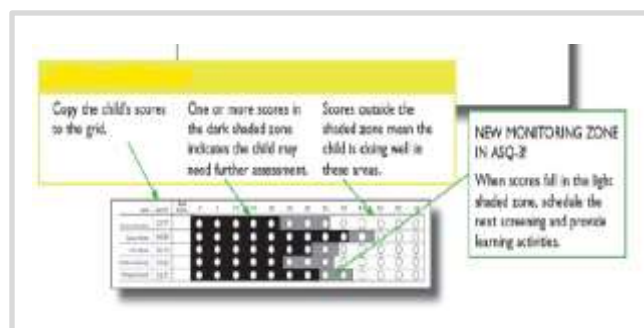


Figure 1. ASQ3 summary score (9).

Statistical analysis

Excel version 2021 and SPSS (Statistical Package for the Social Sciences) version 26 - 2022, were used for statistical analysis, t-test and chi-square was applied to calculate p value between variables, a level below 0.05 was considered significant (10), in addition to basic calculations of numbers and percent.

Results

Demographic criteria: A total of 330 children were enrolled in the study, distributed into 12 age groups (260 months), 140 (42.2%) were

males and 190 (57.8%) were girls with a ratio of 0.7:1 of male: female (Table 1).

Table 1. Demographic criteria for the study sample.

Gender		Age(months)												Total
		2	4	6	9	12	14	18	24	30	36	48	60	
Male	no.	11	12	10	9	12	5	12	13	14	15	12	14	140
	%	31.4	46	33	36	42.8	33.4	50	46.4	45.2	42.8	44.4	48.2	42.2
Female	no.	24	14	17	16	16	10	12	15	17	20	15	15	190
	%	68.6	54	63	64	57.2	66.6	50	53.6	54.8	57.2	55.6	51.8	57.8
Total	no.	35	26	27	25	28	15	24	28	31	35	27	29	330
	%	10.6	7.9	8.2	7.6	8.5	4.5	7.3	8.8	9.4	10.6	8.1	8.8	100

The data indicates that the 14-months age group had the lowest number of children, with a total of 15(4.5%), consisting of 5 boys (33.3%) and 10 girls (66.6%). In contrast, the 36-month and 2-month age groups had the highest number of children, with a total of 35(10.6%), consisting of 15 boys (42.8%) and 20 girls (57.2%), 24 girls and 11 males, respectively.

Developmental delay according to domain: It was found that most enrolled children (n= 322, 97.6%) were having normal development across all domains of development (speech and communication, gross motor, fine motor, problem solving and personal- social) while

developmental delay was detected in 8 (2.42%) children, including 2 children (0.6%) were having delayed in speech and communication only and 6 children (1.8%) were having global developmental delay in all areas (speech and communication, gross motor, fine motor, problem solving and personal-social). These results imply that, overall, the developmental screening outcomes were similar across most domains for the studied group, with slight differences observed in communication skills and global developmental delay (Table 2).

Table 2. Developmental delay in each domain for the study sample.

Development Achievement	Domain	No. (%)
Developmental Delay	Communication	2 (0.6%)
	Gross motor	0
	Fine motor	0
	Problem solving	0
	Personal-social	0
	Global DD	6 (1.8%)
	Total	8 (2.4%)
Normal development	322 (97.6%)	
Total	330 (100%)	

Distribution according to white/gray area in ASQ3: The majority of children who underwent assessment using the Ages and Stages Questionnaires, Third Edition (ASQ-3), demonstrated developmental achievements within the white area, indicating age-appropriate attainment of developmental milestones across multiple domains. These results provide evidence of positive developmental progress among the assessed children, implying that they are meeting or surpassing the anticipated developmental expectations for their respective age groups. However, it is important to note that a proportion of children were classified within the gray area, these were: regarding communication (0-16.1%)

the highest percentage in 30-month age group, gross motor (0-22.6%) the highest percentage in 30-month age group, fine motor (0-20.7%) the highest percentage in 60-month age group, problem solving (3.8-34.5%) the highest percentage in 60-month age group and personal-social (3.8-16.1%) the highest percentage in 30-month age group. The gray area on the ASQ-3 typically signifies the need for further assessment to evaluate specific facets of a child's development that may warrant closer attention. This subset of children may exhibit potential areas of concern or require additional monitoring to gain a more comprehensive understanding of their developmental trajectory, (Table 3).

Table 3. Distribution of normal developed children according to white/gray area in ASQ3.

Age	area	Communication		Gross motor		Fine motor		Problem solving		Personal-social	
		number	%	number	%	number	%	numbers	%	numbers	%
2 mo.	white	30	90.9	30	88.2	29	85.3	32	94.1	31	91.2
	Gray	3	9.1	4	11.8	5	14.7	2	5.9	3	8.8
	Total	33		34		34		34		34	
4 mo.	white	22	91.7	23	92	22	88	23	92	22	88
	Gray	2	8.3	2	8	3	12	2	8	3	12
	Total	24		25		25		25		25	
6 mo.	white	24	92.3	25	96.2	24	92.3	25	96.2	23	88.5
	Gray	2	7.7	1	3.8	2	7.7	1	3.8	3	11.5
	Total	26		26		26		26		26	
9 mon.	white	23	92	23	92	22	88	23	92	24	96
	Gray	2	8	2	8	3	12	2	8	1	4
	Total	25		25		25		25		25	
12 mo.	white	24	85.7	26	92.9	27	96.4	26	92.9	27	96.4
	Gray	4	14.3	2	7.1	1	3.6	2	7.1	1	3.6
	Total	28		28		28		28		28	
14 mo.	white	14	93.3	15	100	15	100	13	86.7	14	93.3
	Gray	1	6.7	0	0	0	0	2	13.3	1	6.7
	Total	15		15		15		15		15	
18 mo.	white	24	100	23	95.8	21	87.5	21	87.5	22	91.7
	Gray	0	0	1	4.2	3	13.5	3	13.5	2	8.3
	Total	24		24		24		24		24	
24 mo.	white	22	84.6	21	80.8	22	84.6	25	96.2	24	92.3
	Gray	4	15.4	5	19.2	4	15.4	1	3.8	2	7.7
	Total	26		26		26		26		26	
30 mo.	white	26	83.9	24	77.4	28	90.3	28	90.3	26	83.9
	Gray	5	16.1	7	22.6	3	9.7	3	9.7	5	16.1
	Total	31		31		31		31		31	
36 mo.	white	31	91.2	29	85.3	31	91.2	28	82.4	30	88.2
	Gray	3	8.8	5	14.7	3	8.8	6	17.6	4	11.8
	Total	34		34		34		34		34	
48 mo.	white	23	85.2	21	77.8	22	81.5	24	93.1	25	92.6
	Gray	4	14.8	6	22.2	5	18.5	3	6.9	2	7.4
	Total	27		27		27		27		27	
60 Mo.	white	29	100	27	93.1	23	79.3	19	65.5	29	100
	Gray	0	0	2	6.9	6	20.7	10	34.5	0	0
	Total	29		29		29		29		29	
Total		322		324		324		324		324	

Developmental delay according age and gender: Among all the participating children, 8 were identified as having

developmental delay, with a higher percentage in boys (3.57%) than in girls (1.58%), (Table 4).

Table 4. Developmental delay according to age and gender.

Age (months)		2	4	6	9	12	14	18	24	30	36	48	60	Total	p value
Normal	male	9	10	10	9	12	5	12	13	14	13	12	14	135 (42.4%)	0.245
	female	24	14	16	16	16	10	12	13	17	20	15	15	187 (57.6%)	
Developmental delay	male	2	2	-	-	-	-	-	-	-	1	-	-	5(1.5%)	
	female	-	-	1	-	-	-	-	2	-	-	-	-	3(0.9%)	
		35	26	27	25	28	15	24	28	31	35	27	29	330	

Overall, the differences between males and females regarding the mean calculated score for each age group from the 12 age groups in the study were found to be non-significant for most age groups. However, in 12 specific age-domain sub-groups, notably in the fine motor domain at 12 (p value: 0.02), 48(p value= 0.001), and 60(p value=0.002) months of age, girls displayed significantly higher scores compared to boys. Additionally, girls exhibited significantly higher scores in two age-domain subgroups, specifically in the gross motor domain at 48 (p value= 0.01) months of age and the communication domain at

60 (p value= 0.02). The findings suggest that while the gender differences in mean scores were not statistically significant for most age groups, distinct patterns were observed in specific age-domain subgroups. Girls consistently outperformed boys regarding mean scores in the fine motor domain and at specific ages, highlighting their superiority in these areas. Furthermore, girls also displayed higher scores in the gross motor domain at 48 and the communication domain at 60 months of age, indicating their advantage in these specific age-domain sub-groups (Table 5).

Table 5. Relationship between gender and development according to the calculated score. (* significant, ** very significant).

Age	Gender	number	Speech and Communication			Gross motor			Fine motor			Problem solving			Personal - social		
			mean	SD	p value	mean	SD	p value	mean	SD	p value	mean	SD	p value	mean	SD	p value
2 mo.	male	11 (31.4%)	49.09	15.6	0.4	53.18	15.9	0.8	47.7	8.8	0.4	50.2	14.5	0.9	46.8	16.5	0.6
	female	24(68.6%)	50.6	4.24		54.17	5.1		50.8	2.43		50.4	9.67		49.5	3.56	
	total	35															
4 mo.	male	12(46.2%)	50.8	17.3	0.1	55	9.4	0.2	52.92	10.9	0.2	52.5	8.7	0.5	50.42	8.4	0.2
	female	14 (53.8%)	55	4.22		54.3	2.9		50	7.5		53.9	5.5		56.97	3.89	
	total	26															
6 mo.	male	10(37%)	56.5	4.69	0.4	53.8	6.4	0.1	57.7	6.4	0.4	57.7	6.5	0.2	52	6.2	0.2
	female	17 (63%)	57.3	8.67		56.8	10.6		54.7	6.5		54.7	6.1		54.7	6.1	
	total	27															
9 mo.	male	9 (36%)	51.1	8.2	0.2	50	8.3	0.1	50	7.5	0.1	51.1	7.6	0.5	51.1	6.6	0.3
	female	16(64%)	54.7	7.4		54	7.9		54.2	4.5		49.6	10.8		53.3	6.4	
	total	25															
12 mo.	male	12(42.9%)	56.7	7.1	0.4	56.4	4.7	0.1	51.6	6.3	0.02*	50.4	6	0.6	50	6.5	0.9
	female	16(57.1%)	56.5	6.2		54.7	10.1		56.5	7.5		49.7	7.1		50.2	7	
	total	28															
14 mo.	male	5(33.3%)	49	10.9	0.3	50	13.7	0.2	50	8.3	0.5	53	5.1	0.07	50	7.4	0.2
	female	10(66.7%)	54.5	5.7		57	6.2		47.5	6.2		47.5	14.9		55	7.6	
	total	15															
18 mo.	male	12(50%)	58.3	6.7	0.5	54.9	9.8	0.6	52.9	6.3	0.5	49.1	7.5	0.2	54.6	5.18	0.7
	female	12(50%)	57	7.6		56.2	7.8		54.1	6.9		46.2	7.7		55	4.6	
	total	24															
24 mo.	male	13(46.4%)	54.6	5.4	0.5	50.3	6.3	0.08	53.8	5.1	0.02	54.2	6.2	0.3	56.6	5.6	0.3
	female	15(53.6%)	53.6	10.3		47	12.8		49.4	9.9		52.3	13.7		55	11.6	
	total	28															
30 mo.	male	14(45.2%)	50.3	8.9	0.1	47	8.3	0.8	50.7	11.6	0.3	49.6	9.1	0.4	53.2	10.9	0.9
	female	17(54.8%)	53.8	9.3		47.5	8		54	11.6		47.9	7.1		53.5	11.6	
	total	31															
36 mo.	male	15(42.9%)	55.6	14.2	0.6	53	5.4	0.1	56.6	7.9	0.9	48.6	10.3	0.3	55.6	8.7	0.8
	female	20(57.9%)	57.3	7.9		50.7	10.9		56.5	13.1		45.8	13.2		55.2	9.7	
	total	35															
48 mo.	male	12(44.4%)	52.2	6.4	0.5	47.3	7.6	0.01*	58.7	4.6	0.001**	56.6	5.9	0.1	56.7	4.4	0.19
	female	15(55.6%)	53.4	5.8		53.5	10.4		51.3	11.8		54	6.1		55.3	4	
	total	27															
60 mo.	male	14(48.3%)	54.6	4.9	0.02*	50.3	8.1	0.2	41.8	6.8	0.002**	43.6	8.2	0.1	58.9	2.4	0.7
	female	15(51.7%)	58	2.1		53.3	7.8		48.7	7.7		47.3	9.7		59.3	2.3	
	total	29															
Total		330															

Relationship between maturity and developmental delay: Of the 301 (91.2%) children, 301 (91.2%) were born at term and 29 (8.8%) were born preterm. Among the term babies, 295 (98%) were found to be normal, and 6 (2.0%) were found to be developmentally delayed. For the preterm-born children, 2 (6.9%) were developmentally delayed, while the remaining 27 (93.1%) were normal. A chi-square test showed no statistically significant association between preterm birth and developmental delay (p value = 0.9) (Table 6). It's

worth mentioning that the corrected age was used for preterm babies instead of the actual age. When measuring the association between maturity and development, no significant differences were found in all five domains of communication, gross motor, fine motor, problem solving, and personal-social across all 12 age groups. This suggests that maturity and development are not directly related and that other factors may play a more significant role in determining an individual's developmental trajectory (Table 7).

Table 6. Relationship between maturity and developmental delay.

Maturity	Development		Total No (%)	p value
	Normal children No. (%)	Delayed children No. (%)		
Term	295 (98)	6 (2)	301(91.2)	0.9
Preterm	27 (93.1)	2 (6.9)	29 (8.8)	
Total	322(97.58)	8(2.42)	330	

Table 7. The relationship between maturity and development.

Age	Maturity	number (%)	Speech and communication			Gross motor			Fine motor			Problem - solving			Personal - social		
			mean	SD	p value	mean	SD	p value	mean	SD	p value	mean	SD	p value	mean	SD	p value
2 mo.	preterm	5(14.3%)	41	17.2	0.1	47	16.9	0.4	48	14.7	0.8	48.2	11.3	0.6	55	4.5	0.5
	term	30(85.7%)	54.3	7.4		52.8	14.9		49.3	7.6		49.6	9.1		51.5	10.2	
	total	35															
4 mo.	preterm	2(7.7%)	55	7.0	0.6	57.5	2.5	0.2	52.5	2.5	0.3	50	10	0.1	55	2.5	0.3
	term	24(92.3%)	51.6	6.3		51.2	7.7		48.7	7.7		52.2	9.8		51.5	6.4	
	total	26															
6 mo.	preterm	4(14.8%)	48.7	8.5	0.2	56.2	5.6	0.8	53.7	6.8	0.3	51.2	8.1	0.2	50	5.4	0.1
	term	23(85.2%)	42.3	6.5		55.6	6.5		57.6	11.3		56.9	10.3		55.6	4.6	
	total	27															
9 mo.	preterm	3(12%)	45	10.8	0.3	48.3	9.1	0.4	46.7	6.1	0.2	48.3	9.2	0.7	51.7	6.4	0.6
	term	22(88%)	54.7	10.9		53.4	9.9		52.3	8		50.5	10.3		49.8	11	
	total	25															
12 mo.	preterm	1(3.6%)	50	-	-	55	-	-	50	-	-	55	-	-	45	-	-
	term	27(96.4%)	57.8	15.2		54.4	15.1		50.7	11.9		49.1	7.4		49.2	8.4	
	total	28															
14 mo.	preterm	0	-	-	-	-	-	-	-	-	-	-	-	-	-	-	-
	term	15(100%)	53.3	7.9		56	10.7		45.3	6.3		49.3	6.1		55	8.2	
	total	15															
18 mo.	preterm	2(8.3%)	50	10	0.7	57.5	2.5	0.1	45	5	0.4	35	5	0.2	47.5	2.5	0.3
	term	22(91.7%)	53.5	9.3		45.5	10.6		50	10.4		46.6	10.6		53.2	5.8	
	total	24															
24 mo.	preterm	3(10.7%)	38.3	20.1	0.4	36.7	23.2	0.6	45	21.2	0.6	36.6	26.2	0.4	41.6	22.5	0.4
	term	25(89.3%)	49	11.7		44	13.2		53.3	10.8		52.2	7.84		55.6	10.5	
	total	28															
30 mo.	preterm	3(9.7%)	48.3	7.8	0.8	45	8.7	0.4	43.3	3.6	0.5	46.7	11.5	0.9	41.7	12.9	0.2
	term	28(90.3%)	49.6	4.2		49.6	4.5		44.8	9.4		45.5	2.6		56.2	4.5	
	total	31															
36 mo.	preterm	4(11.4%)	43.7	12.9	0.1	48.7	7.4	0.7	51.2	12.8	0.7	42.5	8.3	0.9	56.2	10.2	0.7
	term	31(88.6%)	57.6	8.8		47.5	6.2		53.8	3.3		42.7	4.5		58.5	0.8	
	total	35															
48 mo.	preterm	0	-	-	-	-	-	-	-	-	-	-	-	-	-	-	-
	term	27(100%)	52.1	7.6		48.3	7.9		50	10.1		53.7	7.3		54.1	5.2	
	total	27															
60 mo.	preterm	2(6.9%)	55	7	0.7	47.5	3.5	0.3	50	14.2	0.6	42.5	1.25	0.2	55	3.5	0.4
	term	27(93.1%)	52.6	6.6		51.6	8.1		43.5	8.9		44.8	9.5		58.5	5.8	
	total	29															
Total	330																

Relationship between consanguinity and developmental delay: Regarding consanguinity, of 330 children, 70 (21.2%) were born to consanguineous parents, and 260 (78.8%) were born to non-consanguineous, among the consanguineous group, 3 (4.3%) were found to be developmentally delayed while the remaining 67

(95.7%) were not, in contrast, only 5 (1.9%) children among the non-consanguineous group were found to be developmentally delayed while the remaining 255 (98.1%) were not. A chi-square test showed no statistically significant association between consanguinity and developmental delay (p value = 0.7) (Table 8).

Table 8. Relationship between consanguinity and developmental delay.

	Normal children no.(%)	Delayed development children no. (%)	Total	p value
+ve consanguinity	67 (95.7)	3 (4.3)	70(21.2%)	0.7
-ve consanguinity	255 (98.1)	5 (1.9)	260 (78.8%)	
Total	322 (97.58)	8 (2.42)	330 (100)	

Discussion

The first years of a child's life are critical for physical and cognitive development. As such, it is imperative to establish a comprehensive developmental monitoring and screening program. In the current study conducted in Diyala Province, Iraq, the Arabic version of the Ages and Stages Questionnaire, third edition (ASQ-3), was used to screen for developmental delay in children aged 2 to 60 months. There was a significant difference in the number of children across different age groups, with the 14-month age group having the lowest number of children. In contrast, the 36-month and 2-month age groups had the most children. The study found that among all participating children, 8 were identified as having DD, with a higher percentage in boys than in girls (75% vs 25%), the prevalence of developmental delay was 2.42% which is comparable to a study conducted in Menoufia Governorate, Egypt in 2017, which reported a prevalence of 2.9%. However, the prevalence

of developmental delay in the present study was lower than that reported in a study conducted in Iran in 2017 on 500 children aged 4 to 60 months 8.5% (11), and in multiple primary health care centers in Saudi Arabia in 2020 on 948 children 16.4% (12,13). The speech and communication domain had the highest number of delayed children, 2.4%, in the present study. This finding is consistent with a study conducted in Saudi Arabia, where the speech and communication domain was found to have the highest prevalence of delayed children, 3.8% (13). However, in a study conducted in Iran 2011 on 114 children, the speech and communication domain had the highest prevalence of developmental delay, 20% (14). The percentage of children in the gray area who need monitoring regarding speech and communication was 0-16.1%, the highest percentage was found in the 30-month age group. Regarding the gross motor domain, the percentage of delayed children was 1.8%. This finding is inconsistent with a study conducted in Cairo, Egypt, which reported a prevalence of 3.11% in gross motor skills (15). The percentage of children in the gray area who need monitoring

regarding gross motor (0-22.6%), the highest percentage was found in the 30-month age group. The differences in prevalence could be attributed to various factors, such as variations in the screening tool used, differences in sample sizes, or disparities in cultural factors. It is worth noting that cultural beliefs can influence parental priorities and expectations regarding child development. For example, in some cultures, motor development milestones like sitting and walking may be considered the most critical indicators of a child's health, leading parents to focus more on helping their children develop these skills. In contrast, other cultures may emphasize early sociability and speech, considering children who are sociable and talk early as clever and healthy. Consequently, parents in these cultures may prioritize fostering these skills in their children (16). Regarding the fine motor domain, the percentage of delayed children was 1.8%. This finding is consistent with a study conducted in Saudi Arabia, which showed the prevalence of developmental delay in fine motor skills of 1.9% (13). Moreover, it is nearly consistent with a study conducted in Cairo, Egypt, which reported a prevalence of 1.04% delay in fine motor skills (15). The highest percentage of children in the gray area who need monitoring regarding fine motor skills (0-20.7%) was found in the 60-month age group. In the problem-solving and personal-social domains, the prevalence of developmental delay was 1.8% for both. This finding is nearly approximate to the study conducted in Cairo, Egypt, which reported an average prevalence ranging from 1.04% to 3.11%. The percentage of children in the gray area who need monitoring regarding problem solving (3.8-20.7%) and personal-social (3.8-34.5%), the highest percentage was found in the 60-month and 30-month age groups, respectively.

Most children scored within the white area on the ASQ-3, indicating age-appropriate development. However, a significant proportion fell into the gray area, suggesting potential areas of concern requiring further assessment. The highest percentages of children in the gray area varied across domains and age groups: communication and gross motor (30 months), fine motor and problem-solving (60 months), and personal-social (30 months). These findings emphasize the importance of targeted monitoring and further evaluation for children in the gray area to ensure timely intervention. In terms of gender differences, there were no significant gender differences across most age groups when considering various domains. However, we did observe notable patterns in specific age-domain subgroups. Specifically, females exhibited significantly higher scores than males in the fine motor domain at 12 and 60 months, while males at 48 months had higher scores than females. Additionally, females had significantly higher scores in the gross motor domain at 48 and the communication domain at 60 months of age. These findings indicate that while gender differences in mean scores were not statistically significant for most age groups, distinct variations were observed in specific age-domain subgroups. A related study by Sajedi and colleagues found similar trends, where the gender differences were mainly non-significant across most age-domain subgroups. However, in 20 age-domain subgroups, females demonstrated significantly higher scores than males, particularly in the personal-social and fine motor domains, and at 36 and 48 months of age. On the other hand, males had significantly higher scores in two age-domain groups, specifically in the gross motor domain at 20 and 22 months of age (17). The findings in previous studies differ from those reported by Richter and Janson in their studies conducted on a Norwegian sample of children using the ASQ. Richter and Janson found that, on average, girls had a higher developmental stage

than boys in all areas except for gross motor function, where no significant differences were observed (18,19). On the other hand, a study by Kapci showed that there were no significant developmental differences between females and males. However, there were two exceptions, namely the 24-month personal-social development domain and the 42-month communication domain, where gender differences were observed (20). The observed differences across populations in various studies may be attributed to several factors. Some studies include gross developmental disorders in their prevalence statistics, while others do not. Different studies may focus on different age ranges, leading to developmental patterns and outcomes variations. According to the association between maturity and development across five domains: communication, gross motor, fine motor, problem solving, and personal-social. Our findings revealed no significant differences in these domains across all 12 age groups. This result aligns with a study conducted in central Iran, which found no association between ASQ domains and premature birth (21). The findings are consistent with a study conducted at the University of Minnesota, which concluded that no significant correlation exists between maturity and development in any of the five domains (22). Therefore, based on the results of this study, it can be concluded that there is no substantial association between maturity and development in the assessed domains. This study had no significant relationship between consanguinity and child development in healthy children under five (p-value of 0.9). These results align with several previous studies that reported no significant relationship between consanguinity and child health and development (24). However, it is

essential to note that other studies have reported significant adverse effects of consanguineous marriages on child health and well-being (25). Notably, the detrimental effects of consanguineous marriages on child health seem to be more prominent in low-income and developing countries (26). It should also be acknowledged that the risks associated with consanguineous marriages extend beyond child health outcomes, encompassing the potential for genetic disorders and disabilities (27). Nevertheless, it is essential to consider the limitations of this study, including its use of cross-sectional data, which restricts the ability to establish causality, as well as the limited geographical scope of the study sample, potentially limiting the generalizability of the findings. Consanguinity has an important role in autosomal recessive disorders, which were excluded from the study, and this might make consanguinity not a significant factor in this study.

Conclusion

The prevalence of developmental delay in healthy children aged 2 to 60 months in Diyala Province, Iraq, was 2.42%. Some children were in a critical area and needed further evaluation, monitoring, and management to avoid progressing to developmental delay. There was no effect of maturity on development, and no significant association between consanguinity and developmental delay. Early intervention is essential for children with developmental delays.

Recommendations

It is crucial to promote the timely identification and intervention for children with developmental delays in Diyala Province, Iraq, to help all children reach their full potential. Well-trained personnel should screen children during routine health visits to identify those at risk. The government and stakeholders must ensure access to early intervention services. Introducing a validated, standardized assessment tool like the ASQ3 (Ages and Stages Questionnaire) in health centers for

routine developmental screening is recommended. Additionally, a special clinic or committee should be established within the neuropsychiatric consultation unit to evaluate, follow up, and manage children with developmental delays. Lastly, further research should investigate risk factors, including socioeconomic influences, contributing to children being at risk for developmental delay.

Source of funding: No source of funding.

Ethical clearance: Ethical approval to perform the research acquired from the scientific and ethical committees / College of Medicine / University of Diyala (No:2023HAM766 Date:18/5/2023).

Conflict of interest: None.

Acknowledgments:

The authors would like to extend my sincere gratitude to the University of Diyala – College of Medicine for their academic support and for providing a stimulating learning environment that greatly contributed to the completion of this research. Also wish to express my deep appreciation to Al-Batool Hospital for their kind cooperation and for granting access to their valuable expertise and practical experience, which significantly enriched the content of this study.

References

1. Kiserud T, Benachi A, Hecher K, Perez RG, Carvalho J, Piaggio G, Platt LD. The World Health Organization fetal growth charts: concept, findings, interpretation, and application. *American journal of obstetrics and gynecology*. 2018 Feb 1;218(2):S619-29.
2. Centers for Disease Control and Prevention. *Developmental milestones*. Atlanta: Centers for Disease Control and Prevention; 2021.
3. Child development: An observational

South African birth cohort. *PLoS Med*. 2019;16(9):e1002920.

<https://doi.org/10.1371/journal.pmed.1002920>.

4. Stuart M, Ottenbacher K. *Pediatric rehabilitation: Principles and practice*. 4th ed. New York: Demos Medical Publishing; 2012. Available from: <https://dokumen.pub/pediatric-rehabilitation-principles-and-practice-4nbsped-1933864370-9781933864372.html>.

5. Shonkoff JP, Boyce WT, McEwen BS. Neuroscience, molecular biology, and the childhood roots of health disparities: building a stronger foundation for health equity. *JAMA*. 2012;308(8):823-824.

<https://doi.org/10.1001/jama.2009.754>.

6. American Academy of Pediatrics, Section on Ophthalmology, Council on Children with Disabilities, American Academy of Ophthalmology, American Association for Pediatric Ophthalmology and Strabismus, American Association of Certified Orthoptists. Joint Statement-Learning Disabilities, Dyslexia, and Vision. *Pediatrics*. 2009;124:837.

<https://doi.org/10.1542/peds.2009-1445>.

7. Kassebaum NJ, et al. Global, regional, and national levels and causes of maternal mortality during 1990-2016: A systematic analysis for the Global Burden of Disease Study 2016. *Lancet*. 2018;390(10100):1684-1735.

[https://doi.org/10.1016/S0140-6736\(16\)31470-2](https://doi.org/10.1016/S0140-6736(16)31470-2).

8. Squires J, Potter LW, Bricker D. *The ASQ User's Guide for the Ages and Stages Questionnaire: A Parent-Completed, Child Monitoring System*. 2nd ed. Baltimore: Paul Brookes Publishing Co; 1990. Available from: https://www.researchgate.net/publication/232498425_The_ASQSE_user's_guide_For_the_Ages_Stages_Questionnaires_Social-emotional.
9. Kerstjens JM, Bos AF, Ten Vergert EM, et al. Support for the global feasibility of the Ages and Stages Questionnaire as a developmental screener.

- Early Hum Dev. 2009;85(7):443-447.
<https://doi.org/10.1016/j.earlhumdev.2009.03.001>.
10. Spiegelhalter D. The Art of Statistics: How to Learn from Data. New York: Basic Books; 2019.
<https://doi.org/10.5038/1936-4660.13.1.7>.
11. Ahmadipour S, Mohammadzadeh M, Mohsenzadeh A, Birjandi M, Almasian M. Screening for developmental disorders in 4 to 60 months old children in Iran (2015–2016). J Pediatr Neuroradiol. 2017;17(1):8-12.
<https://doi.org/10.1055/s-0037-1612620>.
12. El-Ella SSA, Tawfik MAM, Barseem NF, Elatabany AMAM. Assessment of intellectual development in preschool children in the East of Menoufia Governorate, Egypt. Menoufia Med J. 2017;30:741-747.
<https://doi.org/10.4103/1110-2098.218257>.
13. Shatla MM, Goweda RA. Prevalence and risk factors of developmental delays among preschool children in Saudi Arabia. J Health Popul Nutr. 2020;50(1):10-17.
<https://doi.org/10.21608/jhiph.2020.79318>.
14. Dorre F, Bayat GF. Evaluation of children's development (4–60 months) with a history of NICU admission based on ASQ in Amir Kabir Hospital, Arak. J Ardabil Univ Med Sci. 2011;11(2):143-150. Available from:
https://jarums.arums.ac.ir/browse.php?a_id=183&sid=1&slc_lang=en.
15. Abdelbaky OA, Deifallah S, Amin G, Marzouk D. Screening for developmental delays in children 2-36 months of age in a primary health care center in Cairo, Egypt. J Health Popul Nutr. 2013;31(1):12-17.
<https://doi.org/10.21608/JHIPH.2022.254505>
16. Bornstein MH, Lansford JE, editors. Cultural Perspectives on Parenting. Psychology Press; 2010.
<https://doi.org/10.1080/15295192.2012.683359>.
17. Sajedi F, Vameghi R, Kraskian Mujembari A. Prevalence of undetected developmental delays in Iranian children. Child Care Health Dev. 2014;40(3):379-388.
<https://doi.org/10.1111/cch.12042>.
18. Richter J, Janson H. A Validation Study of the Norwegian Version of the Ages and Stages Questionnaires. Acta Paediatr. 2007;96(7):1040-1044.
<https://doi.org/10.1111/j.1651-2227.2007.00246.x>.
19. Janson H, Squires J. Parent completed developmental screening in a Norwegian population sample: a comparison with U.S normative data. Acta Paediatr. 2004;93:1525–1529.
<https://doi.org/10.1111/j.16512227.2004.tb02641.x>.
20. Kapci EG, Kucuker S, Uslu RL. How applicable are age and stages questionnaires for use with Turkish children? Top Early Child Special Educ. 2010;30(3):176–188.
<https://doi.org/10.1177/0271121410373149>.
21. Yaghini O, Kelishadi R, Keikha M, Niknam N, Sadeghi S, Najafpour E, et al. Prevalence of developmental delay in apparently normal preschool children in Isfahan, central Iran. Iran J Child Neurol. 2015;9(3):17-23. PMID: PMC4577694.
22. Degnan JM, Masten JM, Cicchetti D. The association between maturity and development: A longitudinal study of children and adolescents. J Child Dev. 2011;82(3):715-733.
<https://doi.org/10.1111/jcpp.12927>.
23. Chowdhury I, Rahman KM. Consanguineous marriage and child health in Bangladesh: A comparative analysis. J Biosoc Sci. 2012;44(5):607-620.
<https://doi.org/10.1017/s001216220300104x>.
24. Bener A, Hussain R. Consanguineous unions and child health in the State of Qatar. Paediatr

Perinat Epidemiol. 2006;20(5):372-378.

<https://doi.org/10.1111/j.13653016.2006.00750.x>.

25. Kabir S, Rahman M. The effect of consanguinity on child mortality and morbidity in Bangladesh. J Biosoc Sci. 1997;29(3):331-340.

<https://doi.org/10.1371/journal.pone.0241610>

26. Bittles AH, Black ML. Evolution in health and medicine Sackler colloquium: Consanguinity, human evolution, and complex diseases. Proc Natl Acad Sci. 2010;107(suppl_1):1779-1786.

<https://doi.org/10.1073/pnas.0906079106>.

27. Hamamy H. Consanguineous marriages: Preconception consultation in primary health care settings. J Community Genet. 2012;3(3):185-192.

<https://doi.org/10.1007/s12687-011-0072-y>.

التأثير الكبير لتعدد اشكال جين موت الخلية المبرمج - ١ على عدوى فيروس التهاب الكبد نوع ب والحمل الفيروسي

^١ حيدر أسد محمد ، ^٢ نجدة شكر محمود ، ^٣ جليل إبراهيم كاظم

المخلص

الخلفية: تقييم تطور الأطفال هو عملية تهدف الى تقييم تقدم الطفل عبر عدة مجالات تطويرية، بهدف تحديد التأخيرات أو الاعاقات المحتملة. يُجرى هذا التقييم من قبل كوادر الرعاية الصحية مثل أطباء الأطفال وعلماء النفس وخبراء الطفولة المبكرة، ويتضمن مراقبة دقيقة واختبارات منهجية لتقييم تطور الطفل في المجالات البدنية والعقلية واللغوية والاجتماعية والعاطفية.

الأهداف: يساعد التقييم في تحديد العمر التطوري للطفل والمجالات التي يعتقد أنه متأخر فيها، مما يمكن من التعرف عليها والتدخل لعلاجها مبكراً. **المرضى والطرق:** أجريت هذه الدراسة في محافظة ديالى لتقييم تطور الأطفال العراقيين الذين تتراوح أعمارهم بين ٢ و ٦٠ شهراً، باستخدام استبيانات الأعمار والمراحل وهي أداة فحص موثوقة تم تكييفها ثقافياً.

النتائج: أجريت الدراسة على ٣٣٠ طفلاً في مستشفى البتول التعليمي وكانت نسبة ٩٧,٦٪ تُظهر تطور طبيعي عبر مجالات التطور المختلفة، بما في ذلك الكلام والتواصل والمهارات الحركية الكبرى والمهارات الدقيقة وحل المشكلات والمهارات الشخصية والاجتماعية. ومع ذلك، كان لدى ٢,٤٢٪ تأخيرات تطويرية، حيث كان ٠,٦٪ يعانون من تأخر في الكلام والتواصل و ١,٨٪ يواجهون تأخيرات تنموية عامة.

كما تم تحديد أطفال في "المنطقة الرمادية" للتقييم، مما يشير إلى الحاجة إلى تقييم إضافي في مجالات مثل الكلام والتواصل (١٠-١٦٪) والحركة الكبرى (٦٠-٢٢٪) والحركة الدقيقة (٠-٢٠٪) وحل المشكلات (٣,٨-٣٤٪) والمهارات الشخصية والاجتماعية (١٠-١٦٪).

فيما يتعلق بزواج الأقارب، وُلد ٢١,٢٪ من الأطفال لوالدين أقارب، حيث واجه ٤,٣٪ منهم تأخيرات تطويرية. بينما عانى ١,٩٪ من الأطفال الذين لم يكن والديهما أقارب من تأخر في مجالات التطور المختلفة. أظهرت نتائج الدراسة أن لا علاقة بين القرابة والتأخير التطوري ($p = 0.7$).

أما فيما يتعلق بحالة الولادة، وُلد ٩١,٢٪ في موعدها المحدد، حيث كانت نسبة ٩٧,٣٪ تُظهر تطور طبيعي و ٢,٧٪ يعانون من تأخر تطوري. أما الأطفال الذين وُلدوا قبل الموعد المحدد فيكونوا ٨,٨٪، حيث واجه ٦,٩٪ منهم تأخيرات تطويرية وأظهر ٩٣,١٪ تطور طبيعي. أظهرت نتائج الدراسة أن لا علاقة بين الولادة المبكرة والتأخير التطوري ($p = 0.9$).

الاستنتاج: إجمالاً، أظهرت الدراسة أن نسبة صغيرة من الأطفال في محافظة ديالى يعانون من تأخر في التطور في مجالات مختلفة. وكانت نسبة أخرى من الأطفال في المنطقة "الرمادية" وفي حاجة لمتابعة. بشكل عام، لم يكن للجنس أو الولادة المبكرة أو القرابة أي تأثير على التطوري.

الكلمات المفتاحية: التقييم النمائي، التأخر النمائي، ديالى، ASQ3.

المؤلف المراسل: حيدر أسد محمد

الايمل: haider1991asad@yahoo.com

تاريخ الاستلام: ٩ تموز ٢٠٢٣




تاريخ القبول: ٦ اب ٢٠٢٤

تاريخ النشر: ٢٥ نيسان ٢٠٢٥

^١ مديرية صحة ديالى - ديالى - العراق.

^{٣,٢} كلية الطب - جامعة ديالى - ديالى - العراق.

The Impact of *Helicobacter pylori* on Lesion Type and Matrix Metalloproteinase-9 Expression in Laryngeal Tumors

Wasan Abdul-elah Bakir ¹, Refif Sabih Al-Shawk ², Mais Ibrahim Alsikafi ³, Shaimaa Rahem Al-Salihiy ⁴

^{1,2} Department of Microbiology, College of Medicine, Mustansiriyah University, Baghdad, Iraq.

³ Department of Pathology, College of Medicine, Mustansiriyah University, Baghdad, Iraq.

⁴ Department of Microbiology, College of Medicine, University of Diyala, Diyala, Iraq.

OPEN ACCESS

Correspondence: Refif Sabih Al-Shawk
Email:

refifalshawk@uomustansiriyah.edu.iq

Copyright: ©Authors, 2025, College of Medicine, University of Diyala. This is an open access article under the CC BY 4.0 license (<http://creativecommons.org/licenses/by/4.0/>)

Website:
<https://djm.uodiyala.edu.iq/index.php/djm>

Received: 09 January 2025

Accepted: 05 April 2025

Published: 25 April 2025

Abstract

Background: *Helicobacter pylori* and matrix metalloproteinase-9 (MMP-9) play a significant part in the pathophysiological processes and expression of carcinogenesis, particularly in laryngeal Squamous Cell Carcinoma (LSCC).

Objective: Explore the link between the *H. pylori* bacterium, MMP-9 expression, and laryngeal squamous cell carcinoma development by examining the role of chronic inflammation and extracellular matrix remodeling in laryngeal carcinogenesis.

Patients and Methods: This cross-sectional study recruited 118 tissue samples, including 58 malignant LSCC and 60 benign laryngeal polyps (BLP). Histopathological and immunohistochemical methods were used to assess the interplay of *H. pylori*, MMP-9, and smoking status in laryngeal tumors.

Results: The prevalence of *H. pylori* was significantly higher in malignant lesions (63.79%) as compared to benign lesions (51.66%) ($p=0.1$). A significant correlation was found in patients with benign lesions between the level of MMP-9 and smoking and *H. pylori* status ($r = 0.46$, $p = 0.001$), and ($r = 0.5$, $p = 0.001$), respectively. While in patients with malignant lesions, the correlation test revealed a significant negative correlation between the level of MMP-9 and smoking status ($r = -0.41$, $p = 0.001$), while *H. pylori* is a highest positively correlated with MMP-9 expression ($r = 0.5$, $p = 0.001$). The logistic regression analysis revealed that *H. pylori* infection could significantly predict high MMP-9 expression (OR = 3.08, 95% CI: 1.15-8.28, $p = 0.02$).

Conclusion: These findings highlight the crucial role of *H. pylori* infection and smoking in tumor progression through MMP-9-mediated extracellular matrix remodeling, inflammation, and immune modulation. Suggesting the potential impact of targeting *H. pylori* infection and MMP-9 activity for managing carcinogenesis.

Keywords: *Helicobacter pylori*, MMP-9, Laryngeal squamous cell carcinoma, Benign laryngeal polyps.

Introduction

Laryngeal squamous cell carcinoma (LSCC) is the prevalent malignancy of the larynx, comprising a significant part of head and neck cancers. It is the second most common malignancy in the upper respiratory tract after cancer of the lung (1). LSCC accounts for over 95% of all laryngeal malignancies (2). This cancer arises from the epithelial cells of the larynx and is associated with various risk factors, including exposure to environmental toxins, smoking, and alcohol consumption

(3). Smoking, in particular, is a major contributor to head and neck cancers, introducing carcinogens that lead to DNA damage, oxidative stress in respiratory epithelial tissues, and chronic inflammation. Additionally, lifestyle factors and chronic infections, notably *Helicobacter pylori* (*H. pylori*), have been involved in the development of LSCC (4). Smoking introduces a range of toxic substances that further irritate the mucosal lining, leading to chronic inflammation and increased susceptibility to infections. Synergistic effects of *H. pylori* infection, smoking, and chronic inflammation play an essential role in the progression of LSCC (5). *H. pylori* is a gram-negative organism, ordinarily known for its role in gastric diseases. Recent research suggests that *H. pylori* can also be found in the saliva, calculus, lymphoid tissue of the pharynx, nose, and sinus, oropharyngeal aphthous, discharge of the tympanic cavity, and larynx (6,7). It has been found in the upper aerodigestive tract and is supposed to play a role in inflammation-induced carcinogenesis in the larynx (8). Gastroesophageal reflux disease and laryngeal reflux cause an acidic environment for the larynx, where *H. pylori* can live. Due to its chronic inflammatory effect, *H. pylori* can lead to chronic illness and malignant tumor formation in the larynx (9). Thus, *H. pylori*'s damage to the laryngeal protective layers, such as the mucosa and the epithelium, leads to inflammation, which later on could lead to chronic irritation also, abnormal proliferation, the result in laryngeal pathology that can range from a subtle inflammatory process to the most extreme malignant transformation of the cells (10). Matrix metalloproteinases (MMPs) are key regulators of metastatic processes. Their expression and activation have been implicated in various pathological events, including tumor invasion, inflammation, and metastasis. Among the MMP family, matrix metalloproteinase - 9 (MMP-9) is notably in relation to tumor development and

progression (11). Matrix metalloproteinase (MMP) is a proteolytic metalloenzyme that is dependent on zinc. MMP-9 has a big role in pathophysiological processes and can break down extracellular matrix (ECM) components. Numerous illnesses are linked to MMP-9 overexpression and dysregulation. Therefore, controlling and inhibiting MMP-9 is a crucial therapy strategy of battling a number of illnesses involving cancer (12). The tumor in LSCC features excessive tissue and inflammation, processes strongly affected by the activity of protease enzymes like Matrix Metalloproteinase-9. MMP-9 is the enzyme responsible for the degradation of the extracellular matrix, especially IV-type collagen, a major component of basement membranes (13). In cancer, the unorganized MMP-9 expression is linked with tumor metastasis and angiogenesis, enabling cancer cells to breach the basement membrane and tissues (14). The study aims to explore the link between *H. pylori* infection, MMP-9 expression, and the initiation of laryngeal squamous cell carcinoma by examining the role of chronic inflammation and matrix remodeling in laryngeal carcinogenesis. Awareness of these interactions could provide worthy insight into the pathogenesis of laryngeal carcinoma and the way for new therapeutic strategies for managing this aggressive malignancy.

Patients and Methods

Specimens' collection: This cross-sectional study involved tissue samples acquired from 118 paraffin-embedded archived blocks from July 2024 to October 2024 at Educational Laboratories of Medical City, Al-Yarmouk Teaching Hospital, and private laboratories. These samples were divided into two groups. The first group consisted of 58 patients (47 males and 11 females) suffering from laryngeal squamous cell carcinoma (LSCC) (mean age 56.32 years) and was divided into two groups: 24

smokers and 34 non-smokers. The second group consisted of 60 patients (40 males and 20 females) suffering from benign laryngeal polyps (BLP) (mean age of 50.32 years), who included 23 smokers and 37 nonsmokers. The study focused on patients complaining of laryngeal squamous cell carcinoma and benign laryngeal polyps, and those who had received antibiotics or treatment to eradicate *H. pylori* before tissue collections were excluded. Any comorbid condition, such as diabetes or immunocompromised, is also excluded. Archival specimens of lousy quality or insufficient for analysis, such as small biopsy material, damaged tissues, or incomplete data, were excluded. The diagnosis was reaffirmed histopathologically by reviewing newly prepared hematoxylin and eosin-stained slides held in the research laboratory of the College of Medicine / Mustansiriyah University and the Educational Laboratories of Medical City.

Histological evaluation for detection of *H. pylori* infection: To determine whether or not *H. pylori* was found in the larynx tissue specimens, a histopathological examination was performed using standard methods, including the Giemsa stain, to diagnose the specimen and to identify the *H. pylori*, as well as immunohistochemical analysis for *H. pylori* and MMP-9. The diagnostic criteria for malignant and benign biopsies depend on histopathological examination, which includes examining the tissue under a microscope to evaluate cellular structure, morphology, and other criteria. Each block of paraffin was sectioned into a thickness of 4 micrometers. Three sections were taken from blocks: one was stained with hematoxylin and eosin for histopathology review, and the other two were placed on positively charged slides (Fisher brand) and stained with anti- *H. pylori* and anti-MMP-9 monoclonal antibodies using immunohistochemical techniques. Two separate pathologists re-evaluated the hematoxylin and

eosin (H and E-stained sections) to determine the morphological kinds of the tumor, the grade, and other criteria.

Immunostaining for the detection of *H. pylori* infection: For the immunohistochemical examination of *H. pylori*, polyclonal antibodies against *H. pylori* obtained from rabbits were used (Abcam/UK code (ab20459) 1:100). On the other hand, antibodies against human MMP-9 and polyclonal antibodies [Abcam/UK code, anti-MMP-9 antibody (ab73734)] were used. The detection of gene expression by utilizing monoclonal antibodies specific to a particular gene is regarded as the fundamental premise of the immunostaining method, which is used to identify a particular protein in normal, benign, and cancerous cells. These antibodies could bind to the nuclear targets found in the cytoplasm. The detection of bounded primary antibodies, which is achieved by conjugating secondary antibodies with a particular chromogen (3, 3'-diaminobenzidine, DAB), results in the formation of brown-color sediment at the antigen position in tissue that indicates a positive response. In the peroxidase secondary detection technique, a positive response is shown when brown products react at the location of the target antigen. This reaction is connected with the appearance of the brown products. After that, the cell was stained with a counterstain to produce a blue color.

Scoring: After seeing 10 different fields with a high-powered microscope, the immunohistochemistry (IHC) signaling data were analyzed (100x). By dividing the number of stained cells in each field by the total number of cells in each field across all 10 fields, we were able to determine the percentage of positively stained cells in each of these fields using the formula below: mean percentage of the stained cells across all 10 fields.

Evaluation of Immunostaining: The immunostaining was performed by an

independent histopathologist who was blinded to the clinical diagnosis of the tissues at the time of evaluation and expression of *H. pylori* (Negative, meaning no expression) and (Positive, meaning there was expression) (15, 16). When the tissue's IHC signaling values were more than 10% of total tumor cells, it was determined that the tissue contained MMP-9 (17, 18).

Statistical analysis

Data were analyzed using an accessible statistical program, SPSS-28 (Statistical Packages for Social Sciences- version 28). Data analysis was carried out, and the results were presented as the mean and standard deviation, while categorical variables were presented as percentages. For comparing two independent groups, T-tests were used, or the ANOVA was employed to observe the statistical differences between more than two independent variables. Pearson's Chi-square statistic was used to analyze the percentage differences (qualitative data). To investigate the nature of the connection between the variables, qualitative correlation coefficients (r) were calculated. The prediction of lesion type (benign vs. malignant) and high MMP-9 was performed through Logistic regression analysis. The results are presented as beta coefficients and odds ratios with a 95% confidence interval. The P -value ≤ 0.05 was considered statistically significant.

Results

H. pylori Expression in Benign and Malignant

Lesions: Presence of *H. pylori* protein expression, which was measured and confirmed by immunohistochemistry, was heterogeneous dark brown staining in the tissue that was revealed in Figure 1A and Figure 2A in 37 (63.79%) of the malignant lesions and 31 (51.66%) of the benign polyps, as shown in Table 1. The mean age group of patients with malignant lesions was 56.32 ± 9.8 SD, while those with benign lesions were 50.32 ± 8.3 SD, with significant differences.

Regarding sex distribution, a higher prevalence

rate of males was evident in both groups, 47

(81.03%) in patients with malignant lesions and 40 (66.66%) in benign polyps, as illustrated in Table 1. Table 2 demonstrates a combined analysis using chi-square and Pearson correlation, which was done to evaluate the association between demographic features (independent variables: age, sex, and smoking status) and *H. pylori* infection (dependent variable) in patients who have malignant squamous cell carcinoma. The Age didn't show any significant association with *H. pylori* infection regarding ≤ 50 years and ages > 50 years in terms of *H. pylori* positivity ($p = 0.46$), also a weak non-significant positive correlation was observed ($r = 0.15$, $p = 0.25$). No significant correlation was seen between sex and *H. pylori* infection ($p = 0.85$, $r = -0.09$, $p = 0.49$). Smoking status was significantly correlated with *H. pylori* infection ($p = 0.008$, $r = -0.46$, $p = 0.001$). Table 3 evaluates the association between demographic features (independent variables: age, sex, and smoking status) and *H. pylori* infection (dependent variable) in patients who have benign lesions. There was no statistically significant association between age and *H. pylori* infection ($p = 0.404$, $r = 0.04$, $p = 0.76$) and sex ($p = 0.428$, $r = -0.07$, $p = 0.6$). A significant positive correlation was illustrated between smoking status and *H. pylori* infection ($p = 0.036$, $r = 0.36$, $p = 0.004$).

Table 1. Comparative analysis of *H. pylori* infection in benign and malignant lesions. N.S.: not significant ($p > 0.05$).

Variable	No. (118)	Mean age (year) \pm SD	Male	Female	<i>H. pylori</i> positive	<i>H. pylori</i> Negative
Malignant lesion	58	56.32 \pm 9.8	47 (81.03%)	11 (18.96%)	37 (63.79%)	21 (36.20 %)
Benign lesion	60	50.32 \pm 8.3	40 (66.66%)	20 (33.33%)	31 (51.66%)	29 (48.33%)
P value		$p < 0.05$	0.07 NS	NS	0.1 NS	N.S

Table 2. Chi-Square and Pearson correlation analysis of demographic features with *Helicobacter pylori* in malignant squamous cell carcinoma lesions. *Chi-square for independence, the p-value is less than 0.05, indicating a significant correlation. # Pearson Correlation Coefficient Measures linear relationship strength and significance at ($p < 0.05$).

Demographic features	No. 58	<i>H. pylori</i> Positive (37)	<i>H. pylori</i> Negative (21)	<i>P</i> value (Chi-square)	Pearson correlation coefficient P-value
Age. (Years)					
≤ 50	22 (37.93%)	12 (32.43%)	10 (47.61%)	0.46	r=0.15
> 50	36 (62.06%)	25 (67.56%)	11 (52.38%)		p=0.25
Sex					
Male	47 (81.03%)	31 (83.78%)	16 (76.19%)	0.85	r=-0.09
Female	11 (18.96%)	6 (16.21%)	5 (23.80%)		P=0.49
Smoking status					
Smoker	24 (41.37)	9 (24.32%)	15 (71.42%)	0.008*	r=-0.46
Non-smoker	34 (58.62%)	28 (75.67%)	6 (28.57%)		p=0.001#

Table 3. Chi-Square and Pearson correlation analysis of demographic features with *helicobacter pylori* infection in benign lesions. *In the Chi-square test for independence, the p-value was less than 0.05, indicating a significant correlation. # Pearson Correlation Coefficient Measures linear relationship strength and significance at ($p < 0.05$).

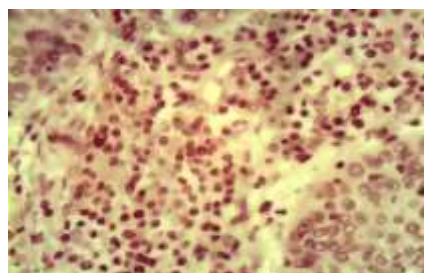
Demographic features	No. 60	<i>H. pylori</i> Positive (31)	<i>H. pylori</i> Negative (29)	<i>P</i> value (Chi-square)	Pearson correlation coefficient P-value
Age. (Years)					
≤ 50	26 (43.33%)	12(38.70%)	14 (48.27%)	0.404	r = 0.04 p = 0.76 NS
> 50	34 (56.66%)	19(61.29%)	15 (51.72%)		
Sex					
Male	40 (66.66%)	22 (70.96%)	18 (62.06%)	0.428	r = -0.07 p = 0.6 NS
Female	20 (33.33%)	9 (29.03%)	11 (37.93%)		
Smoking status					
Smoker	23 (38.33%)	15 (65.21%)	8 (34.78%)	0.036*	r = 0.36 p = 0.004 [#]
Non-smoker	37 (61.66%)	16 (43.24%)	21 (56.75%)		

MMP-9 Expression in Benign and Malignant Lesions: An analysis assessed the link between MMP-9 expression as the dependent variable and independent variables as age, sex, smoking, and *H. pylori* status in patients with malignant lesions. No significant differences in MMP-9 expression with weak, non-significant negative correlation were observed between aged ≤ 50 years and aged > 50 years ($p > 0.05$, $r = -0.2$, $p > 0.05$, respectively). The expression of the mean percentage of MMP-9 did not significantly differ between males and females, with weak and no significant correlation ($p > 0.05$, $r = -0.2$, $p > 0.05$, respectively). Smoking status and *H. pylori* infection significantly affect the level of MMP-9

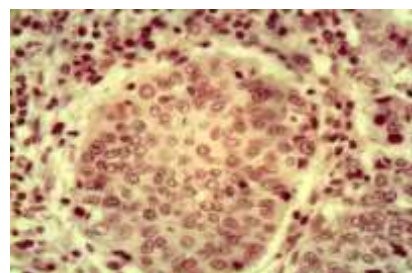
expression, imposing a higher significant increase in MMP-9 expression in the smokers' group and patients with *H. pylori* compared to non-smokers and patients with no *H. pylori* ($p = 0.02$ and $p = 0.001$, respectively). Pearson correlation test revealed a significant negative correlation between the level of MMP-9 and smoking status ($r = -0.41$, $p < 0.001$), while *H. pylori* is a highest positively correlated with MMP-9 expression ($r = 0.5$, $p = 0.001$) as seen in Table 4. MMP-9 protein expression was measured by immunohistochemistry. The tissue has heterogeneous dark brown staining, as shown in Figure 1 B.

Table 4. Association between MMP-9 expression (% positivity) and clinical variables in the malignant lesions. ^t-test for independence, the p-value was less than 0.05, indicating a significant correlation. # Pearson Correlation Coefficient Measures linear relationship strength and significance at ($p < 0.05$).

Variables	No. 58	MMP-9 Expression Mean ± SE %	T-test P value	Pearson Correlation Coefficient P-value
Age (year)				
≤ 50	22 (37.93%)	43.29 ± 6.3	P= 0.438	r = -0.2 P = 0.13
> 50	36 (62.06%)	53.75 ± 2.4		
Sex				
Male	47 (81.03%)	52.44 ± 1.8	P= 0.91	r = -0.2 P = 0.12
Female	11 (18.96%)	53.18 ± 6.54		
Smoking status				
Smoker	24 (41.37%)	57.91 ± 3.06	P= 0.02^	r = -0.41 P = 0.001 [#]
Non-smoker	34 (58.62%)	48.82 ± 2.21		
H. pylori status				
H. pylori Positive	37 (63.79%)	58.92± 1.95	P = 0.001^	r = 0.59 P = 0.001 [#]
H. pylori Negative	21(36.20%)	41.43± 2.54		



A



B

Figure 1. Immunohistochemical staining (IHC) of anti-*H. pylori* and MMP-9 proteins in the tissue of LSCC. Staining by DAB chromogen (dark brown) counterstained with H&E. (A) positive anti-*H. pylori* immunostaining (X400). (B) Positive MMP-9 immunostaining. (X400).

Table 5 demonstrates the results that assessed the link of MMP-9 expression as the dependent variable with the other characteristics that represent independent variables: age, sex, smoking, and *H. pylori* status in patients with benign lesions. No statistically significant differences in MMP-9 expression with weak, non-significant positive correlation were observed between aged ≤ 50 and aged > 50 years ($p > 0.05$, $r = 0.14$, $p = 0.2$, respectively). The mean expression of MMP-9 did not significantly differ between males and females, and no significant correlation ($p > 0.05$, $r = 0.02$, $p =$

0.83, respectively). Smoking and *H. pylori* status significantly affect the level of MMP-9 expression, imposing a higher significant increase in MMP-9 expression in smokers and patients with *H. pylori* compared to non-smokers and patients with no *H. pylori* ($p = 0.001$). Pearson correlation test revealed a significant correlation between the level of MMP-9 and smoking and *H. pylori* status ($r = 0.46$, $p = 0.001$), and ($r = 0.5$, $p = 0.001$), respectively. Figure 2B demonstrates MMP-9 protein expression in dark brown staining in the tissue.

Table 5. Association of MMP-9 expression and clinical variables in the benign lesion. ^t-test for independence, the p-value was less than 0.05, indicating a significant correlation. # Pearson Correlation Coefficient Measures linear relationship strength and significance at ($p < 0.05$).

Variables	No. 60	MMP-9 Expression Mean ± SE %	P value	Pearson Correlation Coefficient P-value
Age (year)				
≤ 50	26 (43.33%)	43.07 ± 2.6	P = 0.2	r=0.14 P= 0.2
> 50	34 (56.66%)	46.91 ± 2.2		
Sex				
Male	40 (66.66%)	45.5 ± 2.0	P= 0.84	r= 0.027 P= 0.83
Female	20 (33.33%)	44.75 ± 3.0		
Smoking status				
Smoker	23(38.33%)	53.04 ± 1.9	P= 0.001^	r= 0.46 P= 0.001#
Non-smoker	37 (61.66%)	40.41 ± 2.1		
H. pylori status				
H. pylori Positive	31 (51.66%)	52.58 ± 1.9	P=0.001^	r= 0.57 P= 0.001#
H. pylori Negative	29 (48.33%)	37.41 ± 2.0		

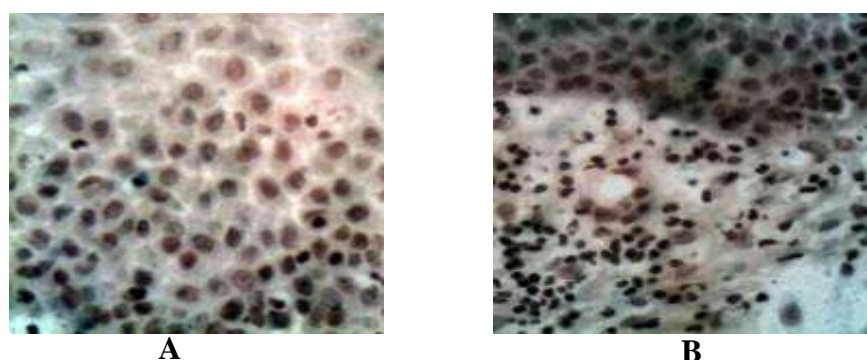


Figure 2: Immunohistochemical staining (IHC) of anti - *H. pylori* and MMP-9 proteins in the tissue of BLP. Staining by DAB chromogen (dark brown) counterstained with H&E. (A) Positive anti-*H. pylori* immunostaining (X400). (B) Positive MMP-9 immunostaining. (X400).

Logistic Regression Analysis: Table 6 presents the results of two logistic models, one for predicting lesion types and the second for predicting high MMP-9 expression. These models were used to estimate the odds ratio (OR) and coefficients using age, sex, smoking, and *H. pylori* status as independent variables and both lesion type and MMP-9 level as dependent variables. To predict malignant lesions, none of the predictors reached the significant level,

although the male sex approached the effect ($p=0.07$, $OR=3.63$, 95% CI: 0.9-14.3). The first model had a strong R^2 of 0.56, which can explain more than half of the variance in the lesion types by the predictors. While the second model assesses the prediction of high MMP-9 level expression, only *H. pylori* significantly predicts the increase in MMP-9 expression ($p=0.02$, $OR=3.08$, 95% CI: 1.15-8.28). The model had a limited explanatory power of R^2 of 0.09.

Table 6. Logistic regression for predicting lesion type and high MMP-9 expression. p -value < 0.05 is statistically significant. odds ratio (OR) > 1 shows a positive association, and < 1 shows a negative association. Confidence interval (CI) at 95% and nagelkerke R-squared values.

Variables	Lesion Type			High MMP-9		
	β (SE)	P value	OR 95% CI	β (SE)	P value	OR 95% CI
Age (> 50)	0.64 (0.49)	0.19	1.89 (0.71-4.96)	-0.34 (0.5)	0.5	0.71 (0.26-1.95)
Sex (Male)	1.29 (0.72)	0.07	3.63 (0.9-14.3)	-0.08 (0.6)	0.89	0.9 (0.72-3.16)
Smoking (yes)	-0.43 (0.67)	0.5	0.65 (0.18-2.3)	-0.5 (0.5)	0.3	0.58 (0.2-1.7)
<i>H. pylori</i> (Positive)	0.84 (0.55)	0.12	2.3 (0.8-6.61)	1.13 (0.51)	0.02*	3.08 (1.15-8.28)
Model Fit (R^2)	0.558			0.093		

Discussion

It is important to explore the associated risk of laryngeal carcinoma and find novel methods and approaches to its prevention and treatment. For many years, there has been debate on the potential link with *H. pylori* and laryngeal and pharyngeal carcinomas. Several investigations have been conducted to illustrate this cause-and-effect relationship. This work studied the relationship between benign and malignant larynx conditions with *H. pylori* and smoking, in addition to the age and sex of the sample. The cases of malignant laryngeal tumors show more association with *H. pylori* infection than benign lesions, which suggests that this is statistically significant. This means *H. pylori* might be associated with malignant tumor formation. *H. pylori*, a colonizing bacterium that is found in the gastric in addition to the laryngeal mucosa, tonsil, and saliva, is linked to specific diseases and can survive in acidic environments (5, 6). This has been supported by many researchers (8). However, it was against a study that postulated no differences among the cases of *H. pylori* and malignancy (9). Gastroesophageal reflux disease and laryngeal reflux cause an acidic environment for the larynx where *H. pylori* can live and lead to chronic illness and malignant tumor formation in the larynx due to its chronic inflammatory effect (19). Thus, the effect of *H. pylori* to damage the laryngeal protective layers, such as the mucosa and the epithelium, leads to inflammation and later on could progress to chronic irritation with abnormal proliferation, in laryngeal pathology that can be a subtle inflammatory process to the most extreme malignant transformation of the cells (20). There is a significant relationship between smoking status and *H. pylori* in cases of squamous cell carcinoma of the larynx, where smokers tend to have an increased proportion of *H. pylori*-negative results, and the Pearson correlation shows a moderate negative relationship between

smoking and *H. pylori* infection. That suggests the smoking may reduce the likelihood of *H. pylori* in patients with malignant tumors of the larynx. This is supported by the study of Ferro et al. (21). Smoking leads to reduced *H. pylori* infection through several mechanisms: nicotine can lead to reduced gastric acid secretion, which creates an unfavorable environment for *H. pylori*, another mechanism is changing in the microbiota in the stomach that is useful for *H. pylori* in addition to its main effect on the immune system where it leads to immune suppression, but also smoking results in the organized of proinflammatory cytokines for example IL-6, TNF- α and IL-1 β . Chronic inflammation can promote gastric mucosal damage and repair processes that may make the stomach less conducive to *H. pylori* survival, especially in gastric ulceration or carcinoma, where significant damage to the stomach lining may occur (11, 22). In benign lesions of the larynx, there is a significant positive role for smoking on *H. pylori*; smoking was associated with higher *H. pylori*-positive cases in comparison to non-smokers. This finding is supported by Bateson (23). Relating to the results as mentioned earlier, the bimodal smoking effect on benign and malignant lesions might be explained by a complex interplay between smoking, the immune system, the gastric environment, the laryngeal environment, and the type of lesion. Nicotine's effect on cellular immunity, especially T cell response, can be summarized in the impairment of the immunity and shift of Th1-IFN γ response (necessary in controlling bacterial infection) to Th2, which may reduce the effectiveness in eradicating *H. pylori*. The immune system's inability to clear the infection due to nicotine's immunosuppressive effects could increase the risk of prolonged inflammation. This persistent inflammation caused by smoking may encourage *H. pylori* infection in benign conditions (24).

However, in malignant lesions, smoking causes damage to the tissue. It reduces the immune system due to the effect of cancer, making the environment less favorable for the organism's life (25). Targeting prevention and treatment strategies for gastric diseases linked with smoking and *H. pylori* can be made easier with an understanding of these dynamics. This is one of the areas that needs to be studied by other researchers to explain in more detail the exact way smoking affects *H. pylori* prevalence. For both the benign and malignant laryngeal lesions, gender does not have a significant effect on *H. pylori*. However, the aging significantly affect results, it is clear that immune system behavior different at aging and a decline with two types of immunity (the adaptive and the native), which makes a person more vulnerable to infection by many organisms, and one of them is *H. pylori* and the infection, inflammation consequences of having tissue changes and finally progression to cancer (26-28). Moreover, a significant positive correlation exists between smoking habit and *H. pylori* with MMP-9 expression in laryngeal malignancy, where smoking and *H. pylori* infection are associated with a higher chance of having MMP-9 expression. These results agree with the study described by Montiel-Jarquin et al. (12), who also found an increase in MMP-9 expression with smoking. The finding of increased *H. pylori* with MMP-9 expression in cancer is confirmed by the study of Liu et al. (22). Gelatinases, particularly MMP-9, play important functions in several inflammatory processes associated with malignancies. MMP-9 affects the tumor environment that favors tumor overrun and metastasis through the effect on the inflammatory cells and their mediators by the cleaving of interleukin-2 α (IL-2 α), shed intercellular adhesion molecule-1 (ICAM-1), and activate the transforming growth factor (TGF- β), all of them are linked to negative regulation of the immunological response to cancer which all

cause tumor growth (28). In addition, MMP-9 influences macrophage polarization to M2 (tumor-activating pathway). The M2 phenotype is crucial for tissue healing, remodeling, and immune tolerance, but its dysregulation can contribute to tumor progression, chronic inflammation, and fibrosis (29). M2 macrophages, which are enriched in tumors, secrete a variety of cytokines (IL-10, TGF- β) that can inhibit immune responses (anti-tumor) and promote cancer cell proliferation (12). This immune suppression, coupled with ECM degradation and tissue remodeling, creates a microenvironment that supports tumor survival, growth, and metastasis. Also, it facilitates the interaction between tumor cells and fibroblasts by breaking down ECM proteins, allowing cancer cells to access growth factors, like vascular endothelial growth factors (VEGF), and fibroblast growth factors (FGFs), that are often sequestered within the ECM. This enhances tumor cell survival, proliferation, and motility; besides these, MMP-9 can affect processing of a novel vessel formation (angiogenesis), which has a significant role in tumorigenesis by degrading the ECM and allowing new vessel formation. As a result, more oxygen and nutrients are delivered to the tumor (29). *Helicobacter pylori*'s effect on the immune system and immune mediator release, like IL-1 β , IL-8, TNF- α , and IL-6, can progress to chronic irritation of the tissue and dysplasia of the mucosal lining cells. At the same time, it can evade the immune cells through the modulation of both regulatory and helper 17-T cells, which allows it to persist in the mucosal lining and causes chronic inflammation and tumor formation. Also, reactive oxygen species cause mutagenic effects on the DNA, with carcinogenic effects. The most virulent factor of *H. pylori* is the CagA protein that causes cell evasion of apoptosis and loss of epithelial-mesenchymal transition and cell survival

through the release of EGF. All of these factors favor cell growth and cancer formation. Tumor invasion and metastasis with more control over the malignant lesion and better survival (19).

Even in benign larynx lesions, smoking and *H. pylori* show a positive correlation with MMP-9 expression. These findings were in agreement with the study of Koyama (30), and there was no effect of age and sex on the level of expressivity. The logistic regression analysis further supported these findings, showing that only *H. pylori* infection emerged as a significant predictor of having high MMP-9 expression with an odds ratio of 3.08 (95% CI: 1.15-8.28), suggesting that this bacterial infection could increase the risk of having high MMP-9 over three times than non-infected individuals. While age, sex, and smoking did not predict the increase in MMP-9, indicating they are less likely to confound this. In the other model that predicts lesion type (malignant vs. benign), none of the predictors achieves a significant level. Still, the male sex ($p=0.07$) and *H. pylori* ($p=0.1$) approach support the impact of this bacterium in laryngeal carcinogenesis (6, 31-33). Although the model was fit for the prediction of lesion type ($R^2=0.558$), its clinical utility is limited because of the lack of significant prediction for the variables. However, it still offers a view of the analytic process, suggesting a validation through a larger, more powerful study. By focusing on these factors, clinicians can better identify at-risk individuals and tailor preventive or therapeutic interventions to improve patient outcomes.

Conclusions

This study highlights the aggravating effect of smoking and *H. pylori* infection on MMP-9 expression, particularly in malignant cases, suggesting their involvement in tumor progression and highlighting the importance of these factors in preventing and management strategies.

Recommendations

Targeting MMP-9 through immunomodulatory therapies or its natural inhibitors shows a promising strategy for controlling tumor invasion and metastasis. Preventing measures, including avoiding smoking and eradicating *H. pylori*, might decrease the chance of this overexpression of MMP-9 and reduce the danger of laryngeal cancer progression.

Source of funding: No source of funding.

Ethical clearance: This study was conducted per the rules outlined in the Declaration of Helsinki. Verbal consent and analytical approval were obtained from all participants before specimen collection. The protocol of the study, along with the subject information and consent form, was reviewed and approved by the local ethics committee of the Microbiology Department at the Medical College of Mustansiriyah University, numbered (13) for the academic year 2024.

Conflict of interest: None.

Acknowledgments:

We sincerely thank the physicians and laboratory staff of Al-Yarmouk Teaching Hospital and Educational Laboratories of Medical City for their invaluable support and contributions, which were instrumental in the successful completion of this study.

References

- 1- Cavaliere M, Bisogno A, Scarpa A, D'Urso A, Marra P, Colacurcio V, et. al. Biomarkers of laryngeal squamous cell carcinoma: a review. *Ann Diagn Pathol.* 2021; 54:151787. <https://doi.org/10.1016/j.anndiagpath.2021.151787>.
- 2- Marioni G, Marchese-Ragona R, Cartei G, Marchese F, Staffieri A: Current opinion in diagnosis and treatment of laryngeal carcinoma. *Cancer Treat Rev* 2006; 32:504–515. <https://doi.org/10.1016/j.ctrv.2006.07.002>.

- 3- Mondal S, Adhikari N, Banerjee S, Amin SA, Jha T. Matrix metalloproteinase-9 (MMP-9) and its inhibitors in cancer: A minireview. *Eur J MedChem.*2020;15;194:112260.
<https://doi.org/10.1016/j.ejmech.2020.112260>.
- 4- Sleeboom JJF, van Tienderen GS, Schenke-Layland K, van der Laan LJW, Khalil AA, Verstegen MMA. The extracellular matrix as hallmark of cancer and metastasis: From biomechanics to therapeutic targets. *Sci Transl Med.*2024;3;16(728):eadg3840.
<https://doi.org/10.1126/scitranslmed.adg3840>.
- 5- Huang Y, Gu M, Wu Q, Zhu J, Wu J, Wang P, et. al. Is Laryngeal Squamous Cell Carcinoma Related to Helicobacter pylori? *Front Oncol.* 2022;28;12:790997.
<https://doi.org/10.3389/fonc.2022.790997>.
- 6- Hsin L, Chuang H, Lin M, Fang T, Li H, Liao C, Kang C, et. al. Article Laryngeal Helicobacter pylori Infection and Laryngeal Cancer-Case Series and a Systematic Review. *Microorganisms.*2021;9:1129.
<https://doi.org/10.3390/microorganisms9061129>
- 7- Jameel NH, Motib AS, Athab AM. The prevalence of Helicobacter pylori infection in Baqubah city. *Diyala Journal of Medicine.* 2020 Oct1;19(1).
<https://doi.org/10.26505/DJM.19015150107>.
- 8- Matić I, Jelić D, Matić I, Maslovara S. and Mendeš T. Helicobacter pylori in the stomach and laryngeal mucosal linings in patients with laryngeal cancer. *Acta Clin Croat.* 2018; 57:91-95. <https://doi.org/10.20471/acc.2018.57.01.10>.
- 9- Zhou J, Zhang D, Yang Y, Zhou L, Tao L. Association between Helicobacter pylori infection and carcinoma of the larynx or pharynx. *Head Neck.* 2016; 38(1): 1-6.
<https://doi.org/10.1002/hed.24214>.
- 10- Genç R, Çağlı S, Yüce İ, Vural A, Okuducu H, Patıroğlu T, Güney E. The role of H. pylori in the development of laryngeal squamous cell carcinoma. *Dis Markers.* 2013; 35(5):447-9.
<https://doi.org/10.1155/2013/95070>.
- 11- Anaa F, Samanthaa M, Claudioc P, Nuriae A, Manolisf K, Lizbethj L, et. al. Smoking and Helicobacter pylori infection: an individual participant pooled analysis (Stomach Cancer Pooling- StoP Project). *European Journal of Cancer Prevention.* 2019; 28(5):390-396,
<https://doi.org/10.1097/CEJ.0000000000000471>.
- 12- Montiel-Jarquín ÁJ, Lara-Cisneros LGV, López-Colombo A, Solís-Mendoza HA, Palmer-Márquez ML, Romero-Figueroa MS. Expression of metalloproteinase-9 in patients with mild and severe forms of gastroesophageal reflux disease. *Cir Cir.* 2019;87(4):436-442. English.
<https://doi.org/10.24875/CIRU.18000691>.
- 13- Patil R, Mahajan A, Pradeep G, Prakash N, Patil S. and Khan S. Expression of matrix metalloproteinase-9 in histological grades of oral squamous cell carcinoma: An immunohistochemical study. *J. of Oral and Maxillo. Path.* 2021; 25(2): 239-46.
<https://doi.org/10.4103/0973-029X.325121>.
- 14- Chen s, Yao H, Zhu S, li Q, Guo G. and Yu J. Expression levels of matrix metalloproteinase-9 in human gastric carcinoma. *Oncology Letters;* 2015;9:915-919.
<https://doi.org/10.3892/ol.2014.2768>.
- 15- Ngaiza A, Yahaya J, Mwakimonga A, Vuhahula E, Mnango L, Mwakigonja A, et. al. Histologic detection of Helicobacter pylori by the immunohistochemical method using anti-Helicobacter pylori polyclonal antibody: A cross-sectional study of patients with gastric pathologies at the Muhimbili National Hospital in Dar-es-salaam, Tanzania. *Arab Journal of Gastroenterology.* 2022; 23(1): 7-14.
<https://doi.org/10.1016/j.ajg.2021.11.002>.
- 16- Akeel M, Elhafey A, Shehata A, Elmakki E, Aboshouk T, Ageely H. and Mahfouz S.

- Efficacy of immunohistochemical staining in detecting *Helicobacter pylori* in Saudi patients with minimal and atypical infection. *European Journal of Histochemistry*. 2021; 65:3222. <https://doi.org/10.4081/ejh.2021.3222>.
- 17- Chen s, Yao H, Zhu S, li Q, Guo G. and Yu J. Expression levels of matrix metalloproteinase-9 in human gastric carcinoma. *Oncology Letters*; 2015;9:915-919. <https://doi.org/10.3892/ol.2014.2768>.
- 18- Lin M, Ashraf N. and Mahjabeen I. Deregulation of MMP-2 and MMP-9 in laryngeal cancer. A retrospective observational study. *Medicine*;2024;103:27. <http://dx.doi.org/10.1097/MD.00000000000038362>.
- 19- Selbach M, Moese S, Backert S, Jungblut PR, Meyer TF. The *Helicobacter pylori* CagA protein induces tyrosine dephosphorylation of ezrin. *Proteomics* 2004; 4:2961–2968. <https://doi.org/10.1002/pmic.200400915>.
- 20- Ozyurt M, Gungor A, Ergunay K, Cekin E, Erkul E, Haznedaroglu T. Real time PCR detection of *Helicobacter pylori* and virulence-associated cagA in nasal polyps and laryngeal disorders. *Otolaryngol Head Neck Surg* 2009; 141:131–135. <https://doi.org/10.1016/j.otohns.2009.04.005>.
- 21- Liu L, Li Y, Zhang X, Zhang H. The correlation of the miR-29a/MMP9 axis with *Helicobacter pylori* infection in gastric cancer. *Am J Transl Res*. 2021 Sep 15;13(9):10155-10162.
- 22- Perlstein Todd S, Lee Richard T. Smoking, Metalloproteinases and Vascular Disease. *Arterioscler Thromb Vasc Biol*. 2006; 26:250–56. <https://doi.org/10.1161/01.ATV.0000199268.27395.4f>.
- 23- Bateson MC. Cigarette smoking and *Helicobacter pylori* infection. *Postgrad Med J* 1993; 69: 41–4. <https://doi.org/10.1136/pgmj.69.807.41>
- 24- Lai S. *Helicobacter pylori* gastric infection in patients with laryngeal cancer. *European Archives of Oto-Rhino-Laryngology*. 2021; 278:1295. <https://doi.org/10.1007/s00405-021-06641-8>.
- 25- Ogihara A, kikuchi S, hasegawa A, kurosawa M, miki K, kanekos E. and mizukoshi H. *Helicobacter pylori* infection, relationship between helicobacter pylori infection and smoking and drinking habits. *Fournal of Gastroenterology and Hepatology* 2000; 15: 271-276. <https://doi.org/10.1046/j.14401746.2000.02077>.
- 26- Idan HM, Motib AS. Incidence of head and neck cancer among Baquba Teaching Hospital Patients. *Diyala Journal of Medicine*. 2024 Oct 25;27(1):86-96. <https://doi.org/10.26505/djm.v27i1.1144>.
- 27- White J, Winteer J, and Rbbinson K. Differential inflammatory response to *Helicobacter pylori* infection: etiology and clinical outcomes. *Journal of Inflammation Research* 2015, 8: 137-147. <https://doi.org/10.2147/JIR.S64888>.
- 28- Bjorklund m and Koivunen E. Gelatinase-mediated migration and invasion of cancer cells. *Biochim. Biophys. Acta*. 2005 25(1):37-69. <https://doi.org/10.1016/j.bbcan.2005.03.001>.
- 29- Jablonska-Trypuc A, Matejczyk M. and Rosochacki S. Matrix metalloproteinases (MMPs), the main extracellular matrix (ECM) enzymes in collagen degradation, as a target for anticancer drugs. *J. Enzym. Inhib. Med. Chem* 2016; 31: 177-183. <https://doi.org/10.3109/14756366.2016.1161620>.
- 30- Koyama S. Significance of Cell-Surface Expression of Matrix Metalloproteinases and their Inhibitors on Gastric Epithelium and Infiltrating Mucosal Lymphocytes in

Progression of Helicobacter pylori-Associated Gastritis. Scand. J. Gastroenterol. 2004;39:1046–1053.

<https://doi.org/10.1080/00365520410003245>.

31- Loosen SH, Mertens A, Klein I, et al. Association between Helicobacter pylori and its eradication and the development of cancer. BMJ Open Gastroenterol 2024;11:e001377. <https://doi.org/10.1136/bmjgast-2024-001377>.

32- Sokolova O, Naumann M. Matrix Metalloproteinases in Helicobacter pylori-

Associated Gastritis and Gastric Cancer. Int J Mol Sci. 2022 Feb 8;23(3):1883. <https://doi.org/10.3390/ijms23031883>.

33- Huang Y, Gu M, Wu Q, Zhu J, Wu J, Wang P, Wang M, Luo J. Is Laryngeal Squamous Cell Carcinoma Related to Helicobacter pylori?. Front Oncol. 2022 Jan28;12:790997. <https://doi.org/10.3389/fonc.2022.790997>.

تأثير بكتيريا الملوية البوابية على نوع الافة وتعبير مصفوفة ميتالوبروتيننايز-٩ في اورام الحنجرة

^١وسن عبد الاله باقر، ^٢ رفيف صبيح الشوك، ^٣ ميس إبراهيم السكافي، ^٤ شيماء رحيم الصالحي

الملخص

الخلفية: تلعب بكتيريا الملوية البوابية ومصفوفة الميتالوبروتيننايز-٩ دوراً مهماً في العمليات المرضية الفسيولوجية والتعبير عن التسرطن، وخاصة سرطان الخلايا الحرشفية الحنجرية.

الأهداف: استكشاف الارتباط المحتمل بين عدوى الملوية البوابية و التعبير عن مصفوفة ميتالوبروتيننايز-٩ ، و تطور سرطان الخلايا الحرشفية الحنجرية من خلال دراسة دور الالتهاب المزمن و التغيرات في تركيب المادة الخلالية خارج الخلية في سرطان الحنجرة.

المرضى والطرق: شملت الدراسة المقطعية ١١٨ عينة نسيجية منها ٥٨ حالة كانت سرطان الخلايا الحرشفية الحنجرية، و ٦٠ حالة كانت سلائل حنجرية حميدة. تم استخدام الفحص النسيجي المرضي الكيميائي المناعي لتقييم تأثير بكتيريا الملوية البوابية وتعبير مصفوفة ميتالوبروتيننايز-٩ وحالة التدخين في اورام الحنجرة.

النتائج: كان انتشار بكتيريا الملوية البوابية ملحوظاً الافة الخبيثة (٦٣,٧٩٪) مقارنة بالآفات الحميدة (٥١,٦٦٪) ($P=0.01$). وجد ارتباط ذو دلالة احصائية لدى مرضى الآفات الحميدة بين مستوى التعبير عن مصفوفة ميتالوبروتيننايز-٩ والتدخين وحالة الإصابة ببكتيريا *H. pylori* ($P=0.46$, $p=0.001$) و ($r=0.5$, $p=0.001$) (على التوالي). اما مرضى الآفات الخبيثة، فقد كشف اختبار الارتباط عن ارتباط سلبي ذي دلالة احصائية بين مستوى مصفوفة ميتالوبروتيننايز-٩ وحالة التدخين ($p=-0.41$, $p=0.001$) بينما كانت بكتيريا *H. pylori* اعلى ارتباط ايجابي مع تعبير مصفوفة ميتالوبروتيننايز-٩ ($r=0.5$, $p=0.001$). كشف تحليل الانحدار اللوجستي ان عدوى بكتيريا *H. pylori* يمكن ان تتنبأ بشكل كبير بارتفاع تعبير مصفوفة ميتالوبروتيننايز-٩ ($OR=3.08$, $95\%CI: 1.15.28$, $p=0.02$).

الاستنتاج: تبرز هذه النتائج الدور الحاسم لعدوى الملوية البوابية بالتزامن مع التدخين في تطور الاورام من خلال إعادة تشكيل المادة الخلالية خارج الخلية بواسطة مصفوفة الميتالوبروتيننايز-٩ و الالتهاب و تعديل الجهاز المناعي.

الكلمات المفتاحية: جرثومة المعدة، MMP-9، سرطان الخلايا الحرشفية في الحنجرة، أورام حميدة في الحنجرة.

المؤلف المراسل: رفيف صبيح الشوك

الايميل: refifalshawk@uomustansiriyah.edu.iq

تاريخ الاستلام: ٩ كانون الثاني ٢٠٢٤

تاريخ القبول: ٥ نيسان ٢٠٢٥


تاريخ النشر: ٢٥ نيسان ٢٠٢٥

^١ فرع الاحياء المجهرية - كلية الطب - الجامعة المستنصرية - بغداد - العراق.

^٢ فرع علم الامراض - كلية الطب - الجامعة المستنصرية - بغداد - العراق.

^٤ فرع الاحياء المجهرية - كلية الطب - جامعة ديالى - ديالى - العراق.

Recurrent Hidradenocarcinoma in the Abdominal Wall with no Distant Metastasis: A Case Report and Literature Review

Yahia Hameed Al-Ani ¹, Raid M. Al-Ani ², Wassan Nori ³,
Israa Mahdi Al-Sudani ⁴

¹ Department of Surgery/General Surgery, College of Medicine, University of Anbar, Anbar, Iraq.

² Department of Surgery/Otolaryngology, College of Medicine, University of Anbar, Anbar, Iraq.

³ Department of Obstetrics and Gynecology, College of Medicine, Mustansiriyah University, Baghdad, Iraq.

⁴ Department of Basic Sciences, College of Medicine, Ibn Sina University of Medical and Pharmaceutical Sciences, Baghdad, Iraq.

OPEN ACCESS

Correspondence: Raid M. Al-Ani

Email:

med.raed.alani2003@uoanbar.edu.iq

Copyright: ©Authors, 2025, College of Medicine, University of Diyala. This is an open access article under the [CC BY 4.0](https://creativecommons.org/licenses/by/4.0/) license (<http://creativecommons.org/licenses/by/4.0/>)

Website:

<https://djm.uodiyala.edu.iq/index.php/djm>

Received: 22 November 2024

Accepted: 28 February 2025

Published: 25 April 2025

Abstract

Background: Hidradenocarcinoma is a rare, aggressive tumor with a high rate of local recurrence and distant metastasis. There are no current management guidelines, and surgery has been used to control the primary disease. Even with wide surgical excision, the course of the tumor is unpredictable, and the prognosis for survival is poor. The most common location is the scalp, followed by the extremities, and rarely the trunk.

Objective: To present a rare recurrent hidradenocarcinoma in the abdominal wall with no distant metastasis.

Case presentation: We present a rare case of recurrent hidradenocarcinoma on the abdominal wall in a 56-year-old male with no known distant metastasis treated with wide surgical excision.

Conclusion: This case represents the second reported case of hidradenocarcinoma involving the abdominal wall in the literature. Wide surgical excisions of the tumor with wide safe margins carry excellent outcomes on 5-year follow-up.

Keywords: Recurrent hidradenocarcinoma; Abdominal wall hidradenocarcinoma; Distant metastasis; Case report.

Introduction

Hidradenocarcinoma is a rare, aggressive, malignant adnexal tumor of the sweat glands (1). It accounts for approximately 6% of all malignant eccrine tumors and less than 0.001% of all tumors (2). It has a slight female predominance (with a male-to-female ratio of 4 to 6) and tends to occur in the fifth to seventh decade of life (3, 4). It was first reported as clear-cell eccrine carcinoma by Keasbey and Hadley in 1954 (5), and it is also known in the literature as clear-cell hidradenocarcinoma, solid-cystic adenocarcinoma, malignant clear-cell hidradenoma, malignant clear-cell myoepithelioma, malignant acrospiroma, and clear-cell eccrine carcinoma (6). They are mainly presented as isolated, hard, asymptomatic intradermal erythematous or violaceous nodules on the head, neck, trunk, limbs, or mouth (1). However, involvement of other body sites like the trunk and extremities occurs on rare occasions (6). Rehman et al. reported the first case of hidradenocarcinoma on the left abdominal wall in a 78-year-old woman. However, no similar cases are reported in the literature (7). Here, we present a rare recurrent hidradenocarcinoma in the

abdominal wall with no distant metastases.

Case presentation

A 56-year-old male presented to the Surgical Department of Al-Ramadi Teaching Hospital, Ramadi City, Iraq, with a gradually growing, painless swelling in the right lower aspect of the anterior abdomen that caused him no discomfort (Figure 1A). The mass started as a small lump and had been growing for the past 6 months before presentation. The patient denied any history of abdominal trauma. On physical examination, the mass measured 5 x 6 cm, solid, firm in consistency with irregular borders. The skin had mild redness over the swelling and the neighboring skin, it was fixed over the mass, but as a whole the mass was mobile to the underlying muscular layer. There were no associated systemic symptoms. Complete blood count and blood chemistries came back with no abnormalities. Differential diagnoses included; sebaceous cyst, lipoma, hemangioma, or an inflamed lymph node. It was excised under local anesthesia and was sent for histopathological evaluation. The patient, however, didn't bring the result of histopathology to the surgeon's attention. Eight months later, the patient comes back to the Surgical Department, complaining of a recurrent mass in the exact location, this time growing around the previous surgical scar. The dimensions were 5 x 4 cm on measurement. The mass looked similar to the previous presentation, having firm skin, irregular borders, mobile, but the skin was a little darker, elevated, reddish-blue, and nodular (Figure 1B). There were no associated systemic symptoms and no palpable lymph nodes in any part of the body. The erythrocyte sedimentation rate returned elevated (58 mm/hour), but all other blood chemistries were within the normal ranges. The previous histopathological report, 8 months earlier, confirmed the diagnosis of hidradenocarcinoma (a malignant tumor of the adnexa). The diagnosis was confirmed as a recurrence of the previously

excised hidradenocarcinoma of the trunk. The mass was excised under general anesthesia, leaving safe margins all around the tumor. The excised mass measured 18 x 11 x 7 cm (Figure 2A), including safe margins: upper and lower excisional margins about 1.5 cm from the mass, both lateral excisional margins about 4-5 cm from the mass, and deep excisional margin about 1 cm from the mass. The tumor itself measured 7 x 5 cm and was encapsulated. Grossly, there were visible necrotic and hemorrhagic foci (Figure 2B). The histopathological examination showed that skin and subcutaneous tissue were infiltrated by deep dermal well-defined tumor masses and nodules composed of atypical large epithelial cells with infrequent mitoses arranged in solid cords and sheets, associated with extensive multifocal necrosis and hemorrhages filling some cystic cavities. The features were consistent with recurrent malignant non-melanocytic skin adnexal tumor/solid and cystic eccrine hidradenocarcinoma-high-grade. All lateral, surrounding excisional safe margins were tumor-free (Figure 3). A positron emission tomography (PET) scan showed no distant metastasis. As such, according to the tumor, node, and metastasis (TNM) classification, the tumor stage was stage II. Since no lymph nodes were detected and after consultation with the Oncology Department, no other adjuvant therapy was suggested. The patient was advised to follow-up monthly for recurrence. After 5 years of follow-up, the patient was free of recurrence or distant metastasis. The patient gave his consent for the publication of the case with its related images.



Figure 1. Pictures of the mass before the surgery. A) Anterior view of the abdomen. B) Lateral view of the abdomen.

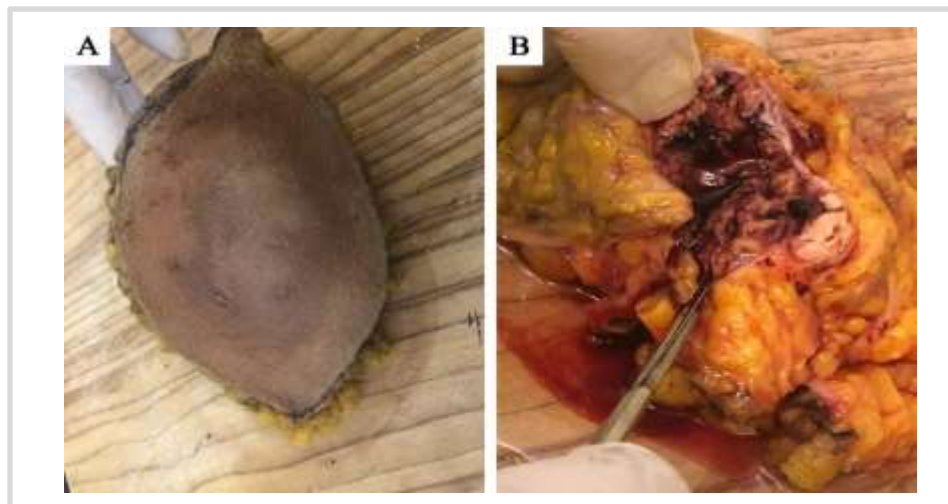


Figure 2. A) Picture of the mass from the outside after excision. B) Visible foci of necrosis and hemorrhages within the mass.

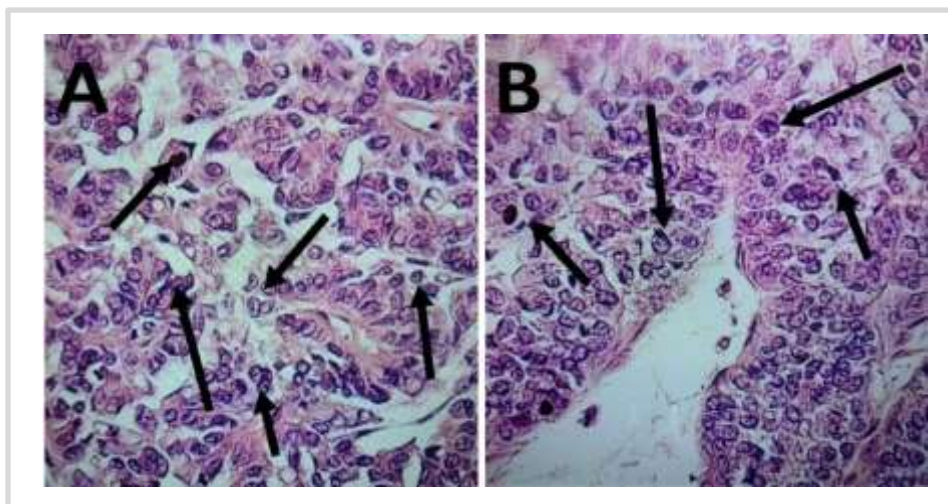


Figure 3. Variable sizes ducts lined by malignant epithelial cells with strong positive for keratin immunohistochemistry as shown by black arrows [Magnification x10 (A) and x40 (B)].

Discussion

Hidradenocarcinoma is an aggressive malignant tumor with a high tendency of local and distant metastasis (8, 9). It arises de novo but can also arise from nodular hidradenoma of the adnexa. The histological study is of prime importance in distinguishing between benign and malignant

forms, which shows increased mitotic activity, local extension, widespread necrosis, and angiolymphatic invasion (10,11). The malignant form is grossly larger, more nodular, and asymmetric (12). Hidradenocarcinoma is further divided into eccrine and apocrine subtypes (Table 1).

Table 1. The characteristics of eccrine and apocrine types of hidradenocarcinoma.

Category	Eccrine Hidradenocarcinoma	Apocrine Hidradenocarcinoma	Supp. Ref.
Gland Location	Found throughout the body, especially on palms, soles, and axillae.	Found only in specific regions such as axillae, anogenital region, abdomen & chest.	(10)
Histological Characteristics	Contains poroid cells with atypical features.	Contains clear, squamoid, poroid cells.	(11)
Differentiation	Generally considered eccrine type if only poroid cells are present.	Considered apocrine type when clear and squamoid cells are also observed.	(13)

Mixed histological features suggest apocrine differentiation, making strict distinction unnecessary (13). This explains the tumor's ability to arise all over the body, even where normally apocrine/eccrine glands are not found (14). Most cases are asymptomatic; they rarely present with symptoms, and when they do, it is primarily due to metastasis. Local symptoms are rarely seen and include bleeding or ulceration. For that, most cases are presented in the late stages. This requires an evaluation of the patient nodal spread (seen in 39%) and visceral metastasis (seen in 28%) at the time of presentation. Indeed, hidradenocarcinomas have an aggressive nature, a high rate of recurrence (50% despite surgery), and metastasis (60% of patients in 2 years). As for the prognosis, although earlier studies had discussed poor prognosis, with an estimated 30% survival for five years yet most of those studies involved small sampling power (15); a recent study by Gao et al. examined 289 cases in 18 years-time and revealed that the hidradenocarcinomas have a good prognosis and the tumor size was the most

important variable that defines overall survival and cancer free period which was reported to be 60.21% and 90.52% respectively (1). The biopsy is the main way to confirm the case. Imaging studies (Ultrasonography, CT, PET scan) are pivotal in excluding other differential diagnoses, guiding biopsy, excluding metastasis, and following up cases for prognostic value. Currently, the mainstay of treatment is wide surgical excision despite the absence of a clear guideline. The usefulness of lymph node dissection is controversial because it has not been clearly shown. Similarly, adjuvant chemotherapy and radiotherapy use has not yet been established (15). Other therapeutic approaches are currently being researched, including PI3K/Akt/mTOR pathway inhibitors, targeted therapy, EGFR inhibitors, and hormonal therapy. However, there is no concrete evidence to implement them due to the lack of sufficient patients owing to the tumor's rarity (3). What is unique about this case is that it represented the second reported case of hidradenocarcinoma involving the abdominal wall without a history

of prior trauma. The first case by Rehman et al. in 2021 was at the site of previous trauma (7). The recurrence was short despite the absence of local and distant metastasis at both consultation times. The cases were well documented and followed for a long time (5 years). It underscores the success of early and aggressive surgical approaches and emphasizes the role of close follow-up, even for such aggressive tumors.

Conclusion

Wide surgical excision with a safe margin was a satisfactory treatment for hidradenocarcinoma.

Recommendations

Owing to the rarity and aggressive behavior of hidradenocarcinoma, particularly in uncommon sites such as the abdominal wall, surgeons should remain aware of its clinical similarity to benign skin or soft tissue swellings. Early detection, accompanied by thorough histopathological examination, is of utmost importance. It is essential for future surgeons to adopt a proactive approach to suspicious or recurrent skin lesions, favoring wide local excision and collaboration within a multidisciplinary team. Long-term follow-up is critical for the early identification of local recurrence or distant metastasis. This case underscores the importance of including hidradenocarcinoma in the differential diagnosis and highlights the value of applying sound surgical oncologic principles in its management.

Source of funding: No source of funding.

Ethical clearance: The study was approved by the Ethical Approval Committee of the University of Anbar, Anbar, Iraq (Reference number 39 on 22-8-2024). Informed consent was obtained from the patient for publication of the case with its related images.

Conflict of interest: None.

Acknowledgments:

The authors would like to express their sincere gratitude and deep appreciation to the University of Anbar for its generous support and for providing the essential resources and facilities

that significantly contributed to the successful completion of this research.

References

1. Gao T, Pan S, Li M, Su R. Prognostic analysis of hidradenocarcinoma: a SEER-based observational study. *Annals of Medicine*. 2022;54(1):454-63. PMID: 35107407, <http://doi.org/10.1080/07853890.2022.2032313>
2. Ba NFK, Ka K, Ba MB, Deh A, Sarr FN, Diallo M, et al. Temporo-frontal and parotidial hidradenocarcinoma: A case report. *World Journal of Advanced Research and Reviews*. 2023;19(2):1325-9. <http://doi.org/10.30574/wjarr.2023.19.2.1718>
3. Soni A, Bansal N, Kaushal V, Chauhan AK. Current management approach to hidradenocarcinoma: a comprehensive review of the literature. *ecancermedicalsecience*. 2015;19;9:517. PMID: 25815059, <http://doi.org/10.3332/ecancer.2015.517>
4. Rafols M, Mejia O, Oh KS, Bendixen B, Jorge I, Narayanan S. An unusual case of lower extremity clear cell hidradenocarcinoma. *Case Reports in Surgery*. 2020;2020(1):6192109. PMID: 32328335, <http://doi.org/10.1155/2020/6192109>.
5. Keasbey LE, Hadley GG. Clear-cell hidradenoma. Report of three cases with widespread metastases. *Cancer*. 1954;7(5):934-52. PMID: 13199772, [http://doi.org/10.1002/10970142\(195409\)7:5<934::aid-cnrcr2820070519>3.0.co;2-5](http://doi.org/10.1002/10970142(195409)7:5<934::aid-cnrcr2820070519>3.0.co;2-5)
6. Kang EY, Fisher SB, Middleton LP. Hidradenocarcinoma involving the male breast: report of a case with emphasis on the differential diagnosis of invasive carcinoma with sweat gland differentiation. *Human Pathology Reports*. 2023;31:300698. <http://doi.org/10.1016/j.hpr.2023.300698>.
7. Rehman R, Squires B, Osto M, Quinn T, Kabolizadeh P. Hidradenocarcinoma of the abdominal wall treated with wide surgical excision and adjuvant radiotherapy. *Cureus*.

- 2021;13(4).. PMID: 34094723,
[http://doi.org/ 10.7759/cureus.14724](http://doi.org/10.7759/cureus.14724).
8. Kent S, Jeha GM, Qiblawi S, Malinosky H, Greenway HT, Kelley B. Hidradenocarcinoma: A Case Series From the Scripps Clinic With a Systematic Review of the Literature. *Dermatologic Surgery*. 2024;50(6):507-11. PMID: 38460197
[http://doi.org/ 10.1097/DSS.0000000000004140](http://doi.org/10.1097/DSS.0000000000004140).
9. Tolkachjov SN, Hocker TL, Hochwalt PC, Camilleri MJ, Arpey CJ, Brewer JD, et al. Mohs micrographic surgery for the treatment of hidradenocarcinoma: the Mayo Clinic experience from 1993 to 2013. *Dermatologic Surgery*. 2015;41(2):226-31. PMID: 25627632
[http://doi.org/ 10.1097/DSS.0000000000000242](http://doi.org/10.1097/DSS.0000000000000242).
10. Jinnah AH, Emory CL, Mai NH, Bergman S, Salih ZT. Hidradenocarcinoma presenting as soft tissue mass: case report with cytomorphologic description, histologic correlation, and differential diagnosis. *Diagnostic Cytopathology*. 2016;44(5):438-41. PMID: 26876052
[http://doi.org/ 10.1002/dc.23449](http://doi.org/10.1002/dc.23449).
11. Gauerke S, Driscoll JJ. Hidradenocarcinomas: a brief review and future directions. *Archives of pathology & laboratory medicine*. 2010;134(5):781-5. PMID: 20441512
[http://doi.org/ 10.5858/134.5.781](http://doi.org/10.5858/134.5.781).
12. Plaza JA, Wakely P, Roman J, Gru AA, Sanguenza JM, Davey J, et al. Low-grade hidradenocarcinomas: a clinicopathologic study of an unusual carcinoma that can mimic its benign counterpart. *The American Journal of Surgical Pathology*. 2023;47(8):907-14. PMID: 37272262
<http://doi.org/10.1097/PAS.0000000000002065>.
13. Belfort FA, de Gouvea Faical LG, De Lima LGCA, de Freitas Perina AL. Appendageal Tumors. *Oncodermatology: An Evidence-Based, Multidisciplinary Approach to Best Practices*: Springer; 2023. p. 393-411.
[http://doi.org/ 10.1007/978-3-031-29277-4_17](http://doi.org/10.1007/978-3-031-29277-4_17).
14. Ko CJ, Cochran AJ, Eng W, Binder SW. Hidradenocarcinoma: a histological and immunohistochemical study. *Journal of cutaneous pathology*. 2006;33(11):726-30. PMID: 17083691
<http://doi.org/10.1111/j.16000560.2006.00536.x>.
15. Ohta M, Hiramoto M, Fujii M, Togo T. Nodular hidradenocarcinoma on the scalp of a young woman: case report and review of literature. *Dermatologic surgery*. 2004;30(9):1265-8. PMID: 15355375
<http://doi.org/10.1111/j.15244725.2004.30390.x>.

تكرار الإصابة بسرطان الغدد العرقية في جدار البطن دون وجود نقائل بعيدة: تقرير حالة ومراجعة أدبية

^١ يحيى حميد العاني، ^٢ راند العاني، ^٣ وسن نوري، ^٤ إسراء مهدي السوداني

الملخص

الخلفية: يُعد سرطان الغدد اللمفاوية ورمًا نادرًا وعدوانيًا، يتميز بمعدل تكرار موضعي مرتفع وانتشار ورم خبيث بعيد. لا توجد إرشادات علاجية حالية، وقد استُخدمت الجراحة للسيطرة على المرض الأساسي. حتى مع الاستئصال الجراحي الواسع، لا يُمكن التنبؤ بمسار الورم، وتوقعات البقاء على قيد الحياة ضعيفة. الموقع الأكثر شيوعًا هو فروة الرأس، تليها الأطراف، ونادرًا ما يكون الجذع.

الأهداف: عرض حالة نادرة من سرطان الغدد اللمفاوية المتكرر في جدار البطن دون انتشار ورم خبيث بعيد.

عرض الحالة: تُقدم حالة نادرة من سرطان الغدد اللمفاوية المتكرر في جدار البطن لدى رجل يبلغ من العمر ٥٦ عامًا، ولم يُكتشف لديه أي انتشار ورم خبيث بعيد، وقد عولج باستئصال جراحي واسع.

الاستنتاج: تُمثل هذه الحالة الثانية المُبلغ عنها لسرطان الغدد اللمفاوية في جدار البطن في الدراسات العلمية. يُحقق الاستئصال الجراحي الواسع للورم مع هوامش أمان واسعة نتائج ممتازة بعد متابعة لمدة ٥ سنوات.

الكلمات المفتاحية: سرطان الغدد اللمفاوية المتكرر؛ سرطان الغدد اللمفاوية في جدار البطن؛ النقائل البعيدة؛ تقرير حالة.

المؤلف المراسل: راند العاني

الايمل: med.raed.alani2003@uoanbar.edu.iq

تاريخ الاستلام: ٢٢ تشرين الثاني ٢٠٢٤

تاريخ القبول: ٢٨ شباط ٢٠٢٥

تاريخ النشر: ٢٥ نيسان ٢٠٢٥

^١ فرع الجراحة العامة - كلية الطب - جامعة الأنبار - الانبار - العراق.

^٢ فرع الجراحة الأنف والأذن والحنجرة - كلية الطب - جامعة الأنبار - الانبار - العراق.

^٣ فرع أمراض النساء والتوليد - كلية الطب - الجامعة المستنصرية - بغداد - العراق.

^٤ قسم العلوم الأساسية - كلية الطب - جامعة ابن سينا للعلوم الطبية والصيدلانية - بغداد - العراق.

DJM

مجلة ديالى الطبية

تصدر عن كلية الطب - جامعة ديالى - ديالى - العراق

هيئة التحرير

رئيس التحرير

أ.م.د. انفال شاكور متعب

دكتوراه بايولوجي جزئي - كلية الطب - جامعة ديالى

anfai_shaker@yahoo.com

مدير التحرير

م.د. سعد احمد علي جدوع العزي

دكتوراه طب مجتمع - كلية الطب - جامعة ديالى

saadalezzi@uodiyala.edu.iq

هيئة التحرير

أ.د. أسماعيل ابراهيم لطيف

دكتوراه مناعة سريرية - كلية الطب - جامعة ديالى

ismail_6725@yahoo.com

أ.د. غانم مصطفى الشيخ

دكتوراه علوم عصبية - كلية امبريال الطبية - المملكة المتحدة

alsheikhg@gmail.com

أ.د. كريم علوان محمد

دكتوراه في علم الأمراض وطب العدلي - رئيس وحدة الأمراض والطب

العدلي في جامعة SEGi الماليزية

jashamy@yahoo.com

أ.د. طالب جواد كاظم

دكتوراه تشريح - كلية الطب - جامعة ديالى

talibjwd@yahoo.com

أ.د. سعد محمود حسين الاركي

بورج جراحة عامة - كلية الطب - جامعة نيوكستل الطبية - ماليزيا

Drsaad1961@gmail.com

أ.د. جليل ابراهيم العزي

دكتوراه طب الاطفال - كلية الطب - جامعة ديالى

jaleel@uodiyala.edu.iq

أ.د. عامر داود مجيد

دكتوراه فيزياء طبية - كلية الطب - جامعة ديالى

amer_dmk@yahoo.com

أ.د. زهير معروف حسين

دكتوراه كيمياء حيائية - كلية الطب - جامعة ديالى

zuhair@medicine.uodiyala.edu.iq

أ.د. مهدي شمخي جبر

بورج طب الاطفال - كلية الطب - جامعة ديالى

meh_sh2000@yahoo.com

أ.د. احمد محمد باذيب

دكتوراه طب باطني و اورام الدم - رئيس قسم الاورام في مستشفى الملك

خالد - نجران - السعودية

abadheeb@moh.gov.sa

أ.د. سلوى شلش عبد الواحد

دكتوراه طب مجتمع - كلية الطب - جامعة ديالى

s_sh_abdulwahid@yahoo.co.uk

أ.د. صالح مهدي سلمان

دكتوراه كيمياء عضوية - كلية الطب - جامعة ديالى

salih@medicine.uodiyala.edu.iq

أ.د. كاملة مراك اوغلو

دكتوراه في طب الأسرة - كلية الطب - جامعة سلجوق - قونية - تركيا

أ.د. ايدن بيادلي

دكتوراه في طب العيون - جامعة أنقرة - تركيا

aydinbeyatli@hotmail.com

أ.د. مروان صالح النمر

دكتوراه في الصيدلة والمداواة - كلية الطب - جامعة ديالى

marwanalnimer@yahoo.com

أ.د. علي محمد باطرفي

جراحة عامة - جامعة العرب - كلية الطب والعلوم الصحية المكلا - حضرموت - اليمن

ambatarfi@yahoo.com

أ.م.د. مقداد فؤاد عبد الكريم

بورج جراحة - كلية الطب - جامعة ديالى

muqdadfuad@yahoo.com

أ.م.د. فايز بن عبد الله الغفيلي

دكتوراه الأحياء الدقيقة الطبية - كلية العلوم التطبيقية - جامعة المجمعة - المملكة

العربية السعودية

F.alghofaily@mu.edu.sa

أ.م.د. مليكة أمير اوغلو

دكتوراه في صحة الطفل وأمراضه - كلية الطب بجامعة سلجوق - قونية - تركيا

mkeser17@gmail.com

د. عمر ليث قاصد

FRCPATH (المملكة المتحدة) IFCAP (الولايات المتحدة الأمريكية) - استشاري

أمراض الأنسجة بجامعة ليستر - المستشفيات الجامعية في ليستر - المملكة المتحدة

Omer.qassid@uhl-tr.nhs.uk

أ.م.د. مصطفى غني طاهر

دكتوراه في أمراض الفم والوجه والفكين - كلية الطب - جامعة ديالى

gheny@uodiyala.edu.iq

أ.د. ناظم غزال نعمان

رئيس قسم طب المجتمع - كلية الطب - جامعة ديالى.

drnadhimg@yahoo.com

تصميم المجلة

احمد جبار محمد

ahmed.jabbar@uodiyala.edu.iq

المراسلة: مكتب مجلة ديالى الطبية /كلية الطب/جامعة ديالى/ ص.ب(٢) مكتب بريد بعلقوبة /بعلقوبة/ديالى/ العراق.

البريد الالكتروني: editor@djmuodiyala.edu.iq, djmuodiyala@yahoo.com